Cover Page

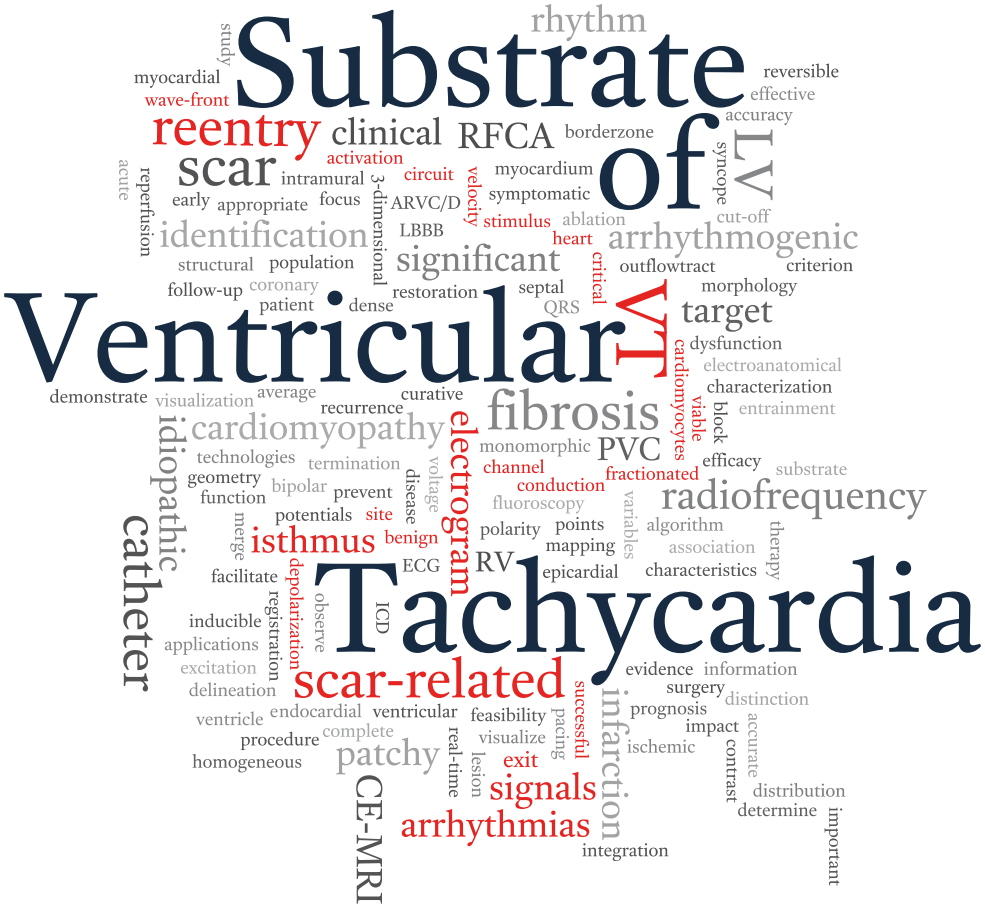


Universiteit Leiden



The handle http://hdl.handle.net/1887/18608 holds various files of this Leiden University dissertation.

Author: Wijnmaalen, Adrianus Pieter
Title: Substrate of ventricular tachycardia
Issue Date: 2012-03-22



A.P. Wijnmaalen

Substrate of Ventricular Tachycardia

Adrianus P. Wijnmaalen

Substrate of Ventricular Tachycardia
Adrianus P. Wijnmaalen

The studies described in this thesis were performed at the Department of Cardiology of the Leiden University Medical Center, Leiden, The Netherlands

Cover: Adrianus P. Wijnmaalen

Lay-out en printing: Optima Grafische Communicatie, Rotterdam, The Netherlands

ISBN: 978-94-6169-213-9

Copyright © Adrianus P. Wijnmaalen, Rotterdam, The Netherlands. All rights reserved. No part of this book may be reproduced or transmitted, in any form or by any means, without permission of the author.

Financial support for the costs associated with the publication of this thesis was received from: Boehringer Ingelheim BV, Biosense Webster, Biotronik Nederland BV, ChipSoft BV, GE Healthcare, J.E. Jurriaanse Stichting, MSD Nederland BV, Servier Nederland Farma BV, St. Jude Medical and Toshiba Medical Systems Nederland.

Substrate of Ventricular Tachycardia

Proefschrift

ter verkrijging van
de graad van Doctor aan de Universiteit van Leiden,
op gezag van de Rector Magnificus Prof.mr. P.F. van der Heijden,

volgens het besluit van het College voor Promoties
te verdedigen op donderdag 22 maart 2012
klokke 13.45 uur

door

Adrianus Pieter Wijnmaalen

geboren te Rotterdam
in 1980

Promotiecommissie

Promotor:	Prof. Dr. M.J. Schalij
Co-promotor:	Dr. K. Zeppenfeld
Overige leden:	Prof. Dr. R.J.M Klautz
	Prof. Dr. J.M.T de Bakker (AMC, Amsterdam)
	Prof. Dr. G. Hindricks (University of Leipzig, Leipzig)
	Dr. D.A. Pijnappels
	Dr. R.J. van der Geest

Financial support by the Netherlands Heart Foundation for
the publication of this thesis is gratefully acknowledged.

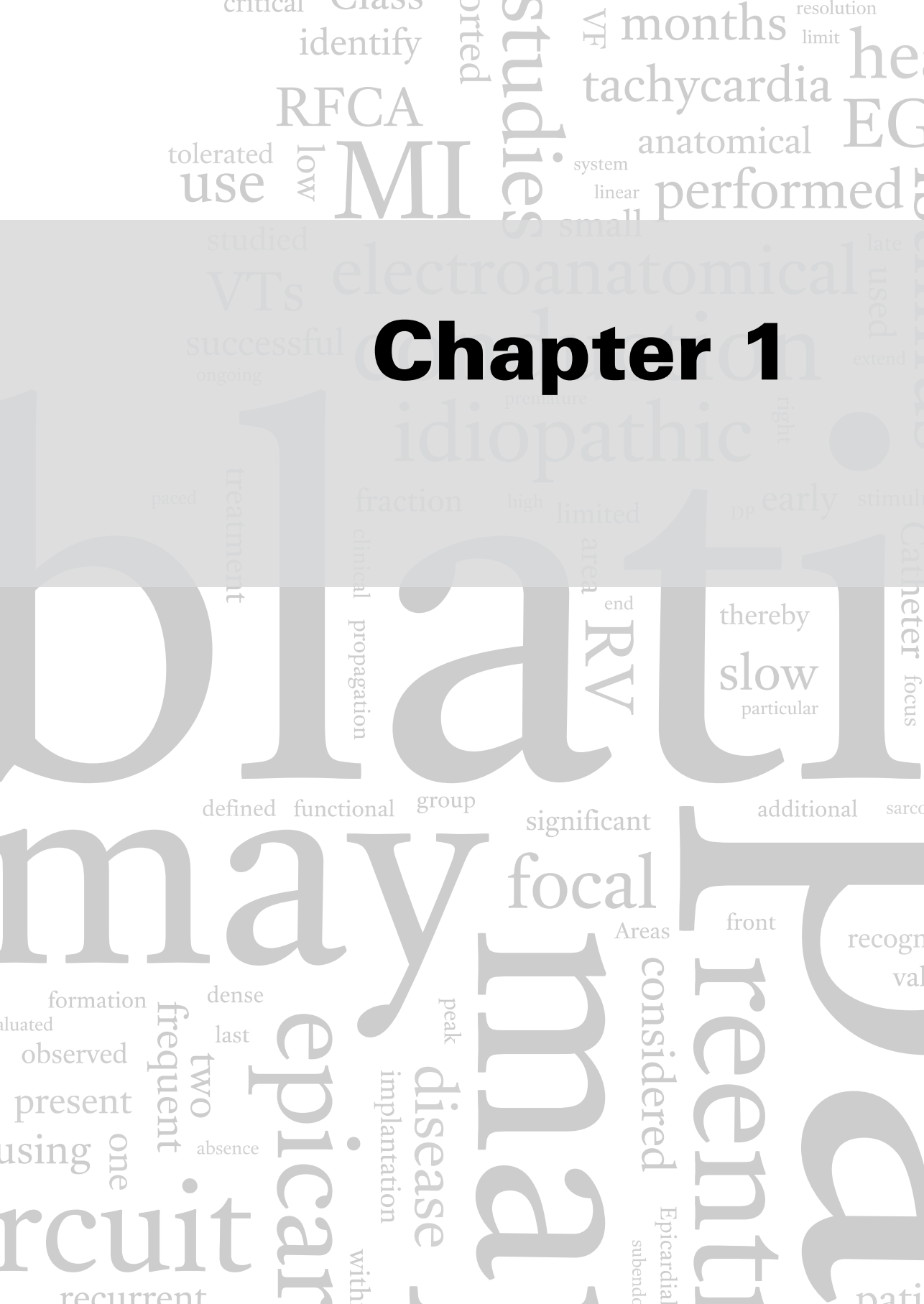
inquietum est cor nostrum, donec requiescat in te

Augustine of Hippo

Contents

Chapter 1	Introduction and outline of the thesis Adapted from Minerva Cardioangiol. 2011 Apr;59(2):149-69.	8
Part I	**Determinants of ventricular tachycardia substrate and techniques for substrate identification**	41
Chapter 2	ECG identification of scar-related ventricular tachycardia with a left bundle branch block configuration Circ Arrhythm Electrophysiol. 2011 Aug 1;4(4):486-93.	42
Chapter 3	Reversed polarity of bipolar electrograms to predict a successful ablation site in focal idiopathic right ventricular outflow tract arrhythmias Heart Rhythm. 2011 May;8(5):665-71.	62
Chapter 4	Early reperfusion during acute myocardial infarction affects ventricular tachycardia characteristics and the chronic electroanatomical and histological substrate Circulation. 2010 May 4;121(17):1887-95.	80
Chapter 5	Head-to-head comparison of contrast-enhanced magnetic resonance imaging and electroanatomical voltage mapping to assess post-infarct scar characteristics in patients with ventricular tachycardias: real-time image integration and reversed registration Eur Heart J. 2011 Jan;32(1):104-14.	100
Chapter 6	Real-time integration of MDCT derived coronary anatomy and epicardial fat: Impact on electroanatomical mapping and ablation for ventricular arrhythmias Submitted.	120

Part II	**Catheter ablation and outcome in different ventricular tachycardia substrates**	145
Chapter 7	Beneficial effects of catheter ablation on left ventricular and right ventricular function in patients with frequent premature ventricular contractions and preserved ejectionfraction Heart. 2010 Aug;96(16):1275-80.	146
Chapter 8	Patients with scar-related right ventricular tachycardia: determinants of long term outcome J Cardiovasc Electrophysiol. 2009 Oct;20(10):1119-27.	162
Chapter 9	Early reperfusion affects inducibility, cycle length and occurrence of VT Circ Arrhythm Electrophysiol. 2011 Apr 1;4(2):195-201.	182
Chapter 10	Catheter ablation of ventricular tachycardia after left ventricular reconstructive surgery for ischemic cardiomyopathy Heart Rhythm. 2012 Jan; 9(1):10-7	200
Summary and conclusions		219
Samenvatting en conclusies		229
List of publications		239
Dankwoord		243
Curriculum Vitae		247
Color section figures		251


Chapter 1

Introduction and outline of the thesis

Adapted from:

Ventricular tachycardia ablation: indications and techniques
Adrianus P. Wijnmaalen and Katja Zeppenfeld

Minerva Cardioangiol. 2011 Apr; 59(2):149-69.

Abstract

The growing role of catheter ablation for ventricular arrhythmias in patients with and without structural heart disease reflects the progress made in this field over the last decades. Due to the high ablation success for non scar-related VA catheter ablation has become a first line therapy for symptomatic idiopathic VT and PVCs or VA presumed to cause ventricular dysfunction. In patients with scar-related VT development of substrate based techniques, irrigated tip catheter ablation and the introduction of an percutaneous epicardial approach in selected patients has rendered many VT previously considered 'unmappable' approachable for ablation. Catheter ablation may be considered in post MI patients even after a first VA episode to prevent VT recurrences during follow-up or to avoid drug therapy, provided that the procedure can be performed safely. The underlying heart disease affects the substrate that determines VT characteristics. Better understanding of the VT substrate in different diseases and individual patients is important for the improvement of mapping and ablation strategies. Advances in substrate imaging technologies and their integration during ablation procedures may provide more insights into the substrates and may guide VT ablation in the future. Since treatment strategies and prognosis of scar-related and non scar-related VT differ, the distinction between these entities is of great relevance and may be enhanced by identification of the VT substrate during catheter mapping. Ablation failure is frequently due to the anatomical localization of the target site. However, evolving new catheter techniques and energy sources may overcome these limitations.

Introduction

Since the first report in 1959 of surgical ventriculoplasty abolishing recurrent ventricular tachycardia (VT) in a patient after myocardial infarction[1] ablation of VT has evolved from surgical treatment to radiofrequency catheter ablation (RFCA). Over the last decennium indications have broadened and techniques have been developed resulting in an increasing use of RFCA for different types of VT.[2]

Patients presenting with VT and underlying structural heart disease are at risk for sudden cardiac death (SCD).[3] The use of implantable cardioverter defibrillators (ICDs) has resulted in a significant reduction in SCD in this patient population.[3-5] ICDs effectively terminate VT but cannot prevent VT recurrence and after an initial episode of VT or ventricular fibrillation (VF) up to two thirds of patients receive one or more appropriate therapies within two years.[6, 7] An important number of VT termination requires shocks which have an significant impact on quality of life.[8] In addition, in patients with heart failure ICD shocks are associated with an increased risk of death.[9] Therapies that prevent episodes of VT are therefore warranted. RFCA can prevent VT recurrence, thereby decreasing the number of ICD shocks in patients with structural heart disease by modifying the VT substrate.[6, 7]

Ventricular arrhythmias (VA) that occur in the absence of structural heart disease are generally considered benign and are associated with a favorable prognosis.[10] Distinction between patients with scar-related and idiopathic (non scar-related) VA is therefore of key relevance. However, a small number of patients presents with malignant VA without (todays) evidence of structural heart disease or scar and some patients have idiopathic VA that cause a potential reversible cardiomyopathy.[11, 12]

Since its first use in 1978 RFCA for idiopathic VA has been proven to be curative and safe and is now considered a first line therapy in highly symptomatic patients.[2]

Even though RFCA for VT is recognized to be of value in structural heart disease, the appropriate patient selection, methods to use, optimal timing and best endpoint are still matter of debate. Individual patient factors and operator experience play an important role in risk-benefit considerations.

Mechanisms and substrates underlying ventricular arrhythmia

Scar-related reentrant ventricular tachycardia

Reentry is the prevailing mechanism for VT related to scar. The requirements for reentry to occur are areas of slow conduction, sites of fixed or functional conduction block and an initiating stimulus or sequence of stimuli.

The time that is needed for propagation through slow conduction areas allows for repolarization of the remaining parts of the circuit so that the reentrant wavefront does not encounter block during its progression.

Histological evaluation of slow conduction areas showed tracts of viable myocardial cells traversing areas of fibrous tissue.[13] Several factors may contribute to the reduction in conduction velocity. Fibrosis between strands of viable cells functionally prolongs the pathway for impulse propagation.[14] In addition, changes in cell coupling by a decreased number of gap-junctions and altered connexin expression may contribute to slow conduction on a cell to cell level.[14, 15]

Conduction velocity is also influenced by the direction of wave front propagation and architecture of fibrosis. Wavefront propagation perpendicular to fiber direction is slower than propagation parallel to the fiber direction.[15]

Areas of fixed or functional conduction block influence reentrant circuit characteristics and form the borders of a protected channel or 'isthmus' of viable myocardial cells. Dense fibrosis and other unexcitable tissue like valve annuli and surgical scars may serve as areas of fixed conduction block.[16, 17] In contrast, functional block is not present during normal rhythm but can evolve due to change in refractoriness in response to a premature excitation and may be equally important defining the reentrant circuit isthmus.[18] The 3-dimensional geometry of myocardial scar plays an important role in the formation of block and may even predict the location of potential reentry circuits.[19]

The critical part of a reentry circuit is an area of slow conduction bordered by two lines of fixed or functional conduction block, the critical isthmus. Reentry is initiated by a premature excitation wavefront that enters this isthmus through its entrance and traverses it slowly. At the exit of the isthmus, often located at the border of the scar, the wavefront emerges to rapidly depolarize the remainder of the ventricles. The activation propagates along the border of the scar (the outer loop) to reactivate the excitable entrance of the circuit thereby closing the circle. (Figure 1) The dimensions of a reentry circuit are 3-dimensional and parts of the circuit may lay subendocardial, intramural and subepicardial, depending on the location and geometry of the structures causing conduction block.[20]

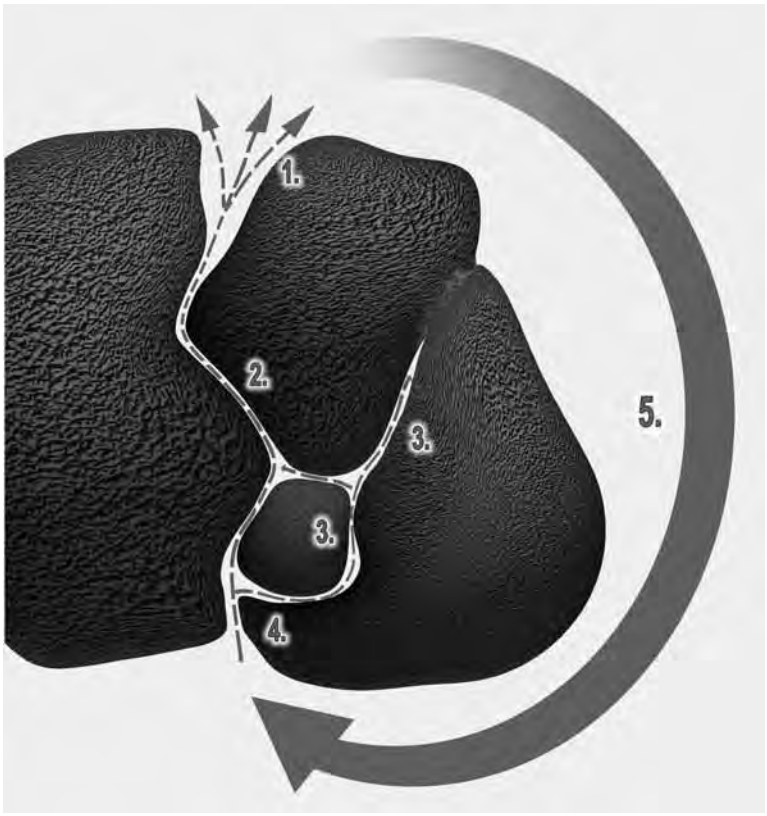


Figure 1. Components of the reentrant circuit and corresponding response to entrainment mapping

Schematic of a scar-related reentrant circuit. The gray areas represent dense scar and white areas represent conducting myocardium. Numbers indicate different reentrant circuit sites encountered during mapping.

1. Exit site. The activation wavefront exits the scar to activate the remainder of the ventricles. During VT concealed entrainment, a difference between post pacing interval (PPI) and VT cycle length ≤30ms and a short stimulus to QRS interval (<30% of VT cycle length) are typically found at this site.

2. Critical isthmus. Protected area of slow conduction through the scar. Concealed entrainment, a difference between PPI and VT cycle length ≤30ms and an intermediate stimulus to QRS interval (31 – 50% of VT cycle length) are encountered at this site during VT.

3. Adjacent bystanders. Slow conducting areas in the scar not part of the reentry circuit under evaluation. Even though during VT concealed entrainment can be found the differnence between PPI and VT cycle length is usually long (>30ms).

4. Entrance site. The activation wave front enters the circuit isthmus. Features: Concealed entrainment, a difference between PPI and VT cycle length ≤30ms and a long stimulus to QRS interval (51-70% of VT cycle length).

5. Outer loop. Rapid activation of the ventricular myocardium from exit toward entrance site. Mapping during VT reveals entrainment with QRS fusion.

Non scar-related idiopathic ventricular arrhythmia

Idiopathic VA is a term used for VA that is known to occur in the absence of clinically apparent structural heart disease.[2] Most idiopathic VA have a focal origin in the ventricular outflowtracts (OT) making them susceptible to discrete radiofrequency ablation. The mechanism underlying focal repetitive monomorphic VT (RMVT) can be triggered activity or automaticity. Most focal VA respond to adenosine, verapamil or beta blockers, agents interfering with the cAMP mediated inward calcium current. In particular the specific effect of adenosine indicates that triggered activity induced by cAMP-mediated delayed afterdepolarizations is the major mechanism underlying these focal VA.[21, 22] More rarely the mechanism of focal VA may be automaticity provoked by adrenergic stimulation or arising from damaged purkinje fibers.[23]

Although most idiopathic VA have a focal origin it has been demonstrated that reentry is the underlying mechanism for a distinct subset of VT, idiopathic left ventricular tachycardia (ILVT), arising from the area of the left posterior or anterior fascicle. The mechanism of this verapamil sensitive form of VT, although not completely understood, may be intrafascicular reentry or involves abnormal Purkinje tissue in which slow conduction is dependent on the slow inward calcium current in partially depolarized cells.[24]

Ablation of VT

Catheter ablation of VT aims to abolish the arrhythmic source in VT with a focal origin or to permanently interrupt the circuit in reentrant VT. The strategy for catheter mapping and ablation is determined by the type of VT and the location of the underlying substrate. The following section summarizes different mapping techniques and potential ablation *target sites*.[2, 25]

Ablation of Scar-related VT

Mapping during VT

When reentrant VT is stable and hemodynamically well tolerated point by point catheter mapping can be performed to identify the critical isthmus allowing for interrupting the circuit with a limited number of RF lesions during ongoing VT.[26, 27] The QRS of the VT begins when the excitation wavefront emerges from the exit of an isthmus often located at the scar border zone.

Thus the depolarization of the slow conducting isthmus occurs prior to QRS onset. Isthmus sites may be recognized by recording isolated low amplitude, presystolic or *diastolic potentials* (DP) during VT. These potentials are generated by the depolarization of isolated bundles of viable myocardial cells within the scar. DP are observed at 50% of isthmus sites

and help to identify sites where RF ablation can terminate VT.[27-29] However, DP are also seen in bystander areas outside the critical isthmus of the VT under evaluation.[27] Isthmus and bystander sites can be discriminated by entrainment mapping or pacing from a remote site to dissociate the DP from the VT.[29]

Entrainment mapping is used to distinguish different components of the reentry circuit. Pacing slightly faster than the VT continuously resets the reentry circuit. Interpretation of entrainment depends on the assumption that pacing does not alter the conduction through the circuit path or initiate another VT. At circuit isthmus sites, pacing entrains VT without changing the ventricular activation remote from the scar, producing *entrainment with concealed fusion* recognizable by the same paced QRS as recorded during VT. Entrainment with QRS fusion is observed when pacing is performed from sites outside the protected isthmus resulting in an altered ventricular activation and consequently a different QRS morphology than during VT.[28]

At reentry circuit sites the post-pacing interval (PPI) is equal to the revolution time through the circuit, which is the tachycardia cycle length. The PPI increases with increasing distance and/or conduction time from the pacing site to the circuit. If the *difference between PPI and VT cycle length is ≤30ms* the pacing site is considered to be part of the reentry circuit. The electrogram (EGM) selected for measuring the PPI is important and should represent the local depolarization at the pacing site. The selection of farfield signals is a common reason for incorrect measurement of the PPI. The local signal is not visible during pacing and reappears when pacing is ceased. Farfield signals are usually not obscured by the stimulus artifact and may be recognized by the fact that they remain visible during pacing.

At reentry circuit isthmus sites the stimulus to QRS interval (S-QRS) equals the conduction time from the pacing site to the reentry circuit exit, and is short (e.g., < 30% of the tachycardia CL) near the exit region, and longer at sites proximal to the exit. At inner loop sites, the stimulus to QRS time may be longer than 70% of the VTCL. Outer loop sites are recognized from a PPI that approximates the VTCL, however at these sites QRS fusion occurs.[28, 30] (Figure 1)

VT unstable for mapping

Only one third of patients after myocardial infarction (MI) and less than 45% of patients with non-ischemic cardiomyopathy referred for ablation of VT are only inducible for VT stable for mapping during ongoing arrhythmia.[25, 31] The majority of patients has 'unstable' VTs that are either hemodynamically not tolerated or not reproducibly inducible. Furthermore, multiple morphologies of VT are frequently inducible while data from the spontaneous VT may only be available from ICD interrogation, preventing the definite identification of the clinical VT.[25, 32] Therefore the focus of VT ablation has shifted away from mapping of single VT reentry circuits during ongoing VT to a substrate based approach targeting broader regions

of scarred myocardium likely containing the critical part of the reentry circuit without the need for mapping during VT.

Substrate mapping

Substrate based mapping and ablation techniques use local EGM characteristics obtained during stable sinus rhythm (SR) or paced rhythm to identify myocardial scar and areas of abnormal electrical conduction. The reduction of myocytes in scar areas reduces the amplitude of recorded EGMs, allowing areas of scar to be recognized from the peak to peak EGM voltage. Animal studies to validate the method were performed in a model of homogeneous dense, infarct scar surrounded by a small scar border zone. It has been shown that a value of ≤1.5mV peak to peak bipolar EGM voltage best demarcated infarct scar areas.[33] In addition, more than 95% of EGMs in normal human ventricles have a voltage of ≥1.55mV.[34] Areas with low voltage EGM can be visualized in 3-dimensional anatomical maps by colour-coding peak-to-peak EGM voltage (voltagemaps). (Figure 2A-C) Ablation of the entire low voltage area or its circumference is usually not feasible. Therefore additional criteria to further select ablation targets within the scar have been applied.

EGM characteristics obtained during SR can be suggestive for potential reentry circuit sites. Slow and heterogeneous conduction through the scar area may result in broadening and fractionation of the local EGM. *Longer duration* (>40ms) and *fractionated* (>4 deflections) EGM have been associated with successful ablation sites for VT after myocardial infarction.[35] Similar to diastolic potentials that precede the QRS complex during VT, *isolated late potentials* that follow the QRS during SR may indicate the presence of slow conducting channels and can be considered as target sites for ablation. Late potentials may be better recognized during right ventricle (RV) apex pacing in selected patients.[36] (Figure 2C)

Conducting channels within dense fibrosis may have larger voltage amplitudes than the surrounding non-conducting areas. Lowering the voltage criteria for the colour coding of dense scar may allow for the identification of these channels.[37]

Pacemapping

Pacemapping can be employed to identify potential VT exit and isthmus sites at the border of the scar during SR. By pacing along the scar-borderzone regions can be identified where the paced 12-lead ECG QRS morphology resembles the VT QRS morphology. *Pacing sites with a matching QRS morphology* are likely to be near the exit of the reentry circuit. During pacemapping a *stimulus-to-QRS (S-QRS) delay of ≥40ms* indicates slow conduction away from the pacing site.(Figure 2C) A paced QRS matching the VT QRS in combination with a long S-QRS interval is consistent with a potential VT isthmus site.[32, 34] Pacing performed at a site more proximal in the circuit may however result in a different QRS morphology since the activation sequence following the stimulus may be opposite to that of the tachycardia.

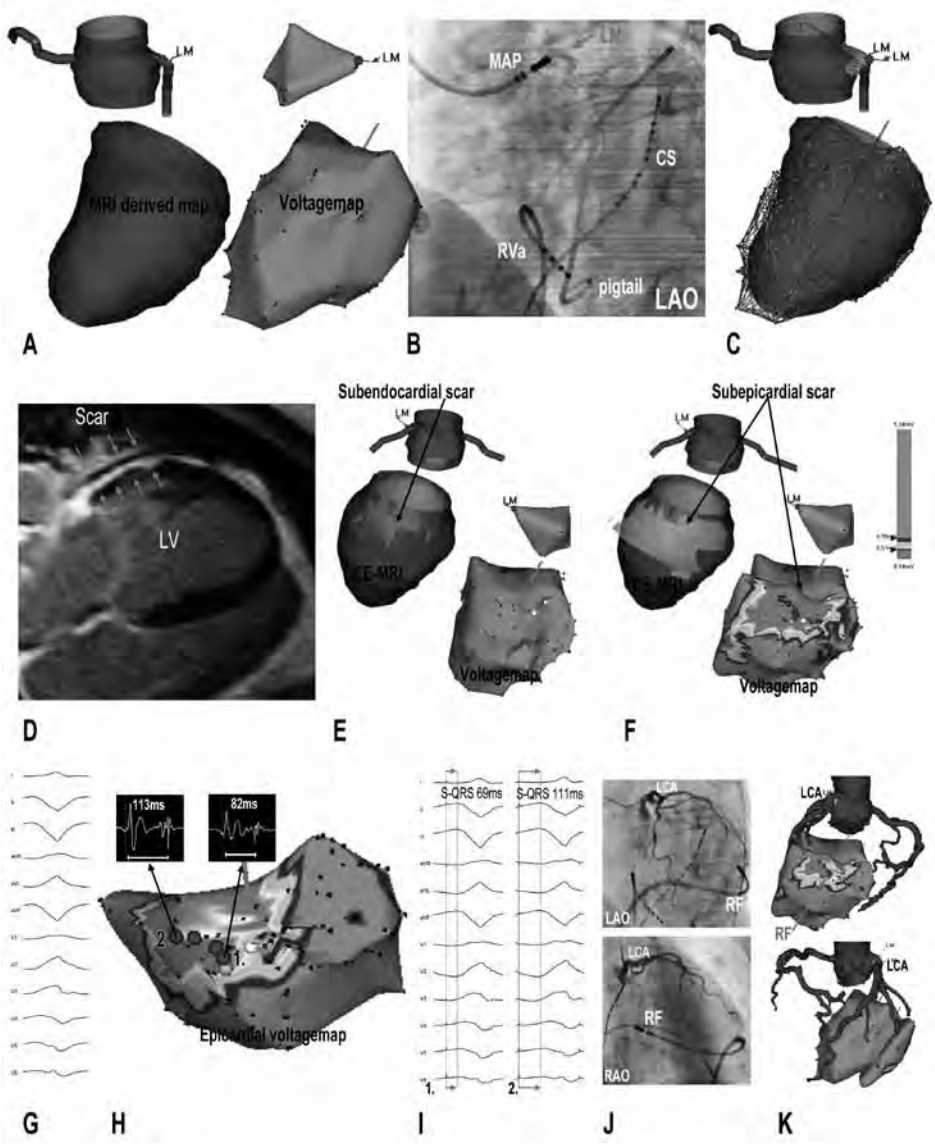


Figure 2. Image integration of electroanatomical voltage mapping and CE-MRI derived data on anatomy and scar characteristics (for figure in color see page: 252)

Example of a patient presenting with VT due to non-ischemic cardiomyopathy in whom combined endocardial and epicardial catheter ablation was performed using image integration of CE-MRI derived data sets and electroanatomical substrate mapping techniques during sinus rhythm.
A and C. Successful integration of the CE-MRI derived LV and aortic cusp anatomy with the LV endocardial electroanatomical voltage map (EAVM) (voltages>1.5mV defined as normal and color coded in purple) using the left main coronary artery (LM) as a single landmark for registration.
B. The fluoroscopy image shows contrast injection through the ablation catheter (MAP) to confirm its position in the LM. Other catheters shown are located at the right ventricular apex (RVa), coronary sinus (CS) and a pigtail catheter in the pericardial space.

D. Identification of mid-wall to subepicardial scar at the posterior base of the LV by contrast enhanced MRI.
E. The location of intramural scar of the inner half of the wall (green) is superimposed on the endocardial MRI derived anatomy. Please note the normal endocardial voltage map which is displayed side by side.
F. The limited epicardial voltage map with a basolateral low voltage area (colors according to the bar) and the endocardial voltage map are displayed side by side with the corresponding MRI data. The location of the non-transmural subepicardial scar was projected on the MRI derived epicardial surface and displayed in blue together with the endocardial MRI derived anatomy. Please note the extend of the subepicardial scar which corresponds to the low voltage area.
G – I. Different substrate based mapping and ablation techniques were used.

G. 12-lead VT QRS morphology.
H. Limited epicardial voltagemapping (color coded according to the bar); green tags represent sites where isolated potentials were recorded. The activation time of the isolated potential at site 1 was 82ms and was longer (113ms) at site 2 located deeper in the scar area which may be consistent with a slow conducting channel.
I. This was confirmed by pacemapping showing a matching pacemap with increasing stimulus to QRS duration between the two sites (69 and 111ms respectively).
J – K. Fluoroscopy (Left anterior oblique (LAO) and right anterior oblique (RAO) views; ablation catheter located at the ablation site (RF). Contrast injection in the left coronary artery (LCA)) showed sufficient distance for ablation between the target site and the coronary artery and confirmed the good registration accuracy between the coronary anatomy derived from multislice computed tomograpy and the electroanatomical map. To exclude vicinity of the phenic nerve high output pacing was performed (not shown). A short linear ablation lesion along the scar borderzone was successful rendering VT not inducible.

Pacing within the scar may further be used to identify area with electrically unexcitable scar (EUS), defined as sites with a unipolar pacing threshold of ≥10mA at 2ms pulse width. Areas of EUS and anatomical boundaries such as valve annuli may form regions of fixed conduction block bordering the VT reentry circuit isthmus; targeting these isthmuses by connecting the anatomical boundaries to EUS or the areas of EUS by linear RF lesions can abolish VT.[17, 38]

Linear ablation lines along the scar border in the region of a presumed exit site or through an identified isthmus performed during SR can be also effective in controlling VT. Additional ablation lesions connecting to dense scar areas or anatomical boundaries or perpendicular to the scar border into the scar have also been applied.[32, 34, 38]

Substrate mapping can also be combined with limited mapping during VT, allowing for identification of the regions of interest during stable SR first. After VT induction evaluation of VT EGMs, entrainment mapping, and ablation can be restricted to predefined regions and may be feasible also for poorly tolerated VT.[32]

Non-contact mapping

Unstable VTs can be mapped aswell using multielectrode mapping arrays that sample and mathematically reconstruct virtual EGMs from multiple distant sites simultaneously. These

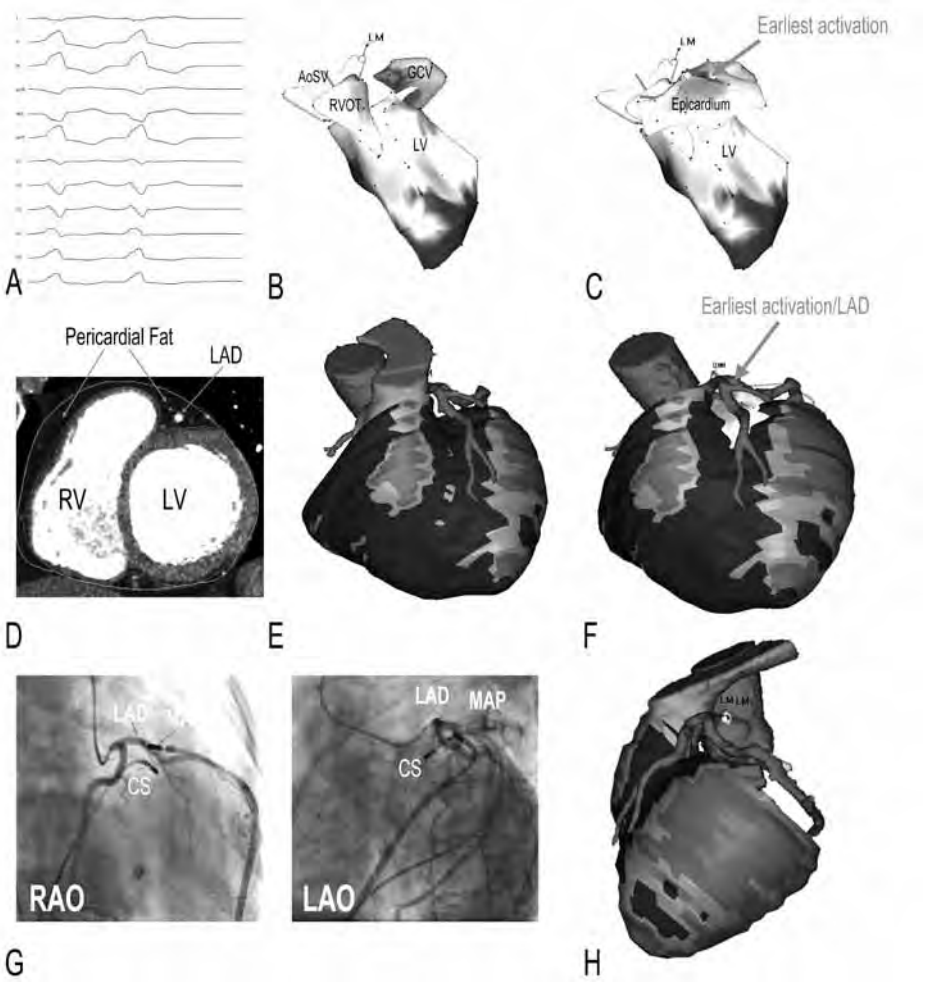


Figure 3. Integration of electroanatomical activation mapping and MSCT derived anatomy during epicardial ablation (for figure in color see page: 253)

Example of a patient presenting with frequent highly symptomatic non-sustained idiopathic VT in whom combined endo- and epicardial electroanatomical mapping and ablation was performed facilitated by integration of CT derived anatomy.

A. 12-lead QRS of the non-sustained VT.

B. Endocardial activation mapping showing limited maps of the aortic cusps (AoSV), great cardiac vein (GCV), right ventricular outflowtract (RVOT) and left ventricle (LV). Earliest local activation time (LAT) was recorded in the GCV but ablation at this site was not successful. C. A limited epicardial activation map overlaying the endocardial maps; epicardial LAT during VT is earlier than the earliest LAT in the GCV.

D. Short axis slice of contrast enhanced multislice computed tomography scan (CT) showing the left and right ventricles (LV and RV) and pericardial fat in the interventricular groove and RV lateral wall.

E and H. Different views of CT derived anatomy showing the proximal aorta, left main coronary artery and pulmonary artery with overlaying CT derived mesh of the epicardial surface. Color

coding of CT derived mesh shows the epicaridal fat distribution. (Purple = >4mm fat thicknes, Orange = >1mm and <4mm fat thickness, Green = no epicardial Fat)
F. Successful integration of the epicardial voltagemaps with the CT derived anatomy and fat distribution. The area of earliest local activation is directly adjacent to the left descending coronary artery, implying that ablation could result in coronary injury. In addition, the area of earliest local activation is in an area of >4mm fat implying that ablation is likely to be unsuccessful. For these reasons no ablation attempt was made.
G. Fluoroscopy images (Right anterior oblique (RAO) and left anterior oblique (LAO) views; the ablation catheter is located epicardially at the earliest LAT site (MAP), reference catheter in the GCV. Contrast injection in the left coronary artery (LAD) confirmed that the target site for ablation is located adjacent to the left descending coronary artery.

systems enable mapping of the ventricular activation in a single beat.[39-41] Non contact mapping may be able to identify the VT exit site in >90% of VTs and some diastolic activity in two-thirds of VTs.[40, 41]

However, a complete diastolic pathway could only be identified in 21% of patients in one study.[41]

Intramural and Epicardial Circuits

Although parts of scar-related reentry circuits are usually located subendocardially, circuits may extend deep into the myocardium. Inability to define an adequate endocardial ablation target where catheter ablation can interrupt the reentry circuit is an important cause for ablation failure. Ablation using open, irrigated tip catheters increases lesion size and may therefore be more effective targeting circuits extending deep into the myocardial wall.[32]

Epicardial ablation

In an important number of patients with scar-related VT RV or left ventricular (LV) endocardial ablation may however be insufficient despite the use of irrigated tip catheters. In these patients part of the reentry circuit may be located at the subepicardium and a transcutaneous epicardial ablation approach should be considered. The necessity of an epicardial ablation may be different according to the underlying disease causing the substrate for VT.[42] The VT surface ECG can be helpful in identifying VT of epicardial origin prior to the procedure. The time needed for the activation wave front to initially traverse the myocardial wall may result in a prolonged initial component of the VT QRS that may be suggestive of an epicardial origin.[43]

Access to the pericardial space can be obtained by a subxyphoid pericardial puncture.[44] If adhesions from prior cardiac surgery or pericarditis limit the access, a surgical approach via a subxyphoid pericardial window may allow at least limited pericardial mapping and ablation.[31, 42]

Epicardial substrate and VT mapping approaches are similar to those employed during endocardial mapping.[44, 45] Epicardial fat however can limit the feasibility of voltage, pace

and entrainment mapping due to the local reduction of the bipolar amplitude and a higher stimulation threshold or no capture of the myocardium covered by fat. In addition, epicardial fat (>5mm) can prevent effective ablation lesion formation in the underlying myocardium.[46, 47] (Figure 3) The real time integration of CT derived coronary anatomy and fat distribution to aid RFCA is further studied in **chapter 6**. RFCA in the vicinity of coronary arteries or the phrenic nerve should be avoided. Coronary arteries may be visualised by coronary angiogram or by integration of pre-acquired multislice CT imaging; a distance of >5mm between the ablation catheter and the coronary artery during RF delivery is recommended.[2, 46, 48](Figure 2 and 3) The course of the phrenic nerve traversing the lateral LV pericardium can be identified by diaphragmatic stimulation during pacing.[49]

The results of epicardial ablation after failed endocardial ablation in selected patients is encouraging; however data are derived from experienced centers and may not be applicable to less experienced operators.[2]

Substrate imaging

Most of 3-dimensional electroanatomical mapping systems allow for the integration of pre-acquired cardiac images with electroanatomical voltagemaps. Currently, different imaging modalities are used to facilitate substrate mapping and ablation. Integration with pre-acquired Multislice computed tomography (MSCT) images can facilitate real-time visualization of the proximal coronary arteries and the distribution of epicardial fat during epicardial mapping and ablation.[48, 50] (Figure 2 and 3)

Information derived from imaging modalities like positron emission tomography (PET) CT and contrast enhanced magnetic resonance imaging (CE-MRI) that provide not only anatomical data but potential information on VT substrate may be of complementary value before and during ablation procedures.

PET can detect non-viable myocardial scar and the combination with CT may accurately delineate location and extend of scar. The integration of PET/CT derived data with electroanatomical mapping has shown to be feasible and accurate. Potential advantages of these techniques are limitation of procedure and fluoroscopy times, the identification of false positive low voltage areas, due to poor catheter contact, and perhaps the identification of viable channels through the scar.[51] However, the substrate information provided by PET represents local glucose metabolism and does not visualize fibrosis. Furthermore, despite the high spatial resolution of CT the resolution of PET is relatively poor thereby limiting the visualization of smaller viable channels within the scar.

CE-MRI allows for the visualisation of the three-dimensional geometry of myocardial fibrosis and is the gold standard for the detection of subendocardial and non-transmural scar.[52, 53] In patients with non ischemic cardiomyopathy (NICM) CE-MRI can sensitively detect intramural and epicardial scars, which might help to choose the appropriate mapping strategy (endocardial, epicardial or combined).[54-56] (Figure 2B) In addition, CE-MRI

can characterize scar heterogeneity based on signal intensity (SI) the extend of which has been associated with spontaneous VT.[57] Furthermore, animal studies have shown that the detailed scar geometry as assessed by in vitro CE-MRI can predict the location of VT reentry circuits.[19, 58]

Real time integration of CE-MRI derived scar information with electroanatomical mapping may allow for visualisation of intramural or epicardial scars and scar characteristics during the procedure and facilitate mapping and catheterablation.[54, 55, 59] (Figure 2A) (This topic is further studied in **chapter 5**)

In the process of merging imaging derived data sets with electroanatomical maps anatomical landmarks are of key importance. Several studies have used the combination of the LV apex, mitral annulus and the aorta for registration.[51, 54, 55, 59] Others have used the ostium of the left main coronary artery located by contrast injection which has the potential to preclude rotation errors.[48, 55] (Figures 2 and 3)

Whether integration of CE-MRI or PET/CT derived information with electroanatomical mapping during ablation procedures translates in to improved outcome needs further evaluation.

Ablation of Focal VT

The activation wavefront of focal arrhythmias spreads radially from the source to depolarize the ventricles creating monomorphic VT or premature ventricular contractions (PVC).

Most focal VA are hemodynamically well tolerated allowing for point by point mapping and evaluation of the recorded local unipolar and bipolar EGM. Unipolar EGMs provide information about the direction of the activation wavefront: an initial positive deflection of the unipolar EGM indicates propagation towards the catheter and has a high negative predictive value for a successful ablation site in focal VA. As the wavefront reaches the electrode and propagates away, the deflection turns negative. When the catheter is located at the focal source the wavefront propagates away producing a monophasic QS configuration.(Figure 4) However, unipolar EGMs provide information about a relatively large area and contain important far field signals. In contrast, in bipolar EGMs the far field signal is subtracted out thereby providing information about the local electrical activity, but do not contain information about the direction of the wavefront. Currently, most ablation procedures for focal arrhythmias are guided by local activation time defined by the initial peak of the bipolar EGM or the rapid negative deflection of the unipolar EGM and in addition by an unipolar QS configuration.[60] (Figure 4)Targeting the arrhythmia focus based on local activation time is successful in >85% of patients.[61]

However, additional mapping criteria that can increase mapping resolution may be helpful to enhance effectiveness and limit the number of required radiofrequency lesions. Reversed polarity of adjacent bipolar EGMs has shown to be useful in ablation of atrial

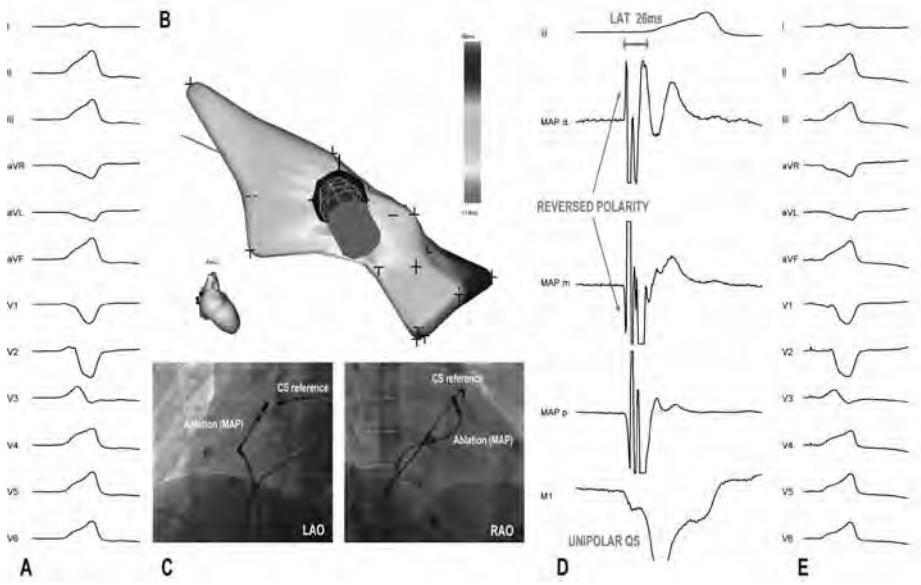


Figure 4. Mapping criteria for focal idiopathic ventricular arrhythmias (for figure in color see page: 254)

Example of a patient presenting with frequent symptomatic premature ventricular contractions (PVCs) successfully ablated from the right ventricular outflow tract (RVOT).

A. 12-lead ECG of the PVC QRS. B. Limited activation map or the RVOT (local activation time (LAT) color coded according to the colorbar, reference R-peak of surface ECG lead II)

C. Fluoroscopy images showing the left anterior oblique (LAO) and right anterior oblique (RAO) views. The ablation catheter is located at the successful ablation site (MAP) and the reference catheter in the CS/GCV.

D. Intracardiac signals at the successful site show (1) LAT of 26ms prior to the PVC QRS onset, (2) the presence of reversed polarity of bipolar adjacent electrograms recorded from the distal and mid electrode pair of the mapping catheter and (3) an unipolar QS configuration.

E. Good pace-match of the PVC QRS with the paced QRS at this site.

fibrillation, **chapter 3** further studies the use of this mapping criterion for idiopathic RVOT VA.[62] (Figure 4)

When mapping during arrhythmia is not feasible due to infrequent occurrence of the arrhythmia pacemapping may be an alternative mapping strategy. Pacemapping compares the 12-lead surface ECG QRS morphology while pacing at a particular site to the morphology of the spontaneous arrhythmia. A good match or 'pacemap' however might have an inferior mapping resolution as compared to mapping of local activation time.[63]

Idiopathic VA usually originate from the ventricular outflowtract region that includes a number of anatomical structures confined to a limited 3-dimensional space. Prior to the ablation procedure the surface ECG QRS morphology may already indicate the site of origin.[22, 43, 64] In > 80%of idiopathic VT the RVOT is the site of origin. However, focal VT can also

originate from the pulmonary artery, the parahisian region, the left ventricular outflow tract (LVOT), the mitral annulus, aortic sinuses of Valsalva and the epicardium (in particular in the proximity of the venous system) requiring a transvenous or trans-pericardial approach.[43]

In addition, VA arising from the papillary muscle or the Purkinjesystem are described. Ablation of PVC's originating form the purkinje system may be effectively abolished by targeting sharp purkinje potentials preceding the local EGM during arrhythmia and local activation during SR.[11, 65]

New technologies

The reason for VA ablation failure and recurrence after ablation is often unclear. One important cause for may be insufficient lesion formation due to poor catheter contact, which might be improved by the use of real time ablation tip contact force measurement.[66] Effective ablation of deep septal reentry circuits or intramural circuits and focal sources that are not abolished from the endo- or epicardium may require deeper ablation lesions. In animal studies enhancement of ablation lesions was demonstrated by using bipolar ablation between two catheters on either side of the interventricular septum or by the use of intramural needle ablation.[67, 68]

Specific Substrates

Ischemic Cardiomyopathy

The incidence of VT in patients late after myocardial infarction (MI) is 1-2%, often occurring after an interval of several years.[2] Most research on VT reentry circuits and catheter ablation of VT was performed in animal models of MI and in patients after MI.

Substrate

The substrate of VT after MI is determined by the geometry of myocardial fibrosis which is influenced by the extent of irreversible injury and surviving myocyte bundles. During MI the injury develops as a wave front beginning in the subendocardial myocardium progressing towards the subepicardium.[69] Scar size and geometry are among others determined by the duration of coronary artery occlusion. Timely reperfusion of the infarct related artery terminates the wave front of necrosis resulting in non-transmural necrosis whereas late reperfusion or permanent coronary occlusion may result in a uniform transmural necrosis.[70] Infarct size is also influenced by collateral perfusion during the acute MI[71], which may be present in variable degrees in humans. The finding that in post MI patients the endocardial scar area as defined by voltagemapping is generally larger than the epicardial scar[47] is consistent with the ´wave front´ theory.

Much of our understanding of the VT substrate after MI is based first on animal models of a chronically occluded coronary artery which typically results in a dense scar with only a small scar borderzone; and secondly on interaoperative mapping studies in post-MI patients with a chronically occluded artery and typically aneurism formation. However, currently early reperfusion strategies have become the standard treatment of acute MI. Whether early reperfusion affects electroanatomical scars and impacts late VT characteristics is studied in **chapter 4 and 9**.[72]

Outcome

Early single-center studies reported acute ablation success rates of up to 90% abolishing the targeted or clinical VT. Recurrence rates were 26-37 % over a follow-up of 34-41 months.[73, 74] In these studies only selected patients with drug refractory, monomorphic, hemodynamically tolerated and reproducibly inducible VTs were included and mapping and ablation was performed using standard RF catheters. Due to the formation of larger and deeper lesions cooled or irrigated RF ablation has proved to be more effective for terminating scar-related VT compared with standard RF and is now preferred for ablation of scar related VT. In the first multicenter study, which evaluated the efficacy and safety of irrigated tip catheter ablation only stable VTs were targeted in 146 patients; all mappable VT's were successfully ablated in 75% of patients. The 1-year recurrence rate was 56%; however a major reduction of VT frequency was observed in most patients. Importantly in 40% of patients fast VTs (<300ms) could be induced that were not targeted.[75]

The high incidence of VT unstable for mapping during ongoing tachycardia has lead to the development of substrate based ablation approaches. In small single-center studies including 9-40 post MI patients all inducible VTs were treated by using additional substrate based criteria to identify ablation target areas. In these series linear RF lesions were applied. In 45-47% of patients no monomorphic VT was inducible after the procedure. The recurrence rate was 25-38% during 8- 10 months follow-up and was higher if VT was still inducible after the procedure or if a VT isthmus could not be identified.[32, 34]

The current status and outcome of VT-ablation in post MI patients is probably best reflected by two recently conducted multi-center trails. The Multicenter Thermocool Ventricular Tachycardia Ablation Trail reported on 231 patientes from 18 centers and the Euro-VT-study on 63 patients from 8 centers.[25, 76] Both trails included patients with recurrent or incessant VT for ablation with irrigated open tip catheters using substrate and entrainment mapping facilitated by a 3-D electroanatomical mapping system. The mean number of inducible VTs was 3±2 per patient and unmappable VTs were present in 69 and 63% of patients.[25, 76]

In the Thermocool study ablation abolished at least one VT in 81% and all VTs in 49% of patients. During a follow-up period of 6 months 51% of patients experienced a recurrent VT. However, the frequency of VT episodes was reduced by ≥75% in 67% of patients. The periprocedural mortality rate was 3%, mainly attributable to uncontrollable arrhythmia.[25]

In the Euro-VT study ablation was acutely successful in 81% of patients. During 12 months follow-up 37% of successfully ablated and 49% of all patients experienced a VT recurrence. One patient experienced a major complication in this study.[76]

In a subgroup of patients presenting with incessant VT or VT storm catheter ablation can be life saving. Acute termination of VT can be achieved in 89% of patients, with a VT recurrence rate of 34% in 22 months as reported by Carbucicchio et al.[77]

An epicardial ablation approach to control recurrent VT seems to be less frequently needed in post MI patients as compared to patients with NICM. Surgical mapping studies have demonstrated that only a minority of VT reentry circuits was located in the subepicardium, in particular in patients after inferior MI.[20] In a large observational study epicardial ablation was performed in only 7% of 278 ablation procedures for post MI VT.[42] However, a significant number of these patients has undergone coronary artery bypass graft (CABG) surgery in the past which has perhaps restricted the epicardial ablation approach.

Early ablation for VT

Recent studies indicate that there might be a role of early catheter ablation after a first episode of VT in post-MI patients concomitant with ICD implantation.

The Substrate Mapping and Ablation in Sinus Rhythm to Halt Ventricular Tachycardia (SMASH-VT) trail included 128 post MI patients with a planned or recent ICD implantation for secondary prevention for hemodynamically untolerated VT, syncope with inducible VT during EP study or VF. Patients were randomized to implantation of ICD alone or ICD implantation with adjunctive catheter ablation of VT using a substrate based approach.[6] During 22.5 months follow-up 12% of patients in the ablation group and 33% of patients in the control group experienced at least one appropriate ICD therapy, a reduction of 65%. Catheter ablation led to a 73% reduction in ICD shocks. Of interest, there was a trend towards a reduced mortality in the ablation group versus the control group (9% vs. 17%).[6]

In the multicenter Ventricular Tachycardia Ablation in Addition to Implantable Defibrillators in Coronary Heart Disesase (VTACH) trail 107 post MI patients presenting with stable VT and reduced LV ejection fraction were randomized to ICD alone or ICD with adjunctive catheter ablation. Mean follow-up was 22.5 months. The median time to first episode of VT or VF was significantly prolonged in the ablation group. The median number of appropriate ICD therapies was reduced by 93% per patient per year.[7]

No procedure related death was reported in both studies. Non-fatal, procedure related complications occurred in 4.7% and 3.8% of patients, respectively. [6, 7] Based on these findings an early use of catheter ablation may be considered in selected patients who receive and ICD as alternative to drug therapy, provided that the procedure can be performed safely.

A recent meta-analysis including 5 studies with a total of 457 participants, 58% treated with adjunctive catheter ablation, showed a 35% reduction in the number of patients with VT recurrence after adjunctive catheter ablation during 6 - 22.5 months of follow-up. No

significant difference in mortality was observed.[78] Further controlled trails with longer follow-up are warranted to evaluate the effect of early catheter ablation on mortality.

Substrate in Dilated Cardiomyopathy.

Even though uncommon, VT also occurs in patients with DCM. The mechanism of VT in DCM is scar-related reentry in 80% of patients, with the remainder being due to bundle branch reentry or a focal origin.[31] At necropsy only 14% of patients with DCM have grossly visible left ventricular scars, in the majority of patients however interstitial or replacement fibrosis is found at histological evaluation.[79] A CE-MRI study performed in patents with clinically defined DCM reported on subendocardial scar in 13% and midwall scar in 28% of patients. No delayed enhancement at all was found in 59% perhaps because of the inability of CE-MRI to detect microscopic interstitial fibrosis.[56] Of interest, the presence of scar detected with CE-MRI and increasing scar thickness have been associated with VT inducibility in DCM patients. Accordingly evidence of scar is often present in patients who undergo catheter ablation for VT. Areas of endocardial abnormal EGMs as depicted by voltagemapping are relatively small, commonly <25% of the endocardial surface.[80] In patients who underwent epicardial voltage mapping the electroanatomical scar tends to be larger on the epicardial surface.[31, 45, 81] Scar areas are commonly found at the basal LV with a predilection at the inferolateral LV wall both endo- and epicardially.[31, 45, 80, 81] Epicardial EGMs in low voltage areas are characterised by low amplitude (<1.0mV) and long duration (>80ms).[45] Late potentials, that likely reflect areas of slow conduction in a fixed substrate, however may be observed less frequently in DCM patients than in post MI patients.[81](Figure 2C) The latter finding may suggest that in DCM patients' functional block, rather than isthmuses bordered by fixed lines of block are important for the occurrence of reentry circuits. This is in line with findings from de Bakker et al. who found short and long strands of fibrous tissue running parallel to the myocardial fiber orientation in human hearts after transplantation for DCM. In these samples activation delay and EGM fractionation was caused by discontinuous and circuitious conduction through zones of patchy fibrosis, which plays an important role for non-uniform anisotropy.[82]

Catheter ablation

Data on catheter ablation for VT in DCM are derived from small single-center studies performed in selected groups of patients. The success of endocardial ablation may be disappointing; acute complete success rates of 27% and 33% have been reported, with a VT recurrence rate of 58% and 47%, respectively in two different series.[31, 80] However, after endocardial ablation failure an epicardial approach might be effective. Eighteen of 22 patients who underwent endo- and epicardial catheter ablation after a previous endocardial ablation failure were rendered non-inducible at the end of the procedure. During 18 months follow-up 71% of patients were free of VT recurrence.[45]

RV scar related VT

Patients with scar-related right ventricular tachycardia (VT) are at risk for VT recurrence and sudden cardiac death. An important cause of RV scar is arrhythmogenic right ventricular cardiomyopathy/dysplasia (ARVC/D), a progressive and most likely genetic disease. However, in more than 50% of affected patients no familial occurrence or disease-specific genetic mutations[83] are found; therefore, diagnosis of ARVC/D is based on criteria proposed by a generally accepted consensus report by an international task force (TF).[84] ARVC/D is histologically characterized by loss of right ventricular myocytes, which may be due to impaired function of the cell adherence complex in combination with mechanical stress, resulting in myocardial cell death with replacement by fibro-fatty tissue. This process begins in the subepicardium and progresses towards the subendocardium.[83, 85]

Although predominantly found in the RV, dysplasia can also involve the LV.[85] Areas of scar as identified by electroanatomical voltage mapping are commonly localized adjacent to the lateral tricuspid annulus, the RVOT, and RV apex.[86, 87] Macroreentrant circuits tend to be clustered around the tricuspid annulus and RVOT and focal activation patterns, perhaps the endocardial breakthrough of an epicardial reentry circuit, have been observed at the RV free wall.[87]

Other diseases like post inflammatory myopathy or sarcoidosis can mimic ARVC/D. [88] In sarcoidosis active granulomatous inflammation can be replaced by fibrosis thereby providing the substrate for reentrant VT. Catheter mapping may reveal low voltage areas in both the RV and LV.[88]

Subtle or early forms of RV fibrosis as substrate for RV tachycardia may only be detected by electroanatomical mapping which may have important prognostic and therapeutic implications by excluding an idiopathic VA. [89, 90]

Outcome

Prior to the widespread use of substrate based ablation techniques two series reported acute ablation success rates, defined as non-inducibility at the end of the procedure, of 46 and 45% using conventional mapping techniques. The two year VT recurrence rate was 71 and 41% respectively.[90, 91] The concept of substrate mapping and ablation including the application of linear lesions to encircle or connect scars facilitated by 3-dimensional mapping systems has evolved over the last decennium. Three more recently conducted studies using a substrate based approach reported much higher acute success rates (74-88%).[86, 87, 92] Long term success rates varied between 53, 76 and 89% of patients who were free of VT recurrence after 36, 26 and 27 months, respectively.

Results of RFCA of scar-related VT due to sarcoidosis seem to be disappointing. In one small series reporting on 8 patients VT remained inducible at the end of the ablation procedure in 7(88%) patients and during follow-up 6(77%) patients experienced recurrent VT.[88]

Both ARVC/D and sarcoidosis are progressive diseases and VT recurrence rates may also be due to further development of substrate over time.

However, similar to DCM patients with ARVC/D have more extensive epicardial scar. A combined endo- and epicardial approach after prior endocardial ablation can be highly effective in abolishing VTs in selected patients and might improve long-term results. Eighty-five percent of patients were non-inducible for VT after ablation and 77% were free of recurrence during 18 months follow-up in one series.[93]

Factors influencing outcome of scar-related VT from the RV including subtle scars only detected by electroanatomical mapping is further evaluated in **chapter 8**.

VT after cardiac surgery

Catheter ablation can be an effective treatment option for scar-related VT occurring after surgical intervention. Surgical scars or patch material may contribute to the substrate for VT late after repair of congenitial heart disease, valve surgery or ventricular reconstructive surgery for heart failure.

Small series of patients who underwent RFCA for recurrent VT after corrected congenital heart disease (CHD), the majority after repair of tetralogy of Fallot have been reported.[17, 94] Ablation guided by mapping during VT can be successful in selected patients who present with stable VT with recurrence rates of up to 40% in 3.8 years.[94] However, the majority of patients after repair of CHD has fast VTs that require a substrate based ablation approach. Electroanatomical mapping performed during SR can identify unexcitable surgical scars, patch material and anatomical boundaries such as valve annuli that anatomically define the critical isthmus for VT. Transecting these isthmuses with linear RFCA lesions resulted in 91% freedom of VT recurrence after a follow-up of 30 months in one series.[17]

VT after aortic or mitral valve surgery in the absence of prior myocardial infarction is rare. In a small series of 20 patients 14(70%) had VT due to scar-related reentry, the majority having scars adjacent to the replaced valve annulus. Ablation abolished 98% of inducible VT and 11(55%) patients remained free of recurrence during a 2.1 year follow-up.[95]

Catheter ablation of VT occurring after surgical ventricular restoration for heart failure in ischemic cardiomyopathy is studied in **chapter 10**.

Idiopathic VT

Despite a good prognosis idiopathic VA can cause severe symptoms including palpitations, chest pain, syncope and fatigue.[22] Catheter ablation for idiopathic VA is associated with a high success rate, 76-100% of patients are without arrhythmia at the end of the procedure and the recurrence rate is very low.[22, 43, 60, 61, 63]

Perhaps due to chronic hemodynamical effects frequent premature ventricular contractions (PVC) may affect the ventricular function. One study following patients with frequent PVCs and normal cardiac function for 4 years showed a modest but significant decline in LV

ejection fraction in 5% of patients.[10] Single center studies have reported on mild to severe reduced LV ejection fraction and increased ventricular dimensions associated with frequent PVCs in selected patients.[12] These detrimental effects of PVCs seem to be reversible after suppression of PVCs by medication or successful catheter ablation.[12] In a recent observational study of 174 patients referred for catheter ablation of PVCs the only independent predictor for LV dysfunction at presentation was PVC burden. The best cut-off was 24% PVCs in 24 hours but some patients with >10% PVCs may also be at risk.[97] However, the clinical relevance of frequent PVCs in asymptomatic patients without LV dysfunction in the unselected general population is not fully understood and a benefit of "preventive" RFCA in these patients has not been proven. Whether subclinical LV dysfunction undetected by normal imaging techniques may be already present in patients with frequent PVCs as compared to normal control patients is studied in **chapter 7**.[96]

It has been demonstrated that the short coupled variant of PVCs originating from the purkinje system or from the outflow tracts can induce episodes of polymorphic VT and VF. These PVCS can be targeted for ablation to prevent VA episodes.[11] Longer coupling intervals in benign RVOT PVC/VT as compared to those associated with malignant polymorphic VT and idiopathic VF have been reported.[98] However, in the largest series including 16 patients with polymorphic VT or VF originating from the RV outflow tract, the frequency of isolated PVCs and their coupling intervals were not different to those observed in 85 patients with idiopathic monomorphic RV tachycardia. Ablation targeting the initiating PVCs prevented recurrence of VF during a follow-up of 54 months.[99]

Indications

Evidence for a benefit of catheter ablation for the treatment of VA is mainly based on uncontrolled trails, single center experience and experts opinion. For patient with structural heart disease the current guidelines of the American College of Cardiology(ACC)/American Heart Association(AHA)/European Society of Cardiology(ESC)[100] state that catheter ablation can be beneficial as a palliative and adjunctive therapy to ICD implantation in patients who receive multiple ICD shocks due to drug refractory sustained VT (Class I, level of evidence C), for incessant VT after failed drug therapy (Class IIa) and in patients with bundle branch reentry (Class I, C). Ablation can be useful in patients with otherwise low risk of SCD, like patients without structural heart disease with idiopathic VA, who present with sustained VT (Class I), symptomatic nonsustained VT (Class IIa) or symptomatic PVCs (Class IIa) for which drug therapy is ineffective, not tolerated or not desired. For patients with prior MI, but relatively preserved left ventricular (LV) ejection fraction (>40%), curative ablation may be considered in lieu of ICD therapy (Class IIb). In patients with congenital heart disease presenting with monomorphic VT ablation is even recommended prior to ICD therapy (Class

I, C). Ablation of ectopic foci that trigger recurrent polymorphic VT is an acceptable strategy for controlling electrical storm (Class IIb).[100]

In the recently published expert consensus document the European Heart Rhythm Association (ERHA) and the Heart Rhythm Society (HRS) recommend to consider ablation for recurrent monomorphic VT in post MI patients with an LVEF >30% as alternative to amiodarone, in post MI patients with LV ejection fraction >35%, even if they have not failed drug therapy and in patients with VA presumed to cause ventricular dysfunction.[2]

Catheter ablation is contra-indicated for NSVT/PVC that are asymptomatic and not suspected to cause ventricular dysfunction and for VT due to transient and reversible causes. Endocardial catheter ablation is furthermore contraindicated in the presence of a mobile ventricular thrombus for the risk of embolization.[2]

Individual patient characteristics, available facilities and technical expertise may determine the possible risks and benefits of the ablation procedure and should therefore be taken into consideration when selecting patients for catheter ablation of VT.

Aim and outline of the thesis

The growing role of catheter ablation for ventricular arrhythmias in patients with and without structural heart disease reflects the progress in this field over the last decades. The aim of the current thesis was to study the determinants for the substrate causing VT, the VT characteristics and outcome specifically after invasive treatment and to develop techniques that facilitate and thereby potentially improve outcome after catheter ablation.

In **part I** determinants of the VA substrate and techniques for substrate identification are studied in patients referred for catheter ablation of VA.

In patients presenting with VA the discrimination between scar-related reentry and an idiopathic focus as underlying mechanism is guiding for further evaluation and treatment. **Chapter 2** studies the diagnostic value of the VA 12-lead surface ECG to determine the presence or absence of myocardial scar underlying the arrhythmia. In this chapter a simple stepwise algorithm based on surface ECG characteristics is developed to aid clinical decision making in patients presenting with VA. Even though non scar-related idiopathic VA is generally considered benign, catheter ablation can be indicated in symptomatic patients. During ablation in otherwise healthy myocardium it is desirable to limit the number of lesions to the minimum. In **chapter 3** catheter mapping is used to evaluate reversed polarity as an additional mapping criterion to improve the determination of successful ablation sites for idiopathic RVOT VA.

Post MI scar is the substrate in the majority of patients presenting with clinically significant scar related VT. Early reperfusion as standard treatment of the acute MI has been

developed over the last decennia. **Chapter 4** describes the affect of early reperfusion on the substrate of VT as determined by electroanatomical mapping and histology and on VT characteristics. Substrate based methods for catheter ablation of VT, rely on delineation of scar by electroanatomical catheter mapping. CE-MRI can be used to visualize the three-dimensional geometry of myocardial fibrosis and is the gold standard for the detection of nontransmural scar. **Chapter 5** focuses on the feasibility of integrating these two modalities to facilitate catheter ablation and evaluates additional value of the use of CE-MRI in a head to head comparison.

Over the last years percutaneous epicardial approach in selected patients has rendered many VT previously considered 'unmappable' approachable for ablation. The determination of VT substrate by electroanatomical mapping and catheter ablation is limited by the presence of epicardial fat and coronary arteries. In **chapter 6** the use of CT derived information to determine fat distribution and coronary artery anatomy during epicardial catheter ablation procedures is studied.

After determination of VA substrate, catheter ablation has the potential to abolish the substrate, reentry circuit or arrhythmogenic focus, for VA. In addition differences in VA substrate between patients may impact clinical outcome. The focus of **Part II** is on the outcome in different ventricular tachycardia substrates.

Non scar-related VA are generally considered benign and in the majority of patients with frequent VA the LV ejection fraction is normal. Reversible deterioration of LV ejection fraction due to, perhaps hemodynamical effects, of frequent PVCs have been described in a limited number of patients. **Chapter 7** assesses the effect of non scar related frequent PVCs on RV and LV function in patients with preserved LVEF. In addition, the effect of successful RFCA of frequent PVCs on LV and RV function is evaluated.

In contrast to non scar-related VA, patients with scar-related VA may be at risk for sudden cardiac death. **Chapter 8** studies determinants of outcome in scar-related VA originating from the right ventricle. Baseline characteristics, diagnosis and acute ablation success are related to VT recurrence during follow-up.

Chapter 9 aims to extend the findings demonstrated in chapter 4 in a larger population of post MI patients who underwent electrophysiological evaluation prior to implantation of an ICD. The effect of early reperfusion during acute MI on inducibility of VT, characteristics of VT and VT recurrence during long-term follow-up is evaluated.

Chapter 10 addresses the substrate, VT characteristics, catheter ablation and VT recurrence in the, until now underexposed, subgroup of patients who present with VT after surgical ventricular restoration for heartfailure after MI.

Reference list

(1) COUCH OA, Jr. Cardiac aneurysm with ventricular tachycardia and subsequent excision of aneurysm; case report. Circulation 1959; 20:251-3.

(2) Aliot EM, Stevenson WG, Almendral-Garrote JM et al. EHRA/HRS Expert Consensus on Catheter Ablation of Ventricular Arrhythmias: developed in a partnership with the European Heart Rhythm Association (EHRA), a Registered Branch of the European Society of Cardiology (ESC), and the Heart Rhythm Society (HRS); in collaboration with the American College of Cardiology (ACC) and the American Heart Association (AHA). Europace 2009; 11:771-817.

(3) van der Burg AE, Bax JJ, Boersma E et al. Standardized screening and treatment of patients with life-threatening arrhythmias: the Leiden out-of-hospital cardiac arrest evaluation study. Heart Rhythm 2004; 1:51-7.

(4) Moss AJ, Zareba W, Hall WJ et al. Prophylactic implantation of a defibrillator in patients with myocardial infarction and reduced ejection fraction. N Engl J Med 2002; 346:877-83.

(5) Bardy GH, Lee KL, Mark DB et al. Amiodarone or an implantable cardioverter-defibrillator for congestive heart failure. N Engl J Med 2005; 352:225-37.

(6) Reddy VY, Reynolds MR, Neuzil P et al. Prophylactic catheter ablation for the prevention of defibrillator therapy. N Engl J Med 2007; 357:2657-65.

(7) Kuck KH, Schaumann A, Eckardt L et al. Catheter ablation of stable ventricular tachycardia before defibrillator implantation in patients with coronary heart disease (VTACH): a multicentre randomised controlled trial. Lancet 2010; 375:31-40.

(8) Schron EB, Exner DV, Yao Q et al. Quality of life in the antiarrhythmics versus implantable defibrillators trial: impact of therapy and influence of adverse symptoms and defibrillator shocks. Circulation 2002; 105:589-94.

(9) Poole JE, Johnson GW, Hellkamp AS et al. Prognostic importance of defibrillator shocks in patients with heart failure. N Engl J Med 2008; 359:1009-17.

(10) Niwano S, Wakisaka Y, Niwano H et al. Prognostic significance of frequent premature ventricular contractions originating from the ventricular outflow tract in patients with normal left ventricular function. Heart 2009; 95:1230-7.

(11) Haissaguerre M, Shoda M, Jais P et al. Mapping and ablation of idiopathic ventricular fibrillation. Circulation 2002; 106:962-7.

(12) Bogun F, Crawford T, Reich S et al. Radiofrequency ablation of frequent, idiopathic premature ventricular complexes: comparison with a control group without intervention. Heart Rhythm 2007; 4:863-7.

(13) De Bakker JM, van Capelle FJ, Janse MJ et al. Reentry as a cause of ventricular tachycardia in patients with chronic ischemic heart disease: electrophysiologic and anatomic correlation. Circulation 1988; 77:589-606.

(14) De Bakker JM, van Capelle FJ, Janse MJ et al. Slow conduction in the infarcted human heart. 'Zigzag' course of activation. Circulation 1993; 88:915-26.

(15) Kawara T, Derksen R, de Groot JR et al. Activation delay after premature stimulation in chronically diseased human myocardium relates to the architecture of interstitial fibrosis. Circulation 2001; 104:3069-75.

(16) De Chillou C, Lacroix D, Klug D et al. Isthmus characteristics of reentrant ventricular tachycardia after myocardial infarction. Circulation 2002; 105:726-31.

(17) Zeppenfeld K, Schalij MJ, Bartelings MM et al. Catheter ablation of ventricular tachycardia after repair of congenital heart disease: electroanatomic identification of the critical right ventricular isthmus. Circulation 2007; 116:2241-52.

(18) Segal OR, Chow AW, Peters NS, Davies DW. Mechanisms that initiate ventricular tachycardia in the infarcted human heart. Heart Rhythm 2010; 7:57-64.

(19) Ciaccio EJ, Ashikaga H, Kaba RA et al. Model of reentrant ventricular tachycardia based on infarct border zone geometry predicts reentrant circuit features as determined by activation mapping. Heart Rhythm 2007; 4:1034-45.
(20) Kaltenbrunner W, Cardinal R, Dubuc M et al. Epicardial and endocardial mapping of ventricular tachycardia in patients with myocardial infarction. Is the origin of the tachycardia always subendocardially localized? Circulation 1991; 84:1058-71.
(21) Lerman BB, Stein K, Engelstein ED et al. Mechanism of repetitive monomorphic ventricular tachycardia. Circulation 1995; 92:421-9.
(22) Iwai S, Cantillon DJ, Kim RJ et al. Right and left ventricular outflow tract tachycardias: evidence for a common electrophysiologic mechanism. J Cardiovasc Electrophysiol 2006; 17:1052-8.
(23) Lopera G, Stevenson WG, Soejima K et al. Identification and ablation of three types of ventricular tachycardia involving the his-purkinje system in patients with heart disease. J Cardiovasc Electrophysiol 2004; 15:52-8.

(24) Okumura K, Matsuyama K, Miyagi H, Tsuchiya T, Yasue H. Entrainment of idiopathic ventricular tachycardia of left ventricular origin with evidence for reentry with an area of slow conduction and effect of verapamil. Am J Cardiol 1988; 62:727-32.
(25) Stevenson WG, Wilber DJ, Natale A et al. Irrigated radiofrequency catheter ablation guided by electroanatomic mapping for recurrent ventricular tachycardia after myocardial infarction: the multicenter thermocool ventricular tachycardia ablation trial. Circulation 2008; 118:2773-82.
(26) El-Shalakany A, Hadjis T, Papageorgiou P et al. Entrainment/mapping criteria for the prediction of termination of ventricular tachycardia by single radiofrequency lesion in patients with coronary artery disease. Circulation 1999; 99:2283-9.
(27) Kocovic DZ, Harada T, Friedman PL, Stevenson WG. Characteristics of electrograms recorded at reentry circuit sites and bystanders during ventricular tachycardia after myocardial infarction. J Am Coll Cardiol 1999; 34:381-8.
(28) Stevenson WG, Khan H, Sager P et al. Identification of reentry circuit sites during catheter mapping and radiofrequency ablation of ventricular tachycardia late after myocardial infarction. Circulation 1993; 88:1647-70.
(29) Bogun F, Bahu M, Knight BP et al. Comparison of effective and ineffective target sites that demonstrate concealed entrainment in patients with coronary artery disease undergoing radiofrequency ablation of ventricular tachycardia. Circulation 1997; 95:183-90.
(30) Stevenson WG, Friedman PL, Sager PT et al. Exploring postinfarction reentrant ventricular tachycardia with entrainment mapping. J Am Coll Cardiol 1997; 29:1180-9.
(31) Soejima K, Stevenson WG, Sapp JL et al. Endocardial and epicardial radiofrequency ablation of ventricular tachycardia associated with dilated cardiomyopathy: the importance of low-voltage scars. J Am Coll Cardiol 2004; 43:1834-42.
(32) Soejima K, Suzuki M, Maisel WH et al. Catheter ablation in patients with multiple and unstable ventricular tachycardias after myocardial infarction: short ablation lines guided by reentry circuit isthmuses and sinus rhythm mapping. Circulation 2001; 104:664-9.
(33) Reddy VY, Wrobleski D, Houghtaling C, Josephson ME, Ruskin JN. Combined epicardial and endocardial electroanatomic mapping in a porcine model of healed myocardial infarction. Circulation 2003; 107:3236-42.
(34) Marchlinski FE, Callans DJ, Gottlieb CD, Zado E. Linear ablation lesions for control of unmappable ventricular tachycardia in patients with ischemic and nonischemic cardiomyopathy. Circulation 2000; 101:1288-96.
(35) Zeppenfeld K, Kies P, Wijffels MC et al. Identification of successful catheter ablation sites in patients with ventricular tachycardia based on electrogram characteristics during sinus rhythm. Heart Rhythm 2005; 2:940-50.

(36) Arenal A, Glez-Torrecilla E, Ortiz M et al. Ablation of electrograms with an isolated, delayed component as treatment of unmappable monomorphic ventricular tachycardias in patients with structural heart disease. J Am Coll Cardiol 2003; 41:81-92.
(37) Arenal A, del CS, Gonzalez-Torrecilla E et al. Tachycardia-related channel in the scar tissue in patients with sustained monomorphic ventricular tachycardias: influence of the voltage scar definition. Circulation 2004; 110:2568-74.
(38) Soejima K, Stevenson WG, Maisel WH, Sapp JL, Epstein LM. Electrically unexcitable scar mapping based on pacing threshold for identification of the reentry circuit isthmus: feasibility for guiding ventricular tachycardia ablation. Circulation 2002; 106:1678-83.
(39) Schalij MJ, van Rugge FP, Siezenga M, van der Velde ET. Endocardial activation mapping of ventricular tachycardia in patients : first application of a 32-site bipolar mapping electrode catheter. Circulation 1998; 98:2168-79.
(40) Della BP, Pappalardo A, Riva S et al. Non-contact mapping to guide catheter ablation of untolerated ventricular tachycardia. Eur Heart J 2002; 23:742-52.
(41) Schilling RJ, Peters NS, Davies DW. Feasibility of a noncontact catheter for endocardial mapping of human ventricular tachycardia. Circulation 1999; 99:2543-52.
(42) Sacher F, Roberts-Thomson K, Maury P et al. Epicardial ventricular tachycardia ablation a multicenter safety study. J Am Coll Cardiol 2010; 55:2366-72.
(43) Daniels DV, Lu YY, Morton JB et al. Idiopathic epicardial left ventricular tachycardia originating remote from the sinus of Valsalva: electrophysiological characteristics, catheter ablation, and identification from the 12-lead electrocardiogram. Circulation 2006; 113:1659-66.
(44) Sosa E, Scanavacca M, d'Avila A, Pilleggi F. A new technique to perform epicardial mapping in the electrophysiology laboratory. J Cardiovasc Electrophysiol 1996; 7:531-6.
(45) Cano O, Hutchinson M, Lin D et al. Electroanatomic substrate and ablation outcome for suspected epicardial ventricular tachycardia in left ventricular nonischemic cardiomyopathy. J Am Coll Cardiol 2009; 54:799-808.
(46) d'Avila A, Gutierrez P, Scanavacca M et al. Effects of radiofrequency pulses delivered in the vicinity of the coronary arteries: implications for nonsurgical transthoracic epicardial catheter ablation to treat ventricular tachycardia. Pacing Clin Electrophysiol 2002; 25:1488-95.
(47) Cesario DA, Vaseghi M, Boyle NG et al. Value of high-density endocardial and epicardial mapping for catheter ablation of hemodynamically unstable ventricular tachycardia. Heart Rhythm 2006; 3:1-10.
(48) Zeppenfeld K, Tops LF, Bax JJ, Schalij MJ. Images in cardiovascular medicine. Epicardial radiofrequency catheter ablation of ventricular tachycardia in the vicinity of coronary arteries is facilitated by fusion of 3-dimensional electroanatomical mapping with multislice computed tomography. Circulation 2006; 114:e51-e52.
(49) Fan R, Cano O, Ho SY et al. Characterization of the phrenic nerve course within the epicardial substrate of patients with nonischemic cardiomyopathy and ventricular tachycardia. Heart Rhythm 2009; 6:59-64.
(50) Desjardins B, Morady F, Bogun F. Effect of epicardial fat on electroanatomical mapping and epicardial catheter ablation. J Am Coll Cardiol 2010; 56:1320-7.
(51) Dickfeld T, Lei P, Dilsizian V et al. Integration of three-dimensional scar maps for ventricular tachycardia ablation with positron emission tomography-computed tomography. JACC Cardiovasc Imaging 2008; 1:73-82.
(52) Kim RJ, Fieno DS, Parrish TB et al. Relationship of MRI delayed contrast enhancement to irreversible injury, infarct age, and contractile function. Circulation 1999; 100:1992-2002.
(53) Wagner A, Mahrholdt H, Holly TA et al. Contrast-enhanced MRI and routine single photon emission computed tomography (SPECT) perfusion imaging for detection of subendocardial myocardial infarcts: an imaging study. Lancet 2003; 361:374-9.

(54) Bogun FM, Desjardins B, Good E et al. Delayed-enhanced magnetic resonance imaging in nonischemic cardiomyopathy: utility for identifying the ventricular arrhythmia substrate. J Am Coll Cardiol 2009; 53:1138-45.
(55) Wijnmaalen AP, van der Geest RJ, van Huls van Taxis CF et al. Head-to-head comparison of contrast-enhanced magnetic resonance imaging and electroanatomical voltage mapping to assess post-infarct scar characteristics in patients with ventricular tachycardias: real-time image integration and reversed registration. Eur Heart J 2011; 32:104-14.
(56) McCrohon JA, Moon JC, Prasad SK et al. Differentiation of heart failure related to dilated cardiomyopathy and coronary artery disease using gadolinium-enhanced cardiovascular magnetic resonance. Circulation 2003; 108:54-9.
(57) Roes SD, Borleffs CJ, van der Geest RJ et al. Infarct tissue heterogeneity assessed with contrast-enhanced MRI predicts spontaneous ventricular arrhythmia in patients with ischemic cardiomyopathy and implantable cardioverter-defibrillator. Circ Cardiovasc Imaging 2009; 2:183-90.
(58) Ashikaga H, Sasano T, Dong J et al. Magnetic resonance-based anatomical analysis of scar-related ventricular tachycardia: implications for catheter ablation. Circ Res 2007; 101:939-47.
(59) Codreanu A, Odille F, Aliot E et al. Electroanatomic characterization of post-infarct scars comparison with 3-dimensional myocardial scar reconstruction based on magnetic resonance imaging. J Am Coll Cardiol 2008; 52:839-42.
(60) Soejima Y, Aonuma K, Iesaka Y, Isobe M. Ventricular unipolar potential in radiofrequency catheter ablation of idiopathic non-reentrant ventricular outflow tachycardia. Jpn Heart J 2004; 45:749-60.
(61) Vestal M, Wen MS, Yeh SJ et al. Electrocardiographic predictors of failure and recurrence in patients with idiopathic right ventricular outflow tract tachycardia and ectopy who underwent radiofrequency catheter ablation. J Electrocardiol 2003; 36:327-32.
(62) van Huls van Taxis CF, Wijnmaalen AP, den Uijl DW et al. Reversed polarity of bipolar electrograms to predict a successful ablation site in focal idiopathic right ventricular outflow tract arrhythmias. Heart Rhythm 2011.
(63) Bogun F, Taj M, Ting M et al. Spatial resolution of pace mapping of idiopathic ventricular tachycardia/ectopy originating in the right ventricular outflow tract. Heart Rhythm 2008; 5:339-44.
(64) Haqqani HM, Morton JB, Kalman JM. Using the 12-lead ECG to localize the origin of atrial and ventricular tachycardias: part 2--ventricular tachycardia. J Cardiovasc Electrophysiol 2009; 20:825-32.
(65) Good E, Desjardins B, Jongnarangsin K et al. Ventricular arrhythmias originating from a papillary muscle in patients without prior infarction: a comparison with fascicular arrhythmias. Heart Rhythm 2008; 5:1530-7.
(66) Yokoyama K, Nakagawa H, Shah DC et al. Novel contact force sensor incorporated in irrigated radiofrequency ablation catheter predicts lesion size and incidence of steam pop and thrombus. Circ Arrhythm Electrophysiol 2008; 1:354-62.
(67) Sivagangabalan G, Barry MA, Huang K et al. Bipolar ablation of the interventricular septum is more efficient at creating a transmural line than sequential unipolar ablation. Pacing Clin Electrophysiol 2010; 33:16-26.
(68) Kovoor P, Daly M, Campbell C et al. Intramural radiofrequency ablation: effects of electrode temperature and length. Pacing Clin Electrophysiol 2004; 27:719-25.
(69) Reimer KA, Lowe JE, Rasmussen MM, Jennings RB. The wavefront phenomenon of ischemic cell death. 1. Myocardial infarct size vs duration of coronary occlusion in dogs. Circulation 1977; 56:786-94.
(70) Miyazaki S, Fujiwara H, Onodera T et al. Quantitative analysis of contraction band and coagulation necrosis after ischemia and reperfusion in the porcine heart. Circulation 1987; 75:1074-82.
(71) Fujiwara Y, Fujiwara H, Matsuda M et al. Reperfusion injury in dog hearts with permanent occlusion of a coronary artery, probably due to reperfusion via collateral vessels. Int J Cardiol 1991; 30:275-84.

(72) Wijnmaalen AP, Schalij MJ, von der Thusen JH, Klautz RJ, Zeppenfeld K. Early reperfusion during acute myocardial infarction affects ventricular tachycardia characteristics and the chronic electroanatomic and histological substrate. Circulation 2010; 121:1887-95.
(73) Borger van der Burg AE, de Groot NM, van Erven L et al. Long-term follow-up after radiofrequency catheter ablation of ventricular tachycardia: a successful approach? J Cardiovasc Electrophysiol 2002; 13:417-23.
(74) Della BP, De Ponti R, Uriarte JA et al. Catheter ablation and antiarrhythmic drugs for haemodynamically tolerated post-infarction ventricular tachycardia; long-term outcome in relation to acute electrophysiological findings. Eur Heart J 2002; 23:414-24.
(75) Calkins H, Epstein A, Packer D et al. Catheter ablation of ventricular tachycardia in patients with structural heart disease using cooled radiofrequency energy: results of a prospective multicenter study. Cooled RF Multi Center Investigators Group. J Am Coll Cardiol 2000; 35:1905-14.
(76) Tanner H, Hindricks G, Volkmer M et al. Catheter ablation of recurrent scar-related ventricular tachycardia using electroanatomical mapping and irrigated ablation technology: results of the prospective multicenter Euro-VT-study. J Cardiovasc Electrophysiol 2010; 21:47-53.
(77) Carbucicchio C, Santamaria M, Trevisi N et al. Catheter ablation for the treatment of electrical storm in patients with implantable cardioverter-defibrillators: short- and long-term outcomes in a prospective single-center study. Circulation 2008; 117:462-9.
(78) Mallidi J, Nadkarni GN, Berger RD, Calkins H, Nazarian S. Meta-Analysis of Catheter Ablation as an Adjunct to Medical Therapy for Treatment of Ventricular Tachycardia in Patients with Structural Heart Disease. Heart Rhythm 2010.
(79) Roberts WC, Siegel RJ, McManus BM. Idiopathic dilated cardiomyopathy: analysis of 152 necropsy patients. Am J Cardiol 1987; 60:1340-55.
(80) Hsia HH, Marchlinski FE. Electrophysiology studies in patients with dilated cardiomyopathies. Card Electrophysiol Rev 2002; 6:472-81.
(81) Nakahara S, Tung R, Ramirez RJ et al. Characterization of the arrhythmogenic substrate in ischemic and nonischemic cardiomyopathy implications for catheter ablation of hemodynamically unstable ventricular tachycardia. J Am Coll Cardiol 2010; 55:2355-65.
(82) De Bakker JM, van Capelle FJ, Janse MJ et al. Fractionated electrograms in dilated cardiomyopathy: origin and relation to abnormal conduction. J Am Coll Cardiol 1996; 27:1071-8.
(83) Sen-Chowdhry S, Syrris P, McKenna WJ. Role of genetic analysis in the management of patients with arrhythmogenic right ventricular dysplasia/cardiomyopathy. J Am Coll Cardiol 2007; 50:1813-21.
(84) Marcus FI, McKenna WJ, Sherrill D et al. Diagnosis of arrhythmogenic right ventricular cardiomyopathy/dysplasia: proposed modification of the Task Force Criteria. Eur Heart J 2010; 31:806-14.
(85) Basso C, Thiene G, Corrado D et al. Arrhythmogenic right ventricular cardiomyopathy. Dysplasia, dystrophy, or myocarditis? Circulation 1996; 94:983-91.
(86) Verma A, Kilicaslan F, Schweikert RA et al. Short- and long-term success of substrate-based mapping and ablation of ventricular tachycardia in arrhythmogenic right ventricular dysplasia. Circulation 2005; 111:3209-16.
(87) Satomi K, Kurita T, Suyama K et al. Catheter ablation of stable and unstable ventricular tachycardias in patients with arrhythmogenic right ventricular dysplasia. J Cardiovasc Electrophysiol 2006; 17:469-76.
(88) Koplan BA, Soejima K, Baughman K, Epstein LM, Stevenson WG. Refractory ventricular tachycardia secondary to cardiac sarcoid: electrophysiologic characteristics, mapping, and ablation. Heart Rhythm 2006; 3:924-9.
(89) Corrado D, Basso C, Leoni L et al. Three-dimensional electroanatomical voltage mapping and histologic evaluation of myocardial substrate in right ventricular outflow tract tachycardia. J Am Coll Cardiol 2008; 51:731-9.

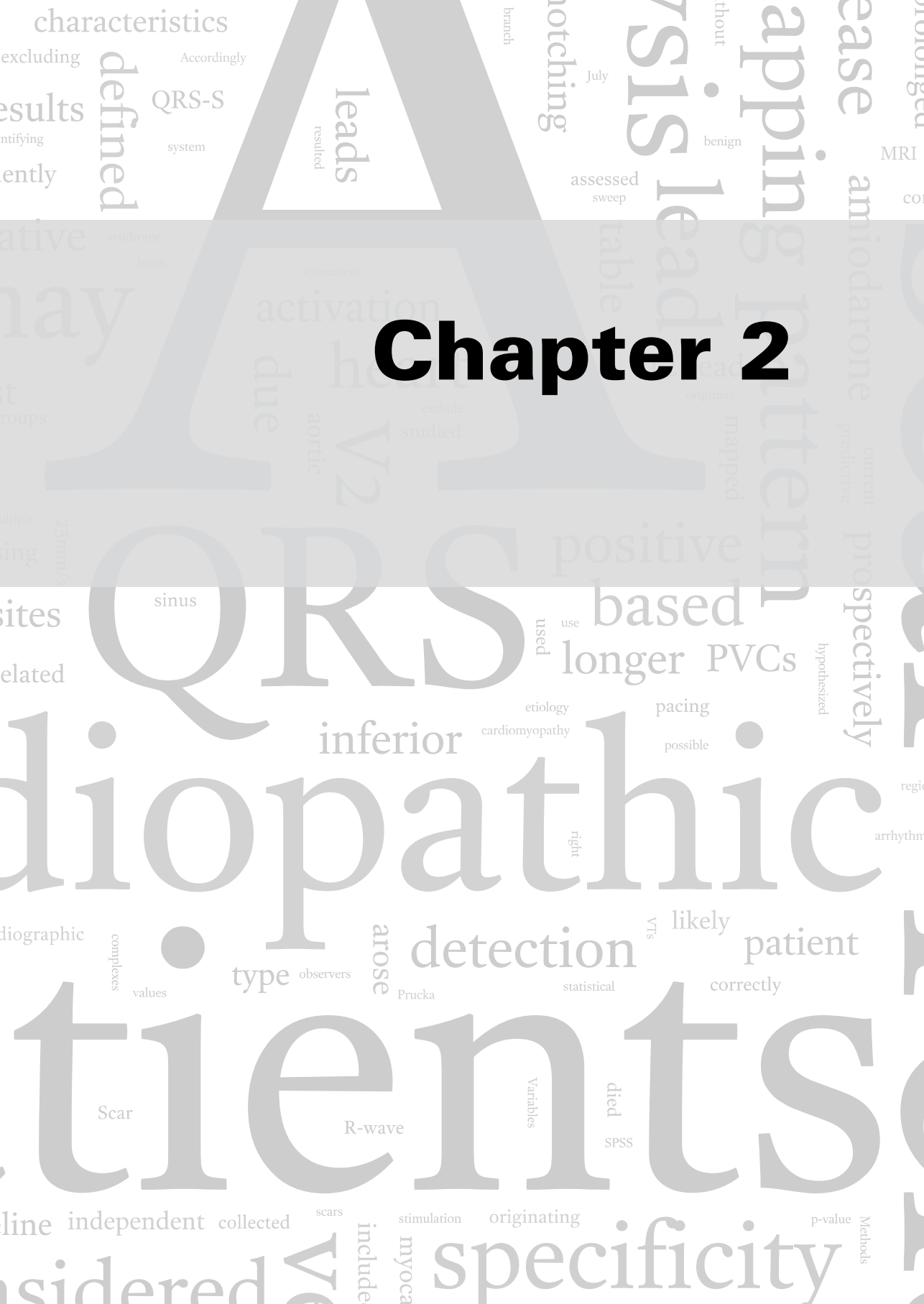
(90) Wijnmaalen AP, Schalij MJ, Bootsma M et al. Patients with scar-related right ventricular tachycardia: determinants of long-term outcome. J Cardiovasc Electrophysiol 2009; 20:1119-27.
(91) Dalal D, Jain R, Tandri H et al. Long-term efficacy of catheter ablation of ventricular tachycardia in patients with arrhythmogenic right ventricular dysplasia/cardiomyopathy. J Am Coll Cardiol 2007; 50:432-40.
(92) Marchlinski FE, Zado E, Dixit S et al. Electroanatomic substrate and outcome of catheter ablative therapy for ventricular tachycardia in setting of right ventricular cardiomyopathy. Circulation 2004; 110:2293-8.
(93) Garcia FC, Bazan V, Zado ES, Ren JF, Marchlinski FE. Epicardial substrate and outcome with epicardial ablation of ventricular tachycardia in arrhythmogenic right ventricular cardiomyopathy/dysplasia. Circulation 2009; 120:366-75.
(94) Morwood JG, Triedman JK, Berul CI et al. Radiofrequency catheter ablation of ventricular tachycardia in children and young adults with congenital heart disease. Heart Rhythm 2004; 1:301-8.
(95) Eckart RE, Hruczkowski TW, Tedrow UB et al. Sustained ventricular tachycardia associated with corrective valve surgery. Circulation 2007; 116:2005-11.
(96) Wijnmaalen AP, Delgado V, Schalij MJ et al. Beneficial effects of catheter ablation on left ventricular and right ventricular function in patients with frequent premature ventricular contractions and preserved ejection fraction. Heart 2010; 96:1275-80.
(97) Baman TS, Lange DC, Ilg KJ et al. Relationship between burden of premature ventricular complexes and left ventricular function. Heart Rhythm 2010; 7:865-9.
(98) Viskin S, Rosso R, Rogowski O, Belhassen B. The "short-coupled" variant of right ventricular outflow ventricular tachycardia: a not-so-benign form of benign ventricular tachycardia? J Cardiovasc Electrophysiol 2005; 16:912-6.
(99) Noda T, Shimizu W, Taguchi A et al. Malignant entity of idiopathic ventricular fibrillation and polymorphic ventricular tachycardia initiated by premature extrasystoles originating from the right ventricular outflow tract. J Am Coll Cardiol 2005; 46:1288-94.
(100) Zipes DP, Camm AJ, Borggrefe M et al. ACC/AHA/ESC 2006 guidelines for management of patients with ventricular arrhythmias and the prevention of sudden cardiac death--executive summary: A report of the American College of Cardiology/American Heart Association Task Force and the European Society of Cardiology Committee for Practice Guidelines (Writing Committee to Develop Guidelines for Management of Patients with Ventricular Arrhythmias and the Prevention of Sudden Cardiac Death) Developed in collaboration with the European Heart Rhythm Association and the Heart Rhythm Society. Eur Heart J 2006; 27:2099-140.

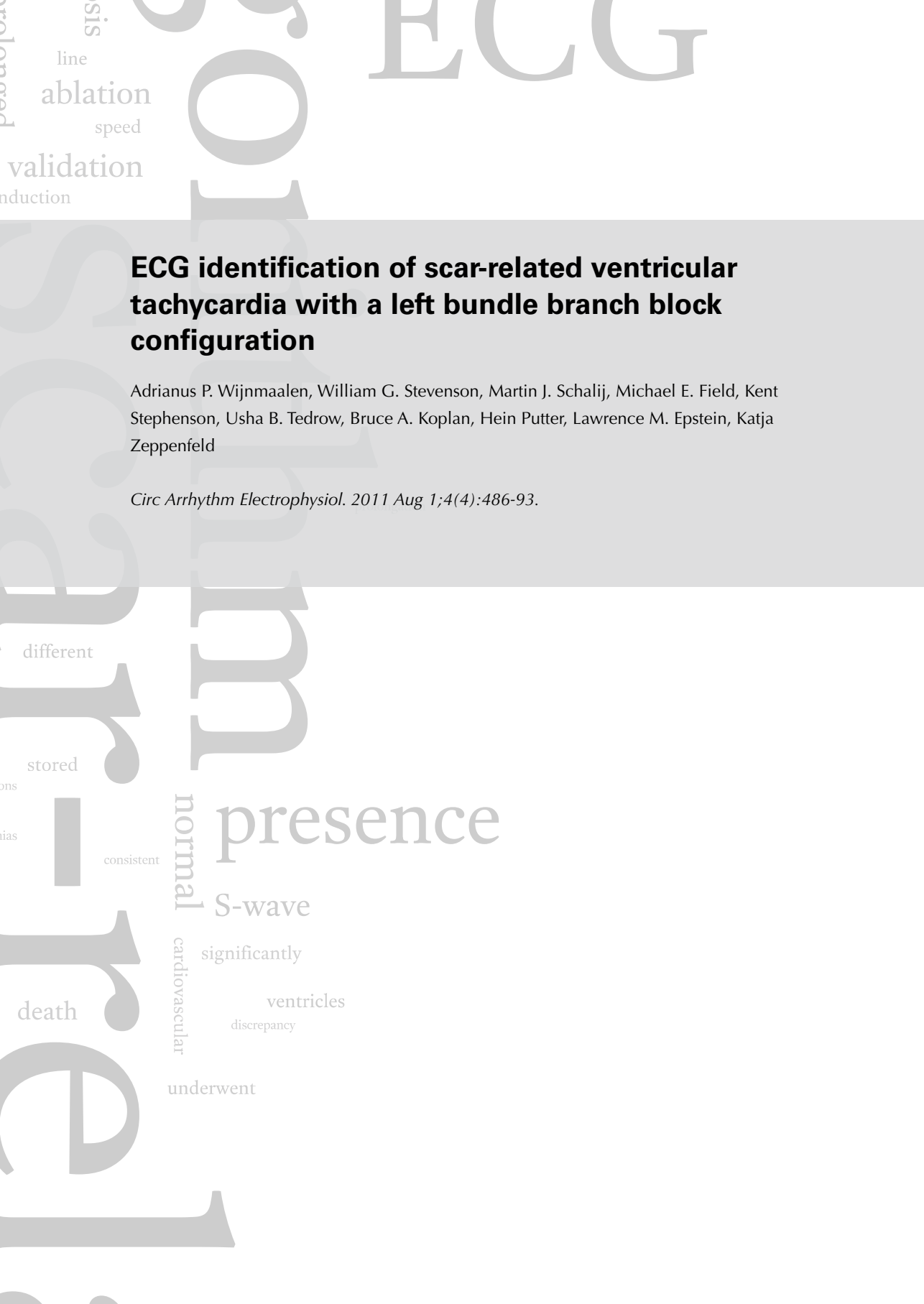

ablation
mapping
patient
VA
scar
catheter
substrate
ventricular
circuit
Ablation
pacing
myocardial
isthmus
voltage
heart
conduction
tachycardia
arrhythmia
fibrosis
areas
based
RV
LV
Figure
also
inducible
potential
VTs
DCM
circuits
selected
effective
prior
EGMs
reduction
patient
reperfusion
structural
wavefront
techniques
block
disease
associated
focal
underlying
number
recurrent
therapy
using
one
Catheter
small
majority
VF
SR
local
two
scars
follow-up
QRS
anatomical
performed
endocardial
information
fixed
approach
fat
ICD
time
exit
RFCA
addition
identify
monomorphic
rates
successful
first
derived
RF
area
sites
considered
study
success
including
experienced
reentrant
due
left
site
months
different
imaging
geometry
left
ventricular
ventricle
ventricles
ventricles
ventricular
ventricular
ventricular



Part I

Determinants of ventricular tachycardia substrate and techniques for substrate identification


Chapter 2
characteristics
excluding
Accordingly
defined
QRS-S
esults
ntifying
system
ently
leads
resulted
branch
notching
July
thout
ease
ysis
lead
appin
benign
MRI
assessed
sweep
amiodarone
ative
syndrome
beats
agreement
activation
hay
due
aortic
V2
exclude
studied
originate
mapped
positive
QRS
based
sinus
sites
elated
use
used
longer
PVCs
prospectively
hypothesized
etiology
pacing
cardiomyopathy
inferior
possible
diopathic
right
arrhythm
diographic
complexes
values
type
observers
arose
Prucka
detection
VTs
likely
patient
statistical
correctly
tients
Scar
R-wave
Variables
died
SPSS
line
independent
collected
scars
stimulation
originating
p-value
Methods
specificity
myoca



ECG identification of scar-related ventricular tachycardia with a left bundle branch block configuration

Adrianus P. Wijnmaalen, William G. Stevenson, Martin J. Schalij, Michael E. Field, Kent Stephenson, Usha B. Tedrow, Bruce A. Koplan, Hein Putter, Lawrence M. Epstein, Katja Zeppenfeld

Circ Arrhythm Electrophysiol. 2011 Aug 1;4(4):486-93.

Abstract

Background: A left bundle branch block-like (LBBB) pattern with a dominant S-wave in V1 is common in idiopathic ventricular arrhythmias (VA). Discrimination between idiopathic and scar-related LBBB pattern VA has important clinical implications. We hypothesized that the VA QRS morphology is influenced by the presence of ventricular scar allowing electrocardiographic discrimination of VA arising from structurally normal versus scarred myocardium.

Methods and results: Twelve-lead ECGs of 297 LBBB pattern monomorphic VA were recorded during catheter ablation procedures. QRS morphology characteristics associated with scar-related VA were identified in retrospective analysis of 118 LBBB pattern VA (95 scar-related, 23 idiopathic) to develop a stepwise algorithm, that was prospectively tested in 179 LBBB pattern VA (120 scar-related, 59 idiopathic). The diagnosis of scar was based on sinus rhythm surface ECG, cardiovascular imaging and electroanatomical catheter mapping. A precordial transition beyond V4, notching of the S-wave downstroke in lead V1 or V2 and a duration from the onset of QRS to the S-nadir in V1>90ms were independent predictors for scar-related VA. The proposed algorithm classified a VA as scar-related if any of these criteria was met. If none of the criteria was present a VA was classified as idiopathic. In prospective validation the algorithm was highly sensitive(96%) and specific(83%) for the identification of scar-related LBBB pattern VA.

Conclusions: The QRS morphology of VA is different between scar-related and idiopathic VA. A simple ECG algorithm is sensitive for identifying scar-related LBBB VA, which could be helpful in guiding further evaluation of these patients.

Introduction

Monomorphic ventricular arrhythmias (VA) in patients without structural heart disease referred to as 'idiopathic' VA are considered benign in the majority of cases.[1, 2] In contrast patients with scar-related monomorphic VA may be at risk for sudden cardiac death (SCD).[3, 4] Discrimination between idiopathic and scar-related VA therefore has important prognostic and therapeutic implications.

Most idiopathic VA have a left bundle branch block (LBBB) like morphology in lead V1.[5] LBBB pattern VA however can also arise from right ventricular (RV) and septal myocardial scars due to cardiomyopathies including arrhythmogenic RV cardiomyopathy and sarcoidosis.

The QRS morphology of a VA is determined by the location of the site from which a focal VA arises or from the location of the reentry circuit exit from which the excitation wavefront emerges to depolarize the surrounding myocardium, but may also be influenced by the presence and extend of myocardial scar.

We hypothesized that the VA QRS morphology may be influenced by the presence of ventricular scar allowing electrocardiographic discrimination of VA arising from structurally normal versus scarred myocardium.

Methods

Data was analyzed from 213 patients with LBBB pattern VA who were referred to Brigham and Women's hospital, Boston, MA, USA and The Leiden University Medical Center, Leiden, The Netherlands for catheter ablation of VA. Twelve-lead ECGs of 297 LBBB pattern monomorphic VA were documented and stored during radiofrequency catheter ablation (RFCA). The ECG algorithm was developed from retrospective analysis of 118 LBBB pattern VA from 81 consecutive patients (65 male, age 53±16years) studied between November 2002 and July 2006. The ECG algorithm was then prospectively validated in 179 LBBB pattern VA registered during RFCA in 132 patients (94 male, age 53±17years) between July 2006 and April 2009.

Algorithm development

All patient records were reviewed to establish or rule out the presence of myocardial scar.

Scar was diagnosed by any of the following: (1) The presence of pathologic Q-waves in ≥2/12 leads of the baseline surface ECG), (2) akinetic or dyskinetic wall motion abnormalities and/or (3) global ventricular dilatation with dysfunction on echocardiography, ventricular angiography or MRI and/or (4) areas of delayed enhancement on contrast enhanced MRI (5) fixed perfusion defects on nuclear imaging; or (6) regions with adjacent, fragmented,

prolonged (≥3 positive deflections, ≥40ms signal duration)[6] and low amplitude bipolar electrograms (≤1.5mV) on contact electroanatomical voltage mapping (EAM).

Electrophysiology study and Electroanatomic Mapping

Electrophysiological evaluation included electrical programmed stimulation (EPS) and EAM. Studies were performed in the post absorptive, non-sedated state. Antiarrhythmic drugs were discontinued for 5 half-lives, with the exception of amiodarone. The EPS-protocol consisted of 2 or 3 drive-cycle lengths (600, 500 and 400ms) and up to 3 ventricular extrastimuli from 2 right ventricular sites and burst pacing. Burst pacing and programmed stimulation during intravenous infusion of isoprotenerol (2-8μg/min) were used if the VA was not inducible at baseline. Twelve-lead ECGs and intracardiac electrograms were recorded simultaneously (Cardio-Lab 4.1; Prucka Engineering, Houston, TX, USA) and stored in digital format for off-line analysis. More than three monomorphic, consecutive beats were classified as ventricular tachycardia (VT) and ≤3 consecutive monomorphic beats as premature ventricular contractions (PVCs). Bipolar EAM of the RV and/or LV was performed in all patients, facilitated by a 3D EA mapping system (CARTO XP EP system Biosense Webster Inc, Diamond Bar, CA, USA) during sinus rhythm in 193(91%) patients and paced rhythm in 20(9%). A 4mm or 3.5mm tip, irrigated quadripolar mapping catheter (NaviStar or Navistar Thermo-Cool, Biosense Webster Inc, Diamond Bar, CA, USA) was used inserted via a transvenous or retrograde aortic approach. In the algorithm development group mapping was restricted to the RV in 35(43%), to the LV in 35(43%), both ventricles were mapped in 11(14%) and epicardial voltage mapping through a subxyphoid puncture was performed in 4 patients.

A VA exit site was determined based on activation and entrainment mapping for mappable VA and based on pace-mapping for unmappable VA. During activation mapping VA exit sites were defined as sites with the earliest ventricular activation and a local unipolar QS-pattern for focal VA and/or sites where pacing entrained the VT with concealed fusion and a postpacing interval within 30ms of the VT cycle length and a S-QRS of ≤30% of VT cycle length for reentry tachycardia. During pace-mapping VA exit sites were defined as sites with a paced QRS morphology that matches the VA QRS morphology (≥11/12 lead QRS pace-match). VA were considered scar-related if a VA exit site was located in or near an area of scar.

ECG analysis

All 12-lead surface ECGs of spontaneous or induced VA were analyzed by two independent observers blinded to the findings of imaging and EAM. In case of discrepancy agreement was reached by consensus. Measurements were performed on the digitally recorded electrograms at a sweep speed of 100mm/s (Cardio-Lab 4.1; Prucka Engineering, Houston, TX, USA) using electronic callipers.

Based on previous literature and theoretical considerations analysis included:

(1) QRS duration (QRSd) measured from the QRS onset, defined as the earliest deflection from the isoelectric line in any ECG lead to the QRS offset, defined as the latest intercept of the S or R-wave with the isoelectric line in any ECG lead.

(2) Frontal plane axis categorized as inferior (≥0° and <180°) or superior (≥180° and <0°).

(3) Precordial transition defined as the first precordial lead with an R/S ratio of >1. An R wave transition beyond V4 (e.g. V5, V6, or negative concordance) was considered 'late' (transition>V4).

(4) QRS-S (QRS-SV1) interval in precordial lead V1 defined as the interval from QRS onset in any lead to the nadir of the S wave in V1.

(5) Total amplitude of the QRS complex (QRSa) in precordial lead V2

(6) The total number of notched QRS complexes in all leads (notch total)

(7) The presence of a notch in the downstroke of the S-wave in precordial lead V1 and V2 (Notch S downstroke V1/2).

Statistical analysis

Continuous variables are expressed as mean±SD, and categorical variables as frequency (%) or percentage (95% confidence interval). Differences between scar-related and non-scar-related VA were assessed using the unpaired student *t*-test. Dichotomous variables were compared using chi-square test. Since the exit site and the propagation wavefront which determine the surface ECG characteristics of a VA differ between VA in one patient, multiple VA in the same patient were regarded as independent for the primary analysis. Variables where the means or frequencies were significantly different between groups were considered for further analysis. Cutoffs were based on choosing the value where the sensitivity and specificity were the same for the prediction of scar. Sensitivity and specificity for each individual value were calculated based on the cut point chosen by the ROC curve.

Variables were categorized accordingly. Next, these variables were analyzed in univariate and multivariable binary logistic regression. Multivariable analysis was performed in a backward stepwise fashion excluding the variable that was the least significant with for each consecutive step until all remaining variables in the model had a p-value lower than 0.25. These variables were incorporated in a stepwise algorithm. If any of the algorithm variable criteria for scar was met, outcome was considered positive for scar. If none of the variable criteria for scar was met, the outcome was considered idiopathic.

All statistical analyses were performed with SPSS software (version 16 SPSS Inc., Chicago, Illinois). For all tests a p-value ≤0.05 was considered significant.

Algorithm validation

The algorithm was then prospectively evaluated in 179 LBBB type VA recorded and stored during RFCA in 132 patients. All 12-lead surface ECGs of the VA were analyzed by two independent observers blinded to the results of scar detection. Each algorithm criterion was

separately classified as positive or negative. In case of discrepancy agreement was reached by consensus. A VA was defined as scar-related if ≥1 out of the variables selected for the algorithm were positive, a VA was classified as idiopathic if all criteria were negative.

These results were compared to the results of scar detection based on baseline ECG, imaging and EAM according to the defined criteria for scar. All patients underwent 12-lead ECG recording, 2-dimensional echocardiography and endocardial EAM as described. In the algorithm development group only the RV was mapped in 76(58%) patients, only the LV in 37(28%), both ventricles in 19(14%) and epicardial voltage mapping was performed in 24(18%). To rule out scar-related VA further analysis was performed including coronary angiography, MRI/contrast enhanced-MRI, nuclear imaging and biopsy if appropriate. Seven VA in 6 patients with evidence of scar on baseline ECG, imaging or EAM but with a VA exit mapped to an area of normal myocardium and remote from scar areas were excluded from the analysis.

Follow-up

Data regarding survival was collected for all patients (from the social security death index for the US patients and from long-term follow-up visits for the Netherlands patients). The date of last contact, heart transplantation or death was considered the date of last follow-up.

Results

Algorithm development

One hundred-eighteen LBBB type VA were analyzed. A total of 95 VA were scar-related and 23 arose from normal myocardium. The etiology of scar and the modality of scar detection are summarized in table 1.

ECG analysis

Scar-related VA had a longer QRSd, a longer QRS-S duration in V1, and a smaller QRS amplitude in V2 as compared to non scar-related VA. In addition, a superior axis, a notch in the downstroke of the S-wave in lead V1 or V2 and a late precordial transition were more frequent in VA that arose from scar areas. The total number of notched QRS complexes was higher in scar-related VA, the difference however did not reach statistical significance between both groups (p=0.055).

The best cutoff values to discriminate between scar-related and non-scar-related VA were a QRSd of >155ms, a QRS-S interval of >90ms and a QRS amplitude in V2 >1.55mV (Table 2).

Table 1. Baseline characteristics

	Algorithm development n=118 VA	**Algorithm validation** n=179 VA
Scar-related	95(81)	120(67)
Underlying disease		
Ischemic cardiomyopathy	48(41)	40(22)
Dilated cardiomyopathy	18(15)	31(17)
ARVC/D	13(11)	20(11)
Congential	6(5)	5(3)
Sarcoidosis	4(3)	0
Valvular	6(5)	2(1)
Hypertrophic cardiomyopathy	0	1(1)
Scar of unknown etiology	0	21(12)
Idiopathic	23(19)	59(33)
Scar detected by		
ECG + imaging + EAM	36(31)	30(17)
Imaging + EAM	51(43)	62(35)
Only ECG	0	0
Only imaging	3(3)	6(3)
Only EAM	5(4)	22(12)
VT/PVCs	107/11	136/43

ARVC/D indicates arrhythmogenic right ventricular cardiomyopathy/dysplasia; ECG, electrocardiogram; EAM, electroanatomical mapping; VT, ventricular tachycardia; PVC, premature ventricular contraction; VA, ventricular arrhythmia. Values are displayed as frequency(%) or mean±SD.

In multivariable analysis a late transition, a notch in the S downstroke of V1 or V2 and a QRS-S interval of >90ms were independently predictive for the presence of scar and therefore selected for the algorithm (table 3, figure 1).

Prospective validation

The developed algorithm was validated in 179 VA collected prospectively in 132 patients during consecutive RFCA procedures. In 31 patients >1 LBBB pattern VA was recorded.

Scar was detected by ECG, imaging and/or EAM in 76 patients with a total of 120 documented VA. The remaining 59 VA recorded in 56 patients were considered to be non scar-related. The results of scar detection and the etiology of scar in scar-related VA are summarized in table 1.

The outcome of the algorithm was positive for scar in 125(70%) VA and negative for scar in 54(30%) VA (table 4). Based on scar detection the outcome of the algorithm was considered true positive in 115 VA, true negative in 49 VA, false positive in 10 VA and false

Table 2. VT QRS variables and test variables in the 118 algorithm development VA

	Scar n=95	**Non scar** n=23	**p=**		**Test Variable**	**Test variable positive** n=
QRSd (ms)	184±43	147±15	**<0.001**	→	QRSd >155ms	76(64)
Superior Axis	35(37)	3(13)	**0.028**	→	Axis 180°≥ and <0°	38(32)
Transition >V4	50(53)	1(4)	**<0.001**	→	Transition >V4	51(43)
QRS-S interval V1 (ms)	107±29	83±18	**<0.001**	→	QRS-SV1 >90ms	77(65)
QRS amplitude V2	1.5±0.7	2.1±1.2	**0.005**	→	QRSa V2 >1.55	55(46)
Notch total	3.0±2.4	1.9±2.0	0.055			
Notch S downstroke V1/2	35(37)	3(13)	**0.028**	→	NotchS downstroke V1/2	38(32)

QRSd indicates QRS duration. Variables are displayed as frequency(%) or mean±SD.

Table 3. Univariable and multivariable logistic regression of test variables in the algorithm development VA

	Univariate OR (95% CI)	p=	**Multivariate** OR (95% CI)	p=
QRSd >155ms	3.7 (1.4–9.5)	0.006		
Superior Axis	3.9 (1.1–14.0)	0.038		
Transition >V4	24.4 (3.2–188.8)	0.006	22.0 (2.8–176.1)	0.004
QRS-S nadir V1 >90ms	6.4 (2.4–17.4)	<0.001	4.6 (1.5–13.7)	0.007
QRS amplitude V2 >1.55	0.6 (0.2–1.5)	0.291		
Notch S downstroke V1/2	3.9 (1.1–14.0)	0.038	3.0 (0.7–12.4)	0.122

OR indicates Odds ratio; QRSd, QRS duration. Variables are displayed as frequency(%) or mean±SD.

negative in 5 VA. This results in a sensitivity of 96%(90-98) and specificity of 83%(71-91) to discriminate between scar-related and non scar-related VA (Figure 2). The values for each algorithm component are provided in table 4.

Since sustained VT was more common in patients with scar (116(85%) scar-related sustained VT) as compared to patients without scar (20(34%) non scar-related sustained VT) the algorithm was separately evaluated for the prediction of scar in VT and PVC subgroups. Sensitivity and specificity were found to be high for the prediction of scar in VT (sensitivity 96%(90-98) and specificity 70%(46-87)) and PVCs (sensitivity 100%(40-100) and specificity 90%(75-97)). Likely attributable to the different prevalence of PVCs and VT in scar-related and non scar-related groups the positive predictive value (PPV) for scar-related VA was low for PVCs (PPV 50%(17-83)) with a negative predictive value (NPV) of 100%(88-100). For VT the PPV was 95%(89-98) and the NPV 74%(49-90).

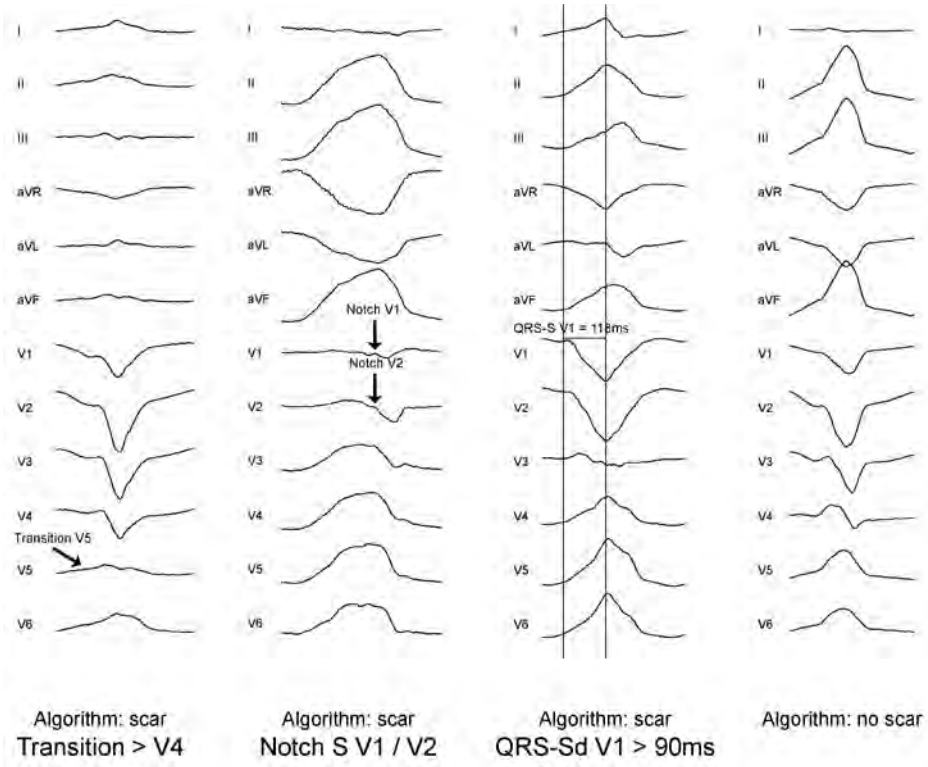


Figure 1. Representative examples of the variables that were used in the algorithm. The first 3 panels show scar-related VT morphologies, the most right panel shows a non scar-related VT.

Table 4. Outcome of the algorithm in 179 validation VA

	Transition >V4	Notch d V1/2	QRS-Sd V1 >90ms	Algorithm
True Positive	83(46)	42(23)	86(48)	115(64)
False Positive	3(2)	5(3)	7(4)	10(6)
True Negative	56(31)	54(30)	52(29)	49(27)
False Negative	37(21)	78(44)	34(19)	5(3)
Sensitivity (%)	69(60-77)	35(27-44)	72(63-79)	96(90-98)
Specificity (%)	95(85-99)	92(81-97)	88(76-95)	83(71-91)
PPV (%)	97(89-99)	89(76-96)	93(85-97)	92(85-96)
NPV (%)	60(50-70)	41(33-50)	61(49-71)	91(79-97)

VA indicates ventricular arrhythmia; PPV, positive predictive value; NPV, negative predictive value. Values are displayed as frequency(%) or percentage(95% confidence interval).

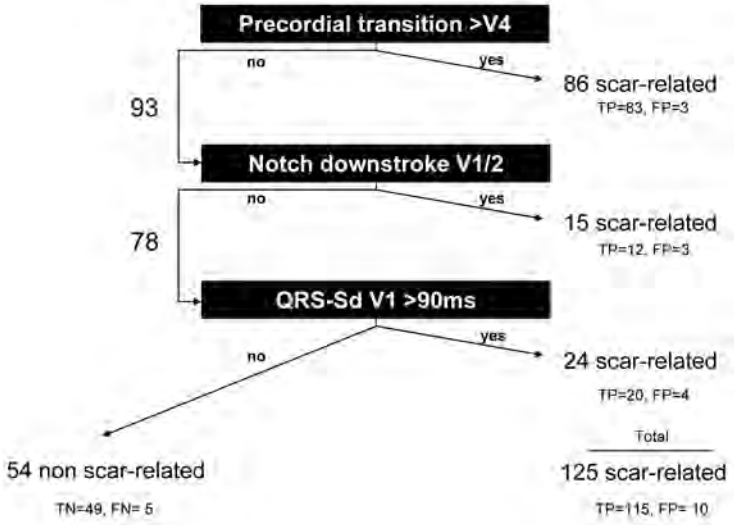


Figure 2. The step by step flow chart of the algorithm for the 179 validation VA. VA indicates ventricular arrhythmia; TP, true positive; FP, false positive; TN, true negative and FN, false negative.

As most idiopathic VTs arise from the outflow tract region, the algorithm was separately evaluated for 105 VA with an inferior axis. Among these VA the algorithm correctly identified 46 out of 51 scar-related VA and 47 out of 54 non scar-related VA. This resulted in a sensitivity of 90%(78-96) and specificity of 87%(75-94).

In patients with known heart disease, VA should be presumed to be related to the underlying disease unless proven otherwise. We therefore assessed the algorithm excluding patients with ischemic heart disease or congenital heart disease, in whom prior knowledge of heart disease may be most likely. In the remaining 101 patients with 134 VA the sensitivity of the algorithm to predict scar was 93%(84-97) with a specificity of 83%(71-91).

Analysis of misclassified VA

Ten VA recorded in 9 patients were classified as scar-related based on the ECG algorithm without scar detection on ECG, imaging or EAM (table 5). Two VA were recorded in one patient in whom mapping revealed a focal endocardial exit of presystolic activity, but where ablation was unsuccessful; no epicardial mapping was performed. We can not exclude the possibility that epicardial EAM would have revealed scar, improving the algorithm performance. Four VA were mapped to the aortic cusp or epicardial LVOT, two arose from the tricuspid annulus and two from the RVOT (figure 3).

Five VA in 4 patients were misclassified as non scar-related. Three were related to a small epicardial scar area not detected by endocardial voltage mapping or imaging, one to a small

Table 5. Misclassified VA according to the ECG algorithm

Patient	VA	Scar	Axis	Transition >V4	Notching V1/V2	QRSs V1>90ms	Site of origin
False positive							
1	1	non-scar	Inf	0	0	1	Endocardial RVOT
2	2	non-scar	Sup	1	0	1	Tricuspid annulus
3	3	non-scar	Sup	1	1	0	Tricuspid annulus
4	4	non-scar	Inf	0	1	0	Aortic cusp
5	5	non-scar	Inf	0	0	1	Likely epicardial VT
5	6	non-scar	Sup	1	1	1	Likely epicardialVT
6	7	non-scar	Inf	0	0	1	Aortic annulus
7	8	non-scar	Inf	0	1	1	Aortic cusp
8	9	non-scar	Inf	0	0	1	Endocardial RVOT
9	10	non-scar	Inf	0	1	0	Epicardial LVOT
False negative							
10	1	Small epicardial scar on EAM	Inf	0	0	0	Epicardial RVOT
10	2	Small epicardial scar on EAM	Inf	0	0	0	Epicardial RVOT
11	3	DCM	Inf	0	0	0	Basal septal
12	4	Posterior RVOT, endocardial scar	Inf	0	0	0	Posterior RVOT
13	5	Epicardial scar RV inferior and RVOT	Inf	0	0	0	Epicardial RVOT

DCM indicates dilated cardiomyopathy; EAM, electroanatomical mapping; RV, right ventricle; RVOT, right ventricular outflowtract; VA, ventricular arrhythmia.

posterior RVOT scar detected by EAM and one to a basal septal scar in a patient with dilated cardiomyopathy.

Interestingly in patients 4, 11 and 13 (table 5) ≥1 other VA were correctly classified as non scar or scar-related.

First induced VA

To adjust for the possible unequal representation of individual patients due to multiple inducible VA an additional analysis was performed testing the algorithm for only the first VA that was induced or recorded spontaneously in each of the 132 patients. When only these

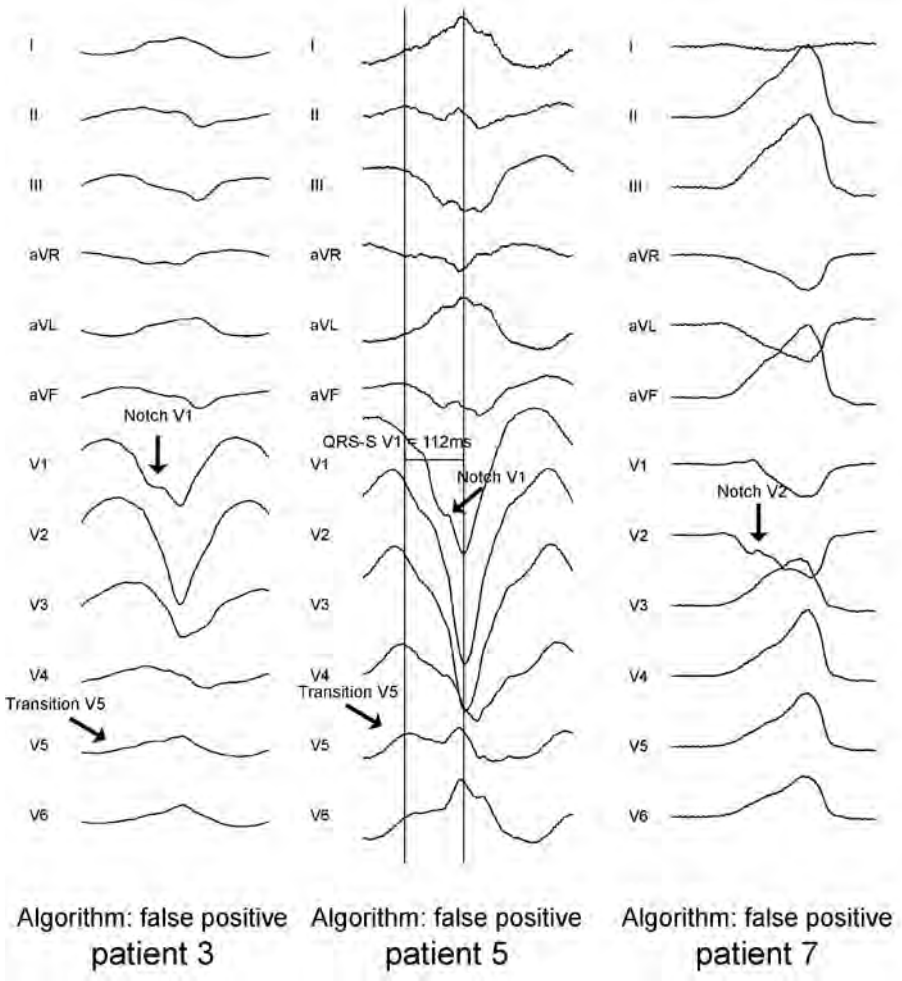


Figure 3. Examples of three QRS morphologies of false positive VA. These VA were originating from the epicardium, aortic cusp and tricuspid annulus (table 5 patient 2, 4 and 5) respectively. Notches in lead V1/2, a late transition and QRS S V1>90ms are indicated.

VA were taken into consideration the algorithm correctly identified 73 of 76 scar-related and 49 of 56 non scar-related VA. This resulted in a similar sensitivity (96%(88-99)) and specificity of (88%(79-95)) as in the analysis of all VA.

Amiodarone

In the algorithm validation group 22 patients with 34 VA were treated with amiodarone, the dosage was 324±247mg daily. The VA QRSd in patients on amiodarone was 218±50ms as compared to 170±121ms(p=0.03) in patients not on amiodarone. Since the use of amiodarone may influence conduction properties an additional analysis excluding all patients

using amiodarone was performed to determine whether the use of amiodarone affected the outcome of the algorithm. In the remaining 145 VA the sensitivity of the algorithm was 94%(86-98) and specificity 83%(71-91) to identify scar-related VA.

Mortality

Patients in whom the algorithm was developed were followed for 42±21months. During follow-up 13(16%) patients with scar-related VA classified by the ECG algorithm died and 2(2%) patients underwent cardiac transplantation. In contrast, all patients who were classified as having non-scar VA survived. The follow-up duration in the prospective analysis group was 14±11 months (median 10, range 0-34 months). Eleven (6%) patients with algorithm based scar-related VA died whereas all patients who were classified as having non scar-related VA survived.

Discussion

Scar-related reentry is the most common cause of sustained monomorphic VT in patients with structural heart disease, and usually warrants implantation of a defibrillator for protection from sudden cardiac death.[7] In contrast, most idiopathic VA have a focal origin not associated with detectable scar, and a benign prognosis. Most have a LBBB pattern morphology and originate in the outflow tract of the RV or LV.[5] LBBB pattern VA however can also be due to scar-related reentry, arising from RV and septal scars.[1-4] A correct diagnosis of scar-related and idiopathic VA is important for long-term prognosis and therapeutic considerations. Diagnosis of idiopathic VA is still one of exclusion and may therefore require extensive non-invasive and invasive assessment.[8]

The current study evaluated the affect of ventricular scar assessed by sinus rhythm ECG, cardiovascular imaging and electroanatomical voltage mapping on QRS morphology characteristics of LBBB pattern VA on 12-lead ECG.

A simple stepwise algorithm of 3 ECG criteria was developed based on 118 retrospectively collected VA ECGs and prospectively tested in 179 LBBB pattern VA allowing for discrimination of VA originating from scarred or structurally normal myocardium with a high sensitivity and specificity.

Ventricular Scar

In the current study only VA ECGs from patients referred for RFCA were included. These patients underwent extensive evaluation including evaluation of the baseline ECG for the presence of Q-waves, cardiac catherization and cardiovascular imaging. In addition, EAM was performed during RFCA in all patients to diagnose or confirm the presence of scar at of

the VT exit. The latter is of importance because EAM has been shown to be highly sensitive to detect scars that may escape detection by imaging.[9] Accordingly, scar associated with VA was diagnosed only by EAM in 5(4%) VA evaluated retrospectively and in 22(12%) VA evaluated prospectively. In the latter group epicardial EAM was applied more frequently. Only patients in whom no scar was detected by any modality were considered to have idiopathic VA. That none of these patients died during follow-up, further suggests that important structural heart disease was unlikely to escape detection in our cohort.

12-lead ECG of the VA and Site of Origin

ECG analysis of the VA included morphology characteristics related to the site of origin, QRS amplitude, duration and notching with special emphasis on the precordial leads V1 and V2.

A superior axis is consistent with a more inferior and apical exit which is frequently observed in patients with ARVD/C but rare in idiopathic VA.[10, 11] An inferior axis with a late transition beyond V4 is consistent with a more inferior and anterior exit below the pulmonary valve and is therefore also not frequently found in idiopathic VA.[11, 12] However, a superior axis or inferior axis with a late precordial transition may occur in VA that arise from the tricuspid annulus region accounting for <5% of idiopathic VA.[12, 13] Of interest, in one series patients with idiopathic VA arising from the tricuspid annulus were older and experienced more often ablation failure than patients with idiopathic VA originating from the RVOT. Although structural abnormalities were excluded by imaging perivalvular fibrosis as observed in other non-ischemic cardiomyopathies can not be fully excluded as a cause of this type of VA.[14] Accordingly, the majority of idiopathic VA in the current study had a transition before or at V4. A transition beyond V4 was only observed in 4 of the VA that were classified as idiopathic. Two arose from the tricuspid annulus, both with a superior axis, one arose from the mid to apical septal region and one occurred in a patient with an epicardial circuit.

A broadly notched QRS(≥160ms) of PVCs has been associated with a dilated and hypokinetic left ventricle.[15] In a study by Ainsworth the mean VA QRSd for all 12 leads was longer in ARVD/C patients (135.1±8.5ms) as compared to patients with idiopathic VA (126.5±13ms) measured on ECG paper copies recorded at 25mm/s. We found longer QRS durations in scar-related (184±43ms) and idiopathic (147±15ms) VA likely due to measurement of QRS duration from simultaneous recordings of all leads, which likely avoids errors introduced due to isoelectric components in some leads.

QRS duration was significantly longer in scar-related VT as compared to idiopathic VA and a QRSd>155ms argues for a scar-related VA. However, scar-related VA that arise from or near the septum might have a short QRS duration. In contrast, idiopathic VA that arise from the free wall of the RV may exhibit a longer QRS duration.[16]

The presence of notches might reflect disturbed conduction and may therefore be a sign of scar tissue but has also been demonstrated in idiopathic VA that arise from the RV free

wall in up to 86% of patients.[15] Although, we found a slightly higher number of total notches in the 12 leads, the difference as compared to idiopathic VA were not significant.

The QRS morphology of VA is determined by the location at which the activation wavefront emerges to activate the ventricles. Areas of delayed conduction at this site, as typically found in scar-related reentry, may contribute to the QRS characteristics by prolongation and notching of its initial portion. In contrast in patients with structurally normal hearts, the spread of activation from the site of origin is rapid. The interval from the QRS onset in any lead to the nadir of the S in V1 was significantly prolonged in scar-related VA and notching of the S-downstroke in V1 or V2 was associated with the presence of ventricular scar. This is in line with the assumption that activation delay due to RV and septal fibrosis translates into a prolonged and notched initial portion of the VA QRS in lead V1 and V2.

Interestingly, longer QRS onset to S nadir in V1 (>60ms) and notching in the S-wave downstroke of V1 or V2 have previously been identified by Kindwell[17] and used by Brugada[18] for the discrimination between supraventricular and ventricular origin of broad complex LBBB type tachycardias. Ninety-five percent of the VTs studied by Kindwell however were originating from structurally abnormal hearts, the majority being related to infarct scar.[17]

Algorithm development and validation

In multivariable analysis a late precordial R-wave transition, notching of the S downstroke in V1 or V2 and the QRS to S duration in V1 were shown to be independently associated with scar-related VA, but individually have a high specificity, but low sensitivity. Combining the three criteria improved sensitivity to 96% with a specificity of 83%. In subgroup analysis the algorithm was sensitive and specific to predict scar in patients with PVCs and with sustained VT. Furthermore if only VA with an inferior axis were taken into consideration, the most frequently observed axis in idiopathic VA, the sensitivity was still 90% and the specificity 88%. Despite the high sensitivity in identifying scar-related VA the algorithm misclassified 10 VA as scar-related. In half of those the origin of the VA was considered to be epicardial or found in the aortic cusps.

Idiopathic VA with an epicardial or aortic cusp origin may have a prolonged QRS duration due to the time needed for the activation wavefront to traverse the myocardial wall and reach the endocardium[19] and could be falsely classified as scar-related by our algorithm based on prolonged initial QRS duration. This QRS prolongation can be present or absent according to the epicardial location or origin of VA.[20, 21] Similarly idiopathic LBBB type VA that originate from the TA may be misclassified due to the late precordial R-wave transition associated with this site of origin. Five VA were misclassified as idiopathic. In three patients small scar areas were only detected by epicardial voltage mapping and in one by endocardial EAM underlying the importance of EAM to differentiate between idiopathic and scar-related VA.

Limitations

In addition to the caveats discussed above there are other limitations to this study. As in previous studies the diagnosis of idiopathic VA was made when evaluation excluded the presence of scar. Even though the extensive evaluation including EAM is a strength of this study the lack of a currently available gold-standard for the diagnosis of idiopathic VA may allow misclassification of patients with a currently undetectable substrate for VA. The studied population did not include patients with known channelopathies, such as Brugada syndrome or long QT syndrome. Commenting on the VA QRS morphology in these patients who may be at risk for sudden death despite the absence of structural heart disease is therefore beyond the scope of this study.

ECG measurements were performed during electrophysiological study at a sweep speed of 100mm/s, standard ECGs in clinical practice however are often printed at 25mm/s. It is possible that some of the observations, such as the QRS-Sd in V1, may be more difficult in standard ECGs recorded at speed of 25mm/s.

Finally although the absence of mortality in the idiopathic group is reassuring and further supports the diagnosis of idiopathic VT, we can not exclude the possibility of small regions of ventricular scar that escape detection with present methods are present in some patients and that could lead to later development of other VA.

Clinical implications

The proposed algorithm detects scar-related VA with high specificity. Although it is not a substitute for imaging to define ventricular function and structural disease, it does provide an immediate electrocardiographic indication of the likelihood of whether ventricular scar is likely to be present, that can inform further evaluation. Furthermore, patients with algorithm positive VA ECG who do not have evidence of structural heart disease on initial clinical assessment may be considered for more detailed imaging, such as MRI.

Reference List

(1) Niwano S, Wakisaka Y, Niwano H, Fukaya H, Kurokawa S, Kiryu M, Hatakeyama Y, Izumi T. Prognostic Significance of Frequent Premature Ventricular Contractions Originating from the Ventricular Outflow Tract in Patients with Normal Left Ventricular Function. Heart 2009; 95:1230-1237.

(2) Lemery R, Brugada P, Bella PD, Dugernier T, van den DA, Wellens HJ. Nonischemic ventricular tachycardia. Clinical course and long-term follow-up in patients without clinically overt heart disease. Circulation 1989; 79:990-999.

(3) Rouleau JL, Talajic M, Sussex B, Potvin L, Warnica W, Davies RF, Gardner M, Stewart D, Plante S, Dupuis R, Lauzon C, Ferguson J, Mikes E, Balnozan V, Savard P. Myocardial infarction patients in the 1990s--their risk factors, stratification and survival in Canada: the Canadian Assessment of Myocardial Infarction (CAMI) Study. J Am Coll Cardiol 1996; 27:1119-1127.

(4) van der Burg AE, Bax JJ, Boersma E, van Erven L, Bootsma M, van der Wall EE, Schalij MJ. Standardized screening and treatment of patients with life-threatening arrhythmias: the Leiden out-of-hospital cardiac arrest evaluation study. Heart Rhythm 2004; 1:51-57.

(5) Haqqani HM, Morton JB, Kalman JM. Using the 12-lead ECG to localize the origin of atrial and ventricular tachycardias: part 2--ventricular tachycardia. J Cardiovasc Electrophysiol 2009; 20:825-832.

(6) Zeppenfeld K, Kies P, Wijffels MC, Bootsma M, van Erven L, Schalij MJ. Identification of successful catheter ablation sites in patients with ventricular tachycardia based on electrogram characteristics during sinus rhythm. Heart Rhythm 2005; 2:940-950.

(7) Aliot EM, Stevenson WG, Almendral-Garrote JM, Bogun F, Calkins CH, Delacretaz E, Della BP, Hindricks G, Jais P, Josephson ME, Kautzner J, Kay GN, Kuck KH, Lerman BB, Marchlinski F, Reddy V, Schalij MJ, Schilling R, Soejima K, Wilber D. EHRA/HRS Expert Consensus on Catheter Ablation of Ventricular Arrhythmias: developed in a partnership with the European Heart Rhythm Association (EHRA), a Registered Branch of the European Society of Cardiology (ESC), and the Heart Rhythm Society (HRS); in collaboration with the American College of Cardiology (ACC) and the American Heart Association (AHA). Heart Rhythm 2009; 6:886-933.

(8) Kies P, Bootsma M, Bax JJ, Zeppenfeld K, van Erven L, Wijffels MC, van der Wall EE, Schalij MJ. Serial reevaluation for ARVD/C is indicated in patients presenting with left bundle branch block ventricular tachycardia and minor ECG abnormalities. J Cardiovasc Electrophysiol 2006; 17:586-593.

(9) Wijnmaalen AP, Schalij MJ, Bootsma M, Kies P, DE RA, Putter H, Bax JJ, Zeppenfeld K. Patients with scar-related right ventricular tachycardia: determinants of long-term outcome. J Cardiovasc Electrophysiol 2009; 20:1119-1127.

(10) Cox MG, Nelen MR, Wilde AA, Wiesfeld AC, van der Smagt JJ, Loh P, Cramer MJ, Doevendans PA, van Tintelen JP, De Bakker JM, Hauer RN. Activation delay and VT parameters in arrhythmogenic right ventricular dysplasia/cardiomyopathy: toward improvement of diagnostic ECG criteria. J Cardiovasc Electrophysiol 2008; 19:775-781.

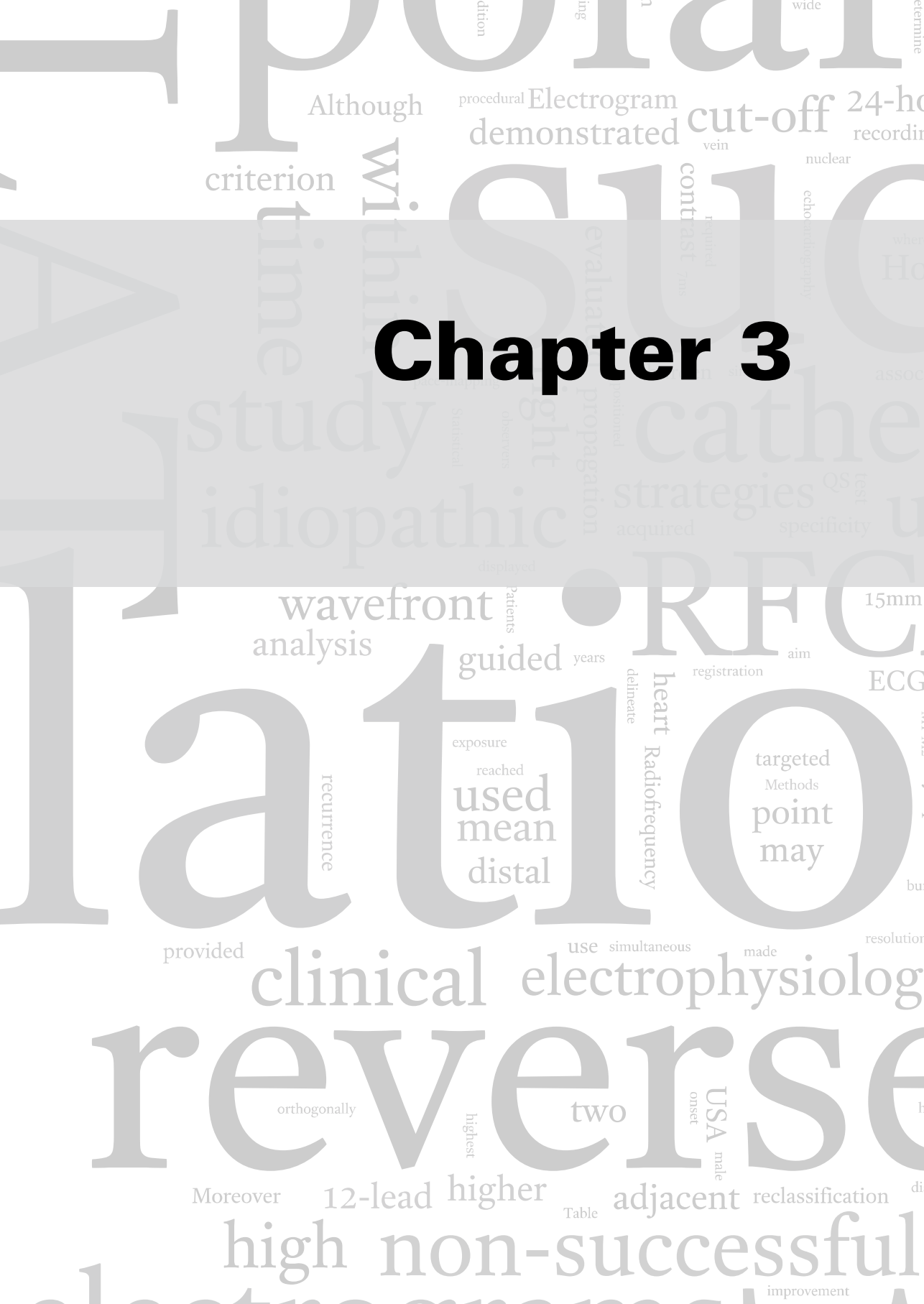
(11) Ainsworth CD, Skanes AC, Klein GJ, Gula LJ, Yee R, Krahn AD. Differentiating arrhythmogenic right ventricular cardiomyopathy from right ventricular outflow tract ventricular tachycardia using multilead QRS duration and axis. Heart Rhythm 2006; 3:416-423.

(12) Jadonath RL, Schwartzman DS, Preminger MW, Gottlieb CD, Marchlinski FE. Utility of the 12-lead electrocardiogram in localizing the origin of right ventricular outflow tract tachycardia. Am Heart J 1995; 130:1107-1113.

(13) Tada H, Tadokoro K, Ito S, Naito S, Hashimoto T, Kaseno K, Miyaji K, Sugiyasu A, Tsuchiya T, Kutsumi Y, Nogami A, Oshima S, Taniguchi K. Idiopathic ventricular arrhythmias originating from the tricuspid annulus: Prevalence, electrocardiographic characteristics, and results of radiofrequency catheter ablation. Heart Rhythm 2007; 4:7-16.

(14) Eckart RE, Hruczkowski TW, Tedrow UB, Koplan BA, Epstein LM, Stevenson WG. Sustained ventricular tachycardia associated with corrective valve surgery. Circulation 2007; 116:2005-2011.
(15) Moulton KP, Medcalf T, Lazzara R. Premature ventricular complex morphology. A marker for left ventricular structure and function. Circulation 1990; 81:1245-1251.
(16) Dixit S, Gerstenfeld EP, Callans DJ, Marchlinski FE. Electrocardiographic patterns of superior right ventricular outflow tract tachycardias: distinguishing septal and free-wall sites of origin. J Cardiovasc Electrophysiol 2003; 14:1-7.
(17) Kindwall KE, Brown J, Josephson ME. Electrocardiographic criteria for ventricular tachycardia in wide complex left bundle branch block morphology tachycardias. Am J Cardiol 1988; 61:1279-1283.
(18) Brugada P, Brugada J, Mont L, Smeets J, Andries EW. A new approach to the differential diagnosis of a regular tachycardia with a wide QRS complex. Circulation 1991; 83:1649-1659.

(19) Daniels DV, Lu YY, Morton JB, Santucci PA, Akar JG, Green A, Wilber DJ. Idiopathic epicardial left ventricular tachycardia originating remote from the sinus of Valsalva: electrophysiological characteristics, catheter ablation, and identification from the 12-lead electrocardiogram. Circulation 2006; 113:1659-1666.
(20) Bazan V, Gerstenfeld EP, Garcia FC, Bala R, Rivas N, Dixit S, Zado E, Callans DJ, Marchlinski FE. Site-specific twelve-lead ECG features to identify an epicardial origin for left ventricular tachycardia in the absence of myocardial infarction. Heart Rhythm 2007; 4:1403-1410.
(21) Bazan V, Bala R, Garcia FC, Sussman JS, Gerstenfeld EP, Dixit S, Callans DJ, Zado E, Marchlinski FE. Twelve-lead ECG features to identify ventricular tachycardia arising from the epicardial right ventricle. Heart Rhythm 2006; 3:1132-1139.


Chapter 3

Reversed polarity of bipolar electrograms to predict a successful ablation site in focal idiopathic right ventricular outflow tract arrhythmias

Carine F.B. van Huls van Taxis, Adrianus P. Wijnmaalen, Dennis W. den Uijl, Marcin Gawrysiak, Hein Putter, Martin J. Schalij, K. Zeppenfeld

Heart Rhythm. 2011 May;8(5):665-71.

Abstract

Background: Radiofrequency catheter ablation (RFCA) for idiopathic right ventricular outflow tract (RVOT) arrhythmias is typically guided by local activation time (LAT) mapping and unipolar electrogram morphology (QS-configuration). However, LAT mapping is limited by the large variation among patients and the area demonstrating a QS-configuration of the unipolar electrogram may be larger than the focal source. Reversed polarity has been proposed as criterion to guide RFCA.

Objective: The aim of this study was to investigate the value of reversed polarity of adjacent bipolar electrograms to predict a successful ablation site in idiopathic RVOT arrhythmias.

Methods: Twenty-five consecutive patients (12 male [48%], 43±15 years) undergoing RFCA for RVOT arrhythmia were studied. Electrograms of ablation sites and of points within a 15mm radius to the successful site were evaluated for LAT, unipolar electrogram morphology and the presence of reversed polarity of adjacent bipolar electrograms. Electrogram characteristics of successful ablation sites were compared to non-successful ablation sites. The spatial distribution of each electrogram characteristic was studied.

Results: Successful ablation sites more often demonstrated reversed polarity and had an earlier LAT than non-successful sites. A wide spatial distribution was observed for unipolar electrograms with a QS-configuration around the successful ablation site. Mapping based on LAT and reversed polarity had a higher predictive value for a successful ablation site than mapping based on LAT and QS-configuration.

Conclusion: The presence of reversed polarity has a high predictive value for successful ablation sites in focal idiopathic RVOT arrhythmias and is likely to reduce the number of RFCA applications.

Introduction

Ventricular arrhythmias (VA) in the absence of structural heart disease are a common entity. Patients presenting with idiopathic VA account for 10% of patients referred for evaluation and treatment of VA and more than 70-80% of idiopathic VA originate from the right ventricular outflow tract (RVOT).[1] Although idiopathic VAs are generally considered benign, they can cause severe symptoms and may be associated with a VA induced cardiomyopathy.[2-6]

Current guidelines indicate anti-arrhythmic drugs as first choice therapy for symptomatic patients; however drugs are often ineffective or hampered by side effects.[1,7,8] Radiofrequency catheter ablation (RFCA) is a reasonable alternative and acutely highly effective with procedural success rates of more than 80%.[1,9-11] Although considered safe, serious complications may occur and the application of a limited number of radiofrequency lesions particular is preferred.[1,12-15]

To guide RFCA, conventional strategies are based on bipolar local activation time (LAT) mapping and the presence of a QS-configuration of the unipolar electrogram to predict a successful ablation site.[16-19] However, the use of LAT is limited by its large variation among patients and the area demonstrating a unipolar QS-configuration may be larger than the focal source.[18,20] A more specific electrogram characteristic to predict a successful ablation site in RVOT arrhythmias is therefore desirable.

The feasibility of guiding ablation by reversed polarity of adjacent bipolar electrograms has been demonstrated in pulmonary vein isolation based on the hypothesis that the excitation wavefront propagates radially from the breakthrough site of the left atrium to the pulmonary vein.[21] A similar reversal of the initial deflection of adjacent bipolar electrograms, indicative for wavefront propagation in opposite directions, has been demonstrated in patients with accessory pathways and focal atrial tachycardias.[22] This phenomenon however, has not been well documented in focal RVOT arrhythmias.

The aim of this study was to investigate the value of reversed polarity mapping to identify an arrhythmogenic focal source and to predict a successful ablation site in focal RVOT arrhythmias.

Methods

Patient population

The patient population consisted of 25 consecutive patients undergoing RFCA of idiopathic focal VA originating from the RVOT. To rule out structural heart disease, a comprehensive clinical evaluation was performed including medical history, 12-lead electrocardiogram (ECG) and two-dimensional transthoracic echocardiography in all patients. If deemed necessary to exclude structural heart disease, exercise testing, coronary angiography, cardiac

multi-detector computed tomography, magnetic resonance imaging and/or nuclear imaging were performed. Prior to RFCA, a 12-lead ECG recording of the VA and a 24-hour Holter registration were acquired in all patients. Ventricular arrhythmias consisting of more than three consecutive monomorphic beats were classified as ventricular tachycardia (VT) and VA ≤3 consecutive monomorphic beats were classified as premature ventricular contraction (PVC).

After RFCA, all patients were monitored for 24 hours to detect early VA recurrence. All patients were evaluated on a regular basis at the outpatient clinic 3 months after discharge. Each visit included a clinical history, 12-lead ECG and 24-hour Holter registration.

Electrophysiological examination and catheter ablation

After informed consent was obtained electrophysiological evaluation was performed comprising electrical programmed stimulation (EPS) and right ventricular electroanatomical activation mapping to identify the site of origin within the RVOT. During mapping and ablation, conscious sedation was avoided whenever possible. Anti-arrhythmic drugs were discontinued for at least 5 half-lives. None of the patients was using amiodarone prior to the procedure. Heparin was administered to maintain an activated clotting time of 250-300s. Catheters were placed through a right femoral vein approach. A quadripolar catheter was inserted in the right ventricle and used for EPS. In the presence of a spontaneous clinical VA, activation mapping was performed using the surface VA QRS as a temporal reference. If no spontaneous VA occurred EPS was performed before and after intravenous isoprotenerol (2-8 µg/min) infusion, if necessary. The EPS protocol consisted of 3 drive-cycle lengths (600, 500 and 400 ms) with up to 3 ventricular extra stimuli and incremental burst pacing from 2 different right ventricular sites.

A 3.5mm irrigated-tip quadripolar mapping catheter (2-5-2mm inter-electrode spacing, Navistar ThermoCool, Biosense Webster Inc, Diamond Bar, CA, USA) was used to create an electroanatomical activation map. Electroanatomical mapping was performed using a 3-D non-fluoroscopic mapping system (CARTO XP™, Biosense Webster Inc, Diamond Bar, CA, USA).

Bipolar electrograms recorded from the distal (M1-M2) and proximal (M3-M4) electrode pair of the mapping catheter (filtered at 30-400Hz), the unipolar electrogram recorded from the distal electrode (M1; filtered at 1-240Hz, Wilson central terminal) and the 12-lead surface ECG were displayed simultaneously and stored on an electrophysiological recording system (Prucka Cardiolab, GE Healthcare, Piscataway, NJ, USA) and on the 3-D mapping system for off line analysis. Bipolar electrograms recorded from the mid electrode pair (M2-M3) were only displayed and stored on the electrophysiological recording system.

To guarantee accurate electroanatomical activation mapping and to avoid annotation of catheter induced PVCs, the VA QRS-morphology of each acquired mapping point was compared to a 12-lead QRS template of the clinical arrhythmia.

Target sites for RFCA were selected based on 1) LAT, 2) the presence of a unipolar QS-configuration and 3) the presence of reversed polarity. Local activation time was measured from the bipolar electrogram recorded from the distal electrode pair of the mapping catheter and was defined as the interval between the initial sharp peak of the electrogram and the onset of the VA QRS. Unipolar electrograms were recorded from the distal electrode of the mapping catheter. The presence of reversed polarity was evaluated from the bipolar electrograms recorded from the distal (M1-M2) and mid (M2-M3) electrode pairs of the mapping catheter and was defined as a rapid simultaneous deflection in opposite direction of the initial part of the bipolar electrograms occurring before the onset of the VA QRS. To record reversed polarity the mapping catheter was positioned parallel or in a shallow angel to the endocardial surface (Figure 1).

Radiofrequency energy was applied at 20-30W with a maximum temperature of 40°C and with external irrigation at 20ml/min to achieve an impedance-fall of 10ohm. If the VA was abolished within 30s, the energy application was continued for 60s. If the VA was not abolished within 30s, the energy application was terminated, the site was tagged as non-successful ablation site on the map and mapping was continued. A successful ablation site was defined as the location where RFCA abolished the VA and was tagged on the map. The procedural endpoint was reached when the targeted VA did not occur spontaneously after a waiting period of 30min after the last application and could not be induced by EPS before and after isoprotenerol infusion.

Electrogram analysis

Electrogram characteristics at successful ablation sites, non-successful ablation sites and at mapping sites within the close vicinity of the successful ablation site (area points) were analyzed. Area points were defined as mapping points acquired within a radius of 15mm from the successful ablation site. The distance between area points and non-successful ablation sites to the VA termination site was measured using the software provided by the CARTO XP system. Area points were further categorized according to the distance to the successful ablation site (1-5mm; 6-10mm; 11-15mm) to study the spatial distribution of the different electrogram characteristics with regard to the successful ablation site. For each analyzed mapping point (1) LAT, (2) unipolar electrogram morphology and (3) the presence of reversed polarity were evaluated. Local activation time, a unipolar QS-configuration and the presence of reversed polarity were compared for successful and non-successful ablation sites.

To further determine the accuracy of LAT, unipolar QS-configuration and the presence of reversed polarity to predict a successful ablation site, electrogram characteristics of successful sites were compared to the characteristics of area points. The cut-off value for LAT to predict a successful ablation site was determined based on the value with the highest combined sensitivity and specificity.

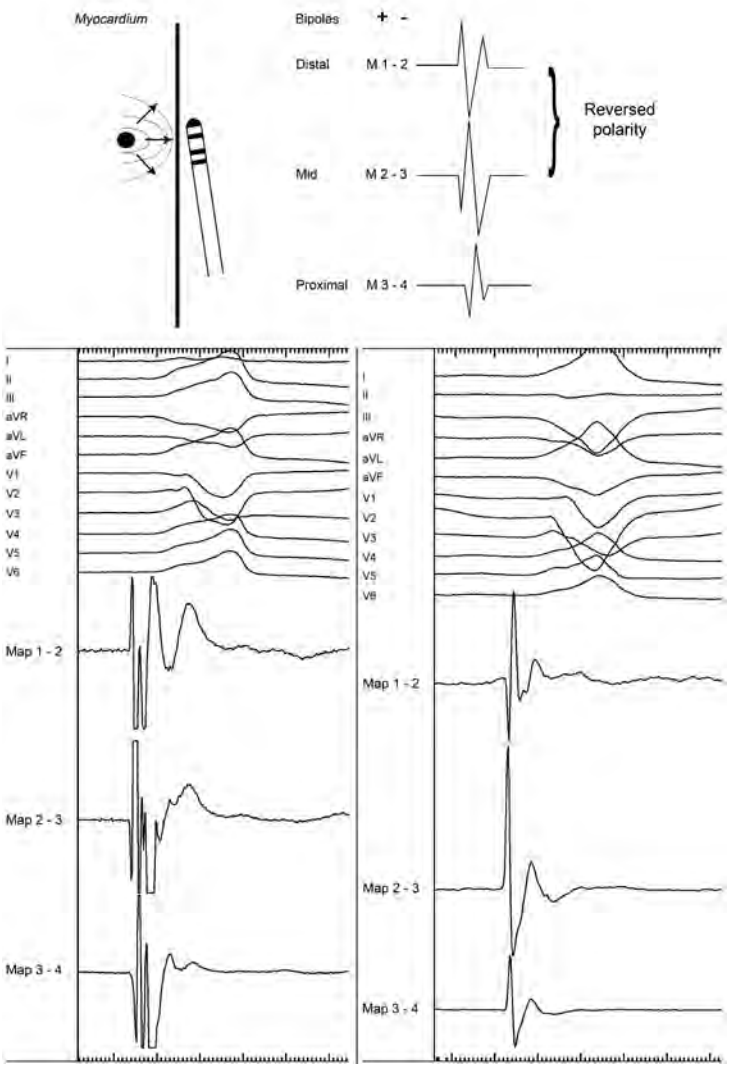


Figure 1.
Panel A. Schematic of an arrhythmogenic focal source within the RVOT (red) with radial wavefront propagation and the position of the quadripolar mapping catheter. The distal (M1-M2) and mid (M2-M3) electrode pairs are simultaneously activated showing a rapid simultaneous deflection in opposite direction of the initial part of the bipolar electrograms defined as reversed polarity.
Panel B. Local bipolar electrograms recorded from the distal (M1-M2), mid (M2-M3) and proximal (M3-M4) electrode pairs of the ablation catheter and the12-lead surface ECG of idiopathic RVOT arrhythmias (sweep-speed 200mm/sec) in two patients. A single radiofrequency application at the recording site abolished the arrhythmia.

To study the impact of reversed polarity on the accuracy to predict successful ablation sites, two different electrophysiological mapping strategies were compared: (1) a conventional approach which was guided by LAT and unipolar QS-configuration and (2) a newly proposed approach guided by LAT and reversed polarity. Both approaches used LAT as a first selection criterion to delineate the area around the focal source within the RVOT. Next, within this area a unipolar QS-configuration or reversed polarity was used to identify the site of origin.

All electrograms were analyzed off-line by two independent observers blinded to the location of the mapping point and to the result of the ablation procedure. In case of discrepancy between the two observers, agreement was reached by consensus.

Statistical analysis

Statistical analysis was performed using SPSS, version 16.0 (SPSS Inc, Chicago, IL, USA). A p-value of <0.05 was considered statistically significant. Normality of distribution was tested using the Kolmogorov-Smirnoff test. Continuous variables are expressed as mean±SD and were compared using the unpaired student's t-test. Categorical variables are expressed as number (%) and were analyzed using the chi-square test. In order to correct for correlations due to multiple measurements within the same patient, robust standard errors were calculated using Sandwich estimators.[23] Adjustment for multiple testing was performed using the Bonferroni correction. To determine the optimal cut-off value for LAT to predict a successful ablation site, a receiver operating characteristic curve was constructed. The cut-off value was based on the LAT value with the highest combined sensitivity and specificity. Finally, to test the clinical impact of electrophysiological mapping based on LAT and reversed polarity on the accuracy to identify a successful RFCA site, the net reclassification improvement compared to conventional mapping was calculated.[24]

Results

Twenty-five consecutive patients (12 male, 43±15 years) with a total of 26 registered VA (22 PVC (85%)) were included in the study. All patients had been symptomatic for 38±40 months and were refractory to therapy with 1.3±1.3 anti-arrhythmic drugs. The VA burden on 24-hour Holter monitoring was 22±17%. All patients had normal left and right ventricular function (mean left ventricular ejection fraction 58±5%) on echocardiography. To rule out structural heart disease additional diagnostic testing was performed and was normal in all patients. Twenty patients underwent exercise testing, coronary angiography was performed in 10 patients, cardiac multi-detector computed tomography in 1 patient, magnetic resonance imaging in 11 patients and nuclear imaging in 3 patients.

Electrophysiology study and radiofrequency catheter ablation

During electrophysiological study, the clinical VA occurred spontaneously in 22/25 (88%) patients. In 3 patients isoprotenerol infusion was required to induce the clinical VA, additional burst pacing was required to initiate the clinical VA in 1 patient. One patient presented with 2 spontaneous VA morphologies (both were targeted).

Electroanatomical activation mapping of the RVOT was performed prior to ablation in all patients (40±29 mapping points per VA). All VA were successfully abolished with a mean of 2.3±1.8 RF applications. Procedural time was 76±24min (including a 30min waiting period after the last RF application) and a fluoroscopy time of 13±8min. Procedural success was achieved in all patients. No procedure related complications occurred and all patients were discharged without in hospital VA recurrence.

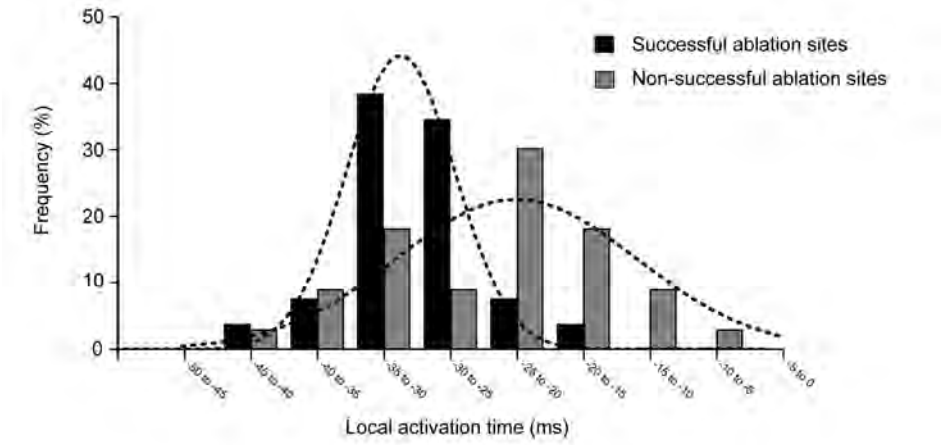


Figure 2. Frequency of local activation time (LAT) at successful ablation sites (black bars) versus non-successful ablation sites (grey bars). The dashed lines indicate the normal distribution of the LAT in the two groups. Please note the important overlap of LAT between successful and non-successful ablation sites.

After 8±7 months of follow-up all patients were free of symptoms without the use of anti-arrhythmic drugs. Twenty patients had a VA burden of <1% on 24-hour Holter monitoring. In 2 patients the VA burden was 2 en 6%, respectively; however the VA QRS-morphology differed from the VA QRS-morphology targeted during the index procedure. In 3 asymptomatic patients, who had disabling symptoms before ablation, 24-hour Holter monitoring was not available.

None of the 4 patients with VT prior to ablation had VT recurrence.

Successful versus non-successful ablation sites

Electrogram characteristics from 26 successful and 33 non-successful ablation sites were compared. Local activation time was significantly earlier at successful ablation sites as compared to non-successful ablation sites (-28±7ms versus -22±8ms, p=0.002). However, there was a considerable overlap in LAT between both groups (Figure 2). Reversed polarity of adjacent bipolar electrograms was observed at 21 of 26 successful ablation sites (85%). In contrast, reversed polarity was absent at all non-successful ablation sites (p<0.001). The presence of a unipolar QS-configuration was similar between successful and non-successful ablation sites (22 (85%) versus 19 (83%), p=0.850).

Spatial distribution of electrogram characteristics

Local activation time, unipolar QS-configuration and the presence of reversed polarity were compared between 26 successful ablation sites and 139 area points within three different categories (Table 1). Local activation time was significantly earlier at successful ablation sites as compared to area points. The best cut-off value to discriminate between a successful ablation site and an area point was a LAT of -23ms. In addition, area points beyond a 5mm radius from the successful ablation site demonstrated less often a unipolar QS-configuration when compared to the successful ablation sites. However, no differences in unipolar electrogram morphology were found between successful ablation sites and area points within a 5mm radius. Moreover, the prevalence of a unipolar QS-configuration at distances between 6-10mm and 11-15mm remained high (63% and 53%, respectively) (Figure 3). Importantly, successful ablation sites showed significantly more often reversed polarity than area points

Table 1. Spatial distribution of electrogram characteristics

	Successful ablation site	Area point		
		1 – 5mm	6 – 10mm	11 – 15mm
N	26	43	51	45
LAT (ms)	-28±7	-21±8*	-18±8*	-18±8*
Unipolar QS-configuration, n (%)	22 (85)	37 (79)	32 (63) †	24 (53) ‡
Reversed polarity, n (%)	21 (81)	2 (5)*	3 (6)*	5 (11)*

LAT= Local activation time; * p<0.001 compared to successful ablation site; † p<0.05 compared to successful ablation site; ‡ p<0.02 compared to successful ablation site

across all categories. The sensitivity to discriminate between a successful ablation site and an area point was slightly higher for LAT (88%) as compared to a unipolar QS (85%) and the presence of reversed polarity (81%), however the specificity to identify a successful site was

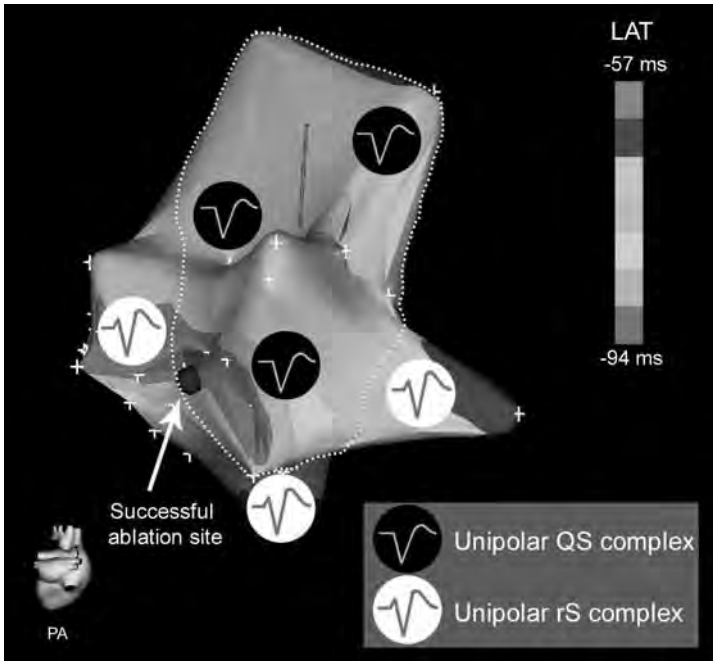


Figure 3. Electroanatomical activation map of a right ventricular outflow tract arrhythmia (posterior view). Local activation time (LAT) is color coded with isochronal steps of 5 ms according to the color bar. The white dotted line delineates the area around the successful ablation site (red tag) that demonstrated a unipolar QS-configuration. Black-with-green icons indicate areas demonstrating unipolar QS-configuration and white-with-red icons correspond to the area demonstrating a unipolar rS configuration. **(for figure in color see page: 254)**

found to be significantly higher for reversed polarity (93%) as compared to LAT (71%) and a unipolar QS-configuration (35%) (Table 2).

Comparison of two mapping strategies to predict a successful ablation site

To study the clinical impact of reversed polarity on the accuracy of electrophysiological mapping of idiopathic RVOT arrhythmias, a comparison was made between a conventional mapping strategy and a newly proposed mapping strategy including reversed polarity. For both strategies, LAT>-23ms was applied as the first criterion. If LAT was >-23ms, this mapping site could be excluded as a successful ablation site with a 97% likelihood. However, if LAT at a certain location was ≤-23ms, the accuracy to positively predict a successful ablation site was only 36%. After excluding mapping sites with LAT>-23ms the conventional mapping strategy used the presence of a unipolar QS-configuration as the second criterion to identify a successful ablation site whereas the new mapping strategy used the presence of reversed polarity. The presence of a unipolar QS-configuration identified the successful

Table 2. Electrogram characteristics

	Sensitivity	Specificity	NPV	PPV
LAT ≤-23ms	88	71	0.97	0.36
Unipolar QS-configuration	85	35	0.92	0.20
Reversed polarity	81	93	0.96	0.68

LAT= Local activation time; NPV= negative predictive value; PPV = positive predictive value

ablation site with 40% accuracy. In contrast, application of reversed polarity as the second criterion led to the identification of the successful ablation site with 86% accuracy (Figure 4). Moreover, mapping based on reversed polarity resulted in a net reclassification improvement of 0.189 (p=0.028). This index of reclassification illustrated that mapping based on LAT and reversed polarity resulted in a significant 'gain of certainty' to identify a successful RFCA site compared to conventional mapping based on LAT and unipolar QS-configuration.[24]

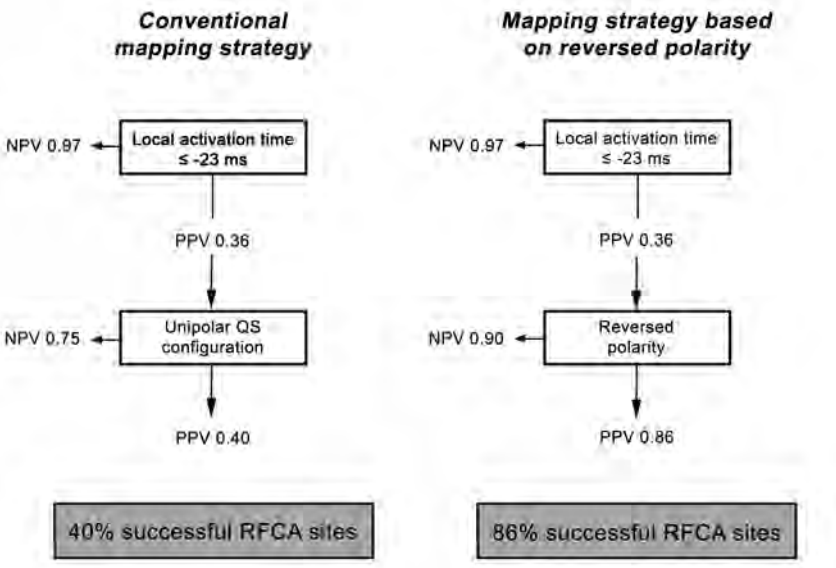


Figure 4. The predictive value of a new mapping strategy guided by local activation time (LAT) and reversed polarity was compared to a conventional mapping strategy guided by LAT and unipolar electrogram morphology. Both approaches use LAT as the primary selection criterion. The new approach uses reversed polarity as the second selection criterion whereas the conventional approach uses the unipolar electrogram morphology (i.e. presence of unipolar QS-configuration). NPV=negative predictive value; PPV=positive predictive value.

Discussion

Key findings of the present study are: (1) the presence of reversed polarity was associated with a high likelihood for a successful RF application; and (2) mapping of idiopathic RVOT arrhythmia based on LAT and reversed polarity resulted in a higher predictive value for a successful ablation, compared to a conventional mapping strategy based on LAT and unipolar electrogram morphology.

Conventional mapping strategies

Several electrophysiological strategies have been described to guide RFCA of focal RVOT arrhythmias. Typically, mapping procedures are guided by unipolar and bipolar electrograms. Unipolar electrograms provide information about the direction of the wavefront: an initial positive deflection of the unipolar electrogram indicates propagation towards the mapping catheter and has a high negative predictive value for a successful ablation site. As the wavefront reaches the electrode and propagates away, the deflection sweeps negative. When the electrode is located at the focal source the wavefront propagates away producing a monophasic QS complex. However, unipolar electrograms provide information about a large area and contain important far-filed signals. In contrast, in bipolar electrograms the far field signal is subtracted out thereby providing information about the local electrical activity, but do not contain information about the direction of the wavefront. Currently, most RFCA procedures for focal arrhythmias are guided by LAT defined by the initial peak of the bipolar electrogram and the rapid negative deflection of the unipolar electrogram, the unipolar electrogram morphology and pace-mapping. Although these criteria have demonstrated their practical value, each technique is associated with its own inherited limitations.[18,20,25,26] The spatial resolution of a good pace-map has been found to be 1.8±0.6cm^2 and inferior to the spatial resolution of activation mapping. Based on this observation pace-mapping was not systematically investigated in our study.[26]

In the current study, LAT was significant earlier at successful ablation sites (-28±7ms) as compared to ablation sites that did not abolish the VA (22±8ms), which is in line with prior studies reporting LAT at effective sites between -24±7 ms and -29±7ms.[3,26] However, we could demonstrate a significant overlap in LAT between successful and non-successful ablation sites. Although the best cut-off value for LAT (-23ms) to discriminate between a successful site and a site in a proximity of less than 15mm provided a high negative predictive value, only a minority of successful sites could be identified correctly. This finding suggests that a cut-off value for LAT can be used to delineate the area of interest, but is not accurate enough to identify a site where RF energy should be applied. Furthermore, the current study confirms and extends prior observations that the area around a site of origin of a focal RVOT VA that exhibits a unipolar QS-configuration is considerably broad.[27] The wide spatial

distribution of a unipolar QS is in line with the low additional value to predict a successful ablation site found in this study.

Reversed polarity

Reversed polarity of bipolar electrograms to guide ablation of focal RVOT arrhythmia was first suggested in a case report by Fisher et al using a custom-built orthogonal electrode array.[28] However, this method to target focal RVOT arrhythmias has not been applied in a large cohort of patients and using a standard quadripolar mapping catheter.

The use of reversed polarity to predict a successful ablation site is based on the hypothesis that rapid radial propagation from a focal source results in simultaneous deflection in opposite direction of the initial part of the bipolar electrograms. Provided that the bipoles are positioned orthogonally to the activation wave front with the focal source ideally located between the bipoles. Due to the cylindrical anatomy of the RVOT it is possible to align a standard quadripolar mapping catheter orthogonally to the myocardial surface.

Indicating wavefront propagation in opposite direction, reversed polarity provides additional information to LAT. A focal source can be assumed if early local activation preceding the VA QRS is present and activation is observed in opposite directions. Combining these two electrogram characteristics is therefore likely to provide a reliable endpoint for catheter mapping. Accordingly, our suggested approach to map focal RVOT arrhythmias by combining LAT with reversed polarity resulted in a high negative predictive value but importantly also in a high positive predictive value to identify a successful ablation site. In contrast, conventional mapping based on LAT and a unipolar QS-configuration had comparable negative predictive but poor positive predictive value.

Procedural aspects

Patients suffering from idiopathic focal RVOT arrhythmias are commonly young and healthy.[29] Therefore important goals when targeting focal RVOT arrhythmias are reduction of radiation exposure and number of RFCA applications needed to terminate the VA. Prior studies reported on mean fluoroscopy time up to 54 minutes targeting RVOT arrhythmias whereas in the current study mean fluoroscopy time was only 13±8min.[19,30] Moreover, the mean number of RFCA applications needed to terminate the VA ranged from 3 to 8 in previous studies but could be reduced to only 2.3±1.8 RFCA applications in the current study.[19,26,30,31] These results indicate that implementation of reversed polarity is likely to reduce both radiation dose and number of RFCA applications.

Limitations

The present study comprised a relatively small number of patients. Therefore the results should be confirmed in a larger population. Furthermore, for statistical purposes LAT was dichotomized according to the cut-off value provided by the ROC-curve analysis, although

this may not fully reflect clinical practice. In addition, during ablation target sites for RFCA were selected based on the combination of early LAT, the presence of a unipolar QS-configuration and the presence of reversed polarity. However, the decision to apply RF energy was made by the operator in a non-randomized fashion. The analyses of LAT, the presence of a unipolar QS-configuration and the presence of reversed polarity have been performed retrospectively. Ideally the newly proposed strategy, combining early LAT and reversed polarity presence, should have been validated prospectively. Finally, based on theoretical considerations the ablation catheter should be pulled back slightly when reversed polarity is recorded to ensure that the catheter tip is in the position of the second electrode. However, this was not systematically evaluated in the present study but seems to be unlikely to further reduce the number of RF applications needed.

Clinical implication

The presence of reversed polarity is easily to obtain and has a high predictive value to identify a successful ablation site in idiopathic focal RVOT arrhythmias. Combining LAT and reversed polarity can predict a successful ablation site with higher accuracy than conventional mapping based on LAT and unipolar QS-configuration. Its clinical application is likely to reduce the number of RFCA applications and radiation exposure to both patient and operator.

Conclusion

The presence of reversed polarity has a high predictive value for a successful ablation site in focal idiopathic RVOT arrhythmias. Combining local activation time and reversed polarity improves the accuracy of identifying the site of origin compared to conventional mapping strategies.

Reference List

(1) Aliot EM, Stevenson WG, Mendral-Garrote JM et al. EHRA/HRS Expert Consensus on Catheter Ablation of Ventricular Arrhythmias: developed in a partnership with the European Heart Rhythm Association (EHRA), a Registered Branch of the European Society of Cardiology (ESC), and the Heart Rhythm Society (HRS); in collaboration with the American College of Cardiology (ACC) and the American Heart Association (AHA). Heart Rhythm 2009;6:886-933.

(2) Takemoto M, Yoshimura H, Ohba Y et al. Radiofrequency catheter ablation of premature ventricular complexes from right ventricular outflow tract improves left ventricular dilation and clinical status in patients without structural heart disease. J Am Coll Cardiol 2005;45:1259-1265.

(3) Sekiguchi Y, Aonuma K, Yamauchi Y et al. Chronic hemodynamic effects after radiofrequency catheter ablation of frequent monomorphic ventricular premature beats. J Cardiovasc Electrophysiol 2005;16:1057-1063.

(4) Bogun F, Crawford T, Reich S et al. Radiofrequency ablation of frequent, idiopathic premature ventricular complexes: comparison with a control group without intervention. Heart Rhythm 2007;4:863-867.

(5) Baman TS, Lange DC, Ilg KJ et al. Relationship between burden of premature ventricular complexes and left ventricular function. Heart Rhythm 2010;7:865-869.

(6) Yarlagadda RK, Iwai S, Stein KM et al. Reversal of cardiomyopathy in patients with repetitive monomorphic ventricular ectopy originating from the right ventricular outflow tract. Circulation 2005;112:1092-1097.

(7) Kobayashi Y, Miyata A, Tanno K et al. Effects of nicorandil, a potassium channel opener, on idiopathic ventricular tachycardia. J Am Coll Cardiol 1998;32:1377-1383.

(8) Gill JS, Mehta D, Ward DE et al. Efficacy of flecainide, sotalol, and verapamil in the treatment of right ventricular tachycardia in patients without overt cardiac abnormality. Br Heart J 1992;68:392-397.

(9) Borger van der Burg AE, de Groot NM, van EL et al. Long-term follow-up after radiofrequency catheter ablation of ventricular tachycardia: a successful approach? J Cardiovasc Electrophysiol 2002;13:417-423.

(10) Calkins H, Kalbfleisch SJ, el-Atassi R et al. Relation between efficacy of radiofrequency catheter ablation and site of origin of idiopathic ventricular tachycardia. Am J Cardiol 1993;71:827-833.

(11) Chinushi M, Aizawa Y, Takahashi K et al. Radiofrequency catheter ablation for idiopathic right ventricular tachycardia with special reference to morphological variation and long-term outcome. Heart 1997;78:255-261.

(12) Coggins DL, Lee RJ, Sweeney J et al. Radiofrequency catheter ablation as a cure for idiopathic tachycardia of both left and right ventricular origin. J Am Coll Cardiol 1994;23:1333-1341.

(13) Zhou L, Keane D, Reed G et al. Thromboembolic complications of cardiac radiofrequency catheter ablation: a review of the reported incidence, pathogenesis and current research directions. J Cardiovasc Electrophysiol 1999;10:611-620.

(14) Joung B, Lee M, Sung JH et al. Pediatric radiofrequency catheter ablation: sedation methods and success, complication and recurrence rates. Circ J 2006;70:278-284.

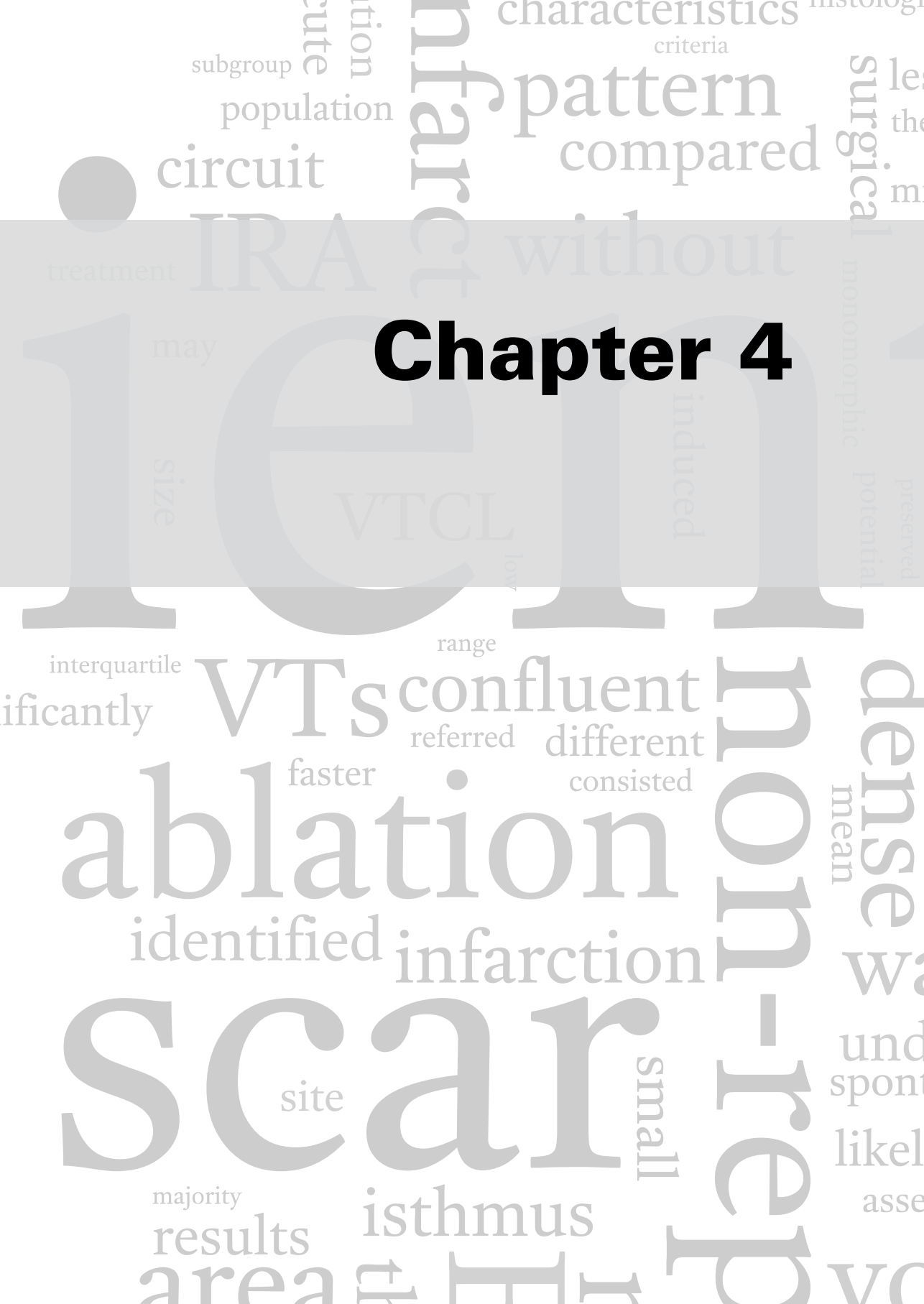
(15) Morwood JG, Triedman JK, Berul CI et al. Radiofrequency catheter ablation of ventricular tachycardia in children and young adults with congenital heart disease. Heart Rhythm 2004;1:301-308.

(16) Weiss C, Willems S, Rueppel R et al. Electroanatomical Mapping (CARTO) of ectopic atrial tachycardia: impact of bipolar and unipolar local electrogram annotation for localization the focal origin. J Interv Card Electrophysiol 2001;5:101-107.

(17) Soejima Y, Aonuma K, Iesaka Y et al. Ventricular unipolar potential in radiofrequency catheter ablation of idiopathic non-reentrant ventricular outflow tachycardia. Jpn Heart J 2004;45:749-760.

(18) Barlow MA, Klein GJ, Simpson CS et al. Unipolar electrogram characteristics predictive of successful radiofrequency catheter ablation of accessory pathways. J Cardiovasc Electrophysiol 2000;11:146-154.
(19) Ribbing M, Wasmer K, Monnig G et al. Endocardial mapping of right ventricular outflow tract tachycardia using noncontact activation mapping. J Cardiovasc Electrophysiol 2003;14:602-608.
(20) Azegami K, Wilber DJ, Arruda M et al. Spatial resolution of pacemapping and activation mapping in patients with idiopathic right ventricular outflow tract tachycardia. J Cardiovasc Electrophysiol 2005;16:823-829.
(21) Yamane T, Shah DC, Jais P et al. Electrogram polarity reversal as an additional indicator of breakthroughs from the left atrium to the pulmonary veins. J Am Coll Cardiol 2002;39:1337-1344.
(22) Damle RS, Choe W, Kanaan NM et al. Atrial and accessory pathway activation direction in patients with orthodromic supraventricular tachycardia: insights from vector mapping. J Am Coll Cardiol 1994;23:684-692.

(23) Zeger SL, Liang KY Longitudinal data analysis for discrete and continuous outcomes. Biometrics 1986;42:121-130.
(24) Pencina MJ, D'Agostino RB, Sr., D'Agostino RB, Jr. et al. Evaluating the added predictive ability of a new marker: from area under the ROC curve to reclassification and beyond. Stat Med 2008;27:157-172.
(25) Joshi S, Wilber DJ Ablation of idiopathic right ventricular outflow tract tachycardia: current perspectives. J Cardiovasc Electrophysiol 2005;16 Suppl 1:S52-S58.
(26) Bogun F, Taj M, Ting M et al. Spatial resolution of pace mapping of idiopathic ventricular tachycardia/ectopy originating in the right ventricular outflow tract. Heart Rhythm 2008;5:339-344.
(27) Man KC, Daoud EG, Knight BP et al. Accuracy of the unipolar electrogram for identification of the site of origin of ventricular activation. J Cardiovasc Electrophysiol 1997;8:974-979.
(28) Fisher WG, Bacon ME, Swartz JF Use of an orthogonal electrode array to identify the successful ablation site in right ventricular outflow tract tachycardia. Pacing Clin Electrophysiol 1997;20:2188-2192.
(29) Nakagawa M, Takahashi N, Nobe S et al. Gender differences in various types of idiopathic ventricular tachycardia. J Cardiovasc Electrophysiol 2002;13:633-638.
(30) Peeters HA, Sippens Groenewegen A, Wever EF et al. Clinical application of an integrated 3-phase mapping technique for localization of the site of origin of idiopathic ventricular tachycardia. Circulation 1999;99:1300-1311.
(31) Klein LS, Shih HT, Hackett FK et al. Radiofrequency catheter ablation of ventricular tachycardia in patients without structural heart disease. Circulation 1992;85:1666-1674.


Chapter 4
characteristics
criteria
subgroup
population
pattern
compared
circuit
IRA
without
treatment
may
size
VTCL
induced
range
interquartile
VTs
confluent
referred
different
faster
consisted
ablation
identified
infarction
scar
non-re
dense
mean
site
small
majority
isthmus
results

Early reperfusion during acute myocardial infarction affects ventricular tachycardia characteristics and the chronic electroanatomical and histological substrate

Adrianus P. Wijnmaalen, Martin J. Schalij, Jan H. von der Thüsen, Robert J.M. Klautz, Katja Zeppenfeld

Circulation. 2010 May 4;121(17):1887-95.

Abstract

Background: Reperfusion therapy during acute myocardial infarction (AMI) results in myocardial salvage and improved ventricular function but may also influence the arrhythmogenic substrate for ventricular tachycardia (VT). This study used electroanatomical (EA) mapping and infarct histology to assess the impact of reperfusion on the substrate and on VT characteristics late after AMI.

Methods and Results: The study population consisted of 36 patients (32 male, 63±15yr) referred for treatment of VT 13±9yrs after AMI. Fourteen patients with early reperfusion during AMI were compared with 22 non-reperfused patients. Spontaneous and induced VTs and the characteristics of EA voltagemaps were analyzed. Twenty-seven patients were treated by radiofrequency catheter ablation. Ten patients (non-reperfused 6) were treated by ventricular restoration with intraoperative cryoablation in 9. During surgery biopsies were obtained from the resected core of the infarct. VT cycle length of spontaneous and induced VTs was shorter in reperfused patients (reperfused 299±52/270±58ms, non-reperfused 378±77/362±74ms, (p=0.01)). An EA patchy scar pattern was present in 71% of reperfused and in 14% of non-reperfused patients (p=0.004). The proportion of EA dense scar was smaller in reperfused patients (24±18% vs. 45±21%, p=0.02). Histological assessment in 10 patients revealed thick layers of surviving myocardium in 75% of reperfused but in none of non-reperfused patients.

Conclusions: Scar size and pattern defined by EA mapping are different between VT patients with and without reperfusion during AMI. Less confluent EA scars match with thick layers of surviving myocardium on histology. Early reperfusion and less confluent electroanatomical scar are associated with faster VTs.

Introduction

Catheter ablation is an important therapeutic option for controlling recurrent ventricular tachycardia (VT) late after acute myocardial infarction (AMI). Mapping studies have shown that reentry circuit locations and VT characteristics vary greatly among patients and are influenced by the 3-dimensional geometry of infarcted areas.[1-3] In animal models, the duration of coronary artery occlusion determines size, transmurality and geometry of myocardial fibrosis after AMI.[4, 5] Thus, it seems likely that early reperfusion, which has become the standard treatment of acute AMI will influence the nature of the VT substrate. Recently, methods have been developed to characterize the VT substrate based on bipolar electrogram characteristics during sinus or paced rhythm. These methods have been applied to ablation of VTs that are not stable for mapping during VT, targeting the substrate with linear radiofrequency lesions at the electrophysiological scar borderzone.[2, 3, 6] Animal studies to validate this substrate based ablation approach were performed in a chronically occluded infarct related artery (IRA) model resulting in a homogeneous dense scar surrounded by a small scar borderzone.[7]

We hypothesized that early reperfusion during AMI results in smaller and less homogeneous scars on electroanatomical voltage maps and faster spontaneous and inducible VT as compared to non-reperfused patients late after MI. To further evaluate the effect of early reperfusion on the VT substrate the results of electroanatomical voltage maps were compared with infarct histology according to the reperfusion strategy in a subgroup of patients undergoing cardiac surgery.

Methods

Patient population

The population comprised of 36 consecutive patients late after AMI referred for catheter ablation or surgical treatment of sustained monomorphic VT without contraindications for LV mapping and without evidence of reversible ischemia. Clinical evaluation consisted of careful history taking regarding the reperfusion strategy during the index myocardial infarction and consecutive ischemic events, arrhythmias and symptoms of heart failure. All patients underwent echocardiography, coronary angiography and nuclear myocardial perfusion imaging to detect ischemia. The results, including the functional status, the presence of a left ventricular (LV) aneurysm, concomitant valvular disease and residual coronary artery disease were evaluated by a team of cardiologists, electrophysiologists and cardiothoracic surgeons according to the institutional protocol. Patients with significant coronary artery stenosis and reversible ischemia on nuclear perfusion imaging, or with a mobile LV thrombus or with NYHA heart failure class IV symptoms were excluded from the study.

Patients presenting with symptoms of heart failure and a dilated or aneurysmatic LV after anterior AMI were considered candidates for a combined surgical approach of ventricular restoration comprising of an endoventricular circular patch plasty and intraoperative VT ablation.[8] In the remaining patients radiofrequency catheter ablation (RFCA) was offered.

Coronary Angiography

All available coronary angiograms obtained during and after the index AMI were reviewed by an interventional cardiologist to assess the effect of the early reperfusion strategy. Based on these results patients were classified as either acutely reperfused with documented open IRA or as not-reperfused. The TIMI (thrombolisis in myocardial infarction) scoring system was used to determine the patency of the infarct related artery (IRA).[9] Patients were considered reperfused when TIMI 3 flow grade was present after reperfusion therapy.

Electrophysiological evaluation

After informed consent all patients underwent electrophysiological evaluation including electrical programmed stimulation (EPS) and LV electroanatomical (EA) voltage mapping.

Studies were performed in the post absorptive, non-sedated state. Antiarrhythmic drugs were discontinued for 5 half-lives, with the exception of amiodarone which was continued in 14 patients. The EPS-protocol consisted of 3 drive-cycle lengths (600, 500 and 400ms) and ≤3 ventricular extrastimuli from 2 right ventricular sites and burst pacing. 12-lead ECGs and intracardiac electrograms were recorded simultaneously with a 48-channel acquisition system (Cardio-Lab 4.1; Prucka Engineering, Houston, TX, USA). The positive endpoint of EPS was reproducible induction of a sustained monomorphic VT lasting ≥30s or requiring termination because of hemodynamic compromise. When catheter ablation was performed the entire protocol was repeated until all inducible VTs were eliminated or until the procedure was classified as ablation failure in the judgment of the physician. Sinus rhythm (SR) EA voltage mapping (CARTO XP EP system Biosense Webster Inc, Diamond Bar, CA, USA) of the LV was performed with a 3.5mm tip quadripolar mapping catheter, interelectrode spacing 2-5-2mm (NaviStar ThermoCooled, Biosense Webster Inc, Diamond Bar, CA, USA) by a retrograde aortic approach. Bipolar voltage maps with a spatial resolution of <15mm were created. Electrical scar in the IRA provided area was defined by voltage criteria. Electrogram amplitudes ≤0.5mV were defined as dense scar, voltages >0.5mV and ≤1.5mV[2, 7] as scar borderzone and a 'patchy pattern' of EA scar as ≥2 low voltage areas separated by areas of preserved voltage (>1.5mV). For each map the surface of the total scar, the scar borderzone and the dense scar were measured using software provided with the CARTO system.

VT was defined as IRA related if the reentry circuit isthmus site was located within the area supplied by the IRA. A reentry circuit isthmus site was defined by either activation and entrainment mapping for tolerated VT or by pace-mapping (≥11/12 lead match between VT QRS and paced QRS morphology and a Stimulus-to-QRS interval (S-QRS) >40ms) in

patients with poorly tolerated VTs or who were scheduled for operation. In the latter, the potential reentry circuit isthmus site was marked by a single RF application to facilitate ablation during surgery.

Ablation

RFCA was performed at isthmus sites during VT for stable VTs and during SR for unstable VTs with an open irrigated tip catheter. Radiofrequency power was applied to a maximum of 50W, provided that the temperature recorded from the electrode remained below 50°C for 60sec. All inducible monomorphic VTs were targeted and RF energy was applied, if a potential isthmus site could be identified.

Cryoablation concomitant to surgery was performed using a Surgifrost® cryoprobe (Cryocath, Montreal Canada). Overlapping applications, up to -150 °C during 90 sec, were applied to the endocardial scar border as identified by the surgeon. The epicardial surface was inspected for the extent of the scar, identified as a white discoloration of the muscular tissue. After opening of the left ventricle the endocardial surface was inspected for the extent of the scar. Next, the thickness of the left ventricular wall was assessed by palpation: a distinction between the normal thickness of the LV wall and the scar can be identified in every patient. In most patients the border at which the ventricular wall changes thickness coincides with the endocardial extention of the visible scar, except for the septal extension. The area for endocardial cryoablation was based on visible extension of the scar tissue or, in rare cases where no visual identification was possible, on the change in wall thickness.[10] Care was taken that the VT reentry circuit isthmus site marked during catheter mapping was included in the ablation line. The encircling cryoablation line coincided with the suture line of encircling endoventricular patch plasty performed after ablation. VTs with a morphology corresponding to 12-lead surface ECG documentation of a spontaneous VT were considered clinical and VTs with a CL corresponding the CL of a VT documented in the ICD as presumptive clinical VT.[11] Complete ablation success was defined as the absence of any inducible monomorphic VT after the ablation procedure. Partial success was defined as successful ablation of one or more clinical/presumptive clinical VT, but other VT remained inducible; and ablation failure was defined by continued inducibility of the clinical/presumptive clinical VT. Acute success was tested immediately after RFCA in patients who underwent catheter ablation and during a second EPS before hospital discharge in patients who underwent surgery.

Histological assessment

In patients treated with surgical ablation and/or ventricular restoration transmural biopsies were taken from the removed central part of the LV scar and were systematically assessed by a pathologist blinded to clinical history and mapping findings. Routine H&E stains were performed on 5 µm formalin-fixed paraffin embedded (FFPE) sections. All sections were

analyzed for the presence and distribution of myocardial fibrosis. Assessment included visual scoring for density, location (predominance of subendocardial or subepicardial fibrosis) and extent of fibrosis and evaluation of the maximum percentage of transmurality. The identified area of most extensive fibrosis was further morphometrically analyzed for total wall thickness, thickness of the remaining viable myocardium and the ratio of remaining myocardium thickness to total wall thickness. In addition, the spatial relation between viable myocardium and fibrous tissue was assessed and scored for each section and compared to the EA mapping results of the core infarct region.

Statistical Analysis

Continuous variables are expressed as mean±SD, and categorical variables as frequency(%). Mann Whitney U-test and Fishers Exact test were used to compare data when appropriate. Mean VTCL was compared after first averaging the VTCL of individual patients and subsequently perform analysis. All statistical analyses were performed with SPSS software (version 16 SPSS Inc., Chicago, Illinois). For all tests a p-value ≤0.05 was considered significant.

Results

Baseline criteria

The 36 patients (63±15yr, 32 male) were referred for treatment of VT 13±9 years after AMI. Fourteen (38%) patients had undergone acute reperfusion therapy. Reperfusion was achieved by PCI in 8 patients and thrombolysis in 5. In one patient with an occluded LAD collateral flow to the IRA (Rentrop grade 3) was present at the time of acute infarction. This was considered spontaneous reperfusion of the infarcted area. The time from onset of symptoms to presentation was available in 12 patients. All patients were admitted within 6 hours after onset of symptoms. The median symptom-onset to presentation time was 2 hours and 45 minutes (interquartile range 1h – 5h40min). The median estimated time to needle or time to balloon was 45min (interquartile range 36min – 1h) and 1h (interquartile range 30min – 2h), respectively resulting in a median symptom onset to balloon/needle time of 3h30min (interquartile range 2h6min – 6h6min). Twenty-two patients did not undergo early reperfusion therapy. Twenty-two (60%) had anterior wall infarction, 11 (31%) inferior wall infarction, 2 (6%) posterior wall infarction and 3 (8%) had more than one infarct location. In these 3 patients the IRA were the left anterior descending (LAD) and right coronary artery (RCA); one patient underwent successful thrombolysis of the LAD and RCA subsequently and was classified as reperfused patient. The remaining two had chronic occlusion of the LAD and RCA and were classified as non-reperfused patients. At referral the IRA was patent in all patients who had undergone early reperfusion and occluded in 17 non-reperfused

patients. In 5 non-reperfused patients the IRA was patent due to late PCI in 4 and late spontaneous reperfusion in 1.

After evaluation 9 (25%) patients were offered a combined approach of surgical ventricular restoration and intraoperative VT ablation. In one patient surgical ventricular restoration without cryoablation was performed after initial catheter ablation. The baseline characteristics of the patients are summarized in table 1.

Table 1. Baseline Characteristics

	All n=36	**Reperfused** n=14	**Non-Reperfused** n=22	**p=**
Male	32(89)	13(93)	19(86)	1.0
Age (year)	63±15	60±11	65±16	0.05
Diabetes	5(14)	1(7)	4(18)	0.6
Atrial Fibrillation	3(8)	2(14)	1(5)	0.3
Time after AMI (year)	13±9	8±5	16±10	0.01
Anterior AMI	22(60)	10(71)	11(50)	0.3
Inferior AMI	11(31)	3(21)	8(36)	0.5
Posterior AMI	2(6)	0	2(9)	0.5
Multiple AMI	3(8)	1(7)	2(9)	1.0
Late PCI of IRA	8(22)	4(29)	5(23)	0.7
Late CABG of IRA	9(25)	1(7)	8(36)	0.06
NYHA class				
1	21(58)	9(64)	12(55)	0.8
2	9(25)	3(21)	6(27)	0.8
3	6(17)	2(14)	4(18)	0.8
Echocardiography				
LVEF (%)	30±13	33±16	28±11	0.5
Anterior aneurysm	18(40)	7(50)	11(50)	1.0
LV hypertrophy	3(8)	0	3(14)	0.3
Failed AAD				
Amiodarone	16(44)	4(29)	12(55)	0.2
Sotalol	10(28)	4(29)	6(27)	1.0
Class I	4(11)	1(7)	3(14)	1.0
B-Blocker	29(81)	11(79)	18(82)	1.0

Medication at referral				
Amiodarone	14(38)	4(29)	10(45)	0.5
Sotalol	6(17)	4(29)	2(9)	0.1
Class I	2(6)	2(14)	0	0.2
B-Blocker	24(67)	10(71)	14(64)	0.7
ACE-I/ATII antagonist	35(97)	14(100)	20(91)	0.5
Diuretics	23(64)	7(50)	16(73)	0.3
Spontaneous VT				
Number distinct VT	1.6±1.7	1.4±1.3	1.7±1.1	0.4
Mean CL (ms)	353±78	299±52	378±77	0.01
Shortest CL (ms)	328±74	279±55	352±72	0.01
Longest CL (ms)	381±94	316±62	411±92	0.01
Mean CL without AAD (ms)	337±65	297±51	351±66	0.07
Mean CL without amiodarone (ms)	334±65	302±53	355±65	0.05
ICD	18(50)	5(36)	13(59)	0.3

AMI indicates acute myocardial infarction; PCI, percutaneous coronary intervention; IRA, infarct related artery; CABG, coronary artery bypass graft; NYHA, New York heart association; LVEF, left ventricular ejection fraction; VT ventricular tachycardia; CL, cycle length; ICD, internal cardiac defibrillator; AAD, anti arrhythmic drugs; ACE-I ACE inhibitor; ATII, angiotensin II. Data are displayed as mean±SD or frequency(%).

Spontaneous VT

Fifty-five different spontaneous VT were registered during 4.7±5 months preceding referral. The number of different VT did not differ between reperfused and non-reperfused patients (1.4±1.3 versus 1.7±1.1, p=0.4). Twenty VTs were documented on 12-lead surface ECGs and 35 on local electrograms stored in the ICD. In the latter group a difference in VTCL of >30ms was considered as different VT. The VTCL was significantly shorter in reperfused patients as compared to non-reperfused patients (299±52ms vs. 378±77ms, p=0.01) (figure 1). To correct for the effect of antiarrhythmic drugs and specifically of amiodarone on VTCL, the mean CL of VTs registered without any AAD and without amiodarone were compared. There was a non-significant tendency to a shorter VTCL without AAD and a significant shorter VTCL without amiodarone in reperfused compared to non-reperfused patients (table 1).

Electrophysiological evaluation

VT was inducible in all patients with a total of 80 different induced VTs. The CL of the first induced VT (the positive endpoint of EPS) was significantly shorter in reperfused patients (278±80ms versus 391±109ms, p=0.002). A similar difference was found for the mean VTCL (270±58 vs. 362±74, p=0.001) (figure 1).

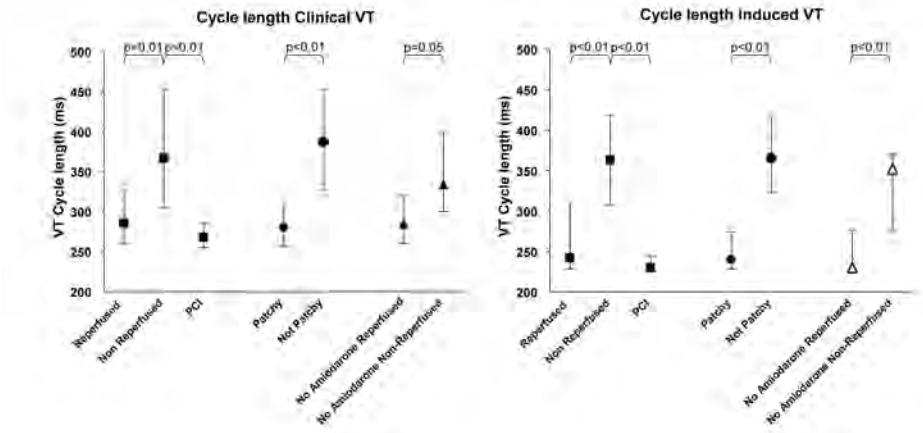


Figure 1. The median and interquartile range for spontaneous (panel A) and induced (panel B) VTCL are displayed for reperfused vs. non-reperfused patients vs. patients after PCI, for patients with a patchy vs. patients without a patchy pattern of electroanatomical scar and for patients with and without amiodarone treatment. CL indicates cycle length; EP electrophysiological study; PCI, percutaneous coronary intervention; VT, ventricular tachycardia.

In 71% of reperfused patients fast VTs with a CL<250ms were inducible compared to 23% non-reperfused patients (p=0.003). After exclusion of patients on amiodarone during EPS the induced VTCL remained significantly shorter in reperfused patients (254±51ms vs. 334±65ms, p=0.006).

Electroanatomical mapping

LV voltage mapping was performed with a mean number of 214±43 mapping points. The total scar surface area (bipolar voltage<1.5mV) was comparable in reperfused and non-reperfused patients (65±48cm^2 vs. 85±46cm^2). However, the surface area of dense scar (bipolar voltage<0.5mV) and the percentage of dense scar in relation to total scar was significantly smaller in the reperfused group (reperfused 21±25 cm^2 and 24±18% vs. non-reperfused 42±32 cm^2 and 45±21%, p=0.02 and p=0.002 respectively).

A patchy scar pattern in the IRA related area was found in 13(36%) patients. Ten of 14 reperfused patients (71%) had a patchy pattern but only 3 (14%) non-reperfused (p=0.001) (figure 2).

In patients who underwent primary PCI the differences as compared to non-reperfused patients were even more pronounced. In these patients the average CL of clinical and induced VTs was 270±23ms and 239±24ms, respectively (figure 1). The average absolute surface area of dense scar was 11±12cm^2, the mean percentage of dense scar was 14±12% and 7(88%) had a patchy scar pattern.

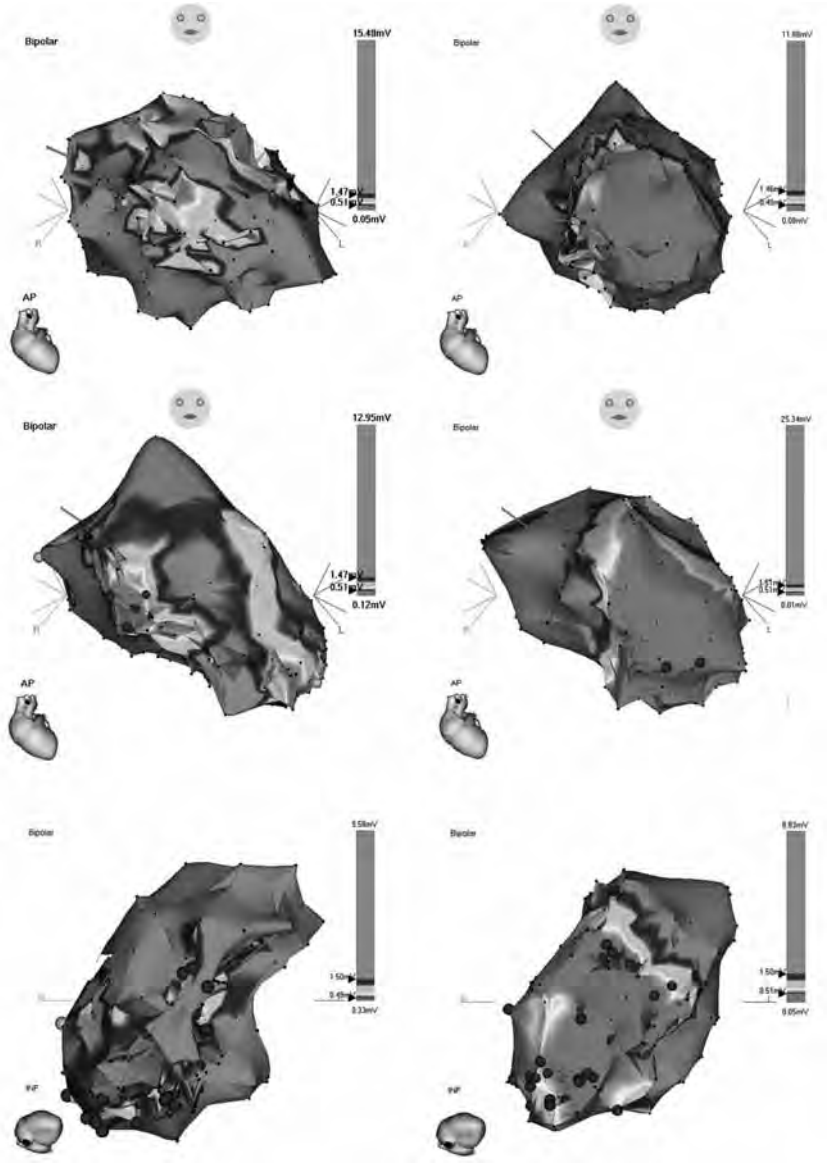


Figure 2. Left ventricular electroanatomical voltagemaps of six patients. Bipolar voltages are color coded according to the colorbar. Voltages <1.5mV were considered abnormal. The 3 maps on the left hand side are obtained in reperfused patients and the 3 on the right in non-reperfused patients. The scar pattern is patchy in reperfused and homogeneous in non-reperfused patients. **(for figure in color see page: 255)**

The targeted reentry circuit sites of VT were located within the scar area supplied by the IRA in 33 patients. In 3 patients no reentry circuit isthmus side could be identified based on the above defined criteria. However, the VT QRS morphology was compatible with an exit site located in the area supplied by the IRA.

The results of the electrophysiological evaluation are summarized in table 2.

Table 2. EPS and electroanatomical mapping

	All n=36	**Reperfused** n=14	**Non-Reperfused** n=22	**p=**
Induced VT at EPS				
Number distinct VT	2.3±1.6	2.1±1.7	2.5±1.6	0.5
CL first induced VT (ms)	347±112	278±80	391±109	0.002
Mean CL (ms)	326±81	270±58	362±74	0.001
Shortest CL (ms)	290±62	251±37	314±63	0.001
Longest CL (ms)	363±117	292±90	409±112	0.002
Mean CL without AAD (ms)	297±70	254±51	334±65	0.006
Points voltagemap	214±43	220±44	211±56	0.6
Surface area map (cm^2)	244±55	249±55	242±55	0.7
Surface area scar (cm^2)	77±47	65±48	85±46	0.2
Surface area dense scar (cm^2)	35±32	21±25	42±21	0.02
Surface area borderzone (cm^2)	43±24	44±29	42±21	0.8
Borderzone % of scar	62±22	76±17	54±21	0.002
Patchy pattern of scar	13(36)	10(71)	3(14)	0.001

CL indicates cycle length; EPS, electrical programmed stimulation; VT, ventricular tachycardia; AAD, antiarrhythmic drugs. Data are expressed as frequency (%) or mean±SD.

Ablation

Catheter ablation was performed in 24/27 patients. In 3 patients, all after early reperfusion with non-tolerated VT (average CL 227±7ms) and a patchy scar pattern no potential VT isthmus site could be identified. In 2 non-reperfused patients epicardial catheter ablation was performed after endocardial ablation failure, which was successful in one. In none of the reperfused patients an epicardial ablation approach was considered appropriate. No procedure related complications were observed.

Ten patients were treated by surgery after electrophysiological evaluation. Nine patients (reperfused 3 (21%), non-reperfused 6 (27%)) were treated by surgical cryoablation and surgical ventricular restoration. One patient underwent surgical ventricular restoration without cryoablation after catheter ablation. There was one peri-operative death due to

Table 3. Treatment and Outcome

	All n=36	Reperfused n=14	Non-Reperfused n=22	p=
RFCA	27(75)	11(79)	16(73)	1.0
Complete	14(52)	5(45)	9(56)	0.3
Partial	9(33)	3(27)	6(38)	0.3
Failure	4(15)	3(27)	1(5)	0.3
Intraoperative EC	9(25)	3(21)	6(27)	1.0
Complete	4(44)	1(33)	3(50)	0.5
Partial	0	0	0	0.5
Failure	3(33)	2(67)	1(17)	0.5
Overall Result				
Complete	18(50)	6(43)	12(55)	0.2
Partial	9(25)	3(21)	6(27)	0.2
No	7(20)	5(36)	2(10)	0.2

Two patients who underwent intraoperative EC did not undergo post-operative EPS, RFCA indicates radiofrequency ablation; EC, encircling cryoablation. Data are expressed as frequency(%).

heart failure. One patient refused post-operative EPS. Outcome after ablation did not differ between reperfused and non-reperfused patients (table 3).

Histological assessment

Histological assessment was performed in the subpopulation of 10 patients undergoing a surgical intervention (reperfused 4, non-reperfused 6). In all non-reperfused patients focal, transmural fibrosis was found; in contrast 3/4 patients with early reperfusion had only non-transmural fibrosis (Figure 3A+B). The average wall thickness of the infarcted area was 1.4±0.7mm. In reperfused patients the average wall thickness was significantly thicker than in non-reperfused patients (2.0±0.6 mm versus 1.0±0.5mm, p=0.03, Figure 3C). The average thickness of viable myocardium even in the most severely fibrotic area was 1.0±0.8 mm in reperfused patients, translating to a ratio of viable myocardium to total wall thickness of 0.5±0.3. In the patients (4 reperfused, 1 non-reperfused) with a patchy pattern of EA scar the average wall thickness was thicker than in patients with a homogeneous EA scar (1.9±0.5mm vs. 0.8±0.2mm, p=0.01). The extent to which viable myocytes were interspersed with fibrosis was categorized (figure 4). Five dominant histological patterns were identified: (A) Contiguous areas of viable myocardium, (B) small confluent areas of fibrosis surrounded by viable myocardium, (C) confluent areas of fibrosis containing only strands of viable cardiomyocytes, (D) confluent areas of fibrosis containing solitary viable cardiomyocytes and (E) transmural confluent fibrosis. The first two patterns were only found in 3 patients after reperfusion and matched with a patchy pattern of EA scar in the core infarct region. In

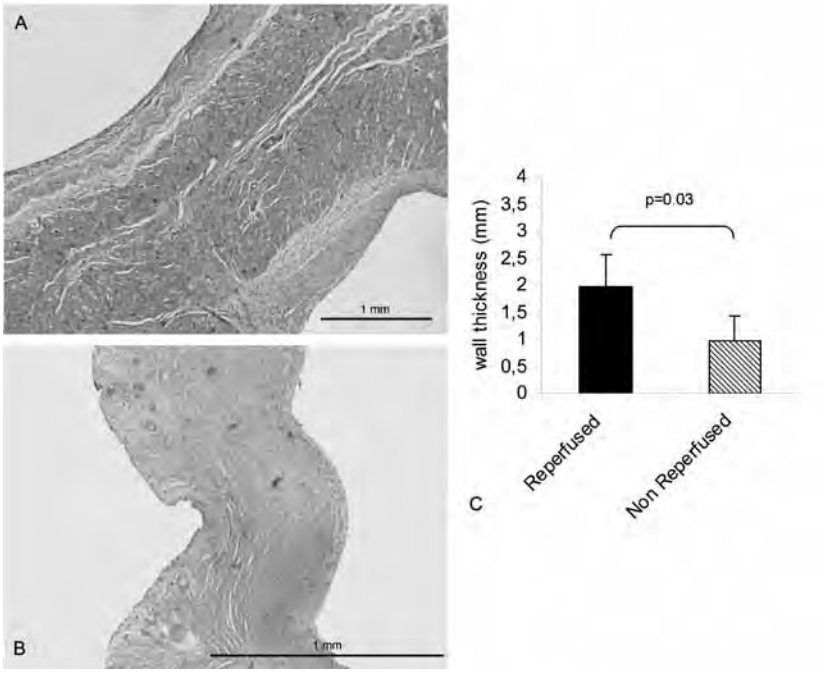
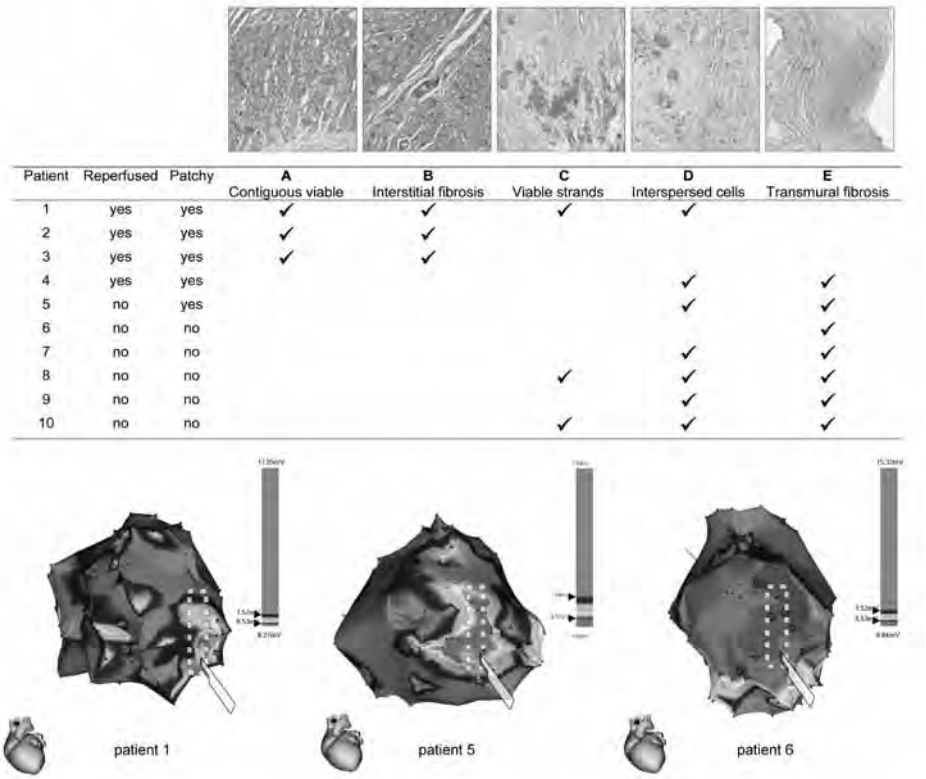


Figure 3. Representative slides of transmural biopsies from the core infarct zone in 2 patients (H&E stain). Panel A: small mid wall fibrosis surrounded by thick viable myocytes bundles in a patient after early reperfusion and with a patchy pattern of EA scar. Panel B: mural thinning with dense transmural fibrosis in a non-reperfused patient with a homogeneous pattern of EA scar with only interspersed cardiomyocytes. Panel C: average wall thickness of the area of most extensive fibrosis in myocardial biopsies of reperfused (n=4; 2.0±0.6 mm) and non-reperfused (n=6; 1.0±0.5 mm) patients. **(for figure in color see page: 256)**

2 patients with a patchy EA pattern of scar (one reperfused, one non-reperfused) transmural fibrosis with solitary viable cardiomyocytes was found at histological assessment. However, in these two patients the core infarct region which was resected consisted of dense scar at mapping (patient 5 in figure 4). In the 5 non-reperfused patients with a homogeneous scar on mapping no contiguous areas of viable myocardium were found. Three representative examples of EA maps (patient 1, 5 and 6) were incorporated in the figure. The assumed area that was resected by the surgeon is indicated on the maps.

Discussion

The current study evaluates the effect of early reperfusion of the infarct related artery on VT characteristics and the VT substrate by EPS, 3-D electroanatomical voltage mapping and histology in patients, who present with VT late after AMI.



Patient	Reperfused	Patchy	A Contiguous viable	B Interstitial fibrosis	C Viable strands	D Interspersed cells	E Transmural fibrosis
1	yes	yes	✓	✓	✓	✓	
2	yes	yes	✓	✓			
3	yes	yes	✓	✓			
4	yes	yes				✓	✓
5	no	yes				✓	✓
6	no	no					✓
7	no	no				✓	✓
8	no	no			✓	✓	✓
9	no	no				✓	✓
10	no	no			✓	✓	✓

Figure 4 The relation between viable myocytes and fibrosis was characterized. Five patterns of local histological scar were identified (A-E). The presence of any of these types in the assessed core infarct region was scored and compared to the presence of reperfusion and the pattern of electroanatomical scar in the 10 patients in whom histological assessment was performed. Three representative examples of EA maps (patient 1, 5 and 6) are shown, the assumed area that was resected by the surgeon is indicated. **(for figure in color see page: 257)**

The main finding of the study is that characteristics of low voltage scars after AMI are different in patients with and without reperfusion therapy. Early reperfusion is associated with less dense and less confluent electroanatomical scars that appear to give rise to faster spontaneous and inducible VTs. The electrophysiological findings match with the histological assessment demonstrating that the LV core infarct area consists of at least 50% viable myocardium in reperfused patients.

To the best of our knowledge this is the first study to report on differences in EA ventricular voltage maps between post-AMI patients with and without successfully reperfused IRA and their potential impact on clinical arrhythmias.

Reperfusion and myocardial scar

Early reperfusion during AMI results in myocardial salvage and reduced mortality during follow-up.[12] Animal studies showed that the duration of coronary artery occlusion is related to infarct size and extend of transmural necrosis.[4, 5] Early reperfusion resulted in necrosis of the inner third of the wall extending towards the midmyocardium, whereas late reperfusion or permanent occlusion resulted in an uniform transmural necrosis.[5] Similar findings were made in human autopsied hearts with acute myocardial infarction after treatment with thrombolysis.[13] These findings from the acute phase of AMI are supported and extended by our data as biopsies were taken in the chronic healing phase 13±9 years after the index MI in 10(28%) of the studied patients. Likely as a result of transmural necrosis the core infarct consisted of transmural fibrosis in non-reperfused patients whereas the majority of early reperfused patients showed no transmural fibrosis at all with thick layers of viable myocardium even in the core infarct region.

The current gold-standard in electrophysiology to define scars after MI is based on electroanatomical voltage criteria. Mapping studies in a porcine model of healed myocardial infarction after chronic occlusion of the IRA revealed large, homogeneous areas of very low voltages surrounded by only a small scar borderzone.[7] These very low voltage areas, arbitrarily defined as <0.5mV, are likely to reflect dense, transmural scar typical for chronic occlusion of the IRA without collateral circulation, whereas the surrounding borderzone may reflect non-transmural scar areas which are partly supplied by non IRAs. A similar pattern of a central homogeneous dense scar area surrounded by the EA borderzone was found in the majority of non-reperfused patients in this study.

Total infarct size defined as areas of electrograms <1.5mV was similar in reperfused and non-reperfused patients. However, acute reperfusion with a median symptom onset to balloon/needle time of 3h30min does not completely abort myocardial infarction but resulted in non-transmural scars as confirmed by histology in a subgroup of patients and contributed to total infarct size using an EA cut-off value of <1.5mV.

Of importance, the total area of electrograms <0.5mV was significantly smaller and the scar borderzone defined by electrograms between 0.5 and 1.5mV significantly larger in reperfused patients which is in line with the histological findings demonstrating only non-transmural scar in the majority of reperfused patients.

In addition, reperfused patients had less confluent EA scar in which areas of lower voltage were frequently interspersed by areas that show relatively preserved or normal bipolar electrograms. These electrograms do not exclude intramural fibrosis as demonstrated by histology. The EA findings likely reflect an inhomogeneous distribution of viable myocardium and fibrosis. Preserved voltage areas are more likely to contain predominantly viable myocardium interspersed by fibrous tissue whereas dense EA scar likely reflects confluent areas of fibrosis containing only strands of viable cardiomyocytes (figure 3).

Arrhythmia and EA scar

Precondition for scar related VT is slow conduction through narrow bundles of surviving myocytes bounded by fibrous tissue.[14]

VTCL is determined by circuit path length and conduction velocity. Increasing isthmus length contributes to circuit path length with consecutive longer VTCL.[15] In a canine infarct model zones of slow conduction and lines of block, bordering the protected isthmus coincided with areas where the borderzone of viable myocardium was thinnest and where the local gradient in borderzone thickness was maximal. In contrast, regions of fast conduction coincided with areas of thicker borderzones with minimal gradients.[1, 16]

Tachycardia related slow conducting channels have been identified within dense EA scar areas in the majority of patients with monomorphic VT after AMI. The mean length of these channels was 23±11mm and the mean CL of the channel related VT was 365±77ms, similar to VLCL found in non-reperfused patients in our study.[17]

The larger and confluent dense scar areas found in patients without reperfusion are more likely to contain longer protected slow conducting channels which may explain the observed longer arrhythmia CL.[15] In contrast, in reperfused patients small areas of dense scars are interspersed with areas of preserved voltages and likely preserved conduction velocity referred to as patchy pattern. Small areas of dense scar and thicker infarct borderzones may result in shorter isthmus length, faster conduction and therefore shorter VTCL. (example provided as online supplement)

Clinical implications

The current study has demonstrated significant differences in the electroanatomical and histological substrate between early reperfused patients and patients with a chronically occluded infarct related artery. In addition, among post-AMI patients who underwent early reperfusion a shift seems to occur towards faster arrhythmias likely because of the reperfusion induced change of the substrate. Previous studies providing insights into the underlying substrate of reentry circuits of VT and the importance of the scar borderzone were performed in patients with a chronically occluded IRA.

Currently RFCA of fast and unstable VT requires a substrate based approach that targets the borderzone of scar relying on voltage mapping and pace-mapping. This substrate based approach was validated in an animal model of chronic occluded IRA with large homogeneous electroanatomical scars surrounded by a small borderzone. The larger border zone in reperfused patients with only small areas of dense scar on mapping and histology, however may require a different mapping approach. Pace-mapping to define VT exit sites, might be less reliable or not applicable if pacing is performed within short protected isthmuses. Whether a 'patchy pattern' of EA scar after reperfusion will pose a challenge in substrate based mapping and ablation needs further evaluation. Studies in animal models that reflect the anatomical substrate in the reperfusion era are warranted to reevaluate the relationship

of the VT circuit and the architecture of the scar which might influence the concept of substrate based ablation.

Limitations

Reperfused patients accounted for one third of the studied population. These patients presented on average 7.7 years earlier than non-reperfused patients. There might be an ascertainment bias such as that the non-reperfused patients represent a subgroup of long term survivors. In addition, alterations in the anatomy of the VT substrate over time that may occur due to increased wall stress, ischemia, hypertension or medication, or due to gradual changes after infarct healing can not be excluded as potential confounders to the presented results. However, the difference in presentation time might reflect advances in recognition and reperfusion strategies of ST-segment elevation AMI in our patient population. The observational nature and relatively small sample size of the study limits the further identification of possible confounders. Since all patients in the current study were referred for ablation of VT, larger studies in a general population of patients after MI are warranted to further elucidate the effect of early reperfusion on arrhythmogenisis and characteristics of VTs.

All biopsies were taken from the central part of the infarcted area as identified by the surgeon. The scar areas were not resected completely, therefore small areas of transmural fibrosis in the core infarcted area in reperfused patients might be missed. In addition, transmural biopsies were only available from the small subgroup of patients who underwent surgery.

Conclusions

There are marked differences in EA scar size and pattern between patients with and without successful reperfusion at the time of myocardial infarction. Less confluent EA scars match with layer of surviving myocyte bundles on biopsy. Early reperfusion and less confluent EA scar are associated with faster ventricular tachycardias which might influence substrate based ablation strategies.

Reference List

(1) Ciaccio EJ, Ashikaga H, Kaba RA, Cervantes D, Hopenfeld B, Wit AL, Peters NS, McVeigh ER, Garan H, Coromilas J. Model of reentrant ventricular tachycardia based on infarct border zone geometry predicts reentrant circuit features as determined by activation mapping. Heart Rhythm. 2007; 4:1034-45.

(2) Marchlinski FE, Callans DJ, Gottlieb CD, Zado E. Linear ablation lesions for control of unmappable ventricular tachycardia in patients with ischemic and nonischemic cardiomyopathy. Circulation. 2000; 101:1288-96.

(3) Verma A, Marrouche NF, Schweikert RA, Saliba W, Wazni O, Cummings J, Abdul-Karim A, Bharqava M, Burkhardt JD, Kilicaslan F, Martin DO, Natale A. Relationship between successful ablation sites and the scar border zone defined by substrate mapping for ventricular tachycardia post-myocardial infarction. Journal of Cardiovascular Electrophysiology. 2005; 16:465-471.

(4) Reimer KA, Lowe JE, Rasmussen MM, Jennings RB. The wavefront phenomenon of ischemic cell death. 1. Myocardial infarct size vs duration of coronary occlusion in dogs. Circulation. 1977; 56:786-94.

(5) Miyazaki S, Fujiwara H, Onodera T, Kihara Y, Matsuda M, Wu DJ, Nakamura Y, Kumada T, Sasayama S, Kawai C, . Quantitative analysis of contraction band and coagulation necrosis after ischemia and reperfusion in the porcine heart. Circulation. 1987; 75:1074-82.

(6) Soejima K, Suzuki M, Maisel WH, Brunckhorst CB, Delacretaz E, Blier L, Tung S, Khan H, Stevenson WG. Catheter ablation in patients with multiple and unstable ventricular tachycardias after myocardial infarction: short ablation lines guided by reentry circuit isthmuses and sinus rhythm mapping. Circulation. 2001; 104:664-9.

(7) Reddy VY, Wrobleski D, Houghtaling C, Josephson ME, Ruskin JN. Combined epicardial and endocardial electroanatomic mapping in a porcine model of healed myocardial infarction. Circulation. 2003; 107:3236-42.

(8) Guiraudon GM, Thakur RK, Klein GJ, Yee R, Guiraudon CM, Sharma A. Encircling endocardial cryoablation for ventricular tachycardia after myocardial infarction: experience with 33 patients. Am Heart J. 1994; 128:982-9.

(9) Sheehan FH, Braunwald E, Canner P, Dodge HT, Gore J, Van NP, Passamani ER, Williams DO, Zaret B. The effect of intravenous thrombolytic therapy on left ventricular function: a report on tissue-type plasminogen activator and streptokinase from the Thrombolysis in Myocardial Infarction (TIMI Phase I) trial. Circulation. 1987; 75:817-29.

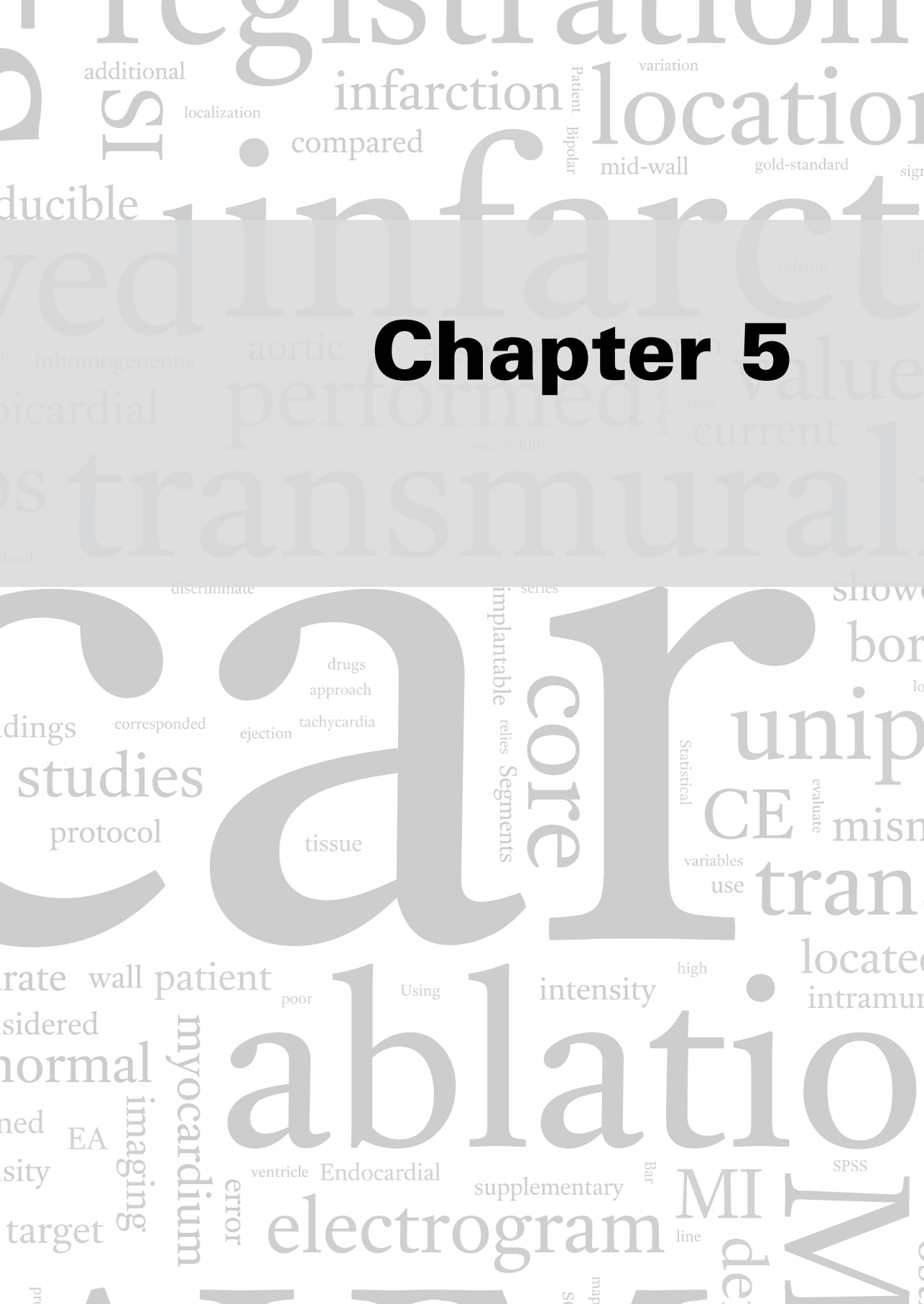
(10) Dor V, Sabatier M, Di DM, Montiglio F, Toso A, Maioli M. Efficacy of endoventricular patch plasty in large postinfarction akinetic scar and severe left ventricular dysfunction: comparison with a series of large dyskinetic scars. J Thorac Cardiovasc Surg. 1998; 116:50-9.

(11) Aliot EM, Stevenson WG, Almendral-Garrote JM, Bogun F, Calkins CH, Delacretaz E, Della BP, Hindricks G, Jais P, Josephson ME, Kautzner J, Kay GN, Kuck KH, Lerman BB, Marchlinski F, Reddy V, Schalij MJ, Schilling R, Soejima K, Wilber D. EHRA/HRS Expert Consensus on Catheter Ablation of Ventricular Arrhythmias: developed in a partnership with the European Heart Rhythm Association (EHRA), a Registered Branch of the European Society of Cardiology (ESC), and the Heart Rhythm Society (HRS); in collaboration with the American College of Cardiology (ACC) and the American Heart Association (AHA). Heart Rhythm. 2009; 6:886-933.

(12) The effects of tissue plasminogen activator, streptokinase, or both on coronary-artery patency, ventricular function, and survival after acute myocardial infarction. The GUSTO Angiographic Investigators. N Engl J Med. 1993; 329:1615-22.

(13) Matsuda M, Fujiwara H, Onodera T, Tanaka M, Wu DJ, Fujiwara T, Hamashima Y, Kawai C. Quantitative analysis of infarct size, contraction band necrosis, and coagulation necrosis in human autopsied hearts with acute myocardial infarction after treatment with selective intracoronary thrombolysis. Circulation. 1987; 76:981-9.

(14) De Bakker JM, van Capelle FJ, Janse MJ, Wilde AA, Coronel R, Becker AE, Dingemans KP, van Hemel NM, Hauer RN. Reentry as a cause of ventricular tachycardia in patients with chronic ischemic heart disease: electrophysiologic and anatomic correlation. Circulation. 1988; 77:589-606.
(15) Ciaccio EJ. Dynamic relationship of cycle length to reentrant circuit geometry and to the slow conduction zone during ventricular tachycardia. Circulation. 2001; 103:1017-24.
(16) Peters NS, Coromilas J, Severs NJ, Wit AL. Disturbed connexin43 gap junction distribution correlates with the location of reentrant circuits in the epicardial border zone of healing canine infarcts that cause ventricular tachycardia. Circulation. 1997; 95:988-96.
(17) Arenal A, del Castillo S, Gonzalez-Torrecilla E, Atienza F, Ortiz M, Jimenez J, Puchol A, Garcia J, Almendral J. Tachycardia-related channel in the scar tissue in patients with sustained monomorphic ventricular tachycardias: influence of the voltage scar definition. Circulation. 2004; 110:2568-74.


registration
additional
infarction
location
localization
compared
Patient
Bipolar
variation
mid-wall
gold-standard
ducible
infarct
inferior
aortic
inhomogeneous
performed
value
current
successfully
transmural
discriminate
series
implantable
relies
Segments
drugs
approach
tachycardia
ejection
corresponded
studies
protocol
tissue
core
unip
CE
Statistical
evaluate
variables
use
tran
locate
intramur
high
intensity
Using
poor
wall
patient
ablatio
myocardium
imaging
error
ventricle
Endocardial
supplementary
electrogram
Bar
line
MI
SPSS
EA
target
normal
sidered
rate

Chapter 5

Head-to-head comparison of contrast-enhanced magnetic resonance imaging and electroanatomical voltage mapping to assess post-infarct scar characteristics in patients with ventricular tachycardias: real-time image integration and reversed registration

Adrianus P. Wijnmaalen, Rob J. van der Geest, Carine F.B. van Huls van Taxis, Hans-Marc J. Siebelink, Lucia J.M. Kroft, Jeroen J. Bax, Johan H.C. Reiber, Martin J. Schalij, Katja Zeppenfeld

Eur Heart J. 2011 Jan;32(1):104-14.

Abstract

Aims: Substrate based ablation of ventricular tachycardia (VT) relies on electroanatomical voltage mapping (EAVM). Integration of scar information from contrast-enhanced magnetic resonance imaging (CE-MRI) with EAVM may provide supplementary information. This study assessed the relation between electrogram voltages and CE-MRI scar characteristics using real-time integration and reversed registration.

Methods and results: 15 patients without implantable cardiac defibrillator (14 male, 64±9yr) referred for VT ablation after myocardial infarction underwent CE-MRI. Contours of the CE-MRI were used to create 3-dimensional surface meshes of the left ventricle (LV), aortic root and left main stem (LM). Real-time integration of CE-MRI derived scar meshes with EAVM of the LV and aortic root was performed using the LM and the CARTO surface registration algorithm. Merging of CE-MRI meshes with EAVM was successful with a registration error of 3.8±0.6mm. After the procedure voltage amplitudes of each mapping point were superimposed on the corresponding CE-MRI location using the reversed registration matrix. Infarcts on CE-MRI were categorized by transmurality and signal intensity. Local bipolar and unipolar voltages decreased with increasing scar transmurality and were influenced by scar heterogeneity. VT reentry circuit isthmus sites were correlated to CE-MRI scar location. In 3 patients VT isthmus sites were located in scar areas not identified by EAVM.

Conclusions: Integration of MRI derived scar maps with EAVM during VT ablation is feasible and accurate. CE-MRI identifies non-transmural scars and infarct gray zones not detected by EAVM according to currently used voltage criteria and may provide important supplementary substrate information in selected patients.

Introduction

Catheter ablation is an important therapeutic option for recurrent ventricular tachycardia (VT) in patients late after myocardial infarction (MI).[1] The majority of these patients are inducible for VTs not suitable for mapping during tachycardia.[2, 3] Substrate based methods have been developed to identify ablation target sites during sinus rhythm.[2, 4] These methods rely on the delineation of myocardial scar by electroanatomical voltage mapping (EAVM).

Contrast enhanced magnetic resonance imaging (CE-MRI) can be used to visualize the 3-dimensional (3-D) geometry of myocardial fibrosis and is the gold-standard for detection of non-transmural scar.[5, 6] Scar heterogeneity on CE-MRI based on signal intensity (SI) has been associated with spontaneous and inducible VT.[7, 8] Furthermore, animal studies showed that CE-MRI defined scar geometry can predict the location of VT reentry circuits.[9] Thus the integration of CE-MRI derived scar information with EAVM may provide important additional information to facilitate VT ablation procedures. Recently post MI scar areas delineated by CE-MRI have been shown to correspond with scar areas defined by EAVM. In two studies different voltage cut-off values were reported to discriminate between the presence and absence of scar based on a post-procedural image comparison.[10, 11] However, a single voltage cut-off value for the presence of scar may not reflect the complex scar architecture and its use may not result in accurate delineation of non-transmural scar and infarct gray-zones.

The purpose of the present study was (1) to show the feasibility and accuracy of real-time integration of CE-MRI derived scar maps and EAVM in post MI patients. Mapping was performed with emphasis on scar borderzone, non-transmural infarcts and gray-zones as assessed by CE-MRI. Then (2), using a post-procedural process bipolar and unipolar voltages of each mapping point were compared to scar transmurality and SI of the corresponding CE-MRI segment. Finally (3) the correlation between VT reentry circuit isthmus sites and CE-MRI scar locations was determined.

Methods

Fifteen consecutive patients referred for catheter ablation of sustained monomorphic VT late after MI without contra-indication for MRI were studied. In 3 patients the indication for ablation was VT that could not be controlled by antiarrhythmic drugs. In 12 patients with a reasonably preserved ejection fraction RF ablation procedure was offered as an alternative for amiodarone therapy or ICD implantation. Informed consent was obtained from all patients. No ethical committee approval was obtained as all performed procedures were part of the routine clinical protocol applied at the Leiden University Medical Center.

MRI acquisition and processing

MRI was performed on a 1.5 T Gyroscan ACS-NT/Intera MR system (Philips Medical Systems, Best, The Netherlands) with patients positioned in the supine position. A standardized clinical cardiac MRI protocol was followed, including cine MR imaging in long-axis (2-chamber and 4-chamber view) and short-axis orientation covering the complete left ventricle. In addition, the proximal aorta including the ostium of the left main coronary artery (LM) and the right coronary artery was imaged in a stack of cross-sectional slices using a black blood TSE sequence. Contrast-enhanced (CE) images were acquired 15 minutes after bolus injection of gadolinium using an imaging protocol as described previously.[8] The heart was imaged in one breath-hold with 20-24 imaging levels (dependent on heart-size) in short-axis and long-axis views. Images were acquired 600-700ms after the R-wave on surface ECG.

Image analysis was performed using in-house developed software (Mass research software, V2008-EXP). In the aorta image series contours were traced describing the lumen of the aorta and the centerline of the LM and the proximal right coronary artery. In the CE short-axis image series, LV endocardial, LV epicardial and right ventricular (RV) endocardial contours were manually traced (figure 1, A). Myocardial tissue with a signal intensity (SI) value ≥35% of the maximum SI within the infarct region was considered scar. The infarct core was defined as myocardium with a SI≥50 and infarct gray zone as myocardium with SI≥35% but SI<50% of the maximum SI (figure 1B).[8] Transmurality of scar was computed for every location for different layers within the LV myocardium. Subsequently, the LV anatomy as described by the endocardial and epicardial contours was converted into 3D mesh files that could be imported into the CARTO system (Biosense Webster, Cordis-Webster, Johnson&Johnson, Diamond Bar, California). 3D meshes were constructed by converting the traced myocardial and aorta contours into 3D coordinates, based on the 3D spatial location and pixel size of the MR images. Assuming minimal patient motion between the various MR sequences, the generated meshes are spatially aligned in the same coordinate system of the MR scanner. A triangularization approach was followed to obtain a surface description of the myocardial walls and the luminal surfaces of the aorta and coronary arteries suitable for importing and visualization with the mapping system.

The vertices of the endocardial and epicardial surface mesh were color coded with the degree of transmurality for the inner and outer half of the LV wall, respectively. Meshes without color-coding were generated of the anatomy of the RV endocardial surface, the proximal aorta and the proximal segments of the left main and right coronary artery (figure 1).

Prior to the ablation procedure all meshes were imported into the CARTO system using pre-commercial CARTO-Merge (IPE) software enabling the registration and fusion of multiple, separate datasets.

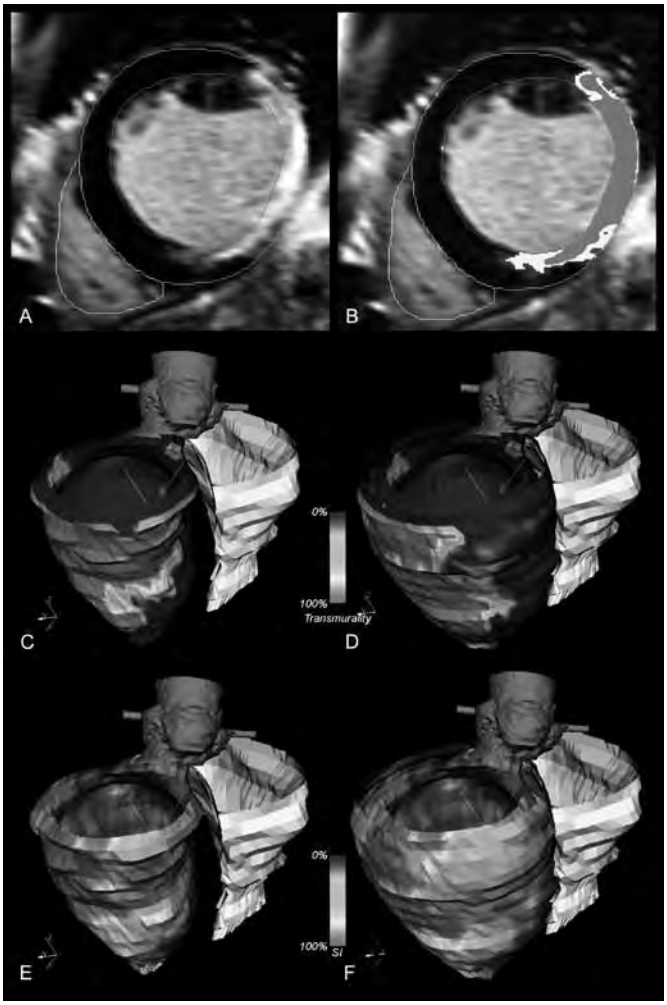


Figure 1. Preprocedural processing consisted of drawing endo- and epicardial ventricular contours using the short axis CE-MRI slices (panel A), defining intensity and transmurality of scar (yellow= gray-zone, red= core infarction, panel B) and creating color coded endocardial (panel C&E) and epicardial (panel D&F) surface meshes. Panels C&D show coding for percentage of transmurality and panels E&F show the same meshes coded for signal intensity according to the colorbar. **(for figure in color see page: 258)**

Electrophysiological evaluation

All patients underwent electrical programmed stimulation and EAVM in the post absorptive, non-sedated state. Antiarrhythmic drugs were discontinued for 5 half-lives. The protocol consisted of 3 drive-cycle lengths and up to 3 extrastimuli from 2 RV sites and burst pacing. The positive endpoint of stimulation was induction of a sustained monomorphic VT lasting for >30s or requiring termination because of hemodynamic compromise.

3-D electroanatomical voltage mapping and image integration

EAVM (CARTO XP) was performed during sinus- or paced rhythm. Using a 3.5mm tip, irrigated mapping catheter (NaviStar ThermoCooled, Biosense Webster Inc, Diamond Bar, CA, USA) and a retrograde approach a voltage map of the aortic root was created. Electrograms were filtered at 30-400Hz(bipolar) and 1-240Hz(unipolar). The catheter was positioned in the left coronary cusp and carefully advanced towards the LM. The position at the ostium was confirmed by undiluted contrast injection through the mapping catheter. The mapping catheter was flushed with saline directly after contrast injection. Secondly a voltage map was created of the LV. Bipolar voltages <1.5mV were considered abnormal and bipolar voltages <0.5mV dense scar.[4, 12] The pre-acquired MRI derived meshes were integrated with the EAVM. A landmark was set at the ostium of the LM on EAVM and MRI mesh. The maps were visually aligned using the location of the LM to overcome rotation errors. Subsequently the surface of the Aortic and LV maps were automatically aligned with the meshes using CartoMERGE software (figure 2). Distances between EAVM and MRI derived maps includ-

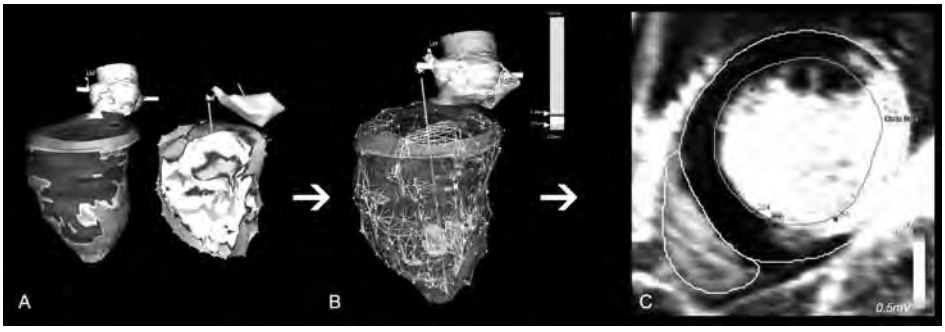


Figure 2. During the procedure 3-D CE-MRI derived meshes (purple represents scar, green represents normal myocardium) were integrated with the electroanatomical voltage maps (color-coding as in the colorbar). After the procedure color-coded mapping points were superimposed on the CE-MRI slice at the corresponding location (color-coding as in the colorbar). **(for figure in color see page: 259)**

ing the LM ostium were calculated to evaluate the registration accuracy. After registration additional mapping points were acquired in areas with a mismatch between EAVM and MRI derived mesh at the EA scar borderzone and at areas with non-transmural scar and gray-zones as assessed by CE-MRI. The location and extent of scar surface on EAVM using a cut-off value of 1.5mV was measured using the software provided with the system and compared with the scar distribution on MRI derived maps.

VT mapping and ablation

A VT reentry circuit isthmus site was defined by activation and entrainment mapping for tolerated VT or by pace-mapping (≥11/12 lead match between VT-QRS and paced-QRS morphology and stimulus-to-QRS interval >40ms) for poorly tolerated VTs.[1] All isthmus sites were tagged on the EAVM and evaluated with respect to scar distribution as assessed by CE-MRI. All inducible monomorphic VTs were targeted and radiofrequency energy was applied if a potential isthmus site could be identified.

Comparison of electroanatomical voltagemaps and contrast enhanced MRI

Post-procedural processing was performed in all cases. The registration matrix, mapping point coordinates and bipolar and unipolar voltages were exported from the CARTO system. Using the reverse registration matrix and point coordinates voltage data were superimposed on the corresponding CE-MRI slice (Mass research software, V2008-EXP) (figure 2).

To enable the assessment of voltages corresponding to different types of CE areas each

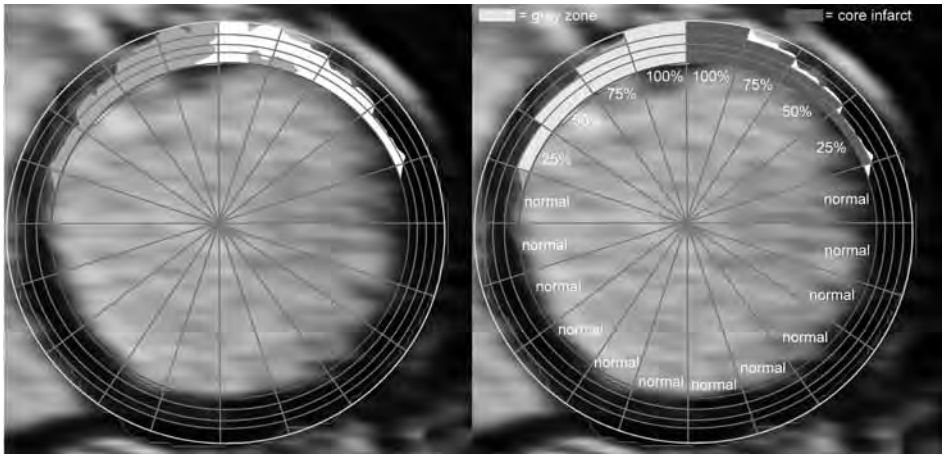


Figure 3. Schematic of the categorization of short axis CE-MRI segments. Panel A shows potential contrast enhancement patterns with regard to transmurality and signal intensity (SI) in different segments. Panel B shows the corresponding coding according to transmurality and SI (yellow= gray-zone, red= core infarction).

short-axis MRI slice was divided into 20 segments. Segments were subdivided into four layers (0-25%, 25-50%, 50-75% and 75-100% transmurality). Each layer was automatically coded as core infarct, infarct gray-zone or normal myocardium based on the mean SI. Based on the characteristics of the 4 layers each segment was assigned to one of 13 subcategories discriminating between location (sub-endocardial, sub-epicardial or mid-wall), transmurality (0%, 25%, 50%, 75% or 100%) and SI (normal, gray-zone or core infarct) of CE scar

(figure 3). The bipolar and unipolar voltages of each mapping point were combined with the scar code of the CE-MRI segment at the corresponding location for analysis.

Statistical Analysis

Continuous variables are expressed as mean±SD or median(interquartile range) when appropriate, and categorical variables as frequency(%). Statistical analysis was performed using SPSS, version 16.0(SPSS, Inc., Chicago). Mann Whitney U-test was used to compare voltages between different CE-MRI segment categories. All tests were two-tailed and a p-value ≤0.05 was considered significant.

RESULTS

Table 1. Patient characteristics at the time of referral for radiofrequency catheter ablation

Age	64±9
Male gender (%)	14 (93)
Time after myocardial infarction (year)	14±12
VT cycle length (ms)	341±76
Drugs	
Amiodarone (%)	0
Sotalol (%)	1 (7)
Beta-Blocker (%)	14 (93)
Class I antiarrhythmic drugs (%)	1 (7)
ACE-I/AT-2 antagonist (%)	13 (87)

LV indicates left ventricle; ACE-I, ACE inhibitor; AT-2, angiotensin 2. Data are expressed as mean±SD or frequency(%).

Patient Population

Fifteen patients (14 male, 64±9 years) were studied. Patient characteristics are summarized in table 1.

Delayed Enhancement MRI

MRI findings are listed in table 2. The mean LV ejection fraction was 44±10%. All patients had evidence of scar tissue on CE-MRI. The infarct was located at the anterior wall in 3(20%), the inferior wall in 9(60%) and the lateral wall in 3(20%) patients. The endocardial surface of segments with transmural infarction (core infarct and infarct gray-zones) was 12±13cm^2 (7.7±7.3% of the total surface) and of sub-endocardial and transmural infarctions 33±20cm^2

Table 2. Results of MRI studies

LV ejectionfraction (%)	44±10
LV end diastolic volume (ml)	232±71
LV end systolic volume (ml)	133±59
LV Mass (g)	140±43
Contrast enhanced mass (g)	26±20
Endocardial surface (cm2)	134±29
Transmural scar (% of surface)	7.7±7.3
Subendocardial and transmural scar (% of surface)	23.0±11.0
Subepicardial and midwall scar (% of surface)	0.7±0.6
Localization contrast enhancement	
Anterior wall	3 (20)
Inferior wall	9 (60)
Lateral wall	3 (20)

LV indicates left ventricle; CE, contrast enhancement. Data are expressed as mean±SD.

(23±11% of the total surface). Segments with intramural or sub-epicardial scar accounted for 1.0±0.91cm^2 (0.74±0.63%) of the total surface.

3-D electroanatomical voltage mapping and image integration

Determination of the location of the LM ostium was uncomplicated in all patients. After contrast injection no dysfunction or obstruction of the mapping catheter was observed. Endocardial voltage maps of the aortic cusps and LV were obtained in all patients. The mean number of LV points was 255±43. The imported MRI meshes were successfully merged with the aortic and LV maps with a mean surface registration error of 3.83±0.57mm. After registration the position error between the LM on EAVM and MRI derived mesh was 4.64±3.58mm. EAVM findings and registration data are summarized in table 3.

Electrical infarct localization (bipolar electrograms <1.5mV) corresponded to infarct localization on CE-MRI (≥25% transmurality) in all patients. The mean endocardial surface area of scar was 30±21cm^2 as determined by EAVM (<1.5mV) and 33±20cm^2 as determined by CE-MRI (correlation R=0.91).

However, despite this correlation visual analysis showed a clear mismatch between EAVM scar areas and MRI maps in particular in 5(33%) patients with inferior MI. In these patients scar areas on MRI were larger than scar areas delineated by EAVM. Of importance, all scar areas not detected by EAVM were non-transmural on CE-MRI (transmurality <75%). Examples are provided in figure 4.

Table 3. 3-D Electroanatomical mapping and image integration

Mean points Aorta map	25±11
Mean points LV map	255±43
Total points LV maps	3023
Points with bipolar voltage<1.5mV	1180(39)
Localization low voltage area	
Anterior	3 (20)
Inferior	9 (60)
Lateral	3 (20)
Distance EAVM points to MRI mesh surface	
Mean (mm)	3.83 ±0.57
Standard Deviation (mm)	2.61±0.49
Minimum (mm)	0.04±0.04
Maximum (mm)	14.2±3.36
Distance LM EAVM to MRI mesh (mm)	4.64±3.58

LV indicates left ventricle; EAVM, electroanatomical mapping; MRI, magnetic resonance imaging. LM, left main coronary artery. Data are expressed as mean±SD or frequency(%)

Mapping and ablation of VTs

A total of 26 sustained monomorphic VTs with a cycle length of 305±85ms was induced in 13 patients (1.9±1.0 VTs/patient). In 2 patients no sustained VT was inducible. A VT isthmus site could be identified and successfully targeted within an endocardial low voltage area corresponding with scar on MRI for 16 VTs in 9 patients. In the remaining 4 patients no endocardial ablation target site could be identified. In 3 the earliest activation during VT or best matching pacemap was at a normal voltage site (>1.5mV). However, at these sites CE-MRI identified sub-endocardial septal scar in 1 and intramural inferoseptal scar in 2 pts. Based on the mapping and CE-MRI findings epicardial mapping was performed in the latter with successful identification of an epicardial ablation target site. In one patient with a poorly tolerated VT no endocardial pace match could be obtained, a mid septal area of CE identified in this patient aswell. RFCA abolished all inducible VTs in 9, the clinical documented VT in 1 and none of the clinical VTs in 3 patients. In 2 patients ablation failed likely to the fact that there was an intramural septal reentrant circuit which was consistent with the finding of contrast enhancement at this location. In one epicardially mapped patient no ablation was performed since the ablation target site was mapped to the close vicinity of the epicardial right coronary artery.

Ten patients received an internal cardiac defibrillator including those in whom ablation failed to abolish all VTs. The median follow-up after ablation was 19 (3 –27) months during which 5 patients experienced recurrent VT.

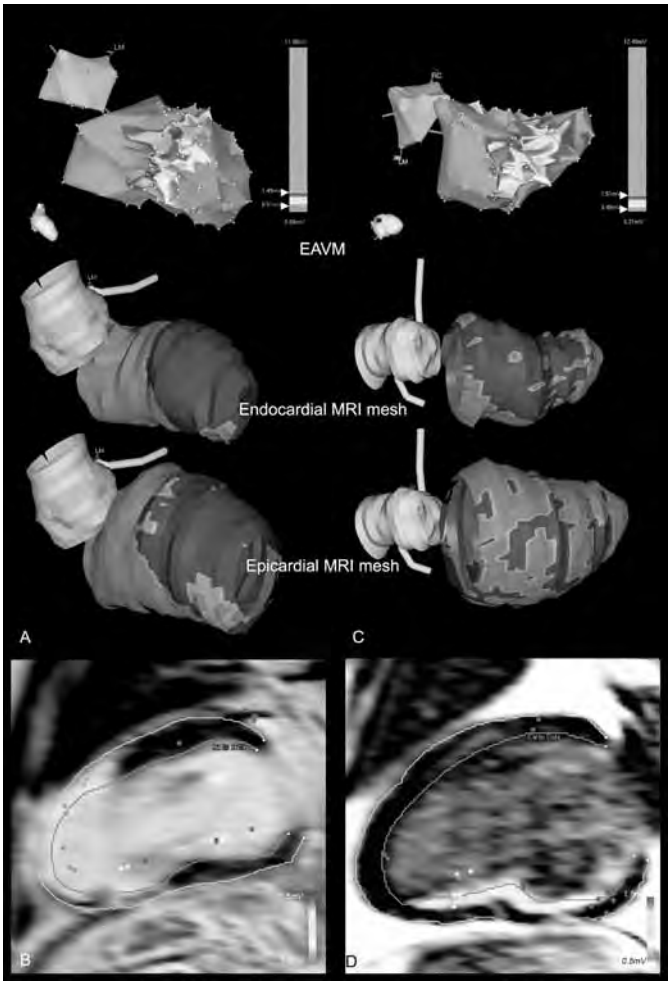


Figure 4. Representative examples of a patient in whom CE-MRI derived mesh matched the EAVM (panel A, B) and of a patient with additional scar-areas identified by CE-MRI not detected by EAVM (panel C, D). Panels A and C show the bipolar voltage maps (color-coding as in the colorbar) and corresponding endo- and epicardial MRI derived surface meshes coded for transmurality (purple represents scar, green represents normal myocardium). Panels B and D show a representative long axis CE-MRI slice with superimposed mapping point locations (mapping point bipolar amplitudes are color coded as in voltage maps).

Comparison of electroanatomical voltagemaps and CE-MRI using reverse registration

Voltages of each mapping point were compared to the CE characteristics of the corresponding segment. 1533(51%) of mapping points were allocated at a segment without CE, 1343(44%) mapping points at a segment with sub-endocardial (684(23%)) or transmural (657(22%)) CE and 112(4%) of mapping points at a segment with mid-wall or sub-epicardial

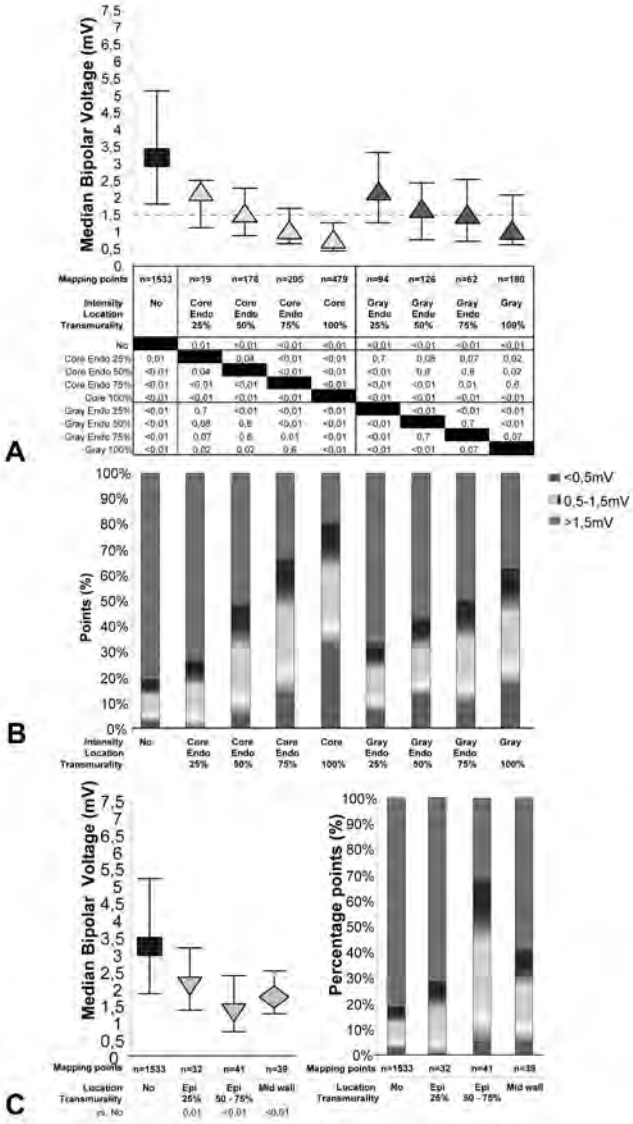
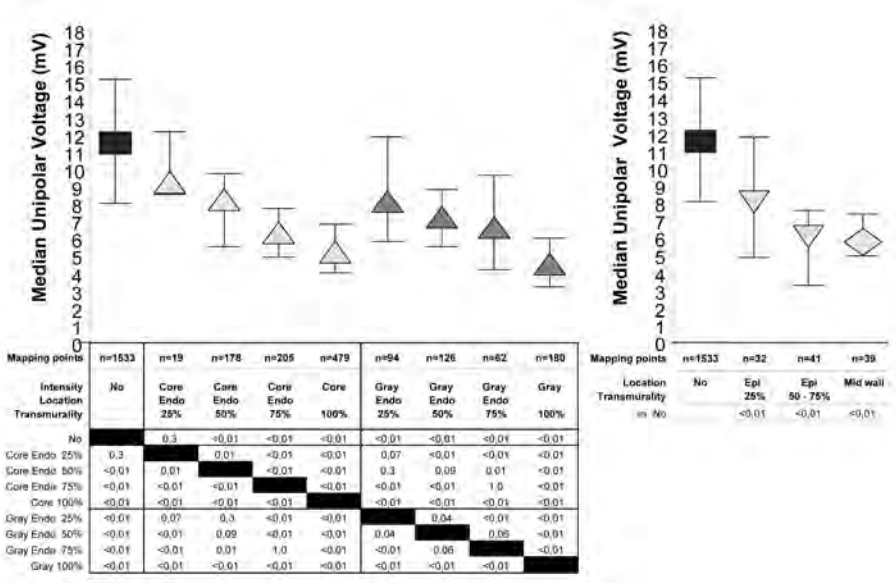


Figure 5. Panel A: median bipolar voltage of points located at short axis CE-MRI segments coded for transmurality and SI of scar. The number of mapping points allocated at each of the 9 segment categories is provided under the X-axis. The p-value of differences (Mann Whitney U-test) between bipolar voltages of each category is displayed. Panel B displays the distribution of points for each segment category according to the current used cut-off values in bipolar voltage mapping (≤0.5mV, >0,5mV - ≤1.5mV and >1.5mV). Panel C displays the mean bipolar voltage and distribution of points at segments with epicardial and mid-wall scar.

CE. The median bipolar voltage at segments with normal myocardium was 3.2mV(1.8-5.1mV). Endocardial bipolar electrogram amplitudes for the core infarct and infarct gray-zone decreased significantly with increasing scar transmurality. The median bipolar voltages for segments with a sub-endocardial to transmural core infarct were 2.2mV(1.1-2.5mV), 1.5mV(0.9-2.2mV), 1.1mV(0.6-1.7mV) and 0.8mV(0.4-1.3mV) for 25%, 50%, 75% and 100% scar transmurality, respectively. For infarct gray-zones median bipolar voltages were 2.2mV(1.3-3.3mV), 1.7mV(0.8-2.4mV), 1.5mV(0.7-2.5mV) and 1.0mV(0.6-2.1mV) for 25%, 50%, 75% and 100% scar transmurality, respectively (figure 5). The mean unipolar voltage was 11.5mV(8.0-15.1mV) at normal segments and decreased significantly with increasing scar transmurality for core infarct and infarct gray-zone. Segments with sub-epicardial and



Mapping points	n=1533	n=19	n=178	n=205	n=479	n=94	n=126	n=62	n=180
Intensity Location Transmurality	No	Core Endo 25%	Core Endo 50%	Core Endo 75%	Core 100%	Gray Endo 25%	Gray Endo 50%	Gray Endo 75%	Gray 100%
No		0.3	<0.01	<0.01	<0.01	<0.01	<0.01	<0.01	<0.01
Core Endo 25%	0.3		0.01	<0.01	<0.01	0.07	<0.01	<0.01	<0.01
Core Endo 50%	<0.01	0.01		<0.01	<0.01	0.3	0.09	0.01	<0.01
Core Endo 75%	<0.01	<0.01	<0.01		<0.01	<0.01	<0.01	1.0	<0.01
Core 100%	<0.01	<0.01	<0.01	<0.01		<0.01	<0.01	<0.01	<0.01
Gray Endo 25%	<0.01	0.07	0.3	<0.01	<0.01		0.04	<0.01	<0.01
Gray Endo 50%	<0.01	<0.01	0.09	<0.01	<0.01	0.04		0.06	<0.01
Gray Endo 75%	<0.01	<0.01	0.01	1.0	<0.01	<0.01	0.06		<0.01
Gray 100%	<0.01	<0.01	<0.01	<0.01	<0.01	<0.01	<0.01	<0.01	

Mapping points	n=1533	n=32	n=41	n=39
Location Transmurality	No	Epi 25%	Epi 50 - 75%	Mid wall
vs No		<0.01	<0.01	<0.01

Figure 6. Panel A: median unipolar voltage of points located at short axis CE-MRI segments coded for transmurality and SI of scar. The number of mapping points allocated at each of the 9 segment categories is provided under the X-axis. The p-value of differences (Mann Whitney U-test) between mean unipolar voltages of each category are displayed. Panel B: median unipolar voltage of points at segments with epicardial and mid-wall scar.

midwall scars between 25% and 75% transmurality showed reduced bipolar and unipolar electrogram voltage (figure 5, 6).

Although bipolar and unipolar electrogram amplitudes were an effective parameter to differentiate between segments of different scar transmurality there was an important overlap between groups. A median bipolar voltage <1.5mV was only found in segments with ≥75% core infarct transmurality and transmural gray-zone infarction.

Discussion

The current study is the first to evaluate the relation between the 3-D geometry of scar and local electrogram voltages using real-time integration and reversed registration of EAVM and CE-MRI in humans. The main findings of this study are: (1) Real-time registration of CE-MRI derived scar information including scar transmurality and heterogeneity and EAVM data during catheter ablation of post-MI VTs is feasible and accurate; (2) Endocardial bipolar and unipolar electrogram amplitudes decrease with increasing scar transmurality and are also influenced by scar heterogeneity as quantified by signal intensity; (3) The current used bipolar electrogram cut-off value of 1.5mV can not fully delineate non-transmural scar, small sub-epicardial scar and infarct gray-zones as identified by CE-MRI.

Imaging derived scar information and EAVM

Surviving myocyte bundles embedded in fibrous tissue are the substrate for reentrant VT in patients after MI. Identification of scar is of importance in substrate based ablation approaches for unstable VT.[2, 4] CE-MRI allows detection of small scars and characterization of infarcts by differentiating the core infarct and infarct gray-zones which extend has been associated with inducible and spontaneous VT.[6-8]

Scar geometry is also an important determinant for conduction properties. The infarct borderzone thickness and the local thickness gradient could predict the location of VT reentry circuit isthmuses in a canine model.[9] Thus, scar information derived from CE-MRI has the potential to improve substrate based ablation.

The currently used gold-standard in electrophysiology to define scar relies on EAVM. Two prior studies have compared CE-MRI data with EAVM in post MI patients. In a post hoc analysis, a good correlation between scar areas on CE-MRI and EAVM was reported using cutoff values of 1.3mV and 1.54mV for bipolar and 5.5mV and 6.52mV for unipolar voltages, respectively.[10, 11] Mismatches between the presence of scar defined by EAVM and CE-MRI found in both studies were thought to be due to the lack of high density mapping at the scar borderzone and poor catheter contact.

Real-time integration

Real-time integration of CE-MRI derived scar information achieved in the current study facilitated high density mapping at the EA scar borderzone and at areas with a mismatch between scar areas on EAVM and CE-MRI. The good registration accuracy prevented delineation of false positive low voltage areas due to poor catheter contact.

Integration of CE-MRI derived data with EAVM was automatically performed with a mean position error of <4mm. This accuracy is in line with studies using CT imaging.[13, 14] In contrast to prior studies in which the position of LV apex, mitral annulus and aorta were used

for registration we tagged the position of the LM ostium. The advantage of using the LM and endocardial surface registration is that it precludes rotation errors.[15]

After image integration and delineation of the EA borderzone we found a good correlation between the surface of scar measured by EAVM using a cutoff value of 1.5mV and scar surface area derived from CE-MRI. However, visual analysis showed a clear mismatch between scar areas defined by EAVM and the area of scar coded on the CE-MRI meshes. CE-MRI scar areas were larger in 33% of the patients. Insufficient mapping density was excluded as a cause of the mismatch by acquiring additional mapping points in these areas after image integration.

The surface of low voltage areas was measured using the CARTO software. This software sums the surface of all individual triangles between mapping points. Therefore the total surface increases with the number of mapping points that are not located in the same plane. Comparing the absolute endocardial scar surface calculated by using the CARTO system with the scar surface measured by the endocardial contours on CE-MRI might therefore be inaccurate.

Reversed registration

The newly proposed technique of reversed registration allowed a head-to-head comparison of voltage data and CE-MRI characteristics independent of surface measurements.

Bipolar and unipolar electrogram amplitudes significantly decreased with increasing scar transmurality for core infarct and infarct gray-zones. A similar correlation between decreasing bipolar voltages and increasing scar transmurality assessed by histology was demonstrated in a dog model of MI.[16] For segments with ≥75% scar transmurality bipolar electrograms were also significantly influenced by scar density defined by SI. Interestingly, the only segments with a median bipolar voltage <1.5mV were segments coded as ≥75% transmural core and completely transmural gray-zone infarction (figure 5).

This finding is in line with prior animal studies as transmural scars are the prevailing type of scar found in pigs after MI in which the cut-off value of 1.5mV was validated.[12] In the current study performed in patients with a relatively preserved LV function, however transmural scars accounted for only 7.7% of the total endocardial surface. Forty-four percent of all mapping points located at a scar area were allocated to a segment with <75% transmural core or infarct gray-zone. The variation in number, size and geometry of surviving myocyte bundles in non-transmural and inhomogeneous scar are likely to influence local electrogram amplitudes.

Accordingly, non-transmural and inhomogeneous scars showed significant higher bipolar and unipolar voltages contributing to the mismatch between EAVM and CE-MRI derived scar maps after image integration and visual comparison.

The total sub-endocardial surface of segments with only mid-wall or sub-epicardial scar was small, which might be expected in a post-MI population.

Defining a voltage cut-off value for the presence of scar, based on real-time image integration like suggested by others[10, 11, 13] is appealing. However, due to the demonstrated complex relation between local electrogram amplitudes and scar characteristics a single cut-off value can not discriminate between the presence or absence of infarct scar at a particular location, because voltage is dependent on infarct transmurality and heterogeneity.

Reentry circuit isthmus sites and scar characteristics

It has been demonstrated that in patients with hemodynamically tolerated VT the majority of successful ablation sites was located in the EA scar borderzone using a cut-off value of 1.5mV. However, some ablation sites were located within normal myocardium as defined by EAVM.[17]

More recently, Desjardins reported that VT isthmus sites, the majority identified by pace-mapping, had a mean bipolar voltage of 0.6±0.9mV and corresponded to core infarct regions or transmural gray-zones on CE-MRI using post-procedure image integration. Of importance, for one third of the induced VT no isthmus could be identified.[10]

In the current study we were unable to identify a VT reentry isthmus site within a low voltage area in 4 patients. However, in 3 patients successful identification of an ablation target site was guided by CE-MRI derived scar information showing non-transmural scar leading to pace-mapping in a normal voltage area in one and an epicardial ablation attempt in 2 patients.

Clinical implications

Real-time integration of CE-MRI derived scar maps and EAVM is feasible and accurate. Of importance, all CE-MRI information including the location of intramural and non-transmural scar and of the core infarct and infarct gray-zone not detectable by EAVM can be visualized during the ablation procedures. This might have important implications for substrate based ablation procedures in particular in patients, in whom variation in collateral circulation and early reperfusion strategies have resulted in inhomogeneous and non-transmural infarction. The technique of reversed registration as described in this study may also provide more insights into the spatial relationship between VT reentry circuit sites and scar characteristics on CE-MRI as successful ablation sites can be superimposed on the CE-MRI.

Limitations

The studied population consisted of post MI patients without contraindications for MRI study. The routine use of MRI in implantable cardioverter defibrillator (ICD) carriers is not considered safe and currently limits the application of the described methods. The increas-

ing availability of 'MRI-safe' implantable defibrillators in the near future may however make the use of MRI derived information during RFCA applicable to a larger population.

The sample size of the patient population included in this study was relatively small. Further studies in larger groups of patients are warranted to further study the supplemental value of the integration of MRI derived scar information during VT ablation.

Conclusions

Real-time integration of CE-MRI derived scar information including scar transmurality and heterogeneity and EAVM data during catheter ablation of post-MI VTs is feasible and accurate.

Electrogram voltages decrease with increasing scar transmurality and are also influenced by scar heterogeneity. The current used bipolar voltage cut-off value of 1.5mV seems to be appropriate to delineate transmural scar. However, local bipolar and unipolar voltages alone are not sufficient to characterize the complex 3-D scar geometry. Merging CE-MRI derived information with EAVM provides supplementary substrate information in particular for non-transmural and heterogeneous infarction.

Reference List

(1) Aliot EM, Stevenson WG, Almendral-Garrote JM, Bogun F, Calkins CH, Delacretaz E, Della BP, Hindricks G, Jais P, Josephson ME, Kautzner J, Kay GN, Kuck KH, Lerman BB, Marchlinski F, Reddy V, Schalij MJ, Schilling R, Soejima K, Wilber D. EHRA/HRS Expert Consensus on Catheter Ablation of Ventricular Arrhythmias: developed in a partnership with the European Heart Rhythm Association (EHRA), a Registered Branch of the European Society of Cardiology (ESC), and the Heart Rhythm Society (HRS); in collaboration with the American College of Cardiology (ACC) and the American Heart Association (AHA). Heart Rhythm. 2009; 6:886-933.

(2) Soejima K, Suzuki M, Maisel WH, Brunckhorst CB, Delacretaz E, Blier L, Tung S, Khan H, Stevenson WG. Catheter ablation in patients with multiple and unstable ventricular tachycardias after myocardial infarction: short ablation lines guided by reentry circuit isthmuses and sinus rhythm mapping. Circulation. 2001; 104:664-9.

(3) Stevenson WG, Wilber DJ, Natale A, Jackman WM, Marchlinski FE, Talbert T, Gonzalez MD, Worley SJ, Daoud EG, Hwang C, Schuger C, Bump TE, Jazayeri M, Tomassoni GF, Kopelman HA, Soejima K, Nakagawa H. Irrigated radiofrequency catheter ablation guided by electroanatomic mapping for recurrent ventricular tachycardia after myocardial infarction: the multicenter thermocool ventricular tachycardia ablation trial. Circulation. 2008; 118:2773-82.

(4) Marchlinski FE, Callans DJ, Gottlieb CD, Zado E. Linear ablation lesions for control of unmappable ventricular tachycardia in patients with ischemic and nonischemic cardiomyopathy. Circulation. 2000; 101:1288-96.

(5) Kim RJ, Fieno DS, Parrish TB, Harris K, Chen EL, Simonetti O, Bundy J, Finn JP, Klocke FJ, Judd RM. Relationship of MRI delayed contrast enhancement to irreversible injury, infarct age, and contractile function. Circulation. 1999; 100:1992-2002.

(6) Wagner A, Mahrholdt H, Holly TA, Elliott MD, Regenfus M, Parker M, Klocke FJ, Bonow RO, Kim RJ, Judd RM. Contrast-enhanced MRI and routine single photon emission computed tomography (SPECT) perfusion imaging for detection of subendocardial myocardial infarcts: an imaging study. Lancet. 2003; 361:374-9.

(7) Schmidt A, Azevedo CF, Cheng A, Gupta SN, Bluemke DA, Foo TK, Gerstenblith G, Weiss RG, Marban E, Tomaselli GF, Lima JA, Wu KC. Infarct tissue heterogeneity by magnetic resonance imaging identifies enhanced cardiac arrhythmia susceptibility in patients with left ventricular dysfunction. Circulation. 2007; 115:2006-14.

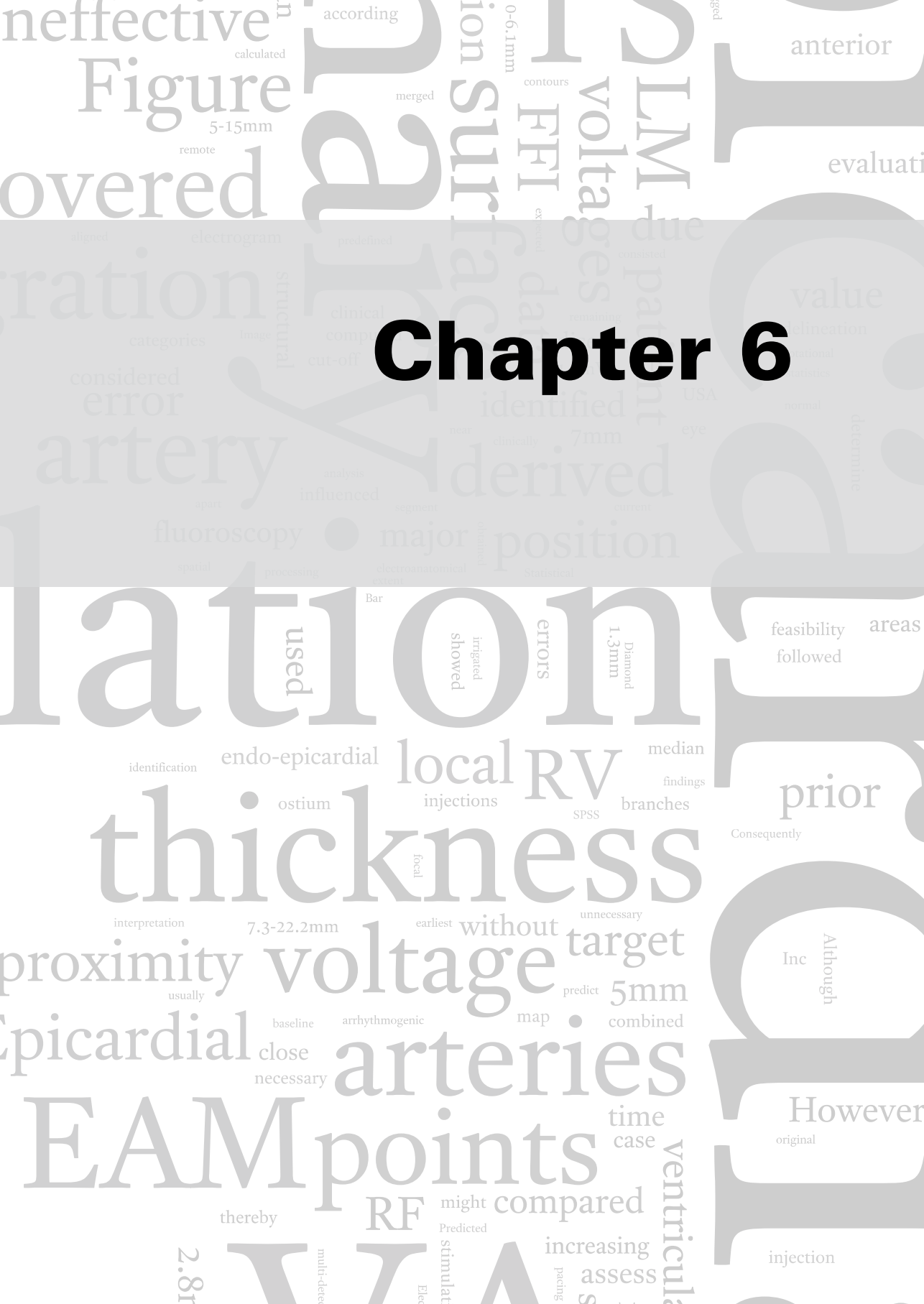
(8) Roes SD, Borleffs CJ, van der Geest RJ, Westenberg JJ, Marsan NA, Kaandorp TA, Reiber JH, Zeppenfeld K, Lamb HJ, DE RA, Schalij MJ, Bax JJ. Infarct tissue heterogeneity assessed with contrast-enhanced MRI predicts spontaneous ventricular arrhythmia in patients with ischemic cardiomyopathy and implantable cardioverter-defibrillator. Circ Cardiovasc Imaging. 2009; 2:183-90.

(9) Ciaccio EJ, Ashikaga H, Kaba RA, Cervantes D, Hopenfeld B, Wit AL, Peters NS, McVeigh ER, Garan H, Coromilas J. Model of reentrant ventricular tachycardia based on infarct border zone geometry predicts reentrant circuit features as determined by activation mapping. Heart Rhythm. 2007; 4:1034-45.

(10) Desjardins B, Crawford T, Good E, Oral H, Chugh A, Pelosi F, Morady F, Bogun F. Infarct architecture and characteristics on delayed enhanced magnetic resonance imaging and electroanatomic mapping in patients with postinfarction ventricular arrhythmia. Heart Rhythm. 2009; 6:644-51.

(11) Codreanu A, Odille F, Aliot E, Marie PY, Magnin-Poull I, Andronache M, Mandry D, Djaballah W, Regent D, Felblinger J, De Chillou C. Electroanatomic characterization of post-infarct scars comparison with 3-dimensional myocardial scar reconstruction based on magnetic resonance imaging. J Am Coll Cardiol. 2008; 52:839-42.

(12) Reddy VY, Wrobleski D, Houghtaling C, Josephson ME, Ruskin JN. Combined epicardial and endocardial electroanatomic mapping in a porcine model of healed myocardial infarction. Circulation. 2003; 107:3236-42.
(13) Dickfeld T, Lei P, Dilsizian V, Jeudy J, Dong J, Voudouris A, Peters R, Saba M, Shekhar R, Shorofsky S. Integration of three-dimensional scar maps for ventricular tachycardia ablation with positron emission tomography-computed tomography. JACC Cardiovasc Imaging. 2008; 1:73-82.
(14) Bogun FM, Desjardins B, Good E, Gupta S, Crawford T, Oral H, Ebinger M, Pelosi F, Chugh A, Jongnarangsin K, Morady F. Delayed-enhanced magnetic resonance imaging in nonischemic cardiomyopathy: utility for identifying the ventricular arrhythmia substrate. J Am Coll Cardiol. 2009; 53:1138-45.
(15) Zeppenfeld K, Tops LF, Bax JJ, Schalij MJ. Images in cardiovascular medicine. Epicardial radiofrequency catheter ablation of ventricular tachycardia in the vicinity of coronary arteries is facilitated by fusion of 3-dimensional electroanatomical mapping with multislice computed tomography. Circulation. 2006; 114:e51-e52.
(16) Wolf T, Gepstein L, Dror U, Hayam G, Shofti R, Zaretzky A, Uretzky G, Oron U, Ben-Haim SA. Detailed endocardial mapping accurately predicts the transmural extent of myocardial infarction. J Am Coll Cardiol. 2001; 37:1590-7.
(17) Verma A, Marrouche NF, Schweikert RA, Saliba W, Wazni O, Cummings J, Abdul-Karim A, Bharqava M, Burkhardt JD, Kilicaslan F, Martin DO, Natale A. Relationship between successful ablation sites and the scar border zone defined by substrate mapping for ventricular tachycardia post-myocardial infarction. Journal of Cardiovascular Electrophysiology.2005; 16:465-471.


Chapter 6

Real-time integration of MDCT derived coronary anatomy and epicardial fat: Impact on epicardial electroanatomical mapping and ablation for ventricular arrhythmias

Carine F.B. van Huls van Taxis, Adrianus P. Wijnmaalen, Sebastiaan R.D. Piers, Rob J. van der Geest, Martin J. Schalij, Katja Zeppenfeld

Submitted

Abstract

Background: Epicardial catheter ablation (CA) for ventricular arrhythmias (VA) is limited by the presence of coronary arteries and epicardial fat. This study aimed to evaluate the feasibility and accuracy of real-time integration of multi-detector computed tomography (MDCT) derived coronary anatomy and fat distribution and its impact on electroanatomical mapping (EAM) and ablation.

Methods and Results: Twenty-eight patients (21 male, 59±16yr) underwent combined endo-epicardial EAM. Prior to the procedure, MDCT derived coronary anatomy and epicardial fat meshes were loaded into the EAM system (CARTO™). Real-time registration of MDCT data was performed after endocardial EAM. The distance between epicardial ablation target sites and coronary arteries was assessed by registered MDCT and angiography. After the procedure, mapping and ablation points were superimposed on the MDCT using a reversed registration matrix for head-to-head comparison of mapping data and local fat thickness. Image registration was successful and accurate (surface error 2.8±1.3mm). Forty-six VA were targeted; 25(54%) were abolished by CA, in 21(46%) ablation failed. In 5 VA no target site was identified and in 3 adhesions prevented mapping. In 2 VA ablation was withheld due to His-bundle vicinity and in 7 due to proximity of coronary arteries. In 4 VA CA was ineffective. At ineffective ablation sites epicardial fat was significantly thicker compared to successful sites (16.9±6.8mm [range 7.3-22.2mm] and 1.5±2.1mm [range 0-6.1mm], $p<0.001$).

Conclusion: Real-time image integration of pre-acquired MDCT information is feasible and accurate. Epicardial fat of >7mm and the presence of coronary arteries are important reasons for epicardial ablation failure.

Introduction

Epicardial electroanatomical mapping (EAM) followed by radiofrequency catheter ablation (RFCA) for ventricular arrhythmia (VA) is an important therapeutic option in patients after endocardial ablation failure. Despite the presence of a subepicardial substrate epicardial EAM and ablation may have important limitations. Bipolar voltage mapping might not be accurate to delineate subepicardial scar and is likely to overestimate its extent as even thin layers of epicardial fat attenuate bipolar electrogram amplitudes.[1-3]

Once a potential ablation target site (TS) has been identified, delivery of RF energy needs to be withheld in the vicinity of coronary arteries, usually visualized by repeated coronary injections, or may be ineffective due to the thickness of epicardial fat which presence can only be assumed when irrigated tip ablation is ineffective.[1,4] Cardiac multi-detector computed tomography (MDCT) can reliably visualize both coronary arteries and epicardial fat.[5,6] Accurate real-time integration of MDCT derived coronary anatomy and fat distribution during the ablation procedure is therefore desirable.

The purpose of this study was (1) to evaluate the extent and distribution of epicardial fat in patients undergoing combined endo-epicardial mapping and ablation, (2) to assess the feasibility and accuracy of real-time integration of MDCT derived coronary anatomy and epicardial fat distribution with EAM, (3) to determine the influence of epicardial fat thickness on bipolar and unipolar voltage and ablation outcome and (4) to evaluate the potential use of the integrated MDCT to identify inappropriate ablation sites.

Methods

Patients and baseline evaluation

The study population consisted of 28 consecutive patients (21 male, 59±16 years) scheduled for combined endo-epicardial EAM and RFCA for drug refractory VA because of previous endocardial ablation failure (n=24) or a high suspicion for an epicardial substrate based on ECG criteria (n=4).[7-9] No ethics committee approval was necessary as all performed procedures were part of routine clinical protocol. Informed consent was obtained from all patients. Prior to the procedure all patients underwent transthoracic echocardiography. When considered necessary, magnetic resonance imaging and/or nuclear imaging were performed to assess the presence of structural heart disease.

Pre-procedural MDCT acquisition and processing

Patients underwent cardiac MDCT prior to EAM. The MDCT data were analyzed using MASS software (V2009-EXP LKEB, Leiden, The Netherlands). The aortic, endocardial, pericardial and epicardial contours and proximal coronary arteries were manually traced (Figure 1A).

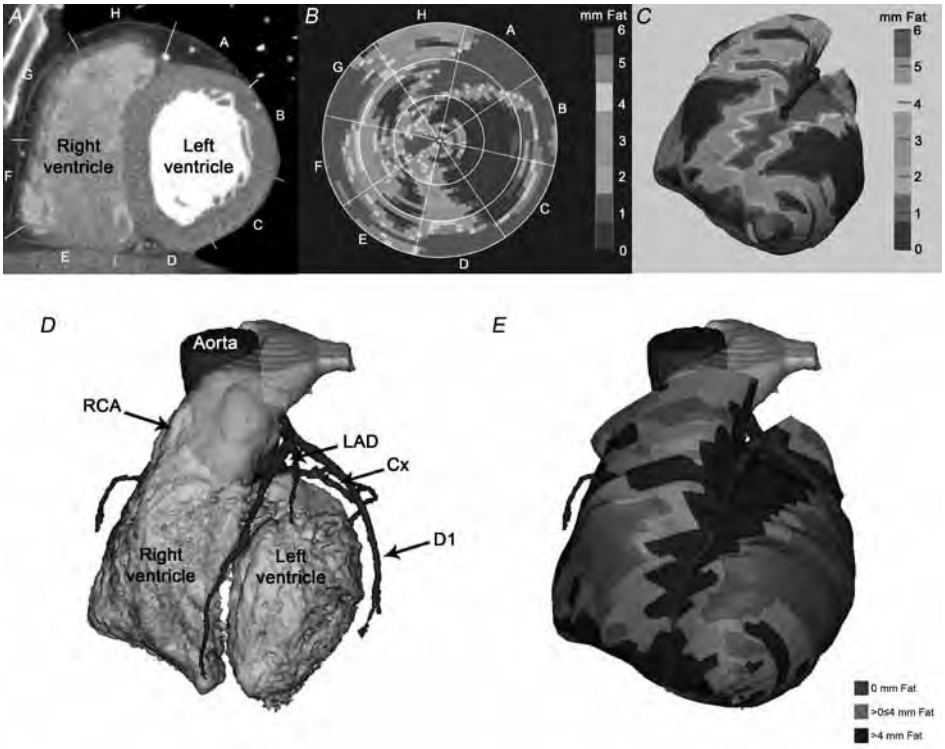


Figure 1. Panel A: Multi-detector computed tomography (MDCT) short axis slice with pericardial (green) and epicardial (red) contours divided into 8 segments A-H. Panel B: Bull's eye reconstruction (8 equal short axis segments A-H and 3 equal long axis segments) of the epicardial surface color coded for fat thickness according to the color bar. Panel C: 3D epicardial surface mesh color coded for fat thickness according to the color bar. Panel D: MDCT derived anatomical structures segmented using the CARTO system. Panel E: Final fusion image. The epicardial fat meshes (color coded for fat thickness as indicated) merged with the segmented MDCT images. Cx=circumflex coronary artery, D1=first diagonal coronary artery, LAD=left anterior descending artery, RCA=right coronary artery.

The distance between the epicardial and pericardial contours was computed to assess fat thickness. A bull's eye reconstruction of the epicardial surface was created and divided into 8 equal short-axis and 3 long-axis segments (Figure 1B).[5] For each segment the mean epicardial fat thickness was calculated.

Contours were converted into 3D meshes and imported into the EAM system (CARTO-XP^{tm}, Biosense Webster Inc, Diamond Bar, CA, USA). The epicardial surface meshes were color coded according to fat thickness (Figure 1C). In addition, the original MDCT data were loaded into the CARTO system and cardiac structures were segmented (Figure 1D). All meshes and segmented images were merged to a final fusion image (FFI) using CARTOMerge (IPE) software (Figure 1E).

Electrophysiological evaluation

Electrophysiological evaluation included programmed electrical stimulation and endo-epicardial EAM. The stimulation protocol consisted of 3 drive-cycle lengths (600, 500 and 400ms) with up to 3 ventricular extra stimuli at 2 RV sites and burst pacing, with and without isoproterenol (2-10μg/min). Positive endpoint for stimulation was induction of a sustained monomorphic VA lasting for >30s or requiring termination because of hemodynamic compromise. Anti-arrhythmic drugs were discontinued for at least 5 half-lives except for amiodarone (n=7).

Electroanatomical mapping and real-time image integration

Pericardial access was established through a subxiphoid puncture (n=26) or by a surgical subxiphoidal window in case of pericardial adhesions (n=2).[10] Limited EAM of the aortic root was performed with a 3.5mm, irrigated-tip catheter (NaviStar ThermoCooled, Biosense Webster Inc, Diamond Bar, CA, USA) using the CARTO system. The mapping catheter was positioned in the ostium of the left main artery (LM) confirmed by undiluted contrast injection through the mapping catheter and the position was tagged on the map.[11] Secondly, an endocardial EAM of the LV and/or RV was created. Electrograms were filtered at 30-400Hz (bipolar) and 1-240Hz (unipolar). Bipolar voltages <1.5mV were considered abnormal and bipolar voltages <0.5mV dense scar.[12] Next, the MDCT-derived images were integrated with the EAM. The images were visually aligned using the location of the LM as a landmark for registration. Subsequently, the surfaces of the LV or RV were automatically aligned using CARTOMerge software. After surface registration the position of the LM was used to assess rotation errors.[11,13] Distances between the EAM and the FFI including the LM were calculated to evaluate registration accuracy.

Identification of ablation target sites

In idiopathic VA LV, RV, aortic sinus and/or coronary venous system activation mapping was performed. If no TS could be identified, the potential epicardial TS was predicted based on the spatial distribution of earliest local activation time.[14] The local epicardial fat thickness and vicinity of coronary arteries was assessed prior to epicardial mapping (Figure 2A).

For scar-related VA TS were selected based on activation and entrainment mapping for tolerated VA. For non-tolerated VA, TS were identified guided by pace-mapping (≥11/12 lead match between VA-QRS, stimulus-to-QRS interval >40ms) and/or the presence of late potentials (potentials separated by an isoelectric segment >20ms and inscribing after QRS).

Epicardial mapping and ablation

For idiopathic VA limited epicardial voltage mapping was performed, followed by detailed activation mapping of the predicted TS. In scar related VA, a regional epicardial voltage map

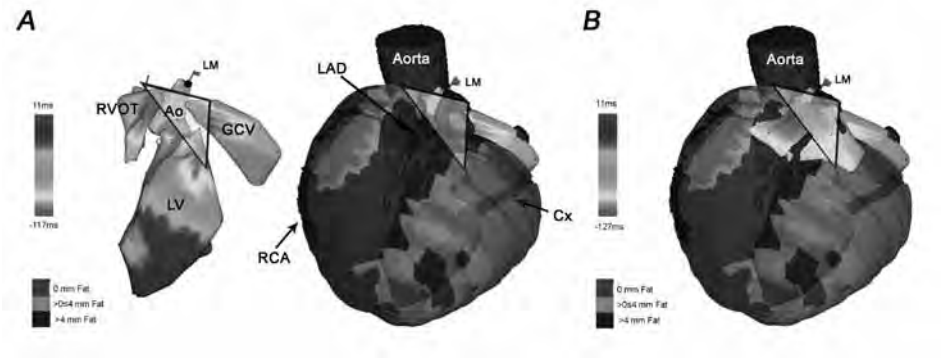


Figure 2. Electroanatomical activation map (EAAM) of an idiopathic ventricular arrhythmia and image integration. Panel A: Endocardial EAAM of the left ventricle (LV), right ventricle outflow tract (RVOT), aorta (Ao) and great cardiac vein (GCV). Similar activation time of the LV, RVOT and GCV was observed. The final fusion image (FFI) was registered with the endocardial EAAM, using the left main artery (LM) (right). The white triangle demonstrates the predicted epicardial target site in the vicinity of the left anterior descending artery (LAD), covered by >4mm fat. Panel B: Limited epicardial EAAM confirmed the earliest activation within the predicted site not suitable for ablation. Cx=Circumflex coronary artery; RCA=right coronary artery. **(for figure in color see page: 260)**

was created of the target area. Ablation TS were defined as for the endocardium and tagged on the epicardial map.

Before epicardial ablation, the vicinity of major coronary arteries branches was estimated on the FFI and categorized into 3 categories (<5mm, 5-15mm, >15mm). Subsequently, coronary angiography (LAO45°, RAO30°) was performed and the distance between catheter tip and coronary artery was evaluated on fluoroscopy using the length of the distal electrode pair (6.7mm) and tip-proximal-electrode distance (14.9mm) as a visual reference (Figure 3). The distance between the catheter tip and major coronary artery branches on the FFI and on fluoroscopy were compared to further evaluate the registration accuracy. If TS were in close proximity to a major branch additional injections were performed to confirm the accuracy of spatial relation as measured on the FFI. Ablation was usually withheld at TS with an estimated distance <5mm. High out put pacing (10mA, 2ms) was performed to determine the location of the phrenic nerve, if appropriate.

Radiofrequency energy was applied at 30-45W (maximum temperature 45ºC, flow 20-30ml/min, 60s) for endocardial sites and up to 50W (flow 20ml/min) for epicardial sites. A successful ablation site was defined as the site where RF energy abolished the VA. In case the VA remained inducible after RF energy was applied, the ablation site was considered non-successful. The endpoint of the procedure was non-inducibility of any VA, inability to identify TS or TS locations that prevented or did not allow effective RF delivery.

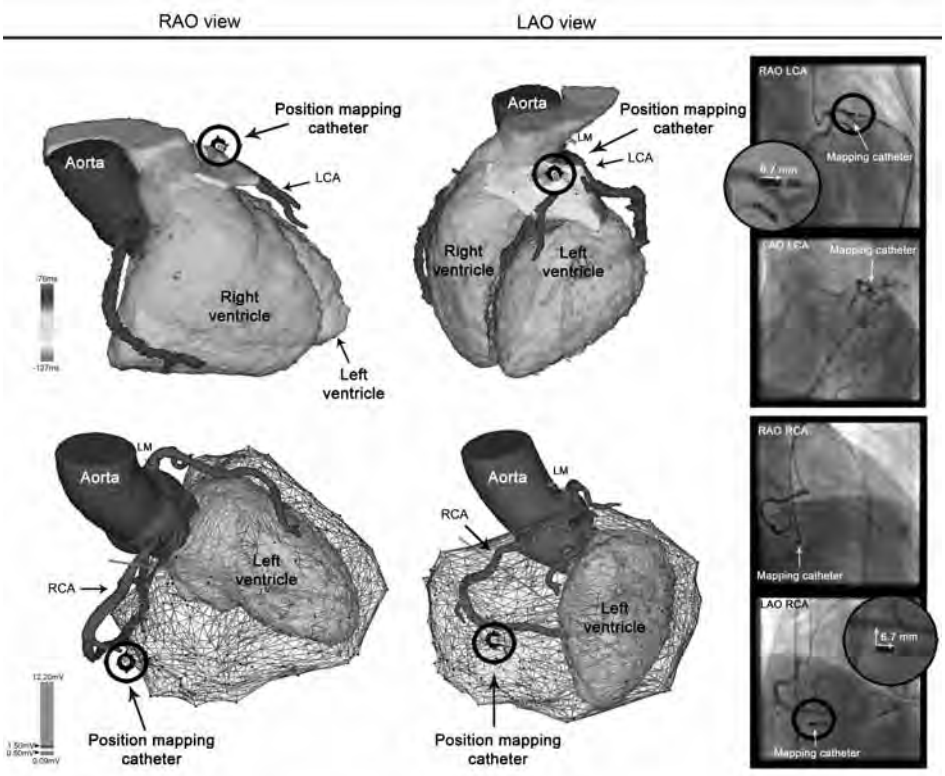


Figure 3. Registration accuracy in 2 patients comparing the distance between the catheter tip and coronary arteries on integrated multi-detector computed tomography (MDCT) images and coronary angiography in a right (RAO) and left (LAO) anterior oblique view. Upper panel: limited activation mapping identified a target site located on the left anterior descending artery (LAD) on both MDCT and angiography. Lower panel: the target site (based on pace-mapping) was located <7mm from the right coronary artery (RCA) confirmed by angiography. **(for figure in color see page: 260)**

Post-procedural evaluation of the impact of epicardial fat

After the procedure, epicardial mapping points and the registration matrix were exported from the CARTO system and superimposed on the original MDCT (Figure 4A). Bipolar and unipolar voltages were correlated to epicardial fat thickness using only mapping points at sites with no evidence for scar on imaging. Mapping points were grouped into three predefined categories according to epicardial fat thickness (0mm, >0≤4mm and >4mm fat).[4] To investigate the impact of epicardial fat on ablation outcome, fat thickness at successful and non-successful ablation sites was compared. In case of linear lesions, the average fat thickness was used.

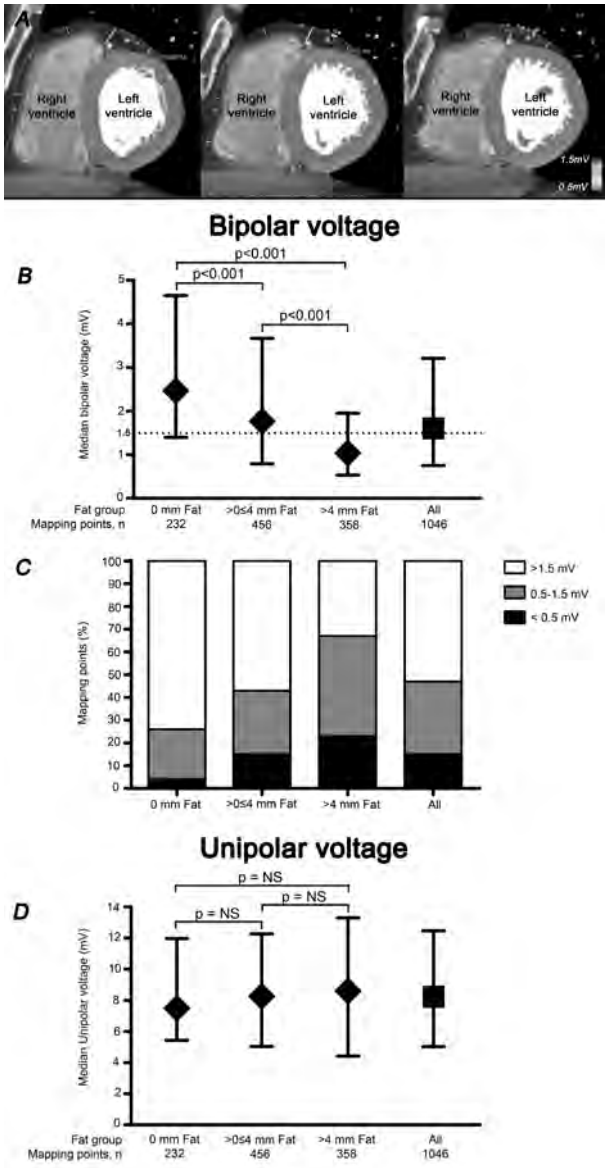


Figure 4. Panel A: Reversed registration of epicardial mapping points projected on the corresponding multi-detector computed tomography (MDCT) location of three sequential short axis images. Points are color coded for bipolar voltage (color bar). Panel B: Median bipolar voltage of epicardial mapping points according to the 3 predefined epicardial fat thickness categories. Panel C: Distribution of epicardial mapping points for each epicardial fat thickness category according to the currently used cut-off values for bipolar voltage mapping. Panel D: Median unipolar voltage of epicardial mapping points according to the 3 epicardial fat thickness categories.

Follow-up

After discharge, patients were followed regularly at our outpatient clinic. Implantable cardioverter defibrillator interrogation was performed every 6 months. Therapy was regarded appropriate when delivered in response to any VA.

Statistical analysis

Statistical analysis was performed using SPSS, version 18.0 (SPSS, Inc., Chicago, IL, USA). Continuous variables are expressed as mean±SD or median (interquartile range) when appropriate, and categorical variables as frequency (%). The Mann-Withney *U*-test or student's T-test were used to compare variables, as appropriate. All tests were two-tailed and a p-value <0.05 was considered statistically significant.

Results

Patient characteristics and pre-procedural MDCT processing

Baseline patient characteristics are summarized in Table 1. The ventricular epicardial surface covered by fat was 65±16%; 25±15% was covered by >4mm fat. Body mass index and age showed a strong association with the percentage of the epicardial surface covered by >4mm fat (p<0.001 and p=0.008, respectively). The basal and apical anterior RV wall and the basal superior LV wall showed the thickest epicardial fat layer (5-6±3mm) (Figure 5).

Table 1. Patient characteristics

Male gender (%)	21 (75)
Age, years	59±16
Body mass index, kg/m^2	25±6
Diabetes mellitus (%)	5(18)
LV ejection fraction,%	46±12
Etiology	
Idiopathic (%)	7 (25)
Ischemic (%)	2 (7)
ARVD/C (%)	3 (11)
LV-cardiomyopathy (%)	10 (36)
Biventricular-cardiomyopathy (%)	6 (21)

ARVD/C=Arrhythmogenic right ventricle dysplasia/cardiomyopathy; LV=left ventricle

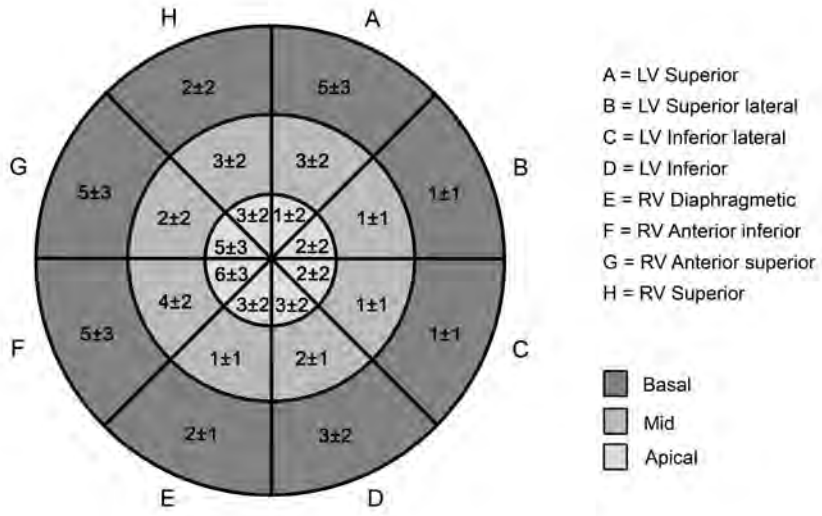


Figure 5. The 24 segments bull's eye reconstruction with 8 short axis segments and 3 long axis segments. For each segment the mean epicardial fat thickness (mm) is indicated.

Real-time image integration and registration accuracy

Endocardial voltage maps of the LV were obtained in 25 patients (structural heart disease 105±65 points, idiopathic VA 50±25 points) with an additional endocardial RV map in 9. In 3 patients only RV mapping was performed (67±23 points). Epicardial mapping was performed in all patients (structural heart disease 150±74 points, idiopathic 87±50 points). The MDCT derived images were successfully merged to the FFI and integrated with the aortic and LV and/or RV EAM with a mean surface registration error of 2.8±1.3mm. After registration, the position error between the LM on the EAM and the FFI was 5.5±2.8mm.

Ablation target sites and procedural outcome

In 22 patients 41 VA (cycle length 382±98ms) could be induced; in 5 patients the clinical VA (idiopathic premature ventricular complexes) was present at baseline; in one patient no VA could be induced. All 46 VA were targeted (Table 2). Seven VA (15%) in 5 patients were successfully ablated from the endocardium and 18 (39%) VA in 13 patients were successfully targeted from the epicardium (7.7±4.3 RF applications/VA).

Ablation of 21 (46%) VA in 13 patients was non-successful. Two VA in 1 LV-cardiomyopathy patient were not targeted due to proximity of the His bundle. For 5 hemodynamic non-tolerated VA in 3 patients (2 LV-cardiomyopathy, 1 arrhythmogenic right ventricular dysplasia/cardiomyopathy) no appropriate TS could be identified. In 1 patient epicardial

mapping for 3 VA was compromised due to pericardial adhesions. Ablation at the TS of the remaining 11 VA in 8 of 13 patients was either ineffective (4 VA in 4 patients) or withheld because of close proximity of a coronary artery (7 VA in 4 patients).

Of interest, all ineffective ablation sites were located at the LV superior wall (2 idiopathic and 1 LV-cardiomyopathy VA) and RV anterior superior wall (1 biventricular-cardiomyopathy VA). These sites were covered by >4mm fat as delineated by the fat meshes.

MDCT-derived coronary anatomy

To further evaluate the registration accuracy, the distance between 28 TS and coronary arteries on the FFI and coronary angiography were compared. Based on the integrated FFI, in 7 patients the TS for 11 VA were located >15mm from a coronary artery, in 8 patients the TS for 8 VA were located 5-15mm and in 6 patients the TS for 9 VA were located <5mm from a coronary artery. In all cases the distance was confirmed by angiography (Figure 3, Table 2). In 4 patients (7 VA) ablation was withheld because of proximity of a coronary artery accounting for ablation failure. In 2 patients ablation was successfully performed without acute complications despite the vicinity of coronary arteries; 1 patient had a TS near a functional occluded coronary artery, the other patient who was in cardiogenic shock because of incessant VA had a TS close to the circumflex artery (distance<5mm) and RF was successfully applied. This patient died 4 weeks later due to progressive heart failure. No coronary artery lesion could be detected at autopsy (Figure 6).

Procedural complications

In 1 patient a major epicardial bleeding (>80cm^3) occurred. Of importance, there was no damage of the LM evaluated by angiography and no procedure related death. Procedural time was 253±89 minutes and fluoroscopy time was 43±15 minutes.

Post-procedural evaluation of the impact of epicardial fat

A total of 1046 epicardial mapping points were located at the epicardium without evidence for scar on imaging. Twenty-two percent of these mapping points (n=232) were located at epicardium not covered by fat with a median bipolar voltage of 2.5mV (1.4-4.6mV) and a median unipolar voltage of 7.5mV (5.4-12.0mV). Bipolar voltages decreased significantly with increasing epicardial fat thickness according to the predefined categories ($p<0.001$). However, using the previously suggested cut-off value of 2.8mm, 37% of mapping points comprised bipolar voltage of >1.5mV. Unipolar voltage was not influenced by epicardial fat (Figure 4B-D). Epicardial fat thickness was 16.9±6.8mm (range 7.3-22.2mm) at 4 non-successful ablation sites, as compared to 1.5±2.1mm (range 0-6.1mm, $p<0.001$) at 17 successful sites.

Table 2. Procedural characteristics

Pt no.	Age	Sex	BMI (kg/cm²)	Epi surface >4mm Fat(%)	Etiology	Epi mapping points	VA no.	VA CL	Mapping strategy	Target site	Mean fat thickness at TS(mm)	Acute ablation outcome	Failure reason	Vicinity to coronary artery
1	68	M	27.5	55	Idiopathic	106	1	PVC	A	LV sup	22.2±3.6	Failure	RF ineffective	LAD 5-15mm
2	76	M	19.9	13	LV-CMP	187	1	300	A+S	NI	NA	Failure	Unstable VA, no TS	NA
3	72	M	24.9	16	LV-CMP	173	1	270	A+S	LV inf-lat	2.2±2.1	Success		>15mm
							2	322	A+S	LV inf	1.3±0.7	Success		>15mm
4	57	F	19.8	17	Idiopathic	128	1	504	A	LV inf-lat	4.8±0.2	Success		RCA 5-15mm
5	59	M	24.9	18	ARVD/C	112	1	480	A+S	RV ant-sup	3.3±1.1	Success		RCA 5-15mm
6	62	M	34.7	37	LV-CMP	190	1	415	A+S	Septal	NA	Failure	TS near His	NA
							2	405	A+S	Septal	NA	Failure	TS near His	NA
7	18	M	20.9	4	Idiopathic	154	1	260	A	LV inf-lat	1.2±0.6	Success		RCA 5-15mm
8	22	M	18.8	12	ARVD/C	259	1	240	A+S	NI	NA	Failure	Unstable VA, no TS	NA
							2	190	A+S	NI	NA	Failure	Unstable VA, no TS	NA
9	40	M	19.9	13	Biv-CMP	246	0	-	S	NA	NA	-		NA
10	62	M	23.1	16	Ischemic	220	1	440	A+S	LV sup-lat	0.4±0.0	Success		>15mm
11	73	M	21.2	13	LV-CMP	189	1	458	A+S	LV inf	5.4±2.6	Failure	TS near RCA	RCA <5mm

Table 2. (continued)

Pt no.	Age	Sex	BMI (kg/cm²)	Epi surface >4mm Fat(%)	Etiology	Epi mapping points	VA no.	VA CL	Mapping strategy	Target site	Mean fat thickness at TS(mm)	Acute ablation outcome	Failure reason	Vicinity to coronary artery
12	74	M	23.3	30	Ischemic	182	1	310	A	RV diaphragmatic	6.1±3.4	Success		Functional occluded LAD <5mm
13	30	F	19.6	10	LV-CMP	172	1	243	S	LV sup-lat	0	Success		>15mm
							2	353	A+S	LV sup-lat	0	Success		>15mm
14	48	F	22.1	6	ARVD/C	97	1	253	A+S	RV sup	0	Success		>15mm
							2	250	A+S	RV sup	0	Success		>15mm
15	61	M	31.8	53	Biv-CMP	37	1	360	A+S	RV ant-inf	7.3±1.1	Failure	RF ineffective	RCA 5-15mm
							2	360	A+S	RV ant-inf-endo	NA	Success		NA
16	48	M	19.7	11	LV-CMP	176	1	520	A+S	LV sup-lat-endo	NA	Success		NA
							2	380	A+S	LV sup-lat-endo	NA	Success		NA
							3	430	A+S	LV inf-endo	NA	Success		NA
							4	430	A+S	LV inf-lat	0.4±1.0	Success		>15mm
17	65	M	29.7	36	Idiopathic	93	1	PVC	A	LV sup	10.8±5.8	Failure	TS near LAD	LAD <5mm
18	45	M	26.7	17	LV-CMP	92	1	340	S	LV sup-lat	0.3±0.3	Success		>15mm
							2	400	S	NI	NA	Failure	pericardial adhesions	NA
							3	440	S	NI	NA	Failure	pericardial adhesions	NA
							4	300	S	NI	NA	Failure	pericardial adhesions	NA

Table 2. (continued)

Pt no.	Age	Sex	BMI (kg/cm²)	Epi surface >4mm Fat(%)	Etiology	Epi mapping points	VA no.	VA CL	Mapping strategy	Target site	Mean fat thickness at TS(mm)	Acute ablation outcome	Failure reason	Vicinity to coronary artery
19	77	F	22.5	28	Biv-CMP	163	1	554	A+S	LV sup-lat	0	Success		Cx <5mm RF not withheld
20	70	M	23.1	48	Biv-CMP	18	1	230	S	RV ant-sup-endo	NA	Success		
21	71	M	34.3	21	LV-CMP	68	1	387	A+S	LV sup	1.3±1.2	Failure	TS near LAD	LAD <5mm
							2	621	A+S	LV sup	1.3±1.2	Failure	TS near LAD	LAD <5mm
							3	356	A+S	LV sup	1.3±1.2	Failure	TS near LAD	LAD <5mm
							4	387	A+S	LV sup	1.3±1.2	Failure	TS near LAD	LAD <5mm
22	54	M	26.8	23	Idiopathic	61	1	PVC	A	LV sup	21.0±5.0	Failure	RF ineffective	RCA 5-15mm
23	69	M	28.4	45	Biv-CMP	80	1	350	A+S	RV ant-inf-endo	NA	Success		
24	71	M	38.7	53	LV-CMP	50	1	375	A+S	LV sup	17.1±2.0	Failure	RF ineffective	LAD 5-15mm
25	66	F	24.2	21	Biv-CMP	273	1	500	A+S	LV inf	0.1±0.3	Success		>15mm
							2	430	A+S	RV sup	0.7±1.4	Success		>15mm
26	69	M	24.0	19	Idiopathic	33	1	PVC	A	LV sup	5.5±0.3	Success		LAD 5-15mm

Table 2. (continued)

Pt no.	Age	Sex	BMI (kg/cm²)	Epi surface >4mm Fat(%)	Etiology	Epi mapping points	VA no.	VA CL	Mapping strategy	Target site	Mean fat thickness at TS(mm)	Acute ablation outcome	Failure reason	Vicinity to coronary artery
							1	430	S	LV sup-lat-endo	NA	Success		NA
							2	360	S	LV inf-lat-endo	NA	Success		NA
27	59	F	25.5	11	LV-CMP	159	3	350	S	NI	NA	Failure	Unstable VA, no TS	NA
							4	280	S	NI	NA	Failure	Unstable VA, no TS	NA
28	57	F	36.8	43	Idiopathic	32	1	PVC	A	LV sup	20.2±7.6	Failure	TS near LAD	LAD <5mm

A=Activation mapping; Ant=Anterior; ARVD/C=Arrhythmogenic right ventricular dysplasia/cardiomyopathy; Biv=Biventricular; CL=Cycle lenght; CMP=Cardiomyopathy; Cx=Circumflex artery; EF=Ejection fraction; Endo=endocardial; Epi=epicardial; F=Female; Inf=Inferior; LAD=Left anterior descending coronary artery; Lat=Lateral; LV=Left ventricle; M=Male; NA=Not applicable; NI=Not identified; PVC=Premature ventricular complex; RCA=Right coronary artery; RF=Radiofrequency energy; S=Substrate mapping; Sup=Superior; VT=Ventricular arrhythmia

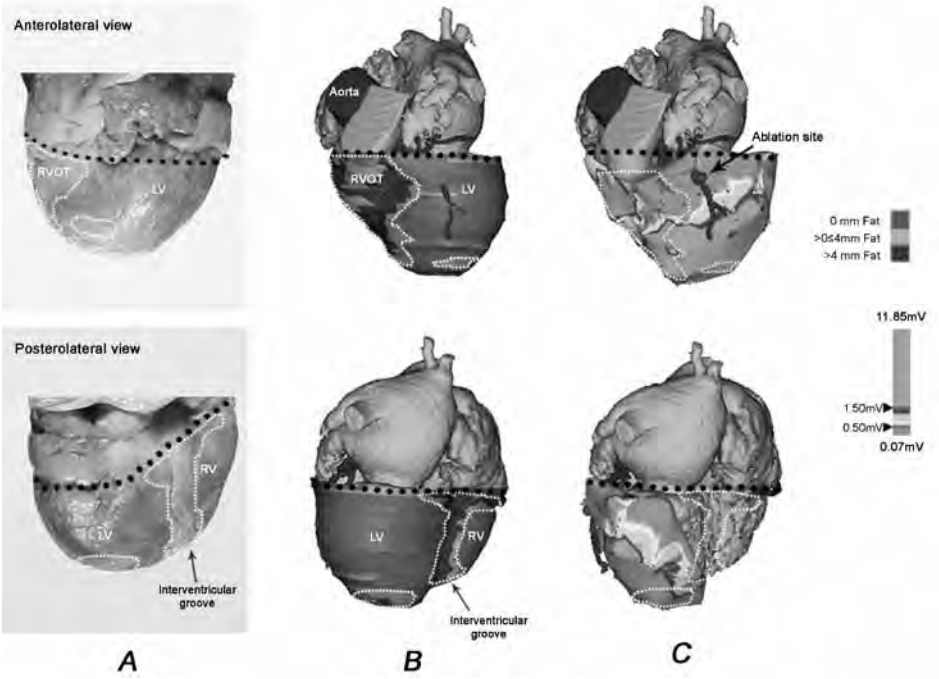


Figure 6. Panel A: Gross pathology of the heart of the patient who died 4 weeks after ablation. Panel B: Final fusion image. Panel C: Fusion of the multi-detector computed tomography (MDCT) anatomy with the epicardial electroanatomical voltage map in a modified anterolateral (top) and posterolateral (bottom) view. The ablation site in the vicinity of the circumflex coronary artery is indicated. Comparison of panel A and B shows a good correlation between epicardial fat distribution by pathology and the MDCT derived epicardial fat mesh (white dotted lines). The black line indicates the atrioventricular groove; the anterolateral low voltage area (color coded as indicated) is compatible with subepicardial scar in the absence of epicardial fat.
LV=left ventricle, RV=right ventricle, RVOT=right ventricle outflow tract. **(for figure in color see page: 261)**

Predicted epicardial target sites in idiopathic VA

In the subgroup of 7 patients without evidence of structural heart disease the earliest local activation time was similar over a broad endocardial area (Δ local activation time ≤10ms at ≥3 endocardial points >1.5cm apart) (n=2), at two remote endocardial sites (Δ local activation time ≤10ms at 2 endocardial points >1.5cm apart) (n=1) or at both an endocardial and an aortic sinus/cardiac venous site (n=4) strongly suggesting an epicardial TS. The predicted epicardial TS and its distance to the coronary arteries and the expected fat layer was confirmed after epicardial EAM and reversed registration in all patients. The area was located near (<5mm) the left anterior descending artery in 2 patients (no ablation performed) (Figure 2B). In 2 other patients, the TS was covered by 22.2mm and 21.0mm fat and ablation at

these sites was ineffective. In 3 patients the TS was located remote (range 7.3-11.5mm) from a coronary artery and covered by 3.8±2.3mm fat. Ablation at these sites abolished the VA.

Follow-up

During a mean follow-up of 27±15 months 5 patients died (4 heart failure; 1 cancer) and 1 patient underwent heart transplantation because of terminal heart failure. Of the remaining 22 patients, 11 patients experienced VA recurrence; all 7 patients with ablation failure (100%) and 4 (27%) who were non-inducible for any VA.

Discussion

The distribution of epicardial fat and coronary arteries varies between patients. Both are of key relevance during epicardial mapping and ablation. This study is the first to demonstrate the feasibility and accuracy of real-time integration of MDCT derived images to visualize both the coronary artery anatomy and the distribution and thickness of epicardial fat *before* epicardial mapping. In 62% of patients with epicardial ablation failure lack of success was related to the proximity of a coronary artery or a thick epicardial fat layer both correctly identified using image integration.

Accuracy of real-time image integration

Image integration was performed using the ostium of the LM as a single landmark and by the surface registration tool provided by CARTO after limited endocardial mapping. This approach resulted in highly accurate integration of EAM and MDCT data. In all patients accuracy was verified with surface registration statistics (surface error 2.8±1.3mm) and the position error between the LM landmark on the EAM and the FFI images (5.5±2.8mm). The registration accuracy of the LM was used to assess rotation errors. The relatively large position error of this landmark is likely due to the fact that the LM is located outside the surface of the LV and RV. The absolute value of the LM position error underestimates the registration accuracy as position errors due to rotation are expected to be larger with increasing distance from the surface. For all points the mean surface registration error was only 2.8mm which is clinically acceptable keeping in mind that the used mapping catheter had a 3.5mm tip.

In contrast to all prior studies, registration accuracy was not only evaluated by the surface registration statistic. We also assessed accuracy by comparing the distance between catheter position and coronary arteries on integrated maps and coronary angiograms. The clinically relevant distance of <5mm, 5-15mm or >15mm was correctly estimated in all 14 patients in whom the TS was located in the proximity of a coronary artery. Others have used the epicardial apex and the most lateral tricuspid and mitral annular points as landmarks for image integration of MDCT derived data after epicardial EAM.[1] However, this strategy may

be prone to rotational errors which do not necessarily result in poor surface registration statistics and in addition this strategy requires extensive epicardial mapping. By using the LM as a landmark, rotational errors can be excluded and epicardial mapping can be restricted to the area of interest.

The demonstrated correspondence of the distance between mapping catheter position and coronary arteries on integrated MDCT image and fluoroscopy has important practical implications. After confirmation of the registration accuracy by a single coronary injection, the distance between further TS and major coronary arteries may be evaluated by integrated MDCT only. In case of close proximity to a major coronary artery or when small coronary arteries, such as diagonal and obtuse marginal branches are present and not accurately visualized on MDCT, additional limited contrast injection may still be necessary. However, in most cases image integration is likely to prevent multiple coronary injections in different angulations. It may even enable more accurate assessment of the proximity of a coronary artery if angiography in caudal angulations is limited by the location triangle of the EAM system.

Although MDCT derived epicardial fat distribution cannot directly be verified using fluoroscopy, the 3D coordinates for epicardial fat meshes and coronary anatomy were derived from the same MDCT suggesting an identical accuracy to delineate fat thickness.

Epicardial fat and voltage mapping

Up to 64% of the epicardial surface was covered with fat; a quarter with a fat layer of >4mm. Of importance, epicardial fat was not restricted to the atrio- and interventricular groove as suggested by others.[1-3] Epicardial fat can attenuate bipolar voltages thereby preventing accurate delineation of subepicardial scar by bipolar voltage mapping. A fat layer ≥2.8mm was found to best separate low voltage (<1.5mV) from normal voltage in a prior study.[1] However, our newly proposed technique of reversed registration allowed a head-to-head comparison of voltage data and local fat thickness. Although we could confirm a decrease in bipolar voltages with increasing fat thickness, nearly 60% of all mapping points acquired in areas with fat and >37% of points acquired in areas with ≥2.8mm fat showed normal bipolar voltages. These findings underline the importance of accurate MDCT derived fat information to avoid overestimation of subepicardial scar and underestimation of epicardial fat.

In contrast to prior observations, this study demonstrates that unipolar voltages are not influenced by epicardial fat which may be caused by the larger field of view.[15,16] Therefore, unipolar voltage mapping may be of value to indicate subepicardial or intramural scar even when a significant epicardial fat layer is present.

Epicardial fat and impact on ablation

Epicardial fat was thickest at the LV superior and RV anterior wall, which is in line with prior investigations.[5] Of interest, all ineffective RF applications were delivered in these areas.

Little is known about the effect of epicardial fat on the efficacy of RF applications. In a prior study, epicardial cooled tip ablation was unable to produce epicardial lesions applied at sites covered by a fat layer >3.5mm.[4] However, this was tested for only 3 applications in an animal model of myocardial infarction. In humans, Desjardins et al. compared epicardial fat thickness of 12 effective and 4 ineffective epicardial cooled-tip ablation sites; all ineffective ablation sites were covered by 10.8-14.6mm fat while effective ablation sites were all located at sites covered by <1.8mm fat.[1] Therefore, a cut-off value for epicardial fat thickness precluding effective epicardial ablation remained undetermined.

In the current study, ablation was performed at 21 sites covered by 0-22.2mm of epicardial fat, including 6 sites covered by 3.0-10.0mm epicardial fat. The epicardial fat thickness at ineffective ablation sites ranged from 7.3-22.2mm. In contrast, all effective ablation sites were covered by 0-6.1mm fat. These findings suggest that an epicardial fat layer <7mm allows for effective irrigated tip ablation in humans.

Predicted epicardial target sites in idiopathic VA

Real-time visualization of the coronary anatomy and fat distribution before epicardial access might be particularly important in patients with a focal arrhythmogenic source typical for idiopathic VA. Based on local activation times we could not only correctly predict the epicardial TS but also, using the pre-acquired and integrated MDCT, the proximity of coronary arteries and local fat thickness at these TS before epicardial access. Consequently, image integration may predict potential ablation failure and may thereby prevent unnecessary epicardial access in selected patients in the future.

Limitations

The comparison of successful and non-successful TS was performed retrospectively. The validation of a cut-off value of >7mm for epicardial fat preventing effective RFCA should be performed in a prospective manner in a larger group of patients.

In addition, the bull's eye reconstruction of epicardial fat reflects a simplified contour of the heart. Consequently, interpretation of the bull's eye should be performed with vigilance and is merely designed to provide a schematic overview of epicardial fat thickness and distribution.

The value of electrogram characteristics for delineation of scar was not analyzed, since the current gold standard to delineate scar (contrast-enhanced magnetic resonance imaging) was not available during the procedure in all patients. However, the objective of this study was to demonstrate the clinical value of real-time image integration of MDCT derived data and to determine the influence of epicardial fat thickness on bipolar and unipolar electrogram voltages. Therefore, only areas without evidence for scar were evaluated.

Conclusion

Real-time image integration of pre-acquired MDCT data on coronary anatomy and fat distribution using the ostium of the LM as a single landmark with EAM is safe, accurate and feasible and available before epicardial access. One fourth of the ventricular epicardial surface is covered by >4mm fat which is predominantly present at the LV superior wall and RV anterior wall. Although bipolar voltages decrease with increasing fat thickness the exact delineation of fat based on bipolar voltage mapping is poor and may be even worse if sub-epicardial scar is present. In contrast, unipolar voltages are not influenced by fat thickness and might therefore be superior for identification of scar covered by epicardial fat.

Epicardial fat layers of >7mm and the presence of coronary arteries are important reasons for epicardial ablation failure. Visualization of the MDCT derived coronary anatomy and epicardial fat thickness prior to epicardial mapping is therefore of importance for the correct interpretation of local bipolar electrograms and the identification of potential harmful and ineffective ablation sites. In addition, accurate image integration after endocardial ablation failure for focal VA may even prevent unnecessary pericardial access and thereby potential complications in selected patients.

Reference List

(1) Desjardins B, Morady F, Bogun F. Effect of epicardial fat on electroanatomical mapping and epicardial catheter ablation. J Am Coll Cardiol 2010; 56:1320-7.

(2) Saba MM, Akella J, Gammie J, Poston R, Johnson A, Hood RE, Dickfeld TM, Shorofsky SR. The influence of fat thickness on the human epicardial bipolar electrogram characteristics: measurements on patients undergoing open-heart surgery. Europace 2009; 11:949-53.

(3) Tung R, Nakahara S, Ramirez R, Lai C, Fishbein MC, Shivkumar K. Distinguishing epicardial fat from scar: analysis of electrograms using high-density electroanatomic mapping in a novel porcine infarct model. Heart Rhythm 2010; 7:389-95.

(4) d'Avila A, Houghtaling C, Gutierrez P, Vragovic O, Ruskin JN, Josephson ME, Reddy VY. Catheter ablation of ventricular epicardial tissue: a comparison of standard and cooled-tip radiofrequency energy. Circulation 2004; 109:2363-9.

(5) Abbara S, Desai JC, Cury RC, Butler J, Nieman K, Reddy V. Mapping epicardial fat with multidetector computed tomography to facilitate percutaneous transepicardial arrhythmia ablation. Eur J Radiol 2006; 57:417-22.

(6) van Werkhoven JM, Heijenbrok MW, Schuijf JD, Jukema JW, Boogers MM, van der Wall EE, Schreur JH, Bax JJ. Diagnostic accuracy of 64-slice multislice computed tomographic coronary angiography in patients with an intermediate pretest likelihood for coronary artery disease. Am J Cardiol 2010; 105:302-5.

(7) Berruezo A, Mont L, Nava S, Chueca E, Bartholomay E, Brugada J. Electrocardiographic recognition of the epicardial origin of ventricular tachycardias. Circulation 2004; 109:1842-7.

(8) Daniels DV, Lu YY, Morton JB, Santucci PA, Akar JG, Green A, Wilber DJ. Idiopathic epicardial left ventricular tachycardia originating remote from the sinus of Valsalva: electrophysiological characteristics, catheter ablation, and identification from the 12-lead electrocardiogram. Circulation 2006; 113:1659-66.

(9) Valles E, Bazan V, Marchlinski FE. ECG criteria to identify epicardial ventricular tachycardia in nonischemic cardiomyopathy. Circ Arrhythm Electrophysiol 2010; 3:63-71.

(10) Sosa E, Scanavacca M, d'Avila A, Pilleggi F. A new technique to perform epicardial mapping in the electrophysiology laboratory. J Cardiovasc Electrophysiol 1996; 7:531-6.

(11) Wijnmaalen AP, van der Geest RJ, van Huls van Taxis CF, Siebelink HM, Kroft LJ, Bax JJ, Reiber JH, Schalij MJ, Zeppenfeld K. Head-to-head comparison of contrast-enhanced magnetic resonance imaging and electroanatomical voltage mapping to assess post-infarct scar characteristics in patients with ventricular tachycardias: real-time image integration and reversed registration. Eur Heart J 2011; 32:104-14.

(12) Marchlinski FE, Callans DJ, Gottlieb CD, Zado E. Linear ablation lesions for control of unmappable ventricular tachycardia in patients with ischemic and nonischemic cardiomyopathy. Circulation 2000; 101:1288-96.

(13) Zeppenfeld K, Tops LF, Bax JJ, Schalij MJ. Images in cardiovascular medicine. Epicardial radiofrequency catheter ablation of ventricular tachycardia in the vicinity of coronary arteries is facilitated by fusion of 3-dimensional electroanatomical mapping with multislice computed tomography. Circulation 2006; 114:e51-e52.

(14) van Huls van Taxis CF, Wijnmaalen AP, den Uijl DW, Gawrysiak M, Putter H, Schalij MJ, Zeppenfeld K. Reversed polarity of bipolar electrograms for predicting a successful ablation site in focal idiopathic right ventricular outflow tract arrhythmias. Heart Rhythm 2011; 8:665-71.

(15) Hutchinson MD, Gerstenfeld EP, Desjardins B, Bala R, Riley MP, Garcia FC, Dixit S, Lin D, Tzou WS, Cooper JM, Verdino RJ, Callans DJ, Marchlinski FE. Endocardial unipolar voltage mapping to detect epicardial ventricular tachycardia substrate in patients with nonischemic left ventricular cardiomyopathy. Circ Arrhythm Electrophysiol 2011; 4:49-55.

(16) Polin GM, Haqqani H, Tzou W, Hutchinson MD, Garcia FC, Callans DJ, Zado ES, Marchlinski FE. Endocardial unipolar voltage mapping to identify epicardial substrate in arrhythmogenic right ventricular cardiomyopathy/dysplasia. Heart Rhythm 2011; 8:76-83.


patient
VT
mappin
catheter
circuit
scar-related
endocardial
QRS
underlying
circuits
potentials
electroanatomical
VA
important
studies
epicardial
myocardial
heart
idiopathic
MI
sites
chapter
RFCA
associated
bipolar
arrhythmia
anatomical
also
site
information
surgical
studied
approach
DCM
LV
rate
left
acute
morphology
reduction
Class
small
post
border
area
first
failure
outcome
isthmus
CE-MRI
selected
fibrosis
slow
EGMs
potential
inducible
ICD
pacing
areas
frequent
However
ejection
presenting
based
number
successful
Substrate
cause
reperfusion
EGM
structural
Catheter
considered
therapy
fraction
geometry
disease
monomorphic
located
time
study
including
reported
VTs
tachycardia
Figure
two
use
conduction
stable
reentrant
scars
success
Chapter
VF
derived
techniques
however
block
RF
wavefront
experienced
DCM
effective

Part II

Catheter ablation and outcome in different ventricular tachycardia substrates

Chapter 7

Beneficial effects of catheter ablation on left ventricular and right ventricular function in patients with frequent premature ventricular contractions and preserved ejection fraction

Adrianus P. Wijnmaalen, Victoria Delgado, Martin J. Schalij, Carine F.B. van Huls van Taxis, Eduard R. Holman, Jeroen J. Bax, Katja Zeppenfeld

* A.P. Wijnmaalen and V. Delgado contributed equally to this article and are shared first author.

Heart. 2010 Aug;96(16):1275-80.

Abstract

Objective: Improvement of left ventricular (LV) ejectionfraction (EF) after radiofrequency catheter ablation (RFCA) of frequent premature ventricular contractions (PVCs) has been reported. However, most patients with frequent PVCs have normal LVEF. In these patients subtle and early forms of PVC induced left and right ventricular (RV) impairment may not be detected by standard echocardiographic techniques. This study aimed to assess the effect of frequent PVCs on ventricular function in patients with preserved LVEF.

Methods: Forty-nine patients (30male, 49±16years) with recent onset (median 1.2years), frequent PVCs (burden 26±13%) and 25 healthy controls were studied. Thirty-four patients with PVCs underwent successful RFCA. Two-dimensional echocardiography was performed at baseline and follow-up. LV volumes and LVEF were calculated by Simpson's rule. Tricuspid annulus plane systolic excursion and fractional area change were calculated to assess RV function. Multidirectional LV strain (radial, circumferential, longitudinal) and RV free wall longitudinal strain were calculated by two-dimensional speckle tracking imaging. At baseline LVEF, volumes and RV dimensions were normal in patients and controls.

Results: Speckle tracking imaging demonstrated reduced LV and RV strain in PVC patients as compared to controls. At follow-up there were no changes in LVEF, LV volumes and RV dimensions and function in successfully treated by RFCA and untreated patients. However, radial, circumferential and longitudinal strain improved significantly in patients after RFCA but remained unchanged in untreated patients.

Conclusions: Frequent PVCs can induce subtle cardiac dysfunction detected by speckle tracking imaging analysis in patients without apparent cardiomyopathy. RFCA can successfully eliminate PVCs and improve cardiac function.

Introduction

Symptomatic ventricular ectopy is frequently encountered in clinical practice. The arrhythmia occurs commonly in patients without structural heart disease and is considered to be without prognostic significance.[1]

In some patients, frequent idiopathic premature ventricular contractions (PVCs) can cause moderate to severe left ventricular (LV) dysfunction.[2-4] Elimination of these PVCs by radiofrequency catheter ablation (RFCA) may result in improved LV ejection fraction (EF).[2-4] The majority of patients presenting with frequent symptomatic PVCs has normal LV volumes and LVEF. It has however been shown that impairment of LV function may evolve after several years of follow-up.[5] Small series demonstrated a reduction of LV dimension after successful RFCA in patients with normal LV function using conventional echocardiography assessment.[6, 7] This finding suggests that frequent PVCs may already have an early subclinical detrimental effect on LV function which may not be unmasked with conventional echocardiography. Whether frequent PVCs have an adverse effect on right ventricular (RV) function is unknown.

Recently, two-dimensional (2D) speckle tracking strain imaging has been introduced.[8, 9] This novel technique enables accurate detection of subtle abnormalities in ventricular function that are not revealed by conventional echocardiographic parameters such as LVEF and RV fractional area change.[10] In addition, 2D speckle tracking strain imaging allows angle-independent evaluation of multidirectional LV strain in radial, circumferential, and longitudinal directions and RV longitudinal strain.[11]

The purpose of this study was to assess the effect of recent-onset, frequent PVCs on RV and LV function in patients with preserved LVEF using 2D speckle tracking strain imaging. In addition, the effect of successful RFCA of frequent PVCs on LV and RV function was evaluated.

Methods

Study population and study protocol

Forty-nine consecutive patients with symptomatic, frequent PVCs (>5% PVC on 24h Holter monitoring) were included. All patients underwent extensive baseline evaluation to rule out structural heart disease including a clinical history with regard to the onset of symptoms, 12-lead electrocardiogram (ECG), exercise testing, 24-hour Holter monitoring and 2D transthoracic echocardiography.

The 12-lead ECG QRS duration, morphology and PVC coupling interval were evaluated. The PVC burden was calculated by dividing the number of PVCs by the total number of beats on Holter recording.

Echocardiographic reference values were obtained from a group of 25 individuals with structural normal hearts. The controls were frequency matched to patients by age, gender, body surface area and LV function. The control group included individuals who were referred for evaluation of chest pain and who had normal echocardiograms. Those individuals referred for echocardiographic evaluation of known valvular heart disease, murmur, syncope, arrhythmias, congestive heart failure or cardiac transplantation were excluded.

Radiofrequency catheter ablation

After informed consent catheter mapping and ablation was performed in the post-absorptive, non-sedated state. Antiarrhythmic drugs were discontinued for 5 half-lives, with the exception of amiodarone.

Mapping was facilitated by an electroanatomical mapping system (CARTO) using a transvenous or retrograde aortic approach. At the site of earliest activation based on the onset of bipolar electrograms with a local unipolar QS-pattern pace-mapping was performed to confirm a ≥11/12 lead QRS pace-match.

Radiofrequency energy was delivered at the site of earliest activation and best pace-map with the target temperature set at 60°C and maximum power output of 50W. After ablation programmed electrical stimulation was performed before and during the administration of isoproterenol (2-10μ/min) to confirm that PVCs were not inducible by adrenergic stimulation. Complete procedural success was defined as the absence of spontaneous or inducible PVC for at least 45 minutes after ablation.

Echocardiography

Two-dimensional echocardiography was performed using a commercially available system (Vivid-Seven, General Electric Vingmed, Horten, Norway) equipped with a 3.5-MHz transducer. Data acquisition was performed in the left lateral decubitus position at a depth of 16cm in the parasternal and apical views. Standard M-mode, grey-scale 2D and color-Doppler images, triggered to the QRS complex, were acquired and saved in cine-loop format for off-line analysis (EchoPAC 7.0.0., GE Medical Systems, Horten, Norway). All echocardiographic measurements were performed on sinus beats, avoiding the first postextrasystolic beat if feasible.

Left ventricular end-diastolic and end-systolic volumes were measured at the apical 2- and 4-chamber views by modified Simpson's rule and LVEF was derived.[12] RV dimensions were measured according to current guidelines.[12] From the apical 4-chamber view, the mid-cavity and basal RV diameters as well as RV longitudinal diameter were measured at end-diastole. From the parasternal short-axis images, the end-diastolic RV outflow tract diameter was measured proximal to the pulmonary valve. RV systolic function was evaluated by calculating the fractional area change and measuring the tricuspid annular plane systolic excursion (TAPSE) index from the apical 4-chamber view.[12]

Two-dimensional speckle tracking imaging analysis

Multidirectional analysis of LV strain (radial, circumferential and longitudinal directions) was performed using 2D speckle tracking imaging. Standard grey-scale 2D images were acquired at a high frame rate to assure adequate tracking of the speckles equally distributed within the myocardium. Myocardial strain can be calculated by measuring the change of the position of the speckles within a myocardial segment along the cardiac cycle.[13, 14]

Applied to the short-axis of the LV, radial strain assesses the thickening and thinning of the myocardial wall whereas circumferential strain assesses the shortening and lengthening of the myocardium along the curvature of the LV wall. The mid-ventricular short-axis of the LV is divided in 6 segments and the values of radial or circumferential strain are derived from the average of the 6 segmental peak systolic strain values (Figure 1A and B).

Applied to LV apical images (2-, 4-chamber and long-axis views), longitudinal strain assesses the shortening of the LV resulting from the excursion of the mitral annulus plane towards the LV apex. Each LV apical view is divided in 6 segments and the global longitudinal strain value is derived from the average of the 18 segmental peak systolic strain values (Figure 1C).

Myocardial deformation of the RV was assessed in the longitudinal direction.[15] From a modified apical 4-chamber view, focused on the RV, longitudinal strain of the free-wall was evaluated. The RV free-wall is divided in 3 segments and the global longitudinal strain value is obtained from the average of the 3 segmental peak systolic strain values (Figure 1D).

All echocardiographic analyses were performed by an independent observer blinded to the clinical history and the treatment. The inter-observer agreement for 2D speckle tracking strain measurements have been previously reported[16, 17], being 6.5±5.4 for radial strain, 2.3±2.4 for circumferential strain, 0.9±1.0 for longitudinal strain and 0.16±3.6% for RV longitudinal strain.

Statistical analysis

Continuous variables are expressed as mean±SD. Categorical variables are expressed as frequencies(%). Comparisons between controls and patients were performed by Student t-test for unpaired data. Patients treated with RFCA and patients who were not treated with RFCA were compared by using Mann-Whitney U-test for unpaired data. Changes in LV and RV dimensions and function at follow-up were compared with Student t-test and Wilcoxon Signed Ranks test for paired data, as appropriate. A p-value <0.05 was considered statistically significant. All statistical analyses were performed with SPSS software (version 16.0, SPSS Inc., Chicago, Illinois).

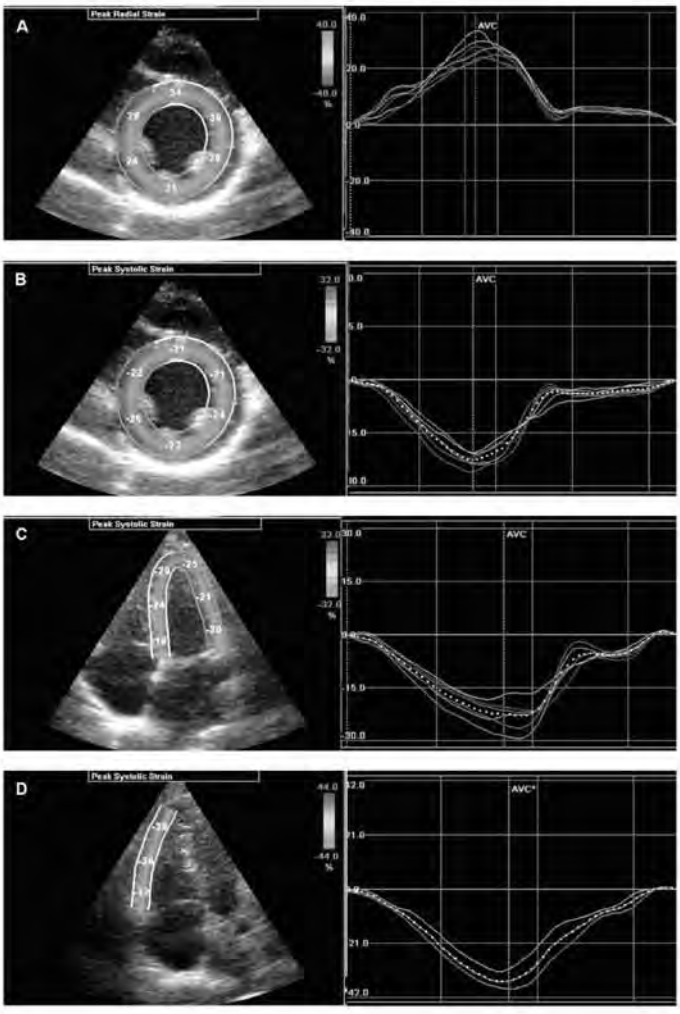


Figure 1. Multidirectional strain analysis with 2-dimensional speckle tracking imaging. In the LV, myocardial strain can be measured in the 3 directions with 2-dimensional speckle tracking imaging. Radial (panel A) and circumferential (panel B) strain are calculated at the mid-ventricular short axis view of the LV. The LV is divided in 6 segments and the segmental peak systolic strain values with the corresponding time-strain curves along the cardiac cycle are obtained. Longitudinal strain of the LV is calculated at the 4-chamber, 2-chamber and long-axis apical views (panel C). In each apical view, the LV is divided in 6 segments, obtaining the segmental peak systolic strain values and the corresponding time-strain curves. Longitudinal strain of the RV free wall (panel D) is measured at modified 4-chamber view, focused on the RV. The free wall is divided in 3 segments, providing the segmental peak systolic strain value and the time-strain curves along the cardiac cycle.

Results

Patient characteristics

Baseline characteristics of the 49 patients (30 men, mean age 49±16 years) are summarized in Table 1. The median duration of symptoms before the first evaluation was 1.2 years (interquartile range 0.4–3 years). In patients who underwent RFCA the 24-hour Holter monitoring was performed 3.0 months (interquartile range 1.0-5.6) prior to the RFCA procedure.

The burden of PVCs was 26±13% of total beats. The PVCs had one dominant morphology in all patients. The mean QRS duration of PVC was 175±24ms. The frontal plane axis was left inferior in 24(49%), left superior in 1(2%), right inferior in 23(47%) and right superior in 1(2%) patient. The average coupling interval was 498±115 ms. No evidence of ischemia was found on exercise testing in any of the patients.

The control group included 25 individuals with normal echocardiograms. By definition, controls were comparable to patients in terms of gender (14(56%) men, p=0.665), age (46±9 years, p=0.333), body surface area (1.8±0.1m^2, p=0.080) and LVEF (58±5%, p=0.201).

Table 1. Baseline characteristics

	n = 49
Age (years)	49 ± 16
Gender (M/F)	30 (61%) / 19 (39%)
Body surface area (m^2)	1.9 ± 0.2
PVC-burden (%)	26 ± 13
Cardiovascular risk factors	
Hypertension	10 (20%)
Hypercholesterolemia	10 (20%)
Family history CAD	13 (27%)
Smoking	7 (14%)
Medical treatment	
Beta-blockers	16 (33%)
ACEI	15 (31%)
Ca-antagonists	5 (10%)
Sotalol	11 (22%)
Amiodarone	1 (2%)
Class I antiarrhythmics	4 (8%)

ACEI = angiotensin-converting enzyme inhibitors, PVC = premature ventricular contraction, CAD = coronary artery disease

Mapping and Radiofrequency catheter ablation

Forty patients were scheduled for mapping and ablation; in nine no RFCA was attempted due to patients' preference. Thirty-four patients could successfully be ablated with a median of 3 RF applications (range 1–14). The PVCs originated from the RV in 24(71%) and the LV

Table 2. Baseline echocardiography and 2-dimensional speckle tracking strain analysis

	Controls (n = 25)	PVC-group (n = 49)	p-value
Heart rate (bpm)	68 ± 10	67 ± 10	0.588
LV end-diastolic volume (ml)	117 ± 29	123 ± 35	0.391
LV end-systolic volume (ml)	49 ± 13	55 ± 19	0.102
LV ejection fraction (%)	58 ± 5	56 ± 7	0.201
RV outflow tract diameter (mm)	29 ± 3	29 ± 4	0.973
RV basal diameter (mm)	31 ± 3	30 ± 4	0.439
RV mid-level diameter (mm)	30 ± 6	29 ± 5	0.421
RV longitudinal diameter (mm)	70 ± 10	71 ± 10	0.481
RV fractional area change (%)	41 ± 9	42 ± 8	0.628
TAPSE (mm)	2.4 ± 0.3	2.4 ± 0.5	0.867
LV Radial strain (%)	43.3 ± 12.7	30.5 ± 12.9	<0.0001
LV Circumferential strain (%)	-20.2 ± 3.1	-15.8 ± 4.0	<0.0001
LV Longitudinal strain (%)	-20.1 ± 1.0	-17.4 ± 3.0	<0.0001
RV Longitudinal strain (%)	-30.1 ± 4.4	-23.8 ± 6.7	<0.0001

LV = left ventricular; PVC = premature ventricular complex; RV = right ventricular; TAPSE = tricuspid annular plane systolic excursion.

in 10(29%) patients. The site of successful RF application was the RV outflow tract in 23, the pulmonary artery in 1, the LV outflow tract in 2, the mitral annulus in 1, the anterior cardiac vein in 3, the aortic cusps in 3 and the Purkinje system in 1 patient. In 2 of these patients 2 different morphologies could be successfully targeted in adjacent areas (RVOT in 1 and Aortic cusps in 1). In 5/6 patients with ablation failure the site of origin could not be determined by an endocardial approach including mapping within the cardiac veins (>1 PVC morphology in 2) and in 1 patient no ablation attempt was made due to the proximity of the His bundle. Procedure and fluoroscopy times were 150±60 min and 17±15 min respectively. In the successfully ablated patients the burden of PVCs was reduced to 0.2±0.8% confirming freedom of PVCs at repeated Holter monitoring 4.1 months (interquartile range 1.4-9.2 months) after RFCA. In contrast, in the 15 patients in whom no mapping and/or ablation attempt was made the PVC burden was stable at follow-up. No complications were observed.

Baseline echocardiography and 2D speckle tracking strain analysis

At baseline, all patients had a non-dilated LV with preserved LVEF (56±7%) and no differences were observed as compared to controls (Table 2). In addition, patients had comparable

RV dimensions and function to controls (fractional area change 42±8% and TAPSE index 2.4±0.5mm) (Table 2).

Multidirectional 2D speckle tracking assessment of the LV demonstrated that patients had significantly impaired LV strain in all the 3 directions (radial, circumferential and longitudinal). Furthermore, patients had lower values of RV longitudinal strain as compared to controls (Table 2). In 7 patients, 2D speckle tracking analysis was performed during sinusal post-extrasystolic beat. However, this had not significant impact on the values of multidirectional strain of the overall population.

Effects of PVC origin

To evaluate the impact of PVC origin on RV and LV function, patients with PVCs originating from the RV confirmed by successful RFCA (n=24) were compared to patients with LV origin (n=10). No differences were observed in LVEF, LV end systolic and diastolic function, RV fractional area change and TAPSE. Myocardial strain was decreased in all the directions to a similar extend in patients with LV and RV site of origin: LV circumferential strain (-16.3±4.0% vs. -15.6±3.3%, p=0.5), LV longitudinal strain (-18.3±3.1% vs. -17.1±2.3%, p=0.7), LV radial strain (30.1±13.8% vs. 33.1±15.6%, p=0.2) and RV longitudinal strain (-25.8±8.4% vs. -22.1±2.3%, p=0.07).

PVC burden and echocardiographic findings

To account for the effect of PVC burden the 30(61%) patients with a PVC burden of >20% (34±9.7%) were compared to 19(39%) patients with a PVC burden <20% (13.3±4.7%). Patients with a high PVC burden tended to have lower LVEF (55±8% vs. 58±6%, p=0.07) and larger LV end-diastolic volume (130±37ml vs. 113±31ml, p=0.13) and LV end-systolic volume (59±20ml vs. 49±17ml, p=0.09) as compared to patients with a moderate PVC burden, however these differences were not significant. Both groups showed comparable values of LV circumferential strain (-16.3±4.4% vs. -15.8±4.0%, p=0.9), radial strain (-31.9±14.2% vs. -32.1±16.0%, p=1.0), longitudinal strain (-17.1±3.5% vs. -17.9±2.2%, p=0.9) and RV longitudinal strain (-23.3±6.0% vs. -25.2±8.3, p=0.3).

Effect of RFCA on LV and RV function

After a median follow up of 13 months (interquartile range 5–22 months) a second echocardiogram was obtained in all patients. The follow-up, the 34 patients successfully treated with RFCA showed a significant decrease in LV end-systolic volume (from 56±21ml to 49±15ml, p=0.018). Changes in LV end-diastolic volumes and LVEF (from 57±8 ml to 59±5%, p=0.245) were not significant. However, with 2D speckle tracking imaging, a significant improvement of strain values was observed in all the 3 directions, with normalization of LV multidirectional myocardial strain. In addition, although there were no significant changes

in RV dimensions and function, RV longitudinal strain also improved at follow-up, with normalization of the longitudinal strain values in successfully treated patients. (Table 3)

In contrast, the group of 15 patients in whom RFCA could not successfully be performed or no RFCA attempt was made the PVC burden was stable and no changes in LV dimensions and function, assessed either by LVEF or multidirectional strain were found. Furthermore, no changes in RV dimensions, function and deformation properties were observed (Table 3).

Discussion

The major finding of the present study is that patients with frequent PVCs of recent onset and normal LV volumes, LVEF and RV dimensions show subtle LV and RV dysfunction. This cardiac impairment normalized after successful ablation of PVCs but remained unchanged in non-treated patients and in patients after unsuccessful RFCA. These findings suggest that recent onset, frequent PVCs can result in reversible biventricular dysfunction not detected by conventional echocardiographic parameters.

Effect of frequent PVCs on ventricular performance

Frequent PVCs are generally considered a benign condition when found in patients without structural heart disease. Small series have demonstrated a link between frequent PVCs and increased LV dimensions and impaired LVEF which improved or normalized after abolishing PVCs by pharmacological treatment or RFCA. However, the majority of patients presenting with frequent PVCs has a preserved LVEF.[1-5] This does not exclude a negative effect of PVCs on systolic function as subtle or early impairment may not be detected by conventional parameters.

Niwano prospectively followed 239 patients with frequent PVCs and only 13, the majority with a high PVC burden, developed a small but significant decline in LVEF after 4 years, suggesting that impaired LV function may develop only over long periods.[5] However, 42 patients with significant symptoms and/or LV dysfunction at baseline were excluded. These patients might represent a subgroup of patients in whom LV dysfunction occurs earlier.[5]

In the present study the median duration of symptoms was 13 months. Despite the short period, these patients had already decreased multidirectional strain as compared to controls, whereas LV volumes, RV dimensions and LV and RV function measured by conventional echocardiographic techniques were normal. This indicates that PVCs may induce early LV and RV dysfunction not detected by conventional 2D echocardiography measurements. The evaluation of multidirectional strain with 2D speckle tracking imaging enables the detection of functional abnormalities by exploring the mechanical properties of the myocardium.[10] 2D speckle tracking imaging may constitute a more sensitive tool to detect subtle ventricular dysfunction, in particular for RV function assessment since quantification of RV volumes

Table 3. Follow-up echocardiography study and 2-dimensional speckle tracking strain analysis

	PVC-RFCA (n = 34)			Non-RFCA PVC (n = 15)		
	Baseline	Follow-up	p-value	Baseline	Follow-up	p-value
Heart rate (bpm)	69 ± 11	68 ± 11	0.790	64 ± 8	68 ± 11	0.670
LV end-diastolic volume (ml)	127 ± 39	120 ± 34	0.077	116 ± 22	114 ± 23	0.551
LV end-systolic volume (ml)	56 ± 21	49 ± 15	0.018	52 ± 14	49 ± 12	0.073
LV ejection fraction (%)	57 ± 8	59 ± 5	0.245	55 ± 5	57 ± 8	0.244
RV outflow tract diameter (mm)	29 ± 4	30 ± 4	0.362	30 ± 4	31 ± 2	0.207
RV basal diameter (mm)	30 ± 4	29 ± 3	0.535	32 ± 4	31 ± 3	0.153
RV mid-level diameter (mm)	29 ± 6	28 ± 5	0.186	28 ± 4	28 ± 5	0.689
RV longitudinal diameter (mm)	73 ± 10	74 ± 10	0.632	68 ± 11	72 ± 11	0.091
RV fractional area change (%)	43 ± 9	45 ± 10	0.261	41 ± 5	40 ± 8	0.783
TAPSE (mm)	2.5 ± 0.5	2.4 ± 0.4	0.327	2.4 ± 0.3	2.2 ± 0.3	0.073
LV Radial strain (%)	31.1 ± 14.2	45.5 ± 16.3*	<0.0001	28.5 ± 9.7	32.0 ± 9.6	0.272
LV Circumferential strain (%)	-16.2 ± 3.9	-18.9 ± 4.2†	0.004	-15.2 ± 4.2	-15.4 ± 3.2	0.925
LV Longitudinal strain (%)	-17.8 ± 2.9	-19.6 ± 2.0*	0.007	-16.4 ± 3.2	-17.1 ± 2.5	0.638
RV Longitudinal strain (%)	-24.2 ± 7.4	-28.4 ± 6.0*	0.009	-22.8 ± 4.2	-23.2 ± 5.2	0.999

*p<0.01 vs. non-RFCA at follow-up; †p = 0.014 vs. non-RFCA at follow-up.
LV = left ventricular; PVC = premature ventricular complex; RFCA = radiofrequency catheter ablation; RV = right ventricular; TAPSE = tricuspid annular plane systolic excursion.

and function with conventional echocardiography remains problematic due to the complex geometry of the RV. However, the present results do not allow to define robust baseline cut-off values of multidirectional myocardial strain to identify and predict which patients will develop cardiomyopathy if RFCA is not applied. Additional studies including larger populations and longer follow-up are warranted to elucidate this aspect.

An inverse relationship between PVC burden and cardiac function has been described and PVC frequency has also been suggested as risk factor for PVC induced cardiomyopathy.[4, 6, 7]

In the current study, patients with a PVC burden of >20% were compared to patients with a PVC burden <20%. Although we did not observe significant differences in LVEF and volumes, there was a tendency to larger LV volumes in patients with a higher PVC burden, still within normal range. LV and RV strain were decreased to a similar extend in patients with a high and moderate PVC burden indicating that even a moderate burden of PVCs (mean 13.3%) can induce subclinical cardiac dysfunction. However, the proportion of patients with a moderate PVC burden was relatively small.

Previous studies reporting on a reversal of cardiomyopathy after RFCA only included patients with PVCs from the RV outflow tract.[3, 7] More recently it was demonstrated that a reversible reduced EF was equally prevalent among patients who had PVCs with a right or left bundle branch block configuration.[4, 18] This was confirmed by our study demonstrating that subtle and reversible LV and RV dysfunction can be induced by PVCs regardless of the site of origin.

RFCA and improvement of LV and RV strain

This study extends the finding of prior reports, that RFCA for PVCs can reverse cardiac functional abnormalities induced by PVCs.[3, 4, 6, 7] While Yarlagadda[3] and Bogun[4] observed reversal of mild to severe dilated cardiomyopathy after ablation of PVCs, Takemoto[7] and Sekiguchi[6] studied patients with normal LVEF detecting no functional abnormalities before RFCA, and demonstrating improvement of LV EF and diameters within the normal range during follow-up. The present study, however, shows that PVC induced LV and RV dysfunction detected at baseline by strain analysis in patients with normal ventricular dimensions and LVEF can be reversed after successful RFCA. In contrast, in the PVC RFCA -control group decreased strain at baseline did not change during short term follow-up. Additional studies with longer follow-up will be warranted to elucidate whether ventricular strain further impairs in patients with frequent PVC non-treated with RFCA.

Clinical implications

Two-dimensional speckle tracking strain imaging detects cardiac functional abnormalities in symptomatic patients with PVCs not detected by conventional echocardiographic measurements. This relatively novel imaging technique has been validated against sonomicrometry and tagged magnetic resonance imaging and several studies have demonstrated its accuracy to measure myocardial strain.[13, 14] By measuring the mechanical properties of the myocardium with this technique, subtle myocardial dysfunction can be detected. Indeed, despite preserved LV or RV functions as assessed with conventional echocardiography, 2D speckle tracking can demonstrate subtle myocardial dysfunction in different clinical conditions (i.e. aortic stenosis, diabetic cardiomyopathy, coronary artery disease).[16, 19, 20] In addition, subtle myocardial dysfunction as detected with 2D speckle tracking has important

prognostic implications.[21-23] As demonstrated in previous studies, LV longitudinal strain showed superior prognostic value than baseline clinical characteristics, LV ejection fraction or wall motion score index measured with conventional echocardiography.[23] Therefore, 2D speckle tracking may constitute a valuable imaging tool to improve the risk stratification of patients with different clinical conditions, including those that potentially can cause cardiomyopathy at long-term follow-up if not treated.

RFCA for PVCs is associated with a high success rate and few complications.[3, 4, 6, 7, 24] Beside its value in relieving patients symptoms, RFCA can play an important role in the management of patients with PVC induced ventricular dysfunction.

Since it has been suggested that advanced PVC induced ventricular dysfunction may lead to irreversible cardiomyopathy in individual patients, the early detection of PVC induced dysfunction might be of clinical relevance.[25] Although there seems to be an association between PVC frequency, duration and decline in LV function some patients with low PVC burden and/or short duration of symptoms have already deterioration of LV function. Therefore PVC burden and duration alone may not identify patients at risk.[2, 4, 5] Until additional risk factors are identified, 2D speckle tracking strain imaging may constitute a valuable test to identify patients that need to be re-assessed during long term follow-up. Whether

Conclusions

Frequent PVCs can induce subtle LV and RV dysfunction in patients without apparent cardiomyopathy. PVCs originating from the LV and RV have similar detrimental effects on ventricular function. RFCA can successfully eliminate PVCs and improve cardiac function. These changes can be evaluated by using 2D speckle tracking imaging.

Reference List

(1) Gaita F, Giustetto C, Di Donna P, et al.: Long-term follow-up of right ventricular monomorphic extrasystoles. J Am Coll Cardiol 2001;38:364-70.

(2) Duffee DF, Shen WK, Smith HC: Suppression of frequent premature ventricular contractions and improvement of left ventricular function in patients with presumed idiopathic dilated cardiomyopathy. Mayo Clin Proc 1998;73:430-3.

(3) Yarlagadda RK, Iwai S, Stein KM, et al.: Reversal of cardiomyopathy in patients with repetitive monomorphic ventricular ectopy originating from the right ventricular outflow tract. Circulation 2005;112:1092-7.

(4) Bogun F, Crawford T, Reich S, et al.: Radiofrequency ablation of frequent, idiopathic premature ventricular complexes: comparison with a control group without intervention. Heart Rhythm 2007;4:863-7.

(5) Niwano S, Wakisaka Y, Niwano H, et al.: Prognostic significance of frequent premature ventricular contractions originating from the ventricular outflow tract in patients with normal left ventricular function. Heart 2009;95:1230-7.

(6) Sekiguchi Y, Aonuma K, Yamauchi Y, et al.: Chronic hemodynamic effects after radiofrequency catheter ablation of frequent monomorphic ventricular premature beats. J Cardiovasc Electrophysiol 2005;16:1057-63.

(7) Takemoto M, Yoshimura H, Ohba Y, et al.: Radiofrequency catheter ablation of premature ventricular complexes from right ventricular outflow tract improves left ventricular dilation and clinical status in patients without structural heart disease. J Am Coll Cardiol 2005;45:1259-65.

(8) Leitman M, Lysyansky P, Sidenko S, et al.: Two-dimensional strain-a novel software for real-time quantitative echocardiographic assessment of myocardial function. J Am Soc Echocardiogr 2004;17:1021-9.

(9) Reisner SA, Lysyansky P, Agmon Y, et al.: Global longitudinal strain: a novel index of left ventricular systolic function. J Am Soc Echocardiogr 2004;17:630-3.

(10) Edvardsen T, Helle-Valle T, Smiseth OA: Systolic dysfunction in heart failure with normal ejection fraction: speckle-tracking echocardiography. Prog Cardiovasc Dis 2006;49:207-14.

(11) Delgado V, Ypenburg C, van Bommel RJ, et al.: Assessment of left ventricular dyssynchrony by speckle tracking strain imaging comparison between longitudinal, circumferential, and radial strain in cardiac resynchronization therapy. J Am Coll Cardiol 2008;51:1944-52.

(12) Lang RM, Bierig M, Devereux RB, et al.: Recommendations for chamber quantification: a report from the American Society of Echocardiography's Guidelines and Standards Committee and the Chamber Quantification Writing Group, developed in conjunction with the European Association of Echocardiography, a branch of the European Society of Cardiology. J Am Soc Echocardiogr 2005;18:1440-63.

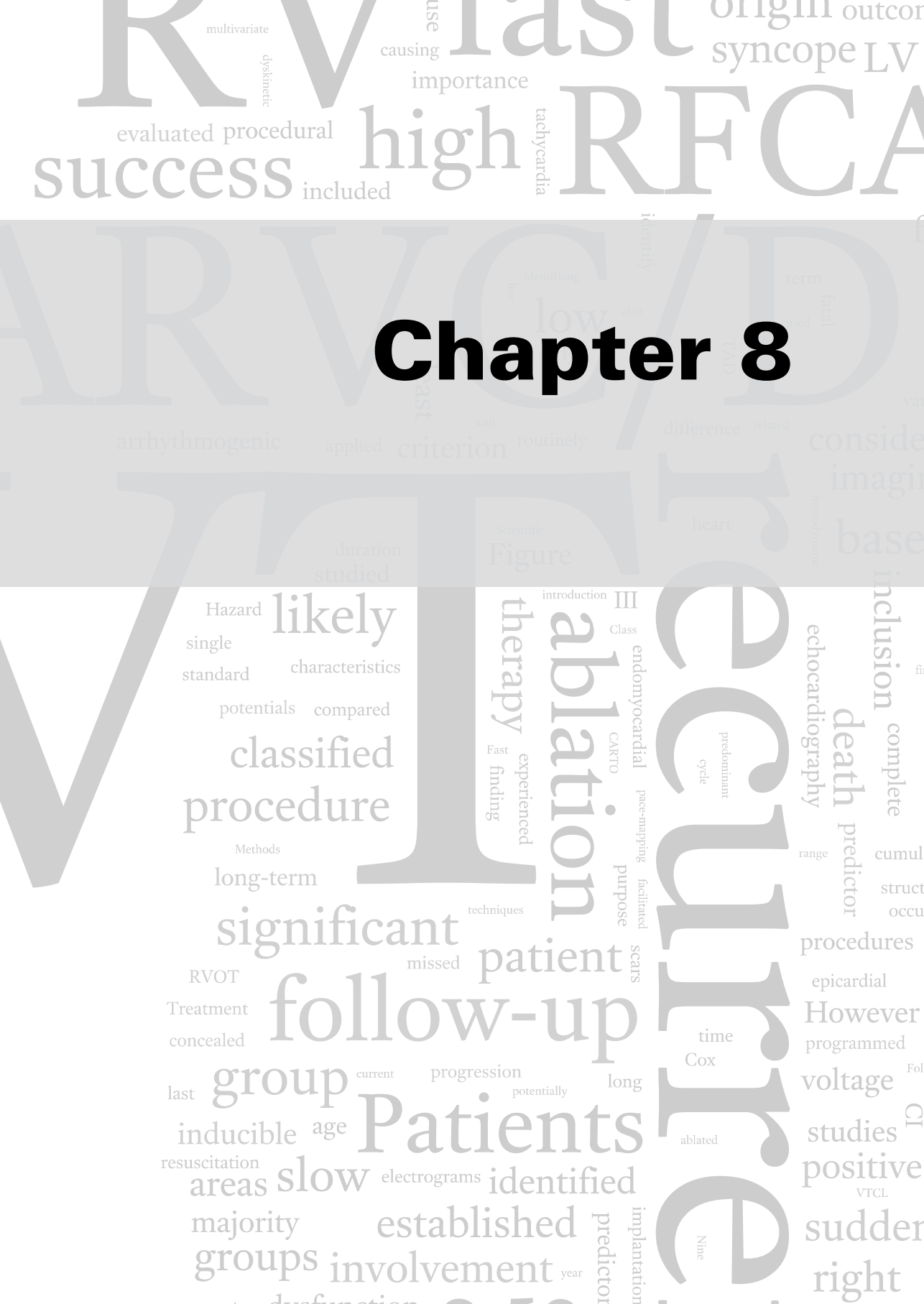
(13) Langeland S, D'hooge J, Wouters PF, et al.: Experimental validation of a new ultrasound method for the simultaneous assessment of radial and longitudinal myocardial deformation independent of insonation angle. Circulation 2005;112:2157-62.

(14) Amundsen BH, Helle-Valle T, Edvardsen T, et al.: Noninvasive myocardial strain measurement by speckle tracking echocardiography: validation against sonomicrometry and tagged magnetic resonance imaging. J Am Coll Cardiol 2006;47:789-93.

(15) Pirat B, McCulloch ML, Zoghbi WA: Evaluation of global and regional right ventricular systolic function in patients with pulmonary hypertension using a novel speckle tracking method. Am J Cardiol 2006;98:699-704.

(16) Ng AC, Delgado V, Bertini M, et al.: Findings from left ventricular strain and strain rate imaging in asymptomatic patients with type 2 diabetes mellitus. Am J Cardiol 2009;104:1398-401.

(17) van Ramshorst J, Mollema SA, Delgado V, et al.: Relation of immediate decrease in ventricular septal strain after alcohol septal ablation for obstructive hypertrophic cardiomyopathy to long-term reduction in left ventricular outflow tract pressure gradient. Am J Cardiol 2009;103:1592-7.
(18) Taieb JM, Maury P, Shah D, et al.: Reversal of dilated cardiomyopathy by the elimination of frequent left or right premature ventricular contractions. J Interv Card Electrophysiol 2007;20:9-13.
(19) Delgado V, Tops LF, van Bommel RJ, et al.: Strain analysis in patients with severe aortic stenosis and preserved left ventricular ejection fraction undergoing surgical valve replacement. Eur Heart J 2009;30:3037-47.
(20) Nucifora G, Bertini M, Marsan NA, et al.: Impact of left ventricular dyssynchrony early on left ventricular function after first acute myocardial infarction. Am J Cardiol 2010;105:306-11.
(21) Cho GY, Marwick TH, Kim HS, et al.: Global 2-dimensional strain as a new prognosticator in patients with heart failure. J Am Coll Cardiol 2009;54:618-24.
(22) Lafitte S, Perlant M, Reant P, et al.: Impact of impaired myocardial deformations on exercise tolerance and prognosis in patients with asymptomatic aortic stenosis. Eur J Echocardiogr 2009;10:414-9.
(23) Stanton T, Leano R, Marwick TH: Prediction of all-cause mortality from global longitudinal speckle strain: comparison with ejection fraction and wall motion scoring. Circ Cardiovasc Imaging 2009;2:356-64.
(24) Zhu DW, Maloney JD, Simmons TW, et al.: Radiofrequency catheter ablation for management of symptomatic ventricular ectopic activity. J Am Coll Cardiol 1995;26:843-9.
(25) Dixit S: Idiopathic premature ventricular complexes causing tachycardia-induced cardiomyopathy: benign arrhythmia with sinister implications. Heart Rhythm 2007;4:868-9.


Chapter 8
RVOT
RFCA
ablation
Patients
follow-up
significant
classified
procedure
likely
therapy
success
high
fast
Lecture
multivariate
dyskinetic
causing
importance
tachycardia
evaluated
procedural
included
syncope
LV
origin
outcom
identify
identifying
term
fatal
low
also
arrhythmogenic
applied
criterion
routinely
difference
related
consider
imagi
base
heart
Scientific
Figure
duration
studied
Hazard
single
standard
characteristics
potentials
compared
Methods
long-term
techniques
missed
patient
RVOT
Treatment
concealed
group
current
progression
long
last
potentially
inducible
age
resuscitation
areas
slow
electrograms
identified
majority
established
groups
involvement
year
implantation
predictor
Nine
ablated
time
Cox
introduction
III
Class
endomyocardial
CARTO
Fast
finding
experienced
pace-mapping
facilitated
purpose
scars
predominant
cycle
echocardiography
death
predictor
range
inclusion
complete
cumul
struct
occu
procedures
epicardial
However
programmed
voltage
studies
positive
VTCL
sudden
right
Fol
CI

Patients with scar-related right ventricular tachycardia: determinants of long-term outcome

Adrianus P. Wijnmaalen, Martin J. Schalij, Marianne Bootsma, Philippine Kies, Albert de Roos, Hein Putter, Jeroen J. Bax, Katja Zeppenfeld

J Cardiovasc Electrophysiol. 2009 Oct;20(10):1119-27.

Abstract

Introduction: Patients with established ARVC/D based on task force (TF) criteria and ventricular tachycardia (VT) are at risk of VT recurrence and sudden death. Data on patients with VT due to right ventricular (RV) scar not fulfilling TF criteria are lacking. The purpose of this study was to assess the long-term arrhythmia recurrence rate and outcome in patients with scar-related right VT with and without a diagnosis of arrhythmogenic right ventricular cardiomyopathy (ARVC/D).

Methods: Sixty-four patients (age 43.5±15yr, 49 male) presenting with non ischemic scar-related VT of RV origin were studied. Scar was identified by electroanatomical mapping, contrast-echocardiography and/or MRI. Patients were evaluated and treated according to a standard institute protocol.

Results: Twenty-nine (45%) patients were diagnosed with ARVC/D according to TF criteria (TF+) and 35 (55%) with RV scar of undetermined origin (TF-) at the end of follow-up (64±42 months). Patients were treated with anti-arrhythmic drugs, Radiofrequency catheter ablation and/or ICD implantation. VT recurrence-free survival for TF+ and TF- was 76% vs. 74% at 1yr and 45% vs. 50% at 4yr (p=ns). Patients with fast index VT (CL≤250ms, n=31) were more likely to experience a fast VT during follow-up than patients with a slow index VT (CL>250ms, n=33) (61% vs. 3%, p<0.001).

Conclusions: Scar-related RV VTs have a high recurrence rate in TF+ and TF- patients. Patients presenting with a fast index VT are at high risk for fast VT recurrence and may benefit most from ICD therapy.

Introduction

Patients with scar-related ventricular tachycardia (VT) of right ventricular (RV) origin are at risk for VT recurrence and sudden cardiac death. RV scar can be due to various diseases, such as ischemic heart disease, viral myocarditis, sarcoidosis, and genetically determined diseases. Subtle forms of RV involvement may not always be detected and classified by clinical evaluation including echocardiography, heart catherization, MRI and endomyocardial biopsy which may have important diagnostic and therapeutic implications. An important cause of RV scar is arrhythmogenic right ventricular cardiomyopathy/dysplasia (ARVC/D), a progressive and most likely genetic disease. In more than 50% of affected patients no familial occurrence[1] or disease specific genetic mutations[2] are found, therefore diagnosis of ARVC/D is based on criteria proposed by a generally accepted consensus report by an international task force (TF).[3]

Prognosis and risk factors for arrhythmia recurrence and sudden cardiac death in patients with ARVC/D have been studied. Class III antiarrhythmic drugs may be effective to control arrhythmia[4]. Radiofrequency catheter ablation (RFCA) is acutely effective in selected patients but hampered by a high recurrence rate during follow-up perhaps due to progression of the disease or subepicardial substrate.[5, 6] ICD implantation for secondary prevention has shown a high incidence of appropriate ICD therapy of 70% to 74%.[7, 8]

Data on patients presenting with scar-related left bundle branch block (LBBB) type VT without an established diagnosis of ARVC/D according to TF criteria are lacking.

The purpose of this study is to compare the clinical presentation, arrhythmia recurrence and outcome in patients with ARVC/D versus TF negative patients with scar-related LBBB type VT's during long term follow-up.

Methods

Patient population

Data from 64 patients referred to the Leiden University Medical Center with non-ischemic scar-related LBBB type VT, defined as predominant S-wave in precordial lead V1 were studied.

Patients had to meet the following criteria for inclusion in the study: documentation of sustained LBBB type VT and evidence of RV scar. RV scar was defined as (1) akinetic or dyskinetic wall motion abnormalities and/or severe right ventricular dilatation with dysfunction[3] on echocardiography[9, 10] or MRI [11-14] and/or (2) as regions of adjacent, fragmented, prolonged (≥3 positive deflections, ≥40ms signal duration) and low amplitude bipolar electrograms (≤1.5 mV) [15, 16] on catheter mapping. Patients with (1) idiopathic LBBB VT without evidence of RV scar, (2) with extensive left ventricular (LV) scar or dysfunction

(LV ejectionfraction <45%) and (3) with significant symptomatic coronary artery disease (defined as positive exercise test and >50% diameter stenosis in one or more coronary arteries) were excluded.

Diagnostic Evaluation

All patients underwent standard invasive and non-invasive testing for ARVC/D according to the criteria defined by the Task Force (TF) of the Working Group Myocardial and Pericardial Disease of the European Society of Cardiology and of the Scientific Council on Cardiomyopathies of the International Society and Federation of Cardiology[3]. In these guidelines major and minor TF criteria have been established encompassing structural, histological, electrocardiographical, clinical and familial aspects of ARVC/D (Table 1).

A 12-lead surface electrocardiogram (ECG) was obtained to determine the presence of T-wave inversion beyond lead V_2, a QRS duration ≥110ms in leads V_1-V_3, the presence of an epsilon wave[3] and terminal activation delay (TAD) >55ms[17]. QRS durations were measured at 100mm/s. Two-dimensional echocardiography with emphasis on wall motion abnormalities and function of the RV and LV with and without intravenous contrast was performed. Images were obtained using a 3.5 MHz transducer, at a depth of 16 cm in the parasternal and apical views (standard long-axis, two-chamber and four-chamber images).

MRI studies were obtained using a 1.5 T MRI system (Philips Medical Systems, Best, The Netherlands). To evaluate regional cardiac function, ECG- triggered multislice, multi-phase gradient-echo MR imaging of the heart was performed encompassing both ventricles with 10-12 imaging planes. MRI studies were evaluated by an experienced cardiac radiologist. Evaluation by signal-averaged electrocardiography was not performed. Endomyocardial biopsies were not obtained routinely because of the well-known sampling error caused by the segmental nature of ARVC/D and the possible risk of perforating the thin walled RV in patients with ARVC/D.[18] All patients were classified according to TF criteria. The diagnosis of ARVC/D was established when at least 2 major criteria or 1 major plus 2 minor criteria or 4 minor criteria were fulfilled. TF negative patients who fulfilled 1 major and 1 minor criterion or 3 minor criteria were classified as 'probable' ARVC/D. In a second analysis the recently proposed TAD was included and considered as diagnostic class IV major criterion.

Arrhythmias

The cycle length (CL) of the index LBBB like VT was measured. In patients presenting with syncope or resuscitation the induced LBBB like VT was considered as index VT. Fast VT was defined as a VT with a CL≤250ms. Syncope without ECG documentation was considered as VT with hemodynamic compromise and registered as fast VT for analysis purpose. Slow VT was defined as VT with a CL>250ms. Electrical programmed stimulation was performed in all patients. The induction protocol consisted of 3 drive-cycle lengths (600, 500 and 400ms) and up to 3 ventricular extrastimuli from 2 right ventricular sites and burst pacing.

Table 1. Diagnostic Criteria

	Definition	TF+ n=29	TF- n=35
Class I Dysfunction and structural alterations			
Major	Severe dilatation and reduction of RV ejection fraction with no (or mild) LV impairment and/or localized RV aneurysms (akinetic or dyskinetic areas with diastolic bulging)	**25**(86)	**6**(17)
Minor	Mild global RV dilatation and/or ejection fraction reduction with normal LV and/or mild segmental dilatation of the RV and/or regional RV hypokinesia	**3**(10)	**14**(40)
Class II Tissue characterization of walls			
Major	Fibrofatty replacement of myocardium on endomyocardial biopsy	-	-
Class III Repolarization abnormalities			
Minor	Inverted T waves in right precordial leads (V2 and V3) (age> 12 yr; in absence of right bundle branch block)	**17**(58)	**1**(3)
Class IV Depolarization abnormalities			
Major	Epsilon waves or localized prolongation (>110 ms) of the QRS complex in right precordial leads (V1-V3)	**17**(58)	**1**(3)
	Terminal activation duration (TAD) ≥55ms*	**17**(58)	**6**(17)
Minor	Late potentials (signal-averaged ECG)	-	-
Class V Arrhythmias			
Minor	Left bundle branch block type ventricular tachycardia and/or frequent ventricular extrasystoles	**29**(100)	**35**(100)
Class VI Family history			
Major	Familial disease confirmed at necropsy or surgery	**0**(0)	**0**(0)
Minor	Familial history of premature sudden death due to suspected right ventricular dysplasia and/or familial history (clinical diagnosis based on present criteria)	**0**(0)	**1**(3)

Diagnostic criteria for ARVC/D as defined by McKenna et al.(3) The number (%) of patients fulfilling each criterion is given for patients with (TF+) and without (TF-) diagnosis of ARVC/D. *Recently proposed diagnostic criteria for ECG depolarisation abnormalities[17], not included to classify patients into TF+ and TF-.

Treatment

Patients were treated according to the routine clinical protocol. The protocol included class III antiarrhythmic drugs (preferably sotalol) in all patients and RFCA if feasible. Patients who were not inducible after RFCA and/or on class III antiarrhythmic drugs were discharged without ICD and antiarrhythmic drug therapy was maintained. Patients who were resuscitated and patients who remained inducible despite AAD received an ICD. In the later course of the study also patients who present with spontaneous or inducible fast VT received an ICD regardless of the results of electrical programmed stimulation and an established diagnosis of ARVC/D.

Hemodynamically tolerated VT were mapped and ablated during VT. Target sites for ablation were sites with an isolated middiastolic potential, and/or sites where pacing entrained the VT with concealed fusion and a postpacing interval within 30ms of the VT cycle length. For fast and hemodynamically untolerated VT the mapping approach was based on the presence of electrograms with low amplitude fragmented signals, double potentials and/or isolated late potentials during sinus rhythm. At these sites pace-mapping was performed. A paced QRS morphology similar to the VT QRS morphology and stimulus to QRS delay >40ms was used to identify target sites for ablation. Ablation for slow and fast VT's was initially performed using roving catheter techniques and later facilitated by electroanatomical mapping (EAM) (CARTO XP EP system, Biosense Webster Inc, Diamond Bar, CA, USA or RPM™ system, Boston Scientific, Natick, MA, USA).

Complete procedural success was defined as the absence of any inducible monomorphic VT at the end of the ablation procedure. Partial success was defined as successful ablation of the clinical tachycardia and ablation failure if the clinical VT could not be successfully ablated.

Follow-up

All patients were followed routinely at our clinic. During visits a detailed history with regard to arrhythmia recurrence was taken. Progression of disease was defined as progressive de- or repolarization abnormalities on ECG, progression of RV dilatation and new a- and dyskinetic areas on echocardiography and/or MRI.

Arrhythmia recurrence was defined as not-otherwise explained syncope or documented VT on 12-lead ECG, 24-hour holter registration, event monitor and/or ICD.

All patients were reevaluated and classified according to TF criteria at last visit.

Statistical Analysis

Continuous variables are expressed as mean±SD, and categorical variables as frequency(%). Comparison of data was performed using the Student's *t*-test. The probability of remaining event free was analyzed by the Kaplan-Meier method, and differences in event-free survival were evaluated with the log-rank test. Multivariate analysis was performed with the use of

Cox regression analysis and variables that were found statistically significant in univariate analysis.

Twenty-one out of 49 patients in the study population underwent more than one ablation procedure because of VT recurrence. In order to judge the long-term effect of RFCA, subsequent procedures were included in the survival analysis using a delayed entry approach, with time from inclusion as analysis time scale. Individuals who had more than one procedure reentered the survival analysis after their initial recurrence. Since multiple occurrences of the same patient are based on disjoint time intervals, correction for dependence is not needed in this approach. For all tests a p-value <0.05 was considered significant.

Results

Study population

The studied population consisted of 49 males and 15 females. Median age at referral was 39yr (range 15–79yr). Thirty-three (52%) patients were younger than 40yr. At presentation 25 patients were diagnosed with ARVC/D according to TF criteria. At the end of follow-up 29 patients fulfilled TF criteria for ARVC/D (TF+) and 35 patients did not fulfill TF criteria (TF-). Nine of the 35 TF- patients were classified as probable ARVC/D. The diagnosis of ARVC/D was based on at least 2 major TF criteria in 11 and at least 1 major and 2 minor TF criteria in 18 patients. In TF- group 14 patients fulfilled only 1 minor, 12 patients fulfilled 2 minor, 2 patients fulfilled 3 minor and 7 patients fulfilled 1 major and 1 minor TF criterion (Table 1). If the newly proposted TAD criterion was applied only one additional patient would have been classified TF+.

RV scar was detected by imaging techniques in 44(69%) patients (TF+ 28 (97%) vs. TF- 16 (46%, p<0.001), in 20 (31%) TF- patients scar was only identified by EAM.

Severe RV dysfunction was present in 7 patients (TF+ 6 vs. TF- 1, p=0.02) and mild left ventricular (LV) involvement in 8 (TF+ 5 vs. TF- 3, p=0.29). In patients with severe RV dilatation and dysfunction the QRS duration was significantly longer as compared to patients with mild RV involvement (149±28ms vs. 110±24 respectively, p<0.001).

Low amplitude, fragmented electrograms were found in 42/49 patients (TF+ 81% vs. TF- 89%, p=0.28) who underwent RFCA. Patient characteristics are summarized in Table 2.

Presentation and treatment

Nine patients (14%) had been resuscitated and 12(19%) had experienced syncope, all of these patients were inducible for LBBB type VT at electrical programmed stimulation. A fast VT (CL ≤250 ms) was documented in 10 (17%) patients and a slow VT (CL>250 ms) in 33 (52%) patients at initial presentation. Forty-nine (72%) patients were treated with Class III antiarrhythmic drugs and 49 (72%) underwent at least one RFCA procedure. A total of 97

Table 2. Patient Characteristics

	TF+ n=29	TF- n=35	P=
Sex M/F	**26/3**	**23/12**	0.02
Age	**41**±13	**46**±18	0.21
Imaging			
Mild TVR	**14**(48)	**16**(46)	0.90
Moderate TVR	**5** (17)	**5**(14)	0.77
Mild PVR	**11**(38)	**19**(54)	0.12
Moderate PVR	**0**(0)	**2**(6)	0.19
Mild RV dilatation	**9**(31)	**3**(11)	0.06
Severe RV dilatation	**10** (34)	**3**(9)	0.011
Mild RV dysfunction	**7**(24)	**2**(6)	0.04
Severe RV dysfunction	**6**(21)	**1**(3)	0.02
LV involvement	**5**(19)	**3**(9)	0.27
Catheter mapping			
Low voltage fragmented electrograms	**17**(59)	**25**(71)	0.28
Located at 1 RV area			
RV outflow tract	**4**(24)	**11**(44)	0.22
RV apex	**1**(6)	**3**(12)	0.48
RV free wall	**0**	**2**(8)	0.24
Adjacent to Tricuspid Annulus	**2**(12)	**1**(4)	0.33
Located at ≥2 RV areas	**10**(59)	**8**(32)	0.07
Presentation			
Resuscitation	**4**(14)	**5**(14)	0.96
Syncope	**8**(28)	**4**(11)	0.09
Fast VT (CL≤250ms)	**6**(21)	**4**(11)	0.31
Slow VT (CL>250ms)	**11**(38)	**22**(63)	0.05
CL VT at baseline (ms)	**260**±55	**286**±67	0.10
Superior axis VT*	**14**(48)	**10**(29)	0.15
Multiple VT morphologies*	**9**(34)	**5**(14)	0.14

CL indicates cycle length; EPS, programmed extrastimulation;TVR, tricuspid valve regurgitation; PVR, pulmonary valve regurgitation; TF+, taskforce positive; TF-, taskforce negative, RV, right ventricular; LV, left ventricular; VT, ventricular tachycardia. * VT's Spontaneous at presentation or at first EPS. Data are expressed as absolute number (%) or mean±SD.

RFCA were performed with complete success in 17 (45%) of the procedures in TF+ patients and in 33 (56%) in TF- patients (p=0.25). Antiarrhythmic drug therapy was continued after RFCA in all patients. 3-Dimensional EAM of the RV was used to facilitate RFCA in 58(59%) procedures in 33 patients (CARTO system in 25 patients, RPM system in 8 patients). RFCA

Table 3. Treatment

	TF+ n=29	TF- n=35	p=
Medication			
Class III	**22**(76)	**27**(77)	0.68
Other	**5**(17)	**8**(23)	0.68
RFCA			
Patients	**21**(72)	**28**(80)	0.48
Number RFCA procedures	**38**	**59**	
Mean no RFCA	**1.31**±1.13	**1.69**±1.99	0.37
Complete success	**17**(45)	**33**(56)	0.25
Partial/No success	**21**(55)	**26**(44)	0.25
3-D EA mapping (% of patients)	**13**(62)	**20**(71)	0.22
ICD	**19**(66)	**7**(20)	<0.001

RFCA indicates radiofrequency catheter ablation; ICD, implantable cardioverter defibrillator; TF+, taskforce positive; TF-, taskforce negative; 3-D EA, 3 dimensional electroanatomical. Data are expressed as absolute number (%) or mean±SD.

success was not influenced by the use of 3-D EAM systems or the site of origin (RVOT vs. none RVOT) of the VT.

An ICD was implanted in 26 patients (41%), 66% of patients in group TF+ and in 20% of patients in TF- (p<0.001) (Table 3).

Patient follow-up

The mean follow-up until last evaluation for VT recurrence was 64±42 months, range 1 to 166 months (TF+ 68±43 months vs. TF- 61±42 months, p=0.51). Follow-up between inclusion and last evaluation for the presence of TF criteria was 57±42 months. During follow-up VT recurrence occurred in 41 patients, (TF+ 20 (72%) and TF- 21 (60%) p=0.21). The cumulative VT recurrence-free survival after the index event was 76% and 74% at 1 year, 59% and 61% at 2 years and 45% and 50% at 4 years, for TF+ and TF- respectively. There was no significant difference in the VT recurrence-free interval between both groups (Figure 1). Within the TF- group (n=35) the VT recurrence free survival was comparable between patients with a probable ARVC/D (n=9) and patients with less than 1 major + 1 minor or 3 minor TF criteria (n=26) (respectively 53% and 49% at 4 years, p=0.54). Three patients died during follow-up (3 TF+).Two deaths were sudden, both occurred in patients without ICD during the early phase of the study when ICD's were not implanted routinely for patients presenting fast VT. One death was non-cardiac.

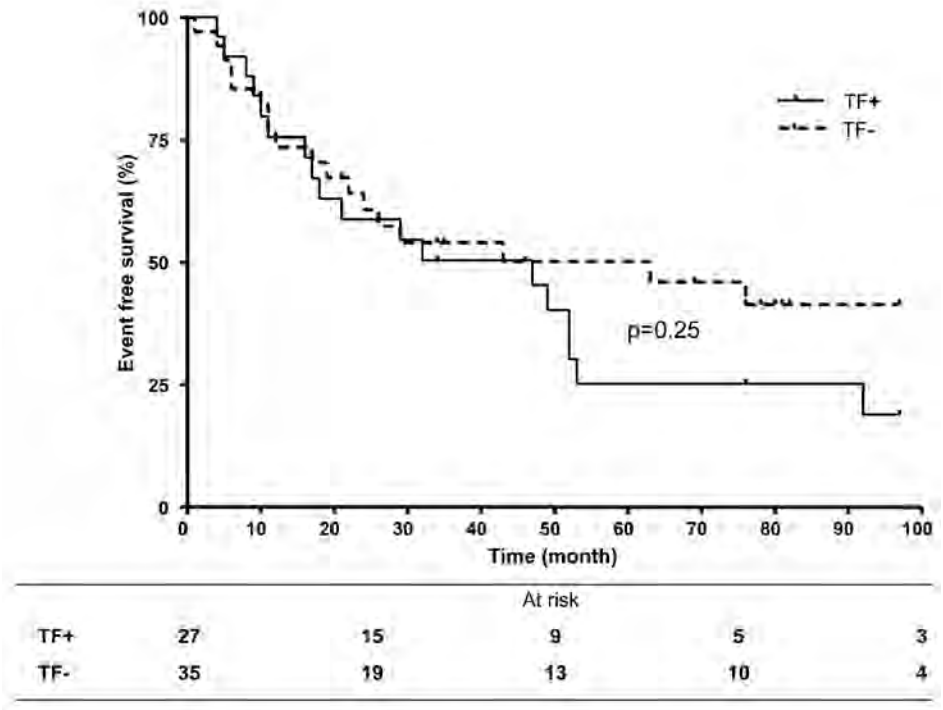


Figure 1. Survival analysis showing the cumulative event free survival for patients with (TF+) and without (TF-) diagnosis of ARVC/D after initial presentation. The table below the graph indicates the numbers of patients at risk.

Cycle length of the index VT

Patients with documented fast VT or syncope at inclusion had a significant lower cumulative recurrence-free interval (35% at 4 years) than patients with documented slow VT (60% at 4 years) (Figure 2). Except for one patient (TF+, index VT CL 260ms), no patient with slow VT at presentation experienced fast VT during follow-up. Figure 3 illustrates the shortest documented VTCL at inclusion and the shortest documented VTCL during follow-up for each individual patient.

Predictors of VT recurrence

Fast VT and/or resuscitation and/or syncope at inclusion and age≤40yr at referral were significant predictors for recurrence after univariate Cox regression analysis of the baseline characteristics. Diagnosis of ARVC/D (hazard ratio TF+ vs. TF- 1.41 (95% CI 0.77-2.62) and severe RV dilatation and RV dysfunction were not predictive for VT recurrence. After multivariate analysis fast VT and/or resuscitation and/or syncope were the only significant predictors for VT recurrence (Hazard Ratio 1.98, 95% CI 1.03-3.81, p=0.04).

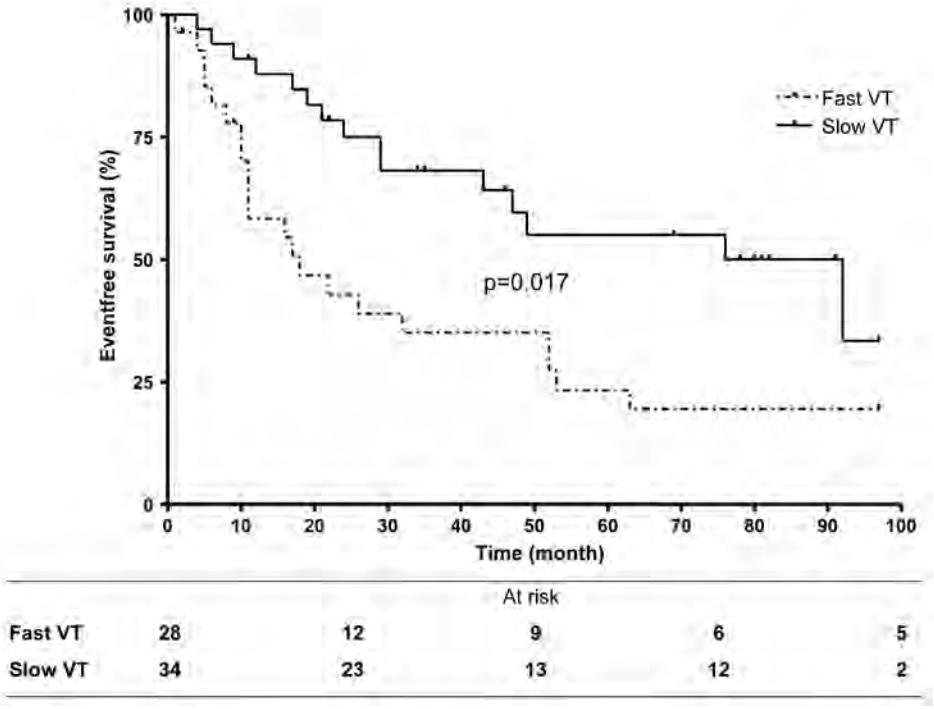


Figure 2. Survival analysis showing the cumulative recurrence free survival for patients presenting with fast VT (cycle length≤250ms) or resuscitation or syncope and patients presenting with a slow VT (cycle length>250ms). The table below the graph indicates the numbers of patients at risk.

Outcome after RFCA

In the subgroup of patients who underwent RFCA the cumulative VT recurrence free survival after a single RFCA procedure was 48% and 58% at 1 year, 31% and 36% at 2 years and 14% and 26% at 4 years, for group TF+ and group TF- respectively. The recurrence free survival was longer after complete success as compared to partial or no success of RFCA (Figure 4). In patients with a fast index VT complete success of RFCA was less likely (32%) than in patients presenting with a slow VT (71%) (p=<0.001). After multivariate analysis fast VT (Hazard Ratio 2.14, 95% CI 1.24-3.69) and incomplete or no success of RFCA were independent predictors of VT recurrence after a single RFCA procedure (Hazard Ratio 2.15, 95% CI 1.24-3.72).

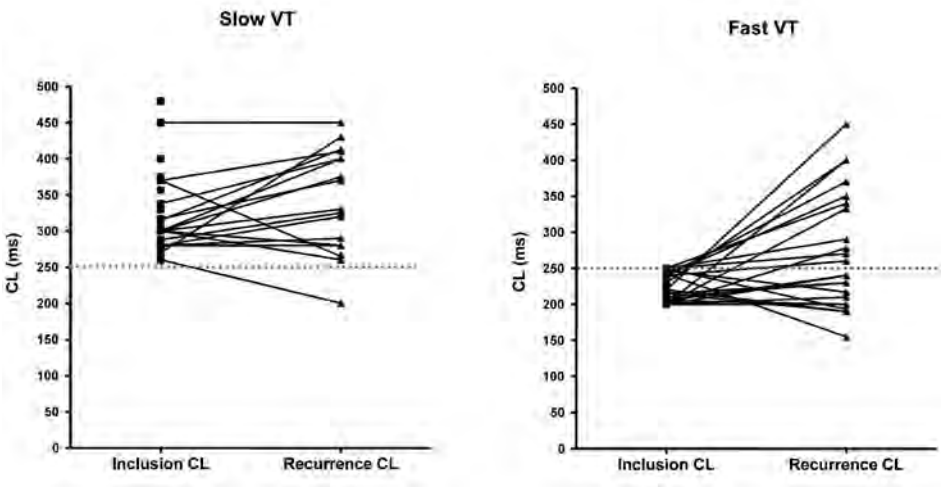


Figure 3. Chart showing the cycle length (CL) of VT at presentation and the shortest documented CL of recurrent VT during follow-up for each individual. Patients who presented with a slow VT (CL>250ms) are shown in the left panel, patients who presented with a fast VT (CL≤250/syncope) are shown in the right panel. Except for 1 patient none of those presenting with a slow VT experienced a fast VT during follow-up.

Discussion

The present study compares the long term clinical outcome of 64 patients presenting with scar-related LBBB type VT. The major finding is that the recurrence rate of ventricular arrhythmias is high in patients with an established diagnosis of ARVC/D and in patients with RV scar of undetermined origin. Patients presenting with a fast VT are at high risk for fast VT recurrence.

RV scar and TF criteria

ARVC/D is a progressive, often inherited cardiomyopathy, but to date molecular diagnosis is not feasible in the majority of cases. The clinical diagnosis is based on the Task Force criteria, however, patients with a confirmed ARVC/D causing mutation may remain TF negative and disease causing mutations are found in less than 50% of TF positive patients.[19-22]

EAM is a sensitive diagnostic modality capable of identifying RV involvement in concealed forms of ARVC/D that are not identified by imaging modalities.[23] In a small series of patients presenting with RVOT VT in the absence of RV dilatation or dysfunction on imaging low voltage areas on EAM correlated with fibrofatty myocardial replacement at biopsy.[23] However, different pathologies such as myocarditis or sarcoidosis may mimic ARVC/D.[24-26] Analysis of endomyocardial biopsies in ARVC/D TF positive patients with LBBB type VT identified myocarditis as underlying cause of RV scar in some of these patients.[25] Despite

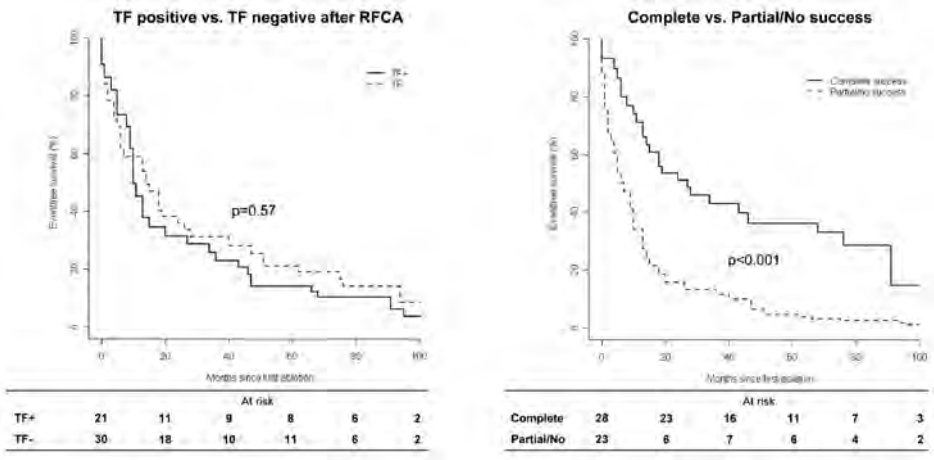


Figure 4. Survival analysis showing the cumulative recurrence free survival for patients with (TF+) and without (TF-) diagnosis of ARVC/D after the first RFCA procedure (left panel) and the cumulative recurrence free survival for patients with acute complete and partial/no success of RFCA (right panel). The table below the graph indicates the numbers of patients at risk.

the clinical importance of the TF criteria these findings highlight their limitations for identification of patients with scar related VT due to mild or early form of ARVC/D and for distinguishing ARVC/D from other potential arrhythmogenic diseases. To date, most available data on outcome and recurrence of scar-related RV VT are derived from TF positive patients or their relatives.

To our best knowledge this is the largest study reporting on long-term arrhythmia recurrence and treatment efficacy in patients with scar-related LBBB type VT of undetermined origin. Of importance, we included bipolar electrogram criteria to define scar and in 54% of the TF- patients scar was only detected by EAM implicating that some of these VT's may have been otherwise classified as idiopathic VT (Figure 5).

Long-term arrhythmia follow-up

ARVC/D is associated with a ventricular arrhythmia recurrence rate of 48 – 74%. [7, 8, 27] The results of the present study confirm the high VT recurrence rate in these patients despite drug therapy and RFCA. However, a remarkable finding is the high VT recurrence rate in patients with RV scar of undetermined origin of whom the majority had no or mild structural alterations of the RV on MRI and/or contrast echocardiography. This finding extends prior observations that localized RV scar, even if detected only by EAM, predispose to VT recurrence, and of importance, to a similar extend as in TF+ ARVC/D patients with obvious structural and functional alterations of the RV. These localized scars may be due to an early/mild form of ARVC/D. Since endomyocardial biopsy was not performed systematically in

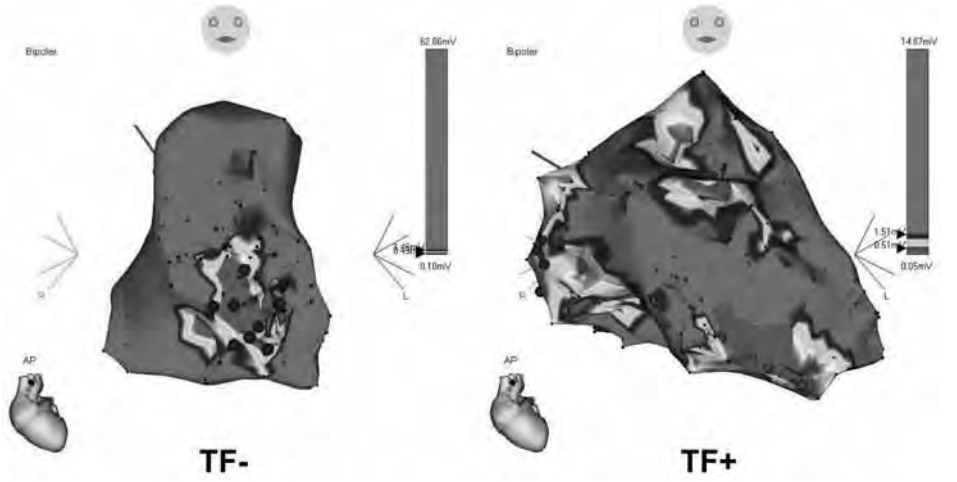


Figure 5. Right ventricular 3-D electroanatomical bipolar voltage maps of a TF- (left) and a TF+ (right) patient. Voltages are color-coded according to the corresponding color bar. Normal voltage is defined as electrogram amplitude >1.5mV displayed in purple. The TF- patient had recurrent VT's with different morphologies originating from a single small RV free wall scar area. Scar was only identified by voltage mapping. The TF+ patient had multiple low voltage areas. VT was successfully terminated at the lateral tricuspid annulus. **(for figure in color see page: 261)**

our patient population because of the predominant non-septal location of the scar areas other causes of RV scars can not be excluded.

Risk stratification

A fast index VT or syncope as presenting symptom, most likely due to a VT with hemodynamic compromise was the only independent predictor for VT recurrence in both groups. The event free survival in these patients was significantly shorter than in patients presenting with slow VT. Of importance, patients who presented with a fast index VT were also more likely to experience recurrence of fast and potentially fatal ventricular arrhythmias during follow-up perhaps identifying a subgroup of patients who benefit most from ICD therapy. This is in line with previous data demonstrating fast VT/VF at presentation as a predictor for potentially fatal VT recurrence in ARVC/D patients.[7, 27]

Several studies seeking risk factors for VT in patients with TF positive ARVC/D have identified younger age, severity of RV failure and LV involvement as factors with predictive value for arrhythmia recurrence. [7, 8, 27] In contrast to these studies severe RV enlargement and LV involvement was not found to be an independent predictor of VT recurrence, however this is likely due to the smaller number of ARVC/D patients with RV enlargement and the exclusion of patients with significant functional LV impairment.

Treatment

Treatment to prevent VT recurrence was similar in both groups. RFCA was offered to all patients and attempted in 49. There was no difference in acute procedural success between both groups. The low acute success rate of RFCA may be at least partly due to a subepicardial substrate typical for patients with ARVD/C, which may not be reachable by an endocardial approach. The recently introduced technique of epicardial mapping and ablation in patients with scar-related RVVT was applied in 4 patients with an unsuccessful endocardial ablation approach leading to complete ablation success in 2 patients. The acute success rate was lower in patients presenting with a fast VT compared to patients in whom a slow VT was targeted. In the latter mapping could be performed during VT which may explain the favourable result. The concept of substrate mapping and ablation during stable rhythm to target unstable VT's based on electrogram characteristics and pace-mapping has evolved during the course of the study. In addition the application of linear lesion to encircle low voltage areas and connect scars was only introduced recently[6]. This approach and the introduction of epicardial ablation is likely to further improve the acute results of RFCA for fast VT.

However, after adjustment fast VT and procedural failure remained independent predictors for VT recurrence. After RFCA the recurrence-free interval was remarkable short for both groups. The high VT recurrence rate in patients with ARVC/D in the first 4 years after ablation is in line with previous studies by Verma et al[6] and Dalal et al[5] and may be due to disease progression. Marchlinski et al.[28] reported a distinctly higher long-term procedural success of RFCA facilitated by EAM in ARVC/D patients. These findings seem to contradict the presented results. However, the current study reported the outcome of all RFCA procedures. In contrast, 68% of the patients reported by Marchlinski et al.[28] underwent a repeated ablation procedure suggesting a lower single procedure success rate. The high VT recurrence after RFCA in patients with RV scar of undetermined origin found in this study may indicate that the arrhythmogenic substrate in these patients is similar to that in patients with established ARVC/D and may be consistent with an early form of ARVC/D.

However, despite the long term follow-up RV involvement remained concealed in the majority of the patients if routine imaging modalities are applied.

In the current study TF+ ARVC/D patients were more likely to receive an ICD than TF- patients. Similar to the strategy that has been adopted for VT treatment and sudden death prevention in patients after myocardial infarction patients with scar related VT and a preserved RV function who did not meet diagnostic criteria for ARVC/D were considered to be at low risk for sudden cardiac death and VT recurrence after drug treatment and RFCA. Although no sudden death occurred in the TF- group during the follow-up period, the high recurrence rate of fast and therefore potential fatal VT's gives cause for concern.

The results of this study indicate that the diagnosis of ARVC/D based on TF criteria does not identify patients at risk for recurrence of RV scar-related VT. Careful decision making

for ICD implantation should include the type of the presenting arrhythmia rather than the definite diagnosis of ARVC/D.

Study Limitations

Our study has several limitations. Not all arrhythmia episodes necessitate hospitalization and episodes may have been missed particularly in patients without ICD.

Due to advances in catheter mapping and the introduction of endo- and epicardial high density 3-dimensional electroanatomical mapping during the course of the study, we can only provide data on the distribution of low voltage areas and not on the scar burden. The extend of the subendocardial and particular the subepicardial scar is likely underestimated in both groups and small low voltage areas may be missed due to the initially performed restricted EAM.

No signal averaged ECG were obtained in our patient population. Therefore a TF class IV minor criterion can be missed which is relevant for the TF- group. If hypothetically the SAECG in all TF- patients had shown late potentials 9 patients in this group would be diagnosed with ARVC/D according to TF criteria resulting in a TF+ group of 38 patients. Repeated analysis of these groups did not result in a significant difference in recurrence free survival between TF+(+9) and TF-(-9) patients. Furthermore univariate Cox regression did not identify a diagnosis of TF+(+9) as predictor for recurrence.

The majority of patients in this study was not evaluated for genetic mutations causing ARVC/D. Genotyping both TF+ and TF- patients is of the greatest relevance and would provide valuable information regarding the underlying cause of RV scar.

Conclusion

Scar-related RV VT are associated with high recurrence rates regardless if the patient was considered TF+ or TF-. In the majority of TF- patients RV scar was only identified by voltage mapping, which might be a diagnostic tool with important prognostic and therapeutic implications. Patients who present with fast VT are at high risk for fast VT recurrence despite intervention and may benefit most from ICD therapy.

Reference List

(1) Hamid MS, Norman M, Quraishi A, Firoozi S, Thaman R, Gimeno JR, Sachdev B, Rowland E, Elliott PM, McKenna WJ: Prospective evaluation of relatives for familial arrhythmogenic right ventricular cardiomyopathy/dysplasia reveals a need to broaden diagnostic criteria. J Am Coll Cardiol 2002;40:1445-50.

(2) Sen-Chowdhry S, Syrris P, McKenna WJ: Role of genetic analysis in the management of patients with arrhythmogenic right ventricular dysplasia/cardiomyopathy. J Am Coll Cardiol 2007;50:1813-21.

(3) McKenna WJ, Thiene G, Nava A, Fontaliran F, Blomstrom-Lundqvist C, Fontaine G, Camerini F: Diagnosis of arrhythmogenic right ventricular dysplasia/cardiomyopathy. Task Force of the Working Group Myocardial and Pericardial Disease of the European Society of Cardiology and of the Scientific Council on Cardiomyopathies of the International Society and Federation of Cardiology. Br Heart J 1994;71:215-8.

(4) Wichter T, Borggrefe M, Haverkamp W, Chen X, Breithardt G: Efficacy of antiarrhythmic drugs in patients with arrhythmogenic right ventricular disease. Results in patients with inducible and noninducible ventricular tachycardia. Circulation 1992;86:29-37.

(5) Dalal D, Jain R, Tandri H, Dong J, Eid SM, Prakasa K, Tichnell C, James C, Abraham T, Russell SD, Sinha S, Judge DP, Bluemke DA, Marine JE, Calkins H: Long-term efficacy of catheter ablation of ventricular tachycardia in patients with arrhythmogenic right ventricular dysplasia/cardiomyopathy. J Am Coll Cardiol 2007;50:432-40.

(6) Verma A, Kilicaslan F, Schweikert RA, Tomassoni G, Rossillo A, Marrouche NF, Ozduran V, Wazni OM, Elayi SC, Saenz LC, Minor S, Cummings JE, Burkhardt JD, Hao S, Beheiry S, Tchou PJ, Natale A: Short- and long-term success of substrate-based mapping and ablation of ventricular tachycardia in arrhythmogenic right ventricular dysplasia. Circulation 2005;111:3209-16.

(7) Corrado D, Leoni L, Link MS, Della BP, Gaita F, Curnis A, Salerno JU, Igidbashian D, Raviele A, Disertori M, Zanotto G, Verlato R, Vergara G, Delise P, Turrini P, Basso C, Naccarella F, Maddalena F, Estes NA, III, Buja G, Thiene G: Implantable cardioverter-defibrillator therapy for prevention of sudden death in patients with arrhythmogenic right ventricular cardiomyopathy/dysplasia. Circulation 2003;108:3084-91.

(8) Wichter T, Paul M, Wollmann C, Acil T, Gerdes P, Ashraf O, Tjan TD, Soeparwata R, Block M, Borggrefe M, Scheld HH, Breithardt G, Bocker D: Implantable cardioverter/defibrillator therapy in arrhythmogenic right ventricular cardiomyopathy: single-center experience of long-term follow-up and complications in 60 patients. Circulation 2004;109:1503-8.

(9) Yoerger DM, Marcus F, Sherrill D, Calkins H, Towbin JA, Zareba W, Picard MH: Echocardiographic findings in patients meeting task force criteria for arrhythmogenic right ventricular dysplasia: new insights from the multidisciplinary study of right ventricular dysplasia. J Am Coll Cardiol 2005;45:860-5.

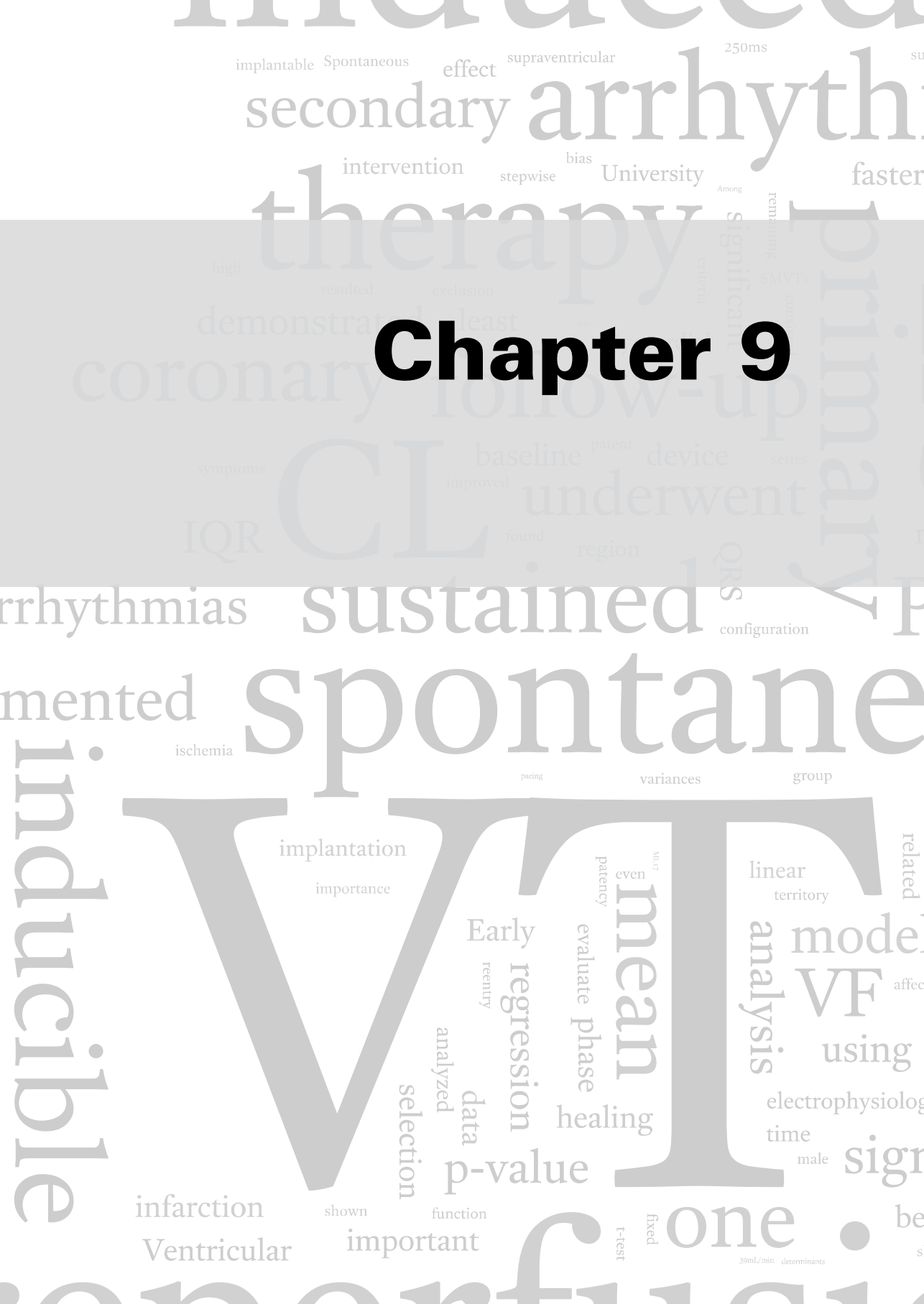
(10) Manyari DE, Duff HJ, Kostuk WJ, Belenkie I, Klein GJ, Wyse DG, Mitchell LB, Boughner D, Guiraudon G, Smith ER: Usefulness of noninvasive studies for diagnosis of right ventricular dysplasia. Am J Cardiol 1986;57:1147-53.

(11) Bomma C, Dalal D, Tandri H, Prakasa K, Nasir K, Roguin A, Tichnell C, James C, Lima JA, Calkins H, Bluemke DA: Regional differences in systolic and diastolic function in arrhythmogenic right ventricular dysplasia/cardiomyopathy using magnetic resonance imaging. Am J Cardiol 2005;95:1507-11.

(12) Midiri M, Finazzo M, Brancato M, Hoffmann E, Indovina G, Maria MD, Lagalla R: Arrhythmogenic right ventricular dysplasia: MR features. Eur Radiol 1997;7:307-12.

(13) Tandri H, Bomma C, Calkins H, Bluemke DA: Magnetic resonance and computed tomography imaging of arrhythmogenic right ventricular dysplasia. J Magn Reson Imaging 2004;19:848-58.

(14) Sen-Chowdhry S, Prasad SK, Syrris P, Wage R, Ward D, Merrifield R, Smith GC, Firmin DN, Pennell DJ, McKenna WJ: Cardiovascular magnetic resonance in arrhythmogenic right ventricular cardiomyopathy revisited: comparison with task force criteria and genotype. J Am Coll Cardiol 2006;48:2132-40.
(15) Zeppenfeld K, Kies P, Wijffels MC, Bootsma M, van Erven L, Schalij MJ: Identification of successful catheter ablation sites in patients with ventricular tachycardia based on electrogram characteristics during sinus rhythm. Heart Rhythm 2005;2:940-50.
(16) Marchlinski FE, Callans DJ, Gottlieb CD, Zado E: Linear ablation lesions for control of unmappable ventricular tachycardia in patients with ischemic and nonischemic cardiomyopathy. Circulation 2000;101:1288-96.
(17) Cox MG, Nelen MR, Wilde AA, Wiesfeld AC, van der Smagt JJ, Loh P, Cramer MJ, Doevendans PA, van Tintelen JP, De Bakker JM, Hauer RN: Activation delay and VT parameters in arrhythmogenic right ventricular dysplasia/cardiomyopathy: toward improvement of diagnostic ECG criteria. J Cardiovasc Electrophysiol 2008;19:775-81.
(18) Strain J: Adipose dysplasia of the right ventricle: is endomyocardial biopsy useful? Eur Heart J 1989;10 Suppl D:84-8.
(19) van Tintelen JP, Entius MM, Bhuiyan ZA, Jongbloed R, Wiesfeld AC, Wilde AA, van der SJ, Boven LG, Mannens MM, van Langen IM, Hofstra RM, Otterspoor LC, Doevendans PA, Rodriguez LM, van Gelder IC, Hauer RN: Plakophilin-2 mutations are the major determinant of familial arrhythmogenic right ventricular dysplasia/cardiomyopathy. Circulation 2006;113:1650-8.
(20) Dalal D, Molin LH, Piccini J, Tichnell C, James C, Bomma C, Prakasa K, Towbin JA, Marcus FI, Spevak PJ, Bluemke DA, Abraham T, Russell SD, Calkins H, Judge DP: Clinical features of arrhythmogenic right ventricular dysplasia/cardiomyopathy associated with mutations in plakophilin-2. Circulation 2006;113:1641-9.
(21) Syrris P, Ward D, Asimaki A, Sen-Chowdhry S, Ebrahim HY, Evans A, Hitomi N, Norman M, Pantazis A, Shaw AL, Elliott PM, McKenna WJ: Clinical expression of plakophilin-2 mutations in familial arrhythmogenic right ventricular cardiomyopathy. Circulation 2006;113:356-64.
(22) Bauce B, Basso C, Rampazzo A, Beffagna G, Daliento L, Frigo G, Malacrida S, Settimo L, Danieli G, Thiene G, Nava A: Clinical profile of four families with arrhythmogenic right ventricular cardiomyopathy caused by dominant desmoplakin mutations. Eur Heart J 2005;26:1666-75.
(23) Corrado D, Basso C, Leoni L, Tokajuk B, Turrini P, Bauce B, Migliore F, Pavei A, Tarantini G, Napodano M, Ramondo A, Buja G, Iliceto S, Thiene G: Three-dimensional electroanatomical voltage mapping and histologic evaluation of myocardial substrate in right ventricular outflow tract tachycardia. J Am Coll Cardiol 2008;51:731-9.
(24) Corrado D, Basso C, Leoni L, Tokajuk B, Bauce B, Frigo G, Tarantini G, Napodano M, Turrini P, Ramondo A, Daliento L, Nava A, Buja G, Iliceto S, Thiene G: Three-dimensional electroanatomic voltage mapping increases accuracy of diagnosing arrhythmogenic right ventricular cardiomyopathy/dysplasia. Circulation 2005;111:3042-50.
(25) Chimenti C, Pieroni M, Maseri A, Frustaci A: Histologic findings in patients with clinical and instrumental diagnosis of sporadic arrhythmogenic right ventricular dysplasia. J Am Coll Cardiol 2004;43:2305-13.
(26) Koplan BA, Soejima K, Baughman K, Epstein LM, Stevenson WG: Refractory ventricular tachycardia secondary to cardiac sarcoid: electrophysiologic characteristics, mapping, and ablation. Heart Rhythm 2006;3:924-9.
(27) Pezawas T, Stix G, Kastner J, Schneider B, Wolzt M, Schmidinger H: Ventricular tachycardia in arrhythmogenic right ventricular dysplasia/cardiomyopathy: clinical presentation, risk stratification and results of long-term follow-up. Int J Cardiol 2006;107:360-8.
(28) Marchlinski FE, Zado E, Dixit S, Gerstenfeld E, Callans DJ, Hsia H, Lin D, Nayak H, Russo A, Pulliam W: Electroanatomic substrate and outcome of catheter ablative therapy for ventricular tachycardia in setting of right ventricular cardiomyopathy. Circulation 2004;110:2293-8.


Chapter 9
implantable
Spontaneous
effect
supraventricular
250ms
secondary
arrhythmias
intervention
bias
stepwise
University
faster
therapy
high
resulted
exclusion
demonstrated
least
coronary
follow-up
baseline
patent
device
symptoms
improved
underwent
IQR
found
region
CL
rrhythmias
sustained
configuration
mented
spontaneous
ischemia
pacing
variances
group
inducible
VT
implantation
importance
even
patency
linear
territory
related
Early
mean
model
regression
evaluate
phase
analysis
VF
reentry
analyzed
data
selection
healing
using
electrophysiolog
time
male
p-value
infarction
shown
function
one
Ventricular
important
fixed
t-test
39mL/min
determinants

Early reperfusion therapy affects inducibility, cycle length and occurrence of ventricular tachycardia late after myocardial infarction

Adrianus P. Wijnmaalen, Sebastiaan R.D. Piers, C. Jan Willem Borleffs, Carine F.B. van Huls van Taxis, Joep Thijssen, Johannes B. van Rees, Suzanne C. Cannegieter, Jeroen J. Bax, Martin J. Schalij, Katja Zeppenfeld

Sebastiaan R.D. Piers and Adrianus P. Wijnmaalen share first authorship on this manuscript

Circ Arrhythm Electrophysiol. 2011 Apr 1;4(2):195-201.

Abstract

Background: This study aimed to evaluate the impact of early reperfusion during acute myocardial infarction (MI) on ventricular tachycardia (VT) inducibility, inducible VT cycle length (CL) and occurrence of spontaneous VT late after MI.

Methods and results: Five-hundred-six patients (440 male, 63±11yr) with prior MI who underwent electrophysiology study before implantation of an implantable cardioverter defibrillator for primary or secondary prevention were assessed. Patients were classified according to the reperfusion strategy {reperfusion (thrombolysis (n=44) or percutaneous coronary intervention (n=65)) vs. no reperfusion (n=397)} during acute MI.

Monomorphic sustained VT was inducible in 351 (69%) patients. Inducibility in reperfused and non-reperfused patients was similar in primary prevention patients (56% vs.58%) but significantly higher for non-reperfused patients in secondary prevention patients (56% vs.79%, p=0.001). Induced VTCL was shorter (247±40 vs.287±63, p<0.001) and very fast VT (CL≤250 ms) was more often induced in reperfused patients (71% vs.47%, p=0.001). In primary prevention patients, non-reperfusion was associated with a doubled risk for first spontaneous VT during follow-up.

Conclusion: There are important differences in VT inducibility, induced VTCL and occurrence of spontaneous VT in the chronic infarct healing phase between patients with and without successful reperfusion during acute MI. These findings suggest differences in the chronic arrhythmogenic substrate.

Introduction

Survivors of acute myocardial infarction (MI) may be at risk for reentrant ventricular tachycardia (VT) originating from infarct scar.[1]

In the past decades, early reperfusion therapies such as thrombolysis and primary percutaneous coronary intervention (PCI) have significantly improved outcome after acute MI.[2] Early reperfusion during MI results in myocardial salvage and improved ventricular function but also influences size, transmurality and geometry of myocardial fibrosis, which may function as a substrate for ventricular arrhythmias.[3-7] A fixed substrate may lead to reentrant tachycardias reproducible induced during electrophysiology study (EPS) and more than 90% of patients with sustained VT late after MI had the arrhythmia induced in the lab.[8] However, these data were derived before the widespread availability of reperfusion therapy and the role for EPS in patients late after reperfused MI is less clear. Mapping studies demonstrated that the 3-dimensional geometry of the infarcted area may determine VT reentry circuit characteristics.[9-12] In a small group of patients referred for treatment of VT late after MI, we previously demonstrated that early reperfusion affects the electroanatomical VT substrate.[13] In addition, cycle length (CL) of spontaneous and induced VTs was shorter in patients who underwent early reperfusion as compared to non-reperfused patients.

The aim of the present study was to evaluate the affect of early reperfusion during acute MI on VT inducibility, induced VTCL and the occurrence of spontaneous VT during follow-up in a larger population of patients with prior MI in one coronary territory who underwent EPS before implantable cardioverter defibrillator (ICD) treatment.

Methods

Patients

Since 1996, information on all patients who received an ICD at the Leiden University Medical Center was prospectively collected in the departmental Cardiology Information System (EPD-Vision®, Leiden University Medical Center). Patient's history, baseline characteristics and results of studies before ICD-implantation were recorded. For the current study, all consecutive patients (1) with a prior MI in a single coronary territory and documented reperfusion strategy during the index MI; (2) without evidence of reversible ischemia assessed by coronary angiogram and nuclear imaging at the time of evaluation, and (3) who underwent EPS before ICD implantation were included. Patients with documented spontaneous monomorphic VT or ventricular fibrillation (VF) in the absence of a reversible cause were considered as secondary prevention ICD recipients and asymptomatic patients with left ventricular ejection fraction (LVEF) <40% without prior documentation of a sustained ventricular arrhythmia primary prevention ICD recipients.[14-16]

All coronary angiograms performed in reperfused patients within 6 months before EPS were reviewed by an interventional cardiologist to evaluate the late patency of the infarct related artery. Patients with ≤ TIMI II flow of the infarct related artery were excluded from analysis. All patients were followed at our institute.

Myocardial infarction

The presence of prior MI was assessed using the definition for MI, as defined by the Task Force for the Redefinition of Myocardial Infarction.[17] Either acute MI had to be documented, or evidence of prior MI had to be present, based on any of the following criteria: 1) development of new pathological Q-waves with or without symptoms; 2) imaging evidence of a region of loss of viable myocardium that is thinned and fails to contract, in the absence of a non-ischemic cause; 3) pathological findings of a healed or healing MI.[17]

MI was considered to be present in more than one coronary artery region if the criteria for acute or prior MI were met for more than one of the regions provided by the three main coronary arteries.

The treatment of prior MI was assessed using the patients' medical charts. Patients were categorized as reperfused when TIMI flow grade 3 was achieved within 9 hours after onset of symptoms. Reperfused patients were subdivided into patients who had underwent primary PCI (defined as angioplasty and/or stenting without prior or concomitant fibrinolytic therapy)[18] and patients who had received thrombolytic therapy. All other patients were categorized as non-reperfused.

Electrophysiology study

Electrophysiological studies to test inducibility of VT were performed according to the current international guidelines.[19] Patients were studied in the post absorptive, non-sedated state. Antiarrhythmic drugs were discontinued for 5 half-lives, with the exception of amiodarone. EPS consisted of up to three basic drive cycle lengths (600, 500 and 400ms) with up to three ventricular extrastimuli and burstpacing from the right ventricular apex and right ventricular outflow tract. The positive endpoint of EPS was reproducible induction of a sustained monomorphic VT (SMVT).[19] Arrhythmias induced by anti-tachycardia pacing (ATP) to terminate the induced VT were not included in the analysis.

Ventricular arrhythmia during electrophysiology study

Ventricular arrhythmias were categorized according to the EHRA/HRS consensus document.[20] SMVT was defined as continuous VT with a similar QRS configuration from beat to beat lasting for more than 30 seconds or requiring an intervention for termination. Separately scored arrhythmia not considered diagnostic for the presence of fixed reentry circuits and therefore aspecific were polymorphic VT, defined as VT with continuously changing QRS configuration from beat to beat and VF.[19]

For each patient, the mean CL of all induced SMVTs was calculated. Patients with missing data on one or more CLs were excluded from all analyses involving VTCL. Monomorphic VTs were categorized into the following four pre-defined subgroups according to CL: ≤250, 251-286, 287-320 and >320 ms (corresponding to a rate of ≥240, 240-210, 210-188 and <188bpm, respectively). A very fast VT was defined as a VT with CL ≤250 ms.

Implantable cardioverter defibrillator settings and follow-up

Defibrillators were programmed as follows: a ventricular arrhythmia monitor zone was programmed in all patients (150-188bpm). Ventricular arrhythmias faster than 188bpm were initially attempted to be terminated with two bursts of ATP followed by a defibrillator shock, if appropriate. In the case of a ventricular arrhythmia faster than 210bpm, device shocks were the initial therapy. Atrial arrhythmia detection was set to >170bpm with supraventricular tachycardia discriminators enabled. Settings were adapted, only when clinically indicated (i.e. hemodynamic well tolerated VT at high rate; VT in the monitor zone).

Patient follow-up was scheduled every three-six months. Device interrogation printouts were checked for appropriate and inappropriate ICD therapy (ATP or shocks). Therapies were classified as appropriate when they occurred in response to VT or VF and as inappropriate when triggered by sinus or supraventricular tachycardia, T-wave oversensing, or electrode dysfunction.

In both primary and secondary prevention ICD recipients, the correlation between treatment of acute MI and the occurrence of first spontaneous monomorphic VT during follow-up was assessed.

Statistical analysis

Dichotomous and categorical data are displayed as numbers and percentages. Continuous data are expressed as mean ± standard deviation or median and interquartile range where appropriate. Patients were grouped according to acute MI treatment. Different groups were compared for 1) inducibility of SMVT, 2) mean CL of induced SMVTs, 3) inducibility of very fast VT (CL ≤250ms), and 4) the occurrence of first spontaneous VT during follow-up in primary and secondary prevention ICD patients. Data were analyzed by means of the Chi-square test, the Student's t-test or the Mann-Whitney U-test as appropriate. For the Student's t-test, equal variances were assumed if Levene's test for equality of variances showed a p-value >0.05. Univariate relationships between baseline parameters and the mean CL of induced VTs were analyzed with linear regression analysis. For each variable, the effect on the mean CL with a 95% confidence interval (95%-CI) was calculated. Variables with a p-value <0.10 were further evaluated in a multivariate model, using backward stepwise selection. At each step, the least significant variable was discarded from the model, until all variables in the model reached a p-value <0.25.

The cumulative incidence of first spontaneous VT during follow-up in primary and secondary prevention ICD patients was analyzed by method of Kaplan-Meier. The effect of acute MI treatment on the risk of spontaneous VT was assessed in a Cox regression model. As with linear regression analysis, first, univariate analyses were performed and variables with a p-value <0.10 were further evaluated in a multivariate model, using backward stepwise selection. At each step, the least significant variable was discarded from the model, until all variables in the model reached a p-value <0.25.

All analyses were performed with SPSS for Windows, version 17.0 (SPSS, Chicago, IL). P-values are all two-sided and for all tests, a p-value <0.05 was considered statistically significant.

Results

Patients

Since 1996, 996 patients with prior MI in one coronary artery region received an ICD at the Leiden University Medical Center. Of these patients, 511 had a documented reperfusion strategy and underwent EPS before ICD implantation and after exclusion of reversible ischemia. Five patients (1%) were excluded due to lack of late patency of the infarct related artery. The remaining 506 patients (87% male, age 63 ± 11 years) comprised the studied sample. The presenting and documented arrhythmia was SMVT in 221 patients (44%) and VF in 113(22%); 172 patients (34%) had no prior sustained arrhythmia. The majority of patients had a depressed left ventricular ejection fraction (36 ± 13%). Mean QRS duration was 115 ± 29 ms and mean creatinin clearance was 79±39mL/min. Medication during EPS included amiodarone in 22% and ACE-inhibitors or ATII-antagonists in 75% of patients. Baseline characteristics are summarized in Table 1.

Myocardial infarction treatment

One-hundred-nine (22%) of 506 patients were treated with reperfusion therapy during the acute MI and 397(78%) were not reperfused. Of the 109 reperfused patients, 65(13%) underwent primary PCI and 44(9%) received thrombolytic therapy. Before electrophysiological evaluation, the infarct-related artery was patent in 97(89%), collaterally perfused in 11(10%) and bypassed in one (1%) of the initially reperfused patients. In non-reperfused patients, the infarct-related artery was patent in 140 (35%), occluded in 116(29%), collaterally perfused in 88(22%) and bypassed in 53(13%). Patients who were reperfused were younger than non-reperfused patients (59±11 vs. 65±10, p<0.001), presented less often with SMVT (22% vs. 49%, p<0.001) and had a shorter interval between MI and electrophysiological evaluation (median 1.6, IQR 0.2 – 5.9 vs. median 10.5, IQR 2.1 – 17.5, p<0.001). In addition, reperfused patients had an anterior MI more frequently (72% vs. 52%, p<0.001), a shorter

Table 1. Baseline characteristics.

	All patients (n=506)	Non-reperfused (n=397)	Reperfused (n=109)	p-value
Male sex	440 (87%)	341 (86%)	99 (91%)	0.176
Age, years	65 (57 – 71)	66 (58 – 73)	60 (51 – 68)	<0.001
Presenting arrhythmia				
Sustained VT	221 (44%)	197 (50%)	24 (22%)	<0.001
Ventricular fibrillation	113 (22%)	94 (24%)	19 (17%)	
No sustained arrhythmia	172 (34%)	106 (27%)	66 (61%)	
Location of MI				
Anterior	285 (56%)	206 (52%)	79 (72%)	<0.001
Non-anterior	221 (44%)	191 (48%)	30 (28%)	
Years from MI to EPS	7.5 (0.9 – 15.0)	10.5 (2.1 – 17.5)	1.6 (0.2 – 5.9)	<0.001
LVEF, %	36 ± 13	35 ± 13	37 ± 13	0.180
NYHA Classification				
I	227 (45%)	172 (43%)	55 (50%)	
II	201 (40%)	164 (41%)	37 (34%)	0.555
III	72 (14%)	56 (14%)	16 (15%)	
IV	6 (1%)	5 (1%)	1 (1%)	
QRS duration, ms	110 (94 – 130)	110 (100 – 138)	100 (90 – 120)	0.001
Renal clearance, mL/min*	79 ± 39	77 ± 41	85 ± 27	0.066
Documented AF or atrial flutter	89 (18%)	69 (17%)	20 (18%)	0.823
Current smoking	126 (25%)	94 (24%)	32 (29%)	0.253
Amiodarone	111 (22%)	98 (25%)	13 (12%)	0.004
ß-blocker	217 (43%)	159 (40%)	58 (53%)	0.014
ACE-inhibitor or ARB	380 (75%)	291 (73%)	89 (82%)	0.070

* Renal clearance was determined with the formula of Cockroft-Gault.
Data are expressed as number (percentages), mean ± standard deviation or median (interquartile range). ACE = angiotensin converting enzyme, AF = atrial fibrillation, ARB = angiotensin receptor blocker, ICD = implantable cardioverter defibrillator, LVEF = left ventricular ejection fraction, MI = myocardial infarction, NYHA = New York Heart Association, EPS = electrophysiology study, VT = ventricular tachycardia

QRS-duration (median 100, IQR 90 – 120 vs. median 110, IQR 100 – 138, p=0.001), were less often treated with amiodarone (12% vs. 25%, p=0.001) but were more likely to receive betablockers (53% vs. 40%, p=0.014).

Inducibility of ventricular arrhythmia

In 422 patients (83%), at least one ventricular arrhythmia was inducible: SMVT was induced in 351(69%) patients, 45 of them were also inducible for polymorphic VT or VF. In 71(14%) patients, only polymorphic VT or VF was induced. Inducibility of SMVT consisted of only

one VT morphology in 222(63%) and two or more different morphologies in 129(37%) patients. Inducibility for SMVT was similar in reperfused and non-reperfused patients without prior documentation of sustained VT or VF (56% vs 58%, p=ns). However, in the secondary prevention group inducibility for SMVT was significantly lower in reperfused patients as compared to non-reperfused patients (56% vs 79%, p=0.001).

Ventricular tachycardia cycle length

In 37(11%) out of 351 patients with inducible SMVT, one or more induced VTCL was unknown, these patients were excluded from VTCL analyses. In the remaining 314 patients, the mean CL was 280±61 ms (Table 2). In 161(51%) patients, at least one monomorphic fast VT (CL ≤250) was induced.

Reperfused patients had a shorter mean CL of the induced VT than non-reperfused patients (247±40ms vs. 287±63ms, p<0.001, Table 2). This difference was even more pronounced when patients who underwent primary PCI were compared to non-reperfused patients (238±40ms vs. 287±63ms, p<0.001). Patients treated with thrombolysis also had a significantly shorter mean CL than non-reperfused patients, but the difference was smaller (260±37ms vs. 287±63ms, p=0.038). After exclusion of patients on amiodarone during EPS the induced VTCL remained significantly shorter in reperfused patients (244±40ms vs. 274±58ms, p<0.001). Of importance, reperfused patients were more often inducible for very fast VT (CL ≤250ms) than non-reperfused patients (71% vs. 47%, p=0.001, Figure 1). The difference was mainly attributable to patients treated with primary PCI, while patients treated with thrombolysis had a similar percentage of very fast VT, as compared to non-reperfused patients. Univariate and subsequent multivariate analysis identified the following five variables as independently affecting the mean CL of induced VTs: no reperfusion, QRS >120 ms, presenting arrhythmia, use of amiodarone and age. After adjustment, no reperfusion at MI was correlated with 17ms (95%-CI 0-34 ms, p=0.048) increase in VT CL at EPS (Figure 2).

Table 2. T-tests for difference of mean cycle length of induced monomorphic ventricular tachycardias.

	N=	Mean CL	Difference* (95%-CI)	p-value
All patients	314	280 ± 61	NA	NA
Non- reperfused	258	287 ± 63	NA	NA
Reperfused	56	247 ± 40	40 (27 – 53)	<0.001
Thrombolysis	23	260 ± 37	27 (2 – 53)	0.038
Primary PCI	33	238 ± 40	49 (27 – 70)	<0.001

*when compared to non-reperfused patients.
CI = confidence interval, CL = cycle length, NA = not applicable, PCI = percutaneous coronary intervention.

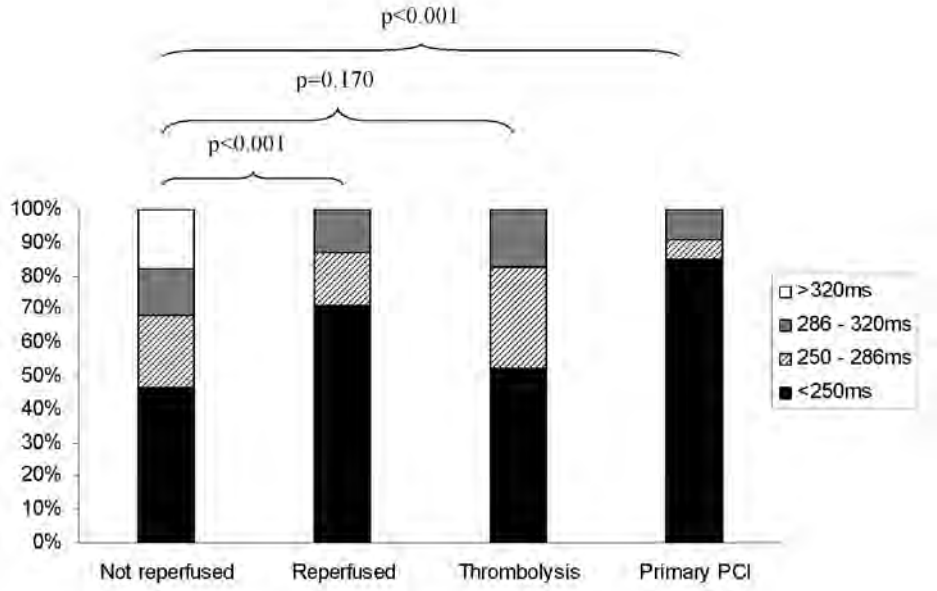


Figure 1. Cycle length of the fastest induced monomorphic ventricular tachycardia, categorized into 4 subgroups. Percentages are for all patients with induced monomorphic ventricular tachycardia in the specific group.

Spontaneous ventricular tachycardia

The 172 primary prevention ICD recipients were followed for a median of 28 months (IQR 11 – 45). During follow-up, spontaneous VT, triggering appropriate ICD therapy was observed in 51(30%) patients. The cumulative incidence of first appropriate therapy was 13% (95% CI 8-18%) at one year, 22% (95% CI 15-28%) at two years, and 30% (95% CI 22-39%) at three years follow-up.

The three year cumulative incidence of first appropriate device therapy was 36% (95% CI 26-47%) in non-reperfused patients and 18% (95% CI 7-29%) in reperfused patients (Figure 3). Cox regression modeling demonstrated that non-reperfused patients exhibited a more than doubled risk for spontaneous VT (hazard ratio 2.2, 95% CI 1.2- 4.3, p=0.010).

The 334 secondary prevention ICD recipients were followed for a median of 37 months (IQR 9–68). Spontaneous VT occurred in 170(51%) patients. The three year cumulative incidence of first appropriate device therapy was 38% (95% CI 32-44%) in non-reperfused patients and 26% (95% CI 12-39%) in reperfused patients (Figure 4). In this population with prior sustained ventricular arrhythmia, MI treatment did not significantly correlate with the occurrence of spontaneous VT during follow-up (hazard ratio 1.4, 95% CI 0.9-2.3).

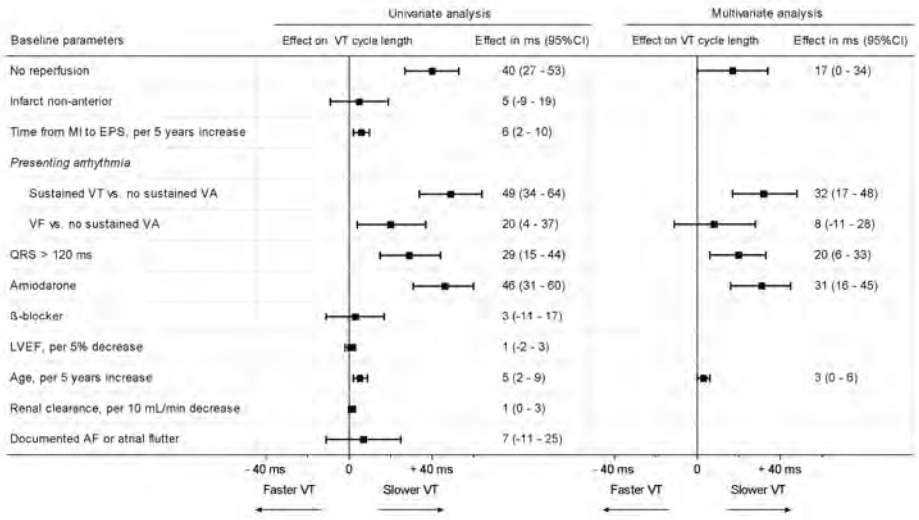


Figure 2. Forest plot of the effect of baseline parameters on the mean cycle length of induced monomorphic ventricular tachycardias. For example, in multivariate analysis, patients who did not receive reperfusion therapy at the index MI on average had a 17 ms (95% CI 0 – 34 ms) longer VT cycle length (i.e., a slower VT), as compared to patients who did receive reperfusion therapy. AF = atrial fibrillation, CI = confidence interval, LVEF = left ventricular ejection fraction, MI = myocardial infarction, EPS = electrophysiology study,VA = ventricular arrhythmia, VF = ventricular arrhythmia, VT = ventricular tachycardia.

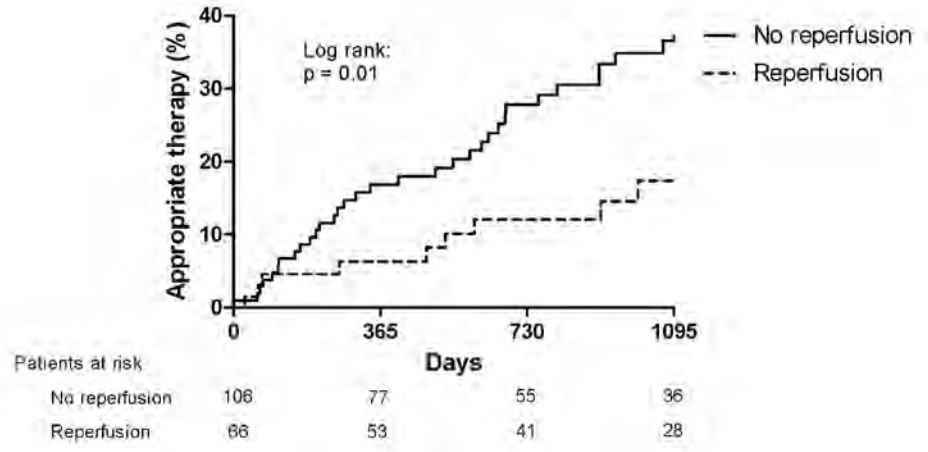


Figure 3. Kaplan-Meier curve for the occurrence of first appropriate ICD therapy in primary prevention ICD patients with reperfusion vs. no reperfusion at prior acute myocardial infarction.

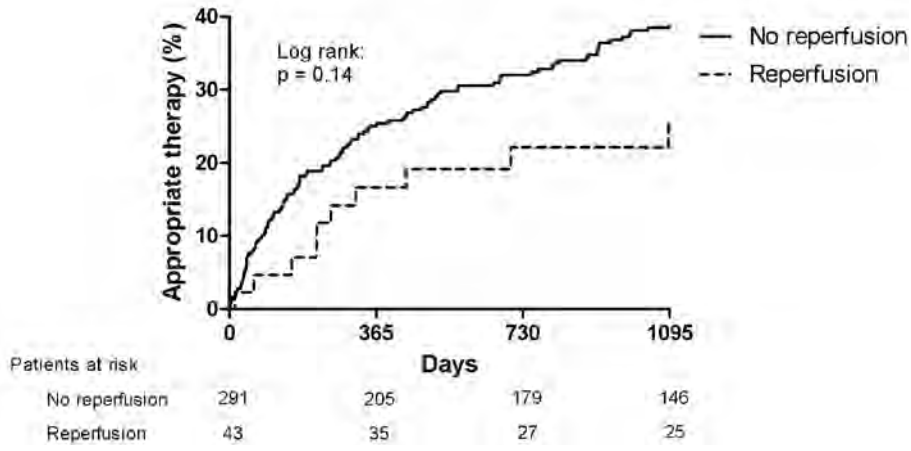


Figure 4. Kaplan-Meier curve for the occurrence of first appropriate ICD therapy in secondary prevention ICD patients with reperfusion vs. no reperfusion at prior acute myocardial infarction.

Discussion

Early reperfusion therapy for acute MI has dramatically increased over the last decenniums and is likely to influence the chronic arrhythmogenic substrate for reentrant tachycardias after infarct healing.

The current study evaluates the effects of early reperfusion during acute MI on VT inducibility, induced VT CL and occurrence of spontaneous VT late after the index MI. Reperfused patients who presented with sustained VT or VF were less likely inducible for monomorphic VT as compared to non-reperfused patients. Reperfused and non-reperfused patients without prior sustained arrhythmia had comparable VT induction rates; however reperfused patients were less likely to experience spontaneous VT during follow-up. Among inducible patients VTCL of induced VTs was significantly shorter and inducible VT was more often very fast VT (CL ≤ 250 ms) in reperfused patients. These differences were even more pronounced in patients treated with primary PCI as compared to thrombolytic therapy. After adjustment for potential confounders, treatment of the index MI appeared to have an independently significant effect on the mean CL of induced VTs.

Early reperfusion during MI and inducibility of VT

Former studies performed before the widespread availability of reperfusion therapy have demonstrated that in patients with coronary artery disease VT was inducible in 92% of patients who presented with sustained VT and in 83% of patients who presented with cardiac arrest due to VF.[8] Accordingly, 79% of the non-reperfused patients in our study who

presented with sustained VT or VF were inducible for monomorphic VT. In contrast, in only 56% of reperfused patients with documented VT or VF monomorphic VT was inducible. Although all patients had a chronic substrate as spontaneous arrhythmias occurred in the absence of a reversible cause the sensitivity of an EPS for substrate assessment after reperfusion therapy seems to be low. This finding is of clinical importance if EPS is performed for the evaluation of patients who present with unexplained syncope due to non-documented VT or during ablation procedures of VT if non-inducibility of monomorphic VT is considered as endpoint for ablation.

Acute reperfusion has resulted in a lower prevalence of spontaneous and induced ventricular arrhythmias in the acute phase of MI.[4, 21-23] In small series, 9-48% of patients receiving thrombolysis were inducible for ventricular arrhythmias as compared to 88-100% of patients without reperfusion therapy.[24, 25] However, the arrhythmogenic substrate causing late ventricular arrhythmias may develop over time. In our series, EPS was performed in the chronic healing phase of MI. Of interest, non-reperfused and reperfused patients without prior spontaneous arrhythmia showed high inducibility rates of 58% and 56%, respectively. However, during follow-up the three year cumulative incidence of appropriate device therapy was 36% in non-reperfused patients and only 17% in reperfused patients. This finding suggest that despite the presence of an arrhythmogenic substrate the value of EPS to predict VT occurrence is lower in reperfused patients as compared to non-reperfused patients.

Effect of early reperfusion and inducible VTCL

Early reperfusion during MI results in myocardial salvage and reduced mortality during follow-up.[3] Histological studies in patients and animal models of acute MI have shown that the duration of coronary artery occlusion is proportionally correlated to the size and transmural extent of myocardial scar.[4, 5, 26] Scar size and geometry are important determinants for the reentrant circuit geometry and may contribute to occurrence and cycle length of VT.[9, 27]

We recently demonstrated that reperfused patients referred for ablation of recurrent VT late after MI appeared to have smaller and less confluent electroanatomical scars with thick layers of surviving myocardium found at histology. Interestingly, the CL of spontaneous and induced VTs was shorter in reperfused than in non-reperfused patients likely due to the observed differences in scar geometry after reperfusion therapy.[13] The association between acute reperfusion therapy and shorter inducible VTCL was confirmed and extended, as the present study is conducted in a large population of post-MI patients also including patients without previously documented ventricular arrhythmia. In addition, we adjusted for all baseline characteristics that affect induced VTCL.

Limitations

Our study was performed in a selected population of ICD recipients with prior MI and low LVEF, who are not representative for the general population with prior MI. In addition, our cutoff of 9 hours for early reperfusion is arbitrarily chosen. Furthermore, we studied induced VTs, and our findings do not necessarily apply to spontaneous VTs. However, in the previous study by Wijnmaalen et al., spontaneous VTs were taken into account and similar differences were found, as compared to induced VTs. Finally, therapy for acute MI was not randomly assigned and time from MI to EPS differs between groups, which could have resulted in selection bias. However, since primary PCI has been shown to be the preferred treatment for acute MI, a study in which patients would be randomly assigned to primary PCI, thrombolysis or conservative treatment is ethically unacceptable and therefore, selection bias is now inevitable in studying the effects of reperfusion. To correct for it, we adjusted for baseline characteristics using linear regression and could demonstrate that reperfusion independently affects the CL of induced VTs.

Conclusions

There are important differences in VT inducibility, induced VTCL and occurrence of spontaneous VT in the chronic phase of MI between patients with and without successful reperfusion during acute MI. Reperfused patients who present with sustained VT/VF are less likely inducible for monomorphic VT. Despite similar VT induction rates in patients without prior documented sustained arrhythmias, reperfused patients are at lower risk for spontaneous VT. However, early reperfusion is associated with faster induced VT.

These findings suggest important differences in the chronic arrhythmogenic substrate after reperfusion, which gives rise to faster VT and which might be less reliably assessable by EPS.

Reference List

(1) Josephson M, Wellens HJ. Implantable defibrillators and sudden cardiac death. Circulation 2004;109:2685-91.

(2) Heidenreich PA, McClellan M. Trends in treatment and outcomes for acute myocardial infarction. 1975-1995. Am J Med 2001;110:165-74.

(3) The effects of tissue plasminogen activator, streptokinase, or both on coronary-artery patency, ventricular function, and survival after acute myocardial infarction. The GUSTO Angiographic Investigators. N Engl J Med 1993;329:1615-22.

(4) Miyazaki S, Fujiwara H, Onodera T, Kihara Y, Matsuda M, Wu DJ, Nakamura Y, Kumada T, Sasayama S, Kawai C. Quantitative analysis of contraction band and coagulation necrosis after ischemia and reperfusion in the porcine heart. Circulation 1987;75:1074-82.

(5) Reimer KA, Lowe JE, Rasmussen MM, Jennings RB. The wavefront phenomenon of ischemic cell death. 1. Myocardial infarct size vs duration of coronary occlusion in dogs. Circulation 1977;56:786-94.

(6) Tarantini G, Cacciavillani L, Corbetti F, Ramondo A, Marra MP, Bacchiega E, Napodano M, Bilato C, Razzolini R, Iliceto S. Duration of ischemia is a major determinant of transmurality and severe microvascular obstruction after primary angioplasty. a study performed with contrast-enhanced magnetic resonance. J Am Coll Cardiol 2005;46:1229-35.

(7) Thiele H, Kappl MJ, Linke A, Erbs S, Boudriot E, Lembcke A, Kivelitz D, Schuler G. Influence of time-to-treatment, TIMI-flow grades, and ST-segment resolution on infarct size and infarct transmurality as assessed by delayed enhancement magnetic resonance imaging. Eur Heart J 2007;28:1433-9.

(8) Prystowsky EN, Miles WM, Evans JJ, Hubbard JE, Skale BT, Windle JR, Heger JJ, Zipes DP. Induction of ventricular tachycardia during programmed electrical stimulation. analysis of pacing methods. Circulation 1986;73:II32-II38.

(9) Ciaccio EJ, Ashikaga H, Kaba RA, Cervantes D, Hopenfeld B, Wit AL, Peters NS, McVeigh ER, Garan H, Coromilas J. Model of reentrant ventricular tachycardia based on infarct border zone geometry predicts reentrant circuit features as determined by activation mapping. Heart Rhythm 2007;4:1034-45.

(10) Marchlinski FE, Callans DJ, Gottlieb CD, Zado E. Linear ablation lesions for control of unmappable ventricular tachycardia in patients with ischemic and nonischemic cardiomyopathy. Circulation 2000;101:1288-96.

(11) Verma A, Marrouche NF, Schweikert RA, Saliba W, Wazni O, Cummings J, Abdul-Karim A, Bhargava M, Burkhardt JD, Kilicaslan F, Martin DO, Natale A. Relationship between successful ablation sites and the scar border zone defined by substrate mapping for ventricular tachycardia post-myocardial infarction. J Cardiovasc Electrophysiol 2005;16:465-71.

(12) Peters NS, Coromilas J, Severs NJ, Wit AL. Disturbed connexin43 gap junction distribution correlates with the location of reentrant circuits in the epicardial border zone of healing canine infarcts that cause ventricular tachycardia. Circulation 1997;95:988-96.

(13) Wijnmaalen AP, Schalij MJ, von der Thüsen JH, Klautz RJM, Zeppenfeld K. Early reperfusion during acute myocardial infarction affects ventricular tachycardia characteristics and the chronic electroanatomical and histological substrate. Circulation 2010;121:1887-1895.

(14) Bardy GH, Lee KL, Mark DB, Poole JE, Packer DL, Boineau R, Domanski M, Troutman C, Anderson J, Johnson G, McNulty SE, Clapp-Channing N, vidson-Ray LD, Fraulo ES, Fishbein DP, Luceri RM, Ip JH. Amiodarone or an implantable cardioverter-defibrillator for congestive heart failure. N Engl J Med 2005;352:225-37.

(15) Buxton AE, Lee KL, Fisher JD, Josephson ME, Prystowsky EN, Hafley G. A randomized study of the prevention of sudden death in patients with coronary artery disease. Multicenter Unsustained Tachycardia Trial Investigators. N Engl J Med 1999;341:1882-90.

(16) Moss AJ, Zareba W, Hall WJ, Klein H, Wilber DJ, Cannom DS, Daubert JP, Higgins SL, Brown MW, Andrews ML. Prophylactic implantation of a defibrillator in patients with myocardial infarction and reduced ejection fraction. N Engl J Med 2002;346:877-83.

(17) Thygesen K, Alpert JS, White HD. Universal definition of myocardial infarction. Eur Heart J 2007;28:2525-38.

(18) Van de Werf F, Bax J, Betriu A, Blomstrom-Lundqvist C, Crea F, Falk V, Filippatos G, Fox K, Huber K, Kastrati A, Rosengren A, Steg PG, Tubaro M, Verheugt F, Weidinger F, Weis M, Vahanian A, Camm J, De CR, Dean V, Dickstein K, Filippatos G, Funck-Brentano C, Hellemans I, Kristensen SD, McGregor K, Sechtem U, Silber S, Tendera M, Widimsky P, Zamorano JL, Silber S, Aguirre FV, Al-Attar N, Alegria E, Andreotti F, Benzer W, Breithardt O, Danchin N, Di MC, Dudek D, Gulba D, Halvorsen S, Kaufmann P, Kornowski R, Lip GY, Rutten F. Management of acute myocardial infarction in patients presenting with persistent ST-segment elevation. the Task Force on the Management of ST-Segment Elevation Acute Myocardial Infarction of the European Society of Cardiology. Eur Heart J 2008;29:2909-45.

(19) Zipes DP, Camm AJ, Borggrefe M, Buxton AE, Chaitman B, Fromer M, Gregoratos G, Klein G, Moss AJ, Myerburg RJ, Priori SG, Quinones MA, Roden DM, Silka MJ, Tracy C, Smith SC, Jr., Jacobs AK, Adams CD, Antman EM, Anderson JL, Hunt SA, Halperin JL, Nishimura R, Ornato JP, Page RL, Riegel B, Priori SG, Blanc JJ, Budaj A, Camm AJ, Dean V, Deckers JW, Despres C, Dickstein K, Lekakis J, McGregor K, Metra M, Morais J, Osterspey A, Tamargo JL, Zamorano JL. ACC/AHA/ESC 2006 guidelines for management of patients with ventricular arrhythmias and the prevention of sudden cardiac death. a report of the American College of Cardiology/American Heart Association Task Force and the European Society of Cardiology Committee for Practice Guidelines (Writing Committee to Develop Guidelines for Management of Patients With Ventricular Arrhythmias and the Prevention of Sudden Cardiac Death). J Am Coll Cardiol 2006;48:e247-e346.

(20) Aliot EM, Stevenson WG, mendral-Garrote JM, Bogun F, Calkins CH, Delacretaz E, Della BP, Hindricks G, Jais P, Josephson ME, Kautzner J, Kay GN, Kuck KH, Lerman BB, Marchlinski F, Reddy V, Schalij MJ, Schilling R, Soejima K, Wilber D. EHRA/HRS Expert Consensus on Catheter Ablation of Ventricular Arrhythmias. developed in a partnership with the European Heart Rhythm Association (EHRA), a Registered Branch of the European Society of Cardiology (ESC), and the Heart Rhythm Society (HRS); in collaboration with the American College of Cardiology (ACC) and the American Heart Association (AHA). Heart Rhythm 2009;6:886-933.

(21) de Chillou C, Sadoul N, Bizeau O, Feldmann L, Gazakure E, Ismail M, Magnin-Poull I, Blankoff I, Aliot E. Prognostic value of thrombolysis, coronary artery patency, signal-averaged electrocardiography, left ventricular ejection fraction, and Holter electrocardiographic monitoring for life-threatening ventricular arrhythmias after a first acute myocardial infarction. Am J Cardiol 1997;80:852-8.

(22) Hohnloser SH, Franck P, Klingenheben T, Zabel M, Just H. Open infarct artery, late potentials, and other prognostic factors in patients after acute myocardial infarction in the thrombolytic era: A prospective trial. Circulation 1994;90:1747-56.

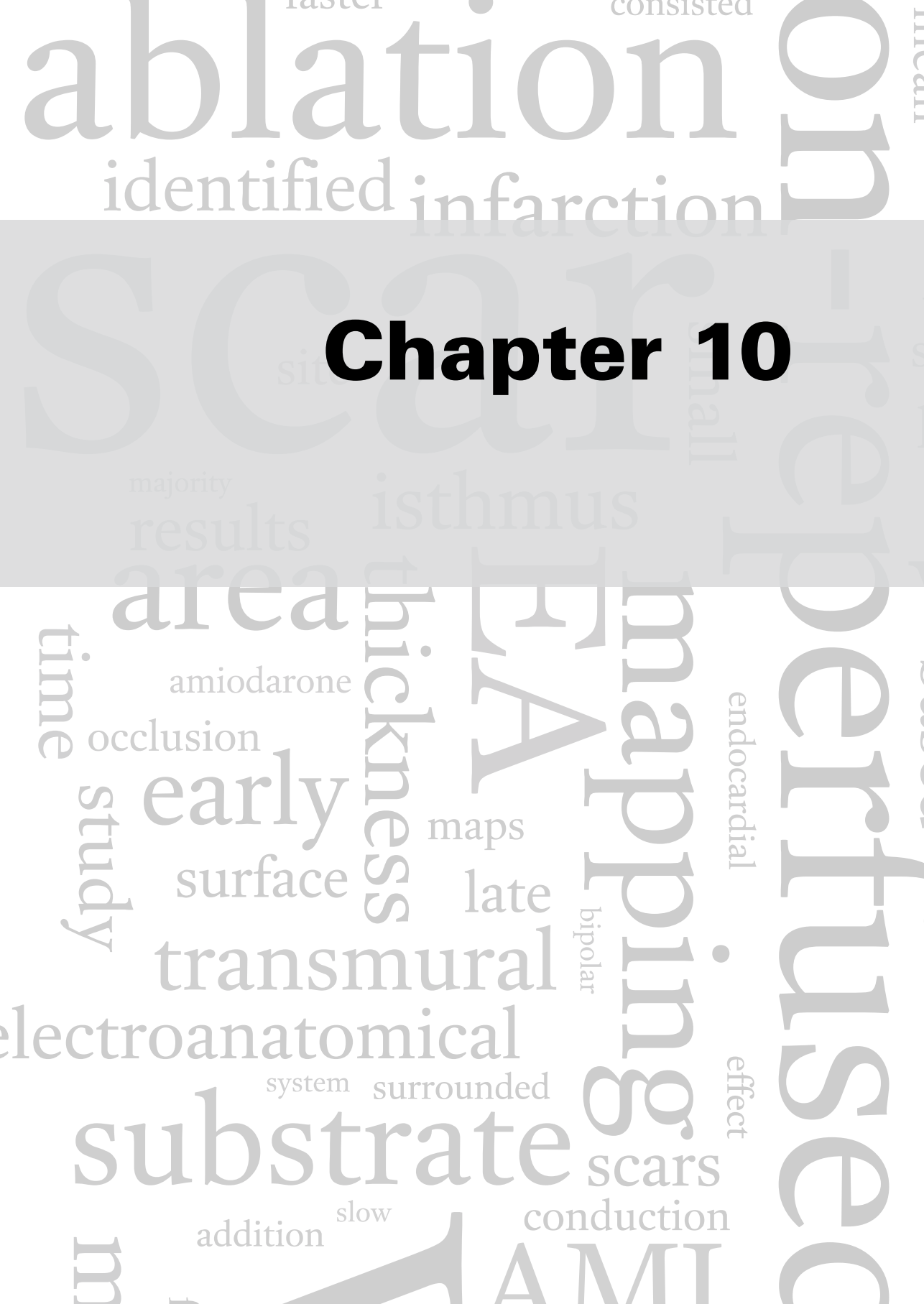
(23) Hohnloser SH, Klingenheben T, Zabel M, Schopperl M, Mauss O. Prevalence, characteristics and prognostic value during long-term follow-up of nonsustained ventricular tachycardia after myocardial infarction in the thrombolytic era. J Am Coll Cardiol 1999;33:1895-902.

(24) Kersschot IE, Brugada P, Ramentol M, Zehender M, Waldecker B, Stevenson WG, Geibel A, De ZC, Wellens HJ. Effects of early reperfusion in acute myocardial infarction on arrhythmias induced by programmed stimulation: a prospective, randomized study. J Am Coll Cardiol 1986;7:1234-42.

(25) Sager PT, Perlmutter RA, Rosenfeld LE, McPherson CA, Wackers FJ, Batsford WP. Electrophysiologic effects of thrombolytic therapy in patients with a transmural anterior myocardial infarction complicated by left ventricular aneurysm formation. J Am Coll Cardiol 1988;12:19-24.

(26) Matsuda M, Fujiwara H, Onodera T, Tanaka M, Wu DJ, Fujiwara T, Hamashima Y, Kawai C. Quantitative analysis of infarct size, contraction band necrosis, and coagulation necrosis in human

autopsied hearts with acute myocardial infarction after treatment with selective intracoronary thrombolysis. Circulation 1987;76:981-9.
(27) Ciaccio EJ, Costeas C, Coromilas J, Wit AL. Static relationship of cycle length to reentrant circuit geometry. Circulation 2001;104:1946-51.


ablation
identified
infarction
scar
non-perfused
Chapter 10
majority
results
isthmus
area
thickness
EA
mapping
time
amiodarone
occlusion
early
endocardial
study
surface
maps
late
bipolar
transmural
electroanatomical
system
surrounded
effect
substrate
scars
addition
slow
conduction

Catheter ablation of ventricular tachycardia after left ventricular reconstructive surgery for ischemic cardiomyopathy

Adrianus P. Wijnmaalen, Kurt C. Roberts-Thomson, Daniel Steven, Robert J.M. Klautz, Stephan Willems, Martin J. Schalij, William G. Stevenson, Katja Zeppenfeld

Heart Rhythm. 2012 Jan; 9(1):10-7

Abstract

Background: After surgical ventricular restoration (SVR) for ischemic cardiomyopathy, ventricular tachycardias (VTs) are an important reason for postoperative morbidity and mortality.

Objective: To elucidate the VT substrate, VT characteristics and outcome of radiofrequency catheter ablation (RFCA) in patients with VT after SVR.

Methods: Twelve(3%) of 416 patients referred for RFCA for VT after myocardial infarction in three centers had underwent SVR. After induction of VT, left ventricular (LV) electroanatomical mapping was performed. Ablation target sites were identified by entrainment, substrate and/or pace mapping.

Results: Four(33%) patients presented within the perioperative period with incessant VT, 8(67%) presented with incessant or recurrent VT late after SVR (VT cycle length 453±102ms). The region of surgical scar was identified by electroanatomical mapping in 11 patients. Twenty-eight VTs (cycle length 384±95ms) were induced. The VT exit was bordering the surgical scar in 20(71%) VTs, 15 of which at the septal side. All VTs were abolished in 5 patients, in 4 only the clinical VTs were abolished, in 1 re-inducibility was not tested. In 2 patients ablation failed after which surgical ablation was performed successfully. During follow-up 3(25%) patients died (non-arrhythmic deaths) all had presented early after SVR. Two(17%) experienced recurrent VT.

Conclusion: VT after LV SVR seems to have a bimodal presentation, one third presented with incessant VT in the acute postoperative phase, having a high mortality. Two thirds presented late after SVR, in these patients RFCA is usually effective. Successful ablation sites are frequently located at the border of surgical scars and patch material.

Introduction

Surgical ventricular restoration (SVR) of the left ventricle (LV) is a potential treatment option for patients with extensive LV scar due to ischemic cardiomyopathy.[1] Commonly used techniques are endoventricular repair with or without the use of a patch and aneurysmectomy with linear repair.[1-3] In the early and late postoperative period ventricular arrhythmias are the second most important cause of death and an important reason for morbidity in these patients.[1, 4] It has been demonstrated that surgical scars and patch material influence occurrence and characteristics of reentrant monomorphic ventricular tachycardias (VTs) in patients after repair of congenital heart disease and in patients after corrective valve surgery.[5, 6] Despite the growing number of patients undergoing SVR, there are no systematic studies of the substrate and the characteristics of sustained monomorphic VTs contributing to the postoperative morbidity and mortality.

This study aimed to elucidate the VT substrate, VT characteristics and outcome of catheter ablation in patients with recurrent VT after SVR.

Methods

Patients

Clinical records of 416 patients referred for radiofrequency catheter ablation (RFCA) for symptomatic VT late after myocardial infarction during 4.0±2.6 (range 2-7) consecutive years in three centers (Brigham and Women's Hospital, Leiden University Medical Center, Hamburg University Hospital) were reviewed and 12 patients (3%) were identified who had LV reconstructive surgery defined as surgical ventricular restoration (SVR) by endoventricular patch-plasty or LV aneurysm resection. General contraindications for endocardial catheter ablation were absence of vascular access to the LV, echocardiographic evidence of mobile LV thrombus, combined aortic and mitral valve replacement and unstable angina. All patients who underwent catheter ablation after SVR were included in the study. Data regarding patient characteristics, clinical history and acute outcome were obtained from the medical record.

Electrophysiological study and mapping

All patients underwent electrical programmed stimulation (EPS) and LV electroanatomical (EA) mapping. The EPS-protocol consisted of 3 drive-cycle lengths (600, 500 and 400ms) and up to 3 ventricular extrastimuli from 2 right ventricular sites and burst pacing. The positive endpoint of EPS was the induction of VT lasting >30s or requiring termination for hemodynamical instability. Bipolar endocardial electroanatomical voltage mapping of the RV and/or LV was performed in all patients, facilitated by a 3D EA mapping system (CARTO

XP EP system, Biosense Webster Inc, Diamond Bar, CA, USA) during sinus or paced rhythm. A 4mm or 3.5mm tip, irrigated quadripolar mapping catheter (NaviStar or Navistar Thermo-Cool, Biosense Webster Inc, Diamond Bar, CA, USA) was used inserted via a transvenous or retrograde aortic approach. Electroanatomical scar was defined by voltage criteria. Electrogram amplitudes ≤0.5mV were defined as dense scar, voltages >0.5mV and ≤1.5mV[7, 8] as scar borderzone. At low amplitude sites pacing was performed with 10mA at 2ms pulse width. Sites with a pacing threshold >10mA were tagged as electrically unexcitable scar (EUS).[9]

Identification and ablation of VT circuits

Hemodynamically tolerated VT were mapped and ablated during VT. Target sites for ablation were sites with an isolated mid-diastolic potential where pacing entrained the VT with concealed fusion and a post pacing interval within 30ms of the VT cycle length (CL) and a stimulus-to-QRS interval <70% of the VTCL. For fast and hemodynamically non-tolerated VT, exit sites were identified and targeted on the basis of pace-mapping during SR, with a paced QRS morphology similar to the VT QRS morphology indicating a potential reentry circuit isthmus site. Pacing was performed at the electroanatomical scar borderzone and at sites where electrograms with low amplitude fragmented components, double potentials and/or isolated late potentials could be recorded during sinus rhythm. Substrate modification by linear ablation lines along the scar border extending lesions at exit sites or through identified isthmus was performed at the discretion of the operator. Complete procedural success was defined as the absence of any inducible monomorphic VT at the end of the ablation procedure. Partial success was defined as successful ablation of the clinical or presumed clinical tachycardia and ablation failure if the clinical or presumed clinical VT could not be successfully ablated. Definitions and ablation strategy used were alike in the three participating centers.

Follow-up

As a rule all antiarrhythmic drugs, with exception of intravenous drugs, were continued after the ablation procedure and at discharge from the hospital. Data regarding survival was collected (from the social security death index for the US patients and from long-term follow-up visits for the Netherlands and German patients). The date of last contact, heart transplantation or death was considered the date of last follow-up.

Results

The characteristics of the 12 patients (all male, age 64±8yr) after myocardial infarction and LV reconstructive surgery included in the study are summarized in table 1. Spontaneous

Table 1. Baseline characteristics

Patient	Age yr	MI	Indication for surgery	Surgery	Patch	Time from Surgery to VT	NHYA class	VT frequency	CL ms	Failed AAD
1	64	Anterior	Heart failure	SVR ablation	Y	< 30 d	4	Incessant	560	Amiodarone Procainamide
2	73	Anterior	Heart failure	SVR	Y	< 30 d	3-4	Incessant	550 600	Amiodarone Procainamide Lidocaine
3	50	Anterior	Heart failure	Aneurysm resection	N	< 30 d	2	Incessant	430	Lidocaine Mexilitine Amiodarone
4	61	Anterior	Heart failure	SVR	Y	< 30 d	3-4	Incessant	460 375	Amiodarone Lidocaine Quinidine
5	62	Anterior	Heart failure	SVR	Y	2 yr	3-4	Incessant	480	Amiodarone Procainamide
6	69	Inferior	Wall rupture	Aneurysm resection	N	2 yr	2	Recurrent	540	Amiodarone
7	61	Anterior	Heart failure	SVR	Y	4 yr	2	Recurrent	380 280	Sotalol
8	63	Anterior	Heart failure	Aneurysm resection	N	2 yr	3-4	Recurrent	560 470	Procainemide Mexilitene Amiodarone
9	51	Anterior	Heart failure	SVR	Y	5 yr	2	Electrical storm	370 270	Lidocaine Sotalol
10	78	Anterior	Heart failure	Aneurysm resection	N	4 yr	3-4	Recurrent	405	Amiodarone
11	64	Posterior	Heart failure	SVR	Y	6 yr	2	Incessant	580	Amiodarone
12	68	Anterior	Heart failure	SVR	Y	3 yr	3	Recurrent	390	Amiodarone

AAD = anti arrhythmic drugs, CL = cycle length, MI = myocardial infarction, n = no, SVR = surgical ventricular restoration, VT = ventricular tachycardia, y = yes, yr = year.

Table 2. VT inducibility, mapping and ablation results and outcome.

Pt	VT N	VT CL (ms)	Lead V1 Lb/ Rb	Axis	Transition	Clinical VT	Mapping	Exit bordering surgical patch/scar	Location LV	Inducible after RF	Number Procedures	Outcome
1	1	526	Rb	RS	V3	y	Activation Entrainment	y	Lateral	n	1	VT free Late death
	2	257	Rb	RS	V4	n	NT	-		-		
2	1	535	Lb	LS	V3	y	RV Activation Entrainment	?	Septal	y	1	Surgery → VT free → Death (Sepsis)
3	1	420	Rb	RS	V3	y	Activation	y	Septal	n	1	VT free
	2	240	Rb	-	-	-	NT	-	-	y		
4	1	400	Rb	RI	No	y	Activation	n	Basal	n	2	VT free Death (heartfailure)
	2	400	Lb	I	V4	n	Activation	y	Inferior septal	n		
	3	350	Rb	RI	V6	n	Activation	n	High lateral	n		
5	1	480	Rb	RI	No	y	Activation Entrainment	y	Anterior septal	n	2	Surgery → VT free
	2	500	Rb	RS	V4	y	Activation Entrainment	y	Inferior septal	y		
	3	330	Rb	RI	V6	n	Pace	y	Lateral	y		
	4	380	Lb	LI	V2	n	Pace	y	Septal	y		
	5	300	Rb	RS	V4	n	Activation	y	Lateral	y		

Table 2. (continued)

Pt	VT N	VT CL (ms)	Lead V1 Lb/ Rb	Axis	Transition	Clinical VT	Mapping	Exit bordering surgical patch/scar	Location LV	Inducible after RF	Number Procedures	Outcome
6	1	540	Rb	LS	V5	y	Activation Entrainment	y	MA - scar	n	1	VT free
	2	300	Lb	LS	V5	n	Pace	y	Apicoseptal	n		
7	1	350	Rb	LS	V2	y	Activation Pace	y	Septal	n	1	VT free
	2	330	Rb	S	V2	n	Pace	y	Septal	n		
8	1	560	Lb	LS	No	y	Activation Pace	y	Septal	n	1	Recurrence
	2	300	Lb	RI	V6	n	Pace	y	Septal	-		
9	1	270	Lb	LS	V2	?	NT	-	-	n	1	Recurrence
	2	290	Lb	LI	No	?	NT	-	-	n		
	3	370	Lb	RI	V3	y	Activation	y	Septal	n		
	4	380	Rb	LI	V3	?	Activation	n	Fascicular	n		
10	1	320	Rb	RI	V2	?	Pace	y	Anteroseptal	-	1	VT free
	2	300	Rb	RS	V3	?	Pace	y	Inferoseptal	-		

Table 2. (continued)

Pt	VT N	VT CL (ms)	Lead V1 Lb/ Rb	Axis	Transition	Clinical VT	Mapping	Exit bordering surgical patch/scar	Location LV	Inducible after RF	Number Procedures	Outcome
11	1	530	Lb	LI	V5	y	Entrainment Pace	y	Inferior septal	n	3	VT free
12	1	390	Rb	LS	V4	y	Entrainment Pace	y	Apicolateral	n	1	VT free
	2	420	Rb	LI	V2	n	Entrainment Pace	y	Circuit behind patch	y		

CL = cycle length, Lb= left bundle branch block, LI = left inferior, LS = left superior, MA = mitral annulus, n = no, NT = not targeted, Pt = patient, Rb = right bundle branch block, RF = radiofrequency ablation, RI= right inferior, RS = right superior, VT = ventricular tachycardia, y = yes. Transition = in Lb the first precordial lead with an R/S ratio of >1, in Rb the first precordial lead with an R/S ratio of <1

VT had occurred before surgery in 3 patients. The indication for surgery had been congestive heart failure in 11 patients and inferior wall rupture due to acute inferior infarction in 1 patient. SVR reshaping the LV with an endoventricular patch was performed in 8 and aneurysm resection in 4 patients respectively. Concomitant procedures were mitral/tricuspid valve repair in 5, coronary artery bypass grafting in 9, and endocardial encircling cryoablation for VT in 1 patient. The LV ejection fraction at referral was 25±9%.

VT had been refractory to class III (amiodarone in 10) or to a combination of class I and III antiarrhythmic drugs in all patients. In 3 patients a previous RFCA attempt in another center had failed. Four (33%) patients presented early, within the perioperative period (<30 days) after surgery with an incessant monomorphic VT. The other 8 (67%) patients presented with incessant monomorphic VT (2), electrical storm (1) or recurrent VT (5) 3.8±1.4 years after LV reconstructive surgery. Prior to ablation, 17 different VT morphologies with a CL of 453±102ms were documented. The mean VTCL of patients presenting in the early postoperative phase was 496±87ms and in those presenting late after SVR 430±106ms. VT was hemodynamically tolerated and was relatively slow (CL >400ms) in 8 patients. At referral, 9 (75%) patients had an implantable cardioverter defibrillator (ICD).

Electrophysiological evaluation and mapping

A total of 28 monomorphic VTs (CL 384±95ms) were induced (2.3±1.2 per patient). VT characteristics are provided in table 2. Sustained polymorphic VT was induced in none of the patients. Electroanatomical mapping of the LV was performed in 11 patients. In 1 patient (patient 2) only RV mapping was performed since the patient presented with left bundle branch block like VT and the LV was not safely accessible due to coexisting mitral valve endocarditis. In the 11 patients with LV mapping an area of EUS or very low voltage was present in the region of reconstructive surgery. In all patients in whom patch material was used at surgery, the location of the endoventricular patch was clearly demarcated as an area of confluent EUS or absence of detectable electrograms (figure 1 and 3). Data regarding mapping strategy and location of VT circuits is summarized in table 2. The exit of the VT reentry circuit was mapped to the border of the EUS or very low voltage area consistent with surgical scar or patch material in 20 of the 28 (71%) induced VTs, including at least one VT in all 11 LV mapped patients. The majority of VT exits (15 of 20 VTs) were on the septal side of the repair whereas 4 VT were mapped to another border of the patch or surgical scar and 1 exited simultaneously at multiple patch borders. Seven of the 15 VTs mapped to the septal portion of the scar had a right bundle branch block (RBBB) type configuration, the remainder had a left bundle branch block configuration. No clear pattern in surface ECG morphology and location of surgical scar or patches was found. The reentry circuit was distant from the surgical scar for 3 VTs in 2 patients. Four VT's in 3 patients were not mapped because they were hemodynamically untolerated, fast VTs (CL<300ms) and were not targeted for ablation

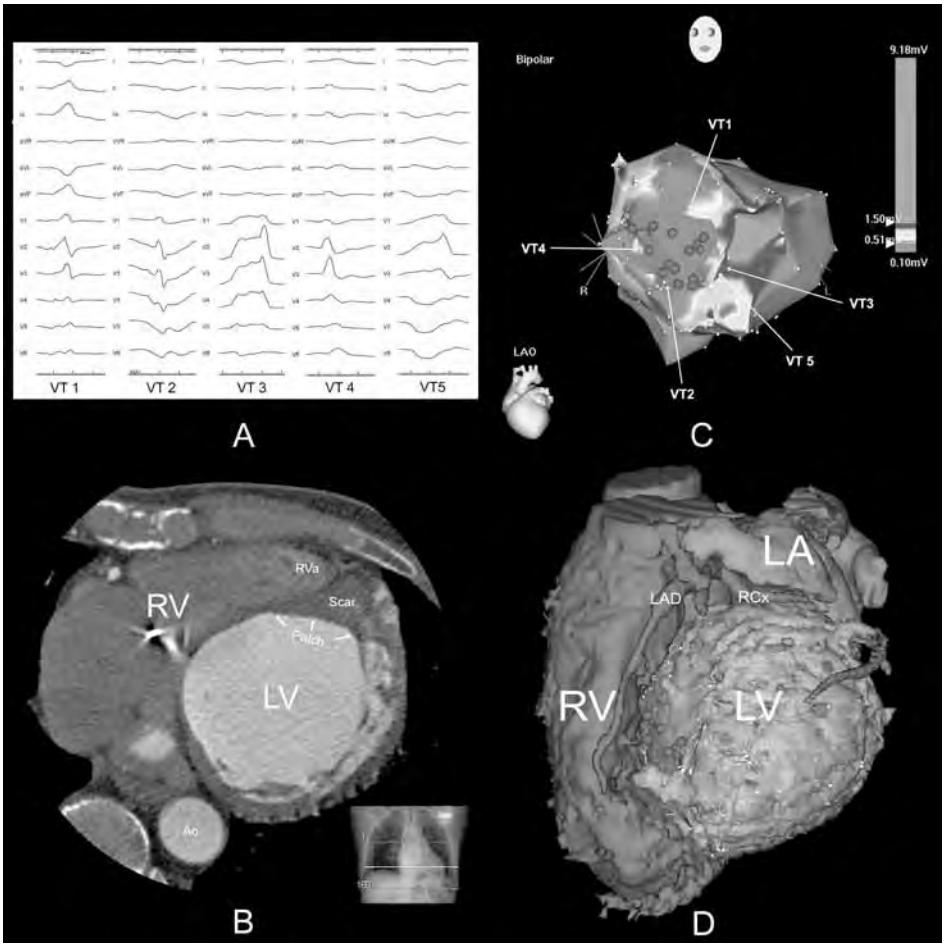


Figure 1. Patient 5, in whom RFCA failed to abolish any of the 5 VTs that appeared to originate from behind the endoventricular patch. Panel A shows the morphologies of VT 1-5 (sweep-speed 100mm/s). Panel B shows the sagittal plane of a multislice CT scan after intravenous contrast demonstrating a space occupied with scar tissue (indicated by the word 'scar') that is excluded from the left ventricular cavity by the endoventricular patch. Panel C shows the endocardial bipolar voltage map with the locations of the exit sites of VT 1-5 bordering the endoventricular patch and indicated by arrows. (colorcoding as in the colorbar, gray is electrically unexcitable scar representing the patch), voltage >1.5 mV is purple. Panel C shows the 3-dimensional reconstruction of the CT images merged with the endocardial voltage map. **(for figure in color see page: 262)**

because of unknown clinical significance in two patients or non-inducibility after ablation of other VTs in one patient.

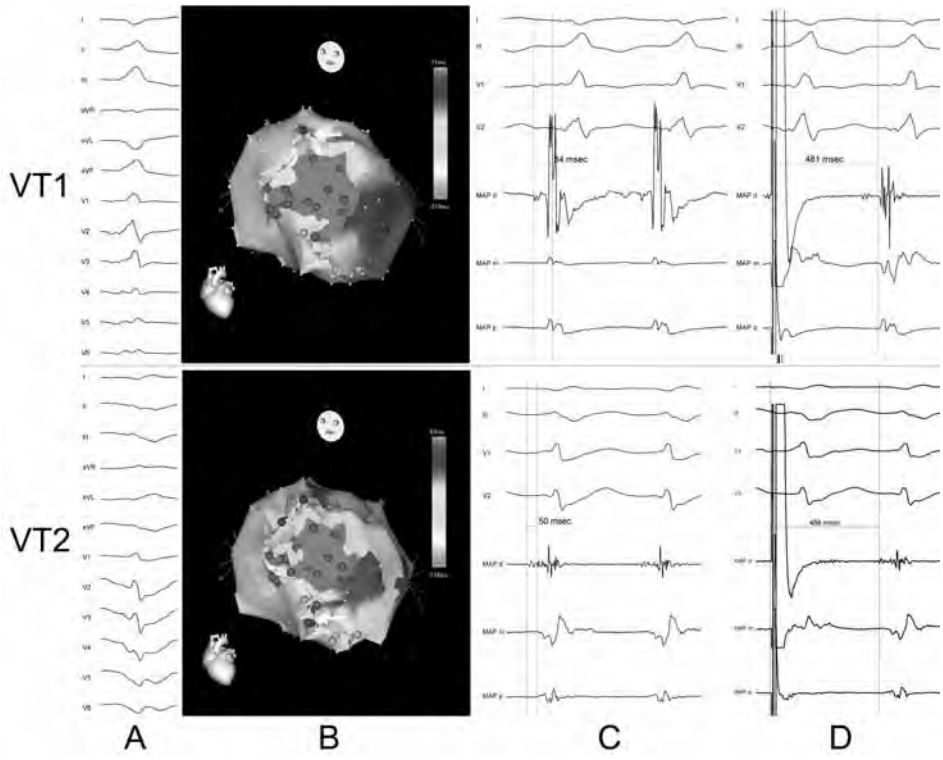


Figure 2. Example showing the activation and entrainment mapping of VT1 and VT2 in patient 5 (figure 1). The exits of VT3 – VT5 were identified using only activation or pacemapping. Panel A: 12 lead QRS morphology of VT1 and VT2. Panel B: Electroanatomical activation maps of the LV during VT1 (top) and VT2 (bottom). The endoventricular patch was identified as an area of unexcitable scar and tagged in gray. Activation time is according to the colorbar with the earliest activation displayed in red. The white arrows indicate the site of earliest endocardial activation, entrainment mapping and RF application (red tags). Panel C: Intracardiac bipolar electrograms recorded from the distal, mid and proximal electrode pairs of the ablation catheter at the border of the endoventricular patch for VT1 and VT2. Panel D: Entrainment mapping of VT1 shows concealed entrainment while capturing the second electrogram component with an S-QRS interval of 25ms identical with the E-QRS, which is consistent with a VT exit site. Pacing at this site entrained the VT with concealed fusion with a post pacing interval (PPI) of 481ms, which equaled VTCL. VT2 could be entrained with concealed fusion with a PPI of 486ms (VTCL = 504ms) and a S-QRS interval of 50ms. **(for figure in color see page: 263)**

Ablation

A single ablation procedure was performed in 9 patients; in 3 patients a repeat procedure was performed because of VT recurrence. RF application consisted of single lesions based on activation and entrainment mapping in 9 and linear lesions based on substrate and pace-mapping in 3 patients.

No sustained VT of any type was inducible in 5 patients, in 4 patients the clinically documented VTs were no longer inducible but another VT remained inducible, in 1 patient

inducibility was not tested at the end of the procedure (patient 10). In 2 patients ablation failed to terminate the clinical VT. Both had presented with incessant VT. In one patient (patient 5) the endocardial exits of 5 VTs were mapped to the border of the repair area (figure 1 and 2), but ablation at these sites failed to terminate VTs suggesting that the critical isthmus of the VTs was located deep to the patch. In this patient cardiac computed tomography scan (MSCT) revealed that the patch was inserted in the LV septum with tissue visible between the patch and the pericardium, and a percutaneous epicardial approach was not attempted (figure 1). In the other patient (patient 2), LV mapping and ablation was not performed due to coexisting mitral valve endocarditis, with a possible risk of embolization. There were no procedural complications. Both patients with ablation failure underwent repeat surgery because of incessant VT with subendocardial resection combined with cryoablation of the residual borderzone in the first and subendocardial resection combined with RF-ablation of the residual borderzone and mitral valve replacement in the second patient.

Outcome

There were no procedure related complications. Two (50%) patients with VT presenting <30 days after initial surgery died within the perioperative period. The cause of death was heart failure in one and sepsis in the other patient. The median follow-up after RF ablation in the remaining 10 patients was 24 months (interquartile range 11 – 39 months). All 10 surviving patients were discharged with an ICD. Eight were free of any VT during follow-up. Two patients had VT recurrence, in both no VT was inducible after the first procedure. One additional patient with VT presenting <30 days after surgery died 3 months after catheter ablation due to heart failure. There were no arrhythmic or sudden cardiac deaths.

Discussion

The number of patients undergoing SVR as treatment for patients with heart failure due to ischemic cardiomyopathy is increasing.[1] Present indications include heart failure after prior myocardial infarction with a dilated or aneurysmal LV.[3, 10, 11] In a pooled analysis of multiple studies, ventricular arrhythmias accounted for 16.6% of early mortality (n=12,331) and 17.2% of late mortality (n=3,729) in patients following SVR.[1] In patients with an ICD implanted for primary or secondary prevention, 14.4% had appropriate ICD shocks in the first year after SVR, the majority within the first two months.[4]

Catheter ablation is an important therapeutic option for controlling recurrent ventricular tachycardia late after acute myocardial infarction. However, although only 12 patients were included, the present study is the largest series of post infarction SVR patients with VT studied with catheter mapping and attempted ablation. Patients (3%) were drawn from a group of 416 patients who underwent RFCA for post myocardial infarction VT in 3 referral

centers. Due to the referral nature of the population, it is not possible to further determine the incidence VT after reconstructive surgery approachable by catheter ablation.

The presentation of patients seems to be bimodal. One third of the patients presented within the early postoperative period. The indication for ablation in these patients was incessant VT refractory to pharmacological treatment, most in the setting of postoperative heart failure or sepsis. Patients were accepted for ablation after consultation of the cardiothoracic surgeon and careful evaluation of possible risks and benefits of the procedure. Considerations included individual patient characteristics, other treatment options, available resources and operator experience. In these severely ill patients catheter ablation was regarded as a last resort to control life threatening ongoing VT.

The other two thirds presented with incessant or frequent episodes of VT late (3.8 years) after surgery. These patients were otherwise in relatively stable condition and selection criteria for ablation were similar to other patients presenting with post myocardial infarction VT.

The majority of patients had relatively slow VT (mean CL 438±100ms) due to myocardial reentry. The long CL may be partly due to the antiarrhythmic drug regime with a combination of class I and III drugs used in 7 patients. However, it is interesting to speculate that the large scars present in patients who are considered for SVR may be more likely to provide large and/or slow reentry circuits.[12-14]

Although SVR improves hemodynamics and reduces wallstress[15] it does not completely eliminate the substrate for myocardial reentry as a significant portion of the myocardial scar is left behind the inserted patch for stability and hemostasis.

Electrophysiologic characteristics and ablation

High density electroanatomical catheter mapping identified a low voltage area consistent with surgical scar or patch material in all LV mapped patients. Importantly, patch material could be demarcated as a confluent area with no detectable electrograms or EUS in all patients in whom endoventricular patch plasty was performed. The border of patch materials and surgical incisions was adjacent to at least some part (usually the exit) of the reentry circuit of 86% of targeted VTs. The majority of VT reentry circuits were mapped to the septal border of the endocardial patch or surgical scar. This is in concordance with previous findings by Josephson et al who found a septal origin in 56% of post-MI VTs mapped during surgery.[16] Of interest, 7 of 15 VTs with a septal exit site had a RBBB like morphology and no clear pattern in surface ECG morphology and location of surgical scar was observed. This suggests that activation of the remaining ventricles might be modified by surgery. A major concern for these patients is the possibility that the VT circuit is beneath the patch material or in the excluded LV, where it would not be amenable to endocardial ablation. Importantly, in the majority of patients (10 of the 12 patients) this was not a major impediment to ablation, as at least portions of reentry circuits were identified on the endocardium. All successful

ablation sites were in the endocardial LV. RFCA acutely abolished all VTs in 5 (42%) and the clinical VT in 4 (33%) patients after one or two RFCA procedures. Two recently conducted multicenter trials assessing the effect of RFCA for recurrent or incessant post MI VT reported acute success rates of 81% abolishing the clinical VT.[17, 18] The similar acute success rate of 75% in the present study despite advanced heart failure and the presence of surgical scar and patch material is encouraging. In one patient, failure of ablation was potentially attributed to exclusion of the reentry circuits, from the endocardium by LV patch material (figure 1). In this patient repeat surgery with subendocardial resection and cryoablation of the borderzone was required to abolish incessant VTs, and was successful. This example suggests that intraoperative treatment of a potentially arrhythmogenic substrate that will be excluded from the endocardium is important, particularly the septal portion of the scar. Routine use of encircling cryoablation[19] or subendocardial resection[16, 20], as previously described for the treatment of VTs, may be considered.

Presentation of incessant sustained monomorphic VT in the early postoperative phase was associated with an in hospital mortality of 50% due to heart failure or sepsis, which likely reflects the poor condition of these patients. In contrast, none of the patients presenting late after SVR died during follow-up. All patients were discharged from hospital with an ICD, and only two (20%) had recurrent VT during a median follow-up of 24 months. Although the patient population was small, the low recurrence rate is remarkable since recent studies have reported that the recurrence rate of VT after RFCA in post MI patients is approximately 50% in the first 6 to 12 months, in both patients with and without incessant VT.[17, 18]

Limitations

The sample size included in the study was relatively small and due to a referral bias the selected population of post SVR patients may not be entirely representative. To our knowledge however this is the first study reporting on the findings and outcome of catheter ablation for VT in this population. Furthermore, the presumption that the reentry circuit of the VTs in one patient was isolated from the ventricles by the patch was based on the fact that endocardial ablation failed. However, it is supported by the distribution of VT exit sites around the patch, the findings at the CT scan (figure 1) and the fact that after surgical removal of the scar behind the patch the patient remains free of any VT recurrence. In addition, a CT scan was available in one patient who underwent successful ablation and in this patient the space behind the inserted patch was evidently smaller. (Figure 3)

Conclusion

Sustained monomorphic VT after LV reconstructive surgery seems to have a bimodal presentation, with one third presenting with incessant VT in the acute postoperative phase, having a high mortality. For the majority, who present with VT years after surgery, RFCA is usually effective despite concerns about potential isolation of arrhythmia substrate outside

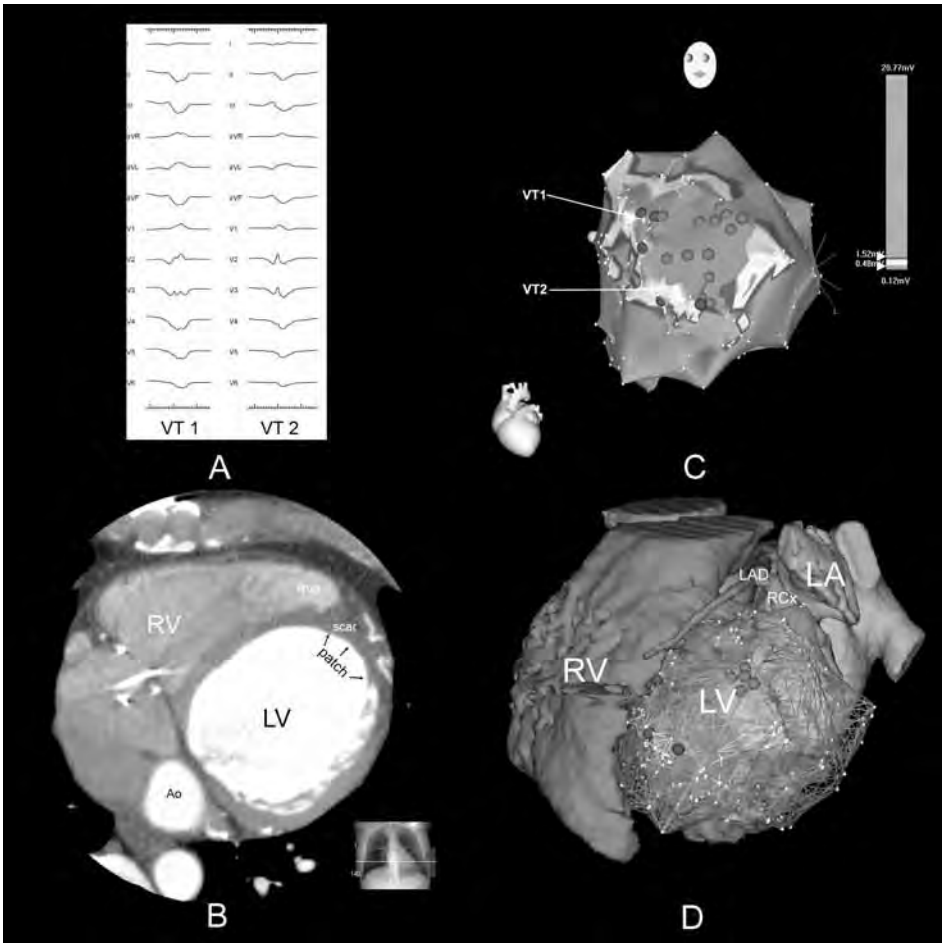


Figure 3. Patient 7, in whom RFCA was successful, abolishing 2 VTs by applying RF energy at the septal side of the endoventricular patch. Panel A shows the morphologies of VT 1-2 (sweep-speed 100mm/s). Panel B shows the sagittal plane of a multislice CT scan after intravenous contrast showing a small apical scar behind the endoventricular patch if compared to patient 5 (figure1). Panel C shows the endocardial bipolar voltage map with the locations of the exit sites of VT 1-2 bordering the endoventricular patch and indicated by arrows (color coding as in the color bar, gray is electrically unexcitable scar representing the patch). Panel C shows the 3-dimensional reconstruction of the CT images merged with the endocardial voltage map. **(for figure in color see page: 264)**

the endocardium. Successful ablation sites are frequently located at the border of surgical scars and patch material. Patch material overlaying the substrate of VT may prevent successful RFCA ultimately necessitating surgical ablation of VT in some patients.

Reference List

(1) Klein P, Bax JJ, Shaw LJ, et al.: Early and late outcome of left ventricular reconstruction surgery in ischemic heart disease. Eur J Cardiothorac Surg 2008;34:1149-57.

(2) COOLEY DA, COLLINS HA, MORRIS GC, Jr., CHAPMAN DW: Ventricular aneurysm after myocardial infarction; surgical excision with use of temporary cardiopulmonary bypass. J Am Med Assoc 1958;167:557-60.

(3) Dor V, Saab M, Coste P, Kornaszewska M, Montiglio F: Left ventricular aneurysm: a new surgical approach. Thorac Cardiovasc Surg 1989;37:11-9.

(4) O'Neill JO, Starling RC, Khaykin Y, et al.: Residual high incidence of ventricular arrhythmias after left ventricular reconstructive surgery. J Thorac Cardiovasc Surg 2005;130:1250-6.

(5) Zeppenfeld K, Schalij MJ, Bartelings MM, et al.: Catheter ablation of ventricular tachycardia after repair of congenital heart disease: electroanatomic identification of the critical right ventricular isthmus. Circulation 2007;116:2241-52.

(6) Eckart RE, Hruczkowski TW, Tedrow UB, et al.: Sustained ventricular tachycardia associated with corrective valve surgery. Circulation 2007;116:2005-11.

(7) Reddy VY, Wrobleski D, Houghtaling C, Josephson ME, Ruskin JN: Combined epicardial and endocardial electroanatomic mapping in a porcine model of healed myocardial infarction. Circulation 2003;107:3236-42.

(8) Marchlinski FE, Callans DJ, Gottlieb CD, Zado E: Linear ablation lesions for control of unmappable ventricular tachycardia in patients with ischemic and nonischemic cardiomyopathy. Circulation 2000;101:1288-96.

(9) Soejima K, Stevenson WG, Maisel WH, Sapp JL, Epstein LM: Electrically unexcitable scar mapping based on pacing threshold for identification of the reentry circuit isthmus: feasibility for guiding ventricular tachycardia ablation. Circulation 2002;106:1678-83.

(10) Athanasuleas CL, Buckberg GD, Stanley AW, et al.: Surgical ventricular restoration in the treatment of congestive heart failure due to post-infarction ventricular dilation. J Am Coll Cardiol 2004;44:1439-45.

(11) Dor V, Civaia F, Alexandrescu C, Sabatier M, Montiglio F: Favorable effects of left ventricular reconstruction in patients excluded from the Surgical Treatments for Ischemic Heart Failure (STICH) trial. J Thorac Cardiovasc Surg 2011;141:905-16.

(12) Woie L, Eftestol T, Engan K, et al.: The heart rate of ventricular tachycardia following an old myocardial infarction is inversely related to the size of scarring. Europace 2011.

(13) Wijnmaalen AP, Schalij MJ, von der Thusen JH, Klautz RJ, Zeppenfeld K: Early reperfusion during acute myocardial infarction affects ventricular tachycardia characteristics and the chronic electroanatomic and histological substrate. Circulation 2010;121:1887-95.

(14) Ciaccio EJ: Dynamic relationship of cycle length to reentrant circuit geometry and to the slow conduction zone during ventricular tachycardia. Circulation 2001;103:1017-24.

(15) ten Brinke EA, Klautz RJ, Tulner SA, et al.: Long-term effects of surgical ventricular restoration with additional restrictive mitral annuloplasty and/or coronary artery bypass grafting on left ventricular function: six-month follow-up by pressure-volume loops. J Thorac Cardiovasc Surg 2010;140:1338-44.

(16) Josephson ME, Horowitz LN, Harken AH: Surgery for recurrent sustained ventricular tachycardia associated with coronary artery disease: the role of subendocardial resection. Ann N Y Acad Sci 1982;382:381-95.

(17) Tanner H, Hindricks G, Volkmer M, et al.: Catheter ablation of recurrent scar-related ventricular tachycardia using electroanatomical mapping and irrigated ablation technology: results of the prospective multicenter Euro-VT-study. J Cardiovasc Electrophysiol 2010;21:47-53.

(18) Stevenson WG, Wilber DJ, Natale A, et al.: Irrigated radiofrequency catheter ablation guided by electroanatomic mapping for recurrent ventricular tachycardia after myocardial infarction: the multicenter thermocool ventricular tachycardia ablation trial. Circulation 2008;118:2773-82.
(19) Guiraudon GM, Thakur RK, Klein GJ, et al.: Encircling endocardial cryoablation for ventricular tachycardia after myocardial infarction: experience with 33 patients. Am Heart J 1994;128:982-9.
(20) Dor V, Sabatier M, Montiglio F, et al.: Results of nonguided subtotal endocardiectomy associated with left ventricular reconstruction in patients with ischemic ventricular arrhythmias. J Thorac Cardiovasc Surg 1994;107:1301-7.

primary
successful
polarity
ocardial
coronary
idiopathic
get
integration
ent
spontaneous
predict
catheter
presence
site
EA
VA
CF
substrate
SVR
without
registration
imaging
unipolar
chapter
ECG
shorter
cardiac
MDCT
LV
assessed
performed
associated
surgical
reversed
myocardium
electrograms
Chapter
QRS
detected
isthmus
identification
cardiomyopathy

Summary and conclusions

Catheter ablation targeting the arrhythmia substrate has become an important therapeutic option for patients with different types of ventricular tachycardia (VT). The aim of the current thesis was to study the determinants for the substrate causing VT, the VT characteristics and outcome specifically after invasive treatment and to develop techniques that facilitate and thereby potentially improve outcome after catheter ablation. **Chapter 1** provides an overview of the current literature regarding the different underlying substrates for monomorphic VT and the applied ablation techniques.

In **part I** determinants of the VA substrate and techniques for substrate identification were studied in patients referred for catheter ablation of VA. After identification and localization of the substrate catheter ablation has the potential to specifically target these regions thereby preventing VA recurrence. The potential advantage of multimodal imaging of the VT substrate and related anatomical structures integrated with the electroanatomical information during catheter ablation could be demonstrated. Differences in VA substrate between patients are likely to impact clinical outcome which was further addressed in **part II.**

Part I

Discrimination between idiopathic (non scar-related) and scar-related LBBB pattern VA has important clinical implications. In **chapter 2** we hypothesized that the VA QRS morphology is influenced by the presence of ventricular scar allowing electrocardiographic discrimination of VA arising from structurally normal versus scarred myocardium. Twelve-lead ECGs of 297 LBBB pattern monomorphic VA were recorded during radiofrequency catheter ablation (RFCA) procedures. QRS morphology characteristics associated with scar-related VA were identified in retrospective analysis of 118 LBBB pattern VA (95 scar-related, 23 idiopathic) to develop a stepwise algorithm, that was prospectively tested in 179 LBBB pattern VA (120 scar-related, 59 idiopathic).

The diagnosis of scar was based on sinus rhythm surface ECG, cardiovascular imaging and electroanatomical catheter mapping. A precordial transition beyond V4, notching of the S-wave downstroke in lead V1 or V2 and a duration from the onset of QRS to the S-nadir in V1>90ms were independent predictors for scar-related VA. The proposed algorithm classified a VA as scar-related if any of these criteria was met. If none of the criteria was present a VA was classified as idiopathic. In prospective validation the algorithm was highly sensitive (96%) and specific (83%) for the identification of scar-related LBBB pattern VA. We therefore concluded that the QRS morphology of VA is different between scar-related and idiopathic VA. A simple ECG algorithm is sensitive for identifying scar-related LBBB VA, which can be helpful in guiding further evaluation of these patients.

In **chapter 3** the value of reversed polarity of adjacent bipolar electrograms to predict a successful ablation site in idiopathic right ventricular outflow tract (RVOT) arrhythmias was

evaluated. Twenty-five consecutive patients undergoing RFCA for RVOT arrhythmia were studied. Electrograms of ablation sites and of points within a 15mm radius to the successful site were evaluated for local activation time (LAT), unipolar electrogram morphology and the presence of reversed polarity of adjacent bipolar electrograms. Electrogram characteristics of successful ablation sites were compared to non-successful ablation sites. The spatial distribution of each electrogram characteristic was studied. Successful ablation sites more often demonstrated reversed polarity and had an earlier LAT than non-successful sites. A wide spatial distribution was observed for unipolar electrograms with a QS-configuration around the successful ablation site. Mapping based on LAT and reversed polarity had a higher predictive value for a successful ablation site than mapping based on LAT and QS-configuration. The presence of reversed polarity therefore has a high predictive value for successful ablation sites in focal idiopathic RVOT arrhythmias and is likely to reduce the number of RFCA applications.

Reperfusion therapy during acute myocardial infarction (AMI) results in myocardial salvage and improved ventricular function but may also influence the arrhythmogenic substrate for ventricular tachycardia (VT). **Chapter 4** used electroanatomical mapping (EAM) and infarct histology to assess the impact of reperfusion on the substrate and on VT characteristics late after AMI. Thirty-six patients referred for treatment of VT 13±9yrs after AMI were studied. Fourteen patients with early reperfusion during AMI were compared with 22 non-reperfused patients. Spontaneous and induced VTs and the characteristics of EAM were analyzed. Twenty-seven patients were treated by RFCA. Ten patients (non-reperfused 6) were treated by ventricular restoration with intraoperative cryoablation in 9. During surgery biopsies were obtained from the resected core of the infarct. VT cycle length of spontaneous and induced VTs was shorter in reperfused patients (reperfused 299±52/270±58ms, non-reperfused 378±77/362±74ms, (p=0.01)). An EA patchy scar pattern was present in 71% of reperfused and in 14% of non-reperfused patients (p=0.004). The proportion of EA dense scar was smaller in reperfused patients (24±18% vs. 45±21%, p=0.02). Histological assessment in 10 patients revealed thick layers of surviving myocardium in 75% of reperfused but in none of non-reperfused patients. Scar size and pattern defined by EAM are different between VT patients with and without reperfusion during AMI. Less confluent EA scars match with thick layers of surviving myocardium on histology. Early reperfusion and less confluent electro-anatomical scar are associated with faster VTs.

Substrate based ablation of VT relies on electroanatomical voltage mapping (EAM). Integration of scar information from contrast-enhanced magnetic resonance imaging (CE-MRI) with EAM may be of additional value during ablation procedures. **Chapter 5** assessed the relation between electrogram voltages and CE-MRI scar characteristics using real-time integration and reversed registration.

Fifteen patients without implantable cardiac defibrillator referred for VT ablation after myocardial infarction underwent CE-MRI. Real-time integration of CE-MRI derived scar meshes with EAM of the left ventricle (LV) and aortic root was performed using the left main stem (LM) and the CARTO surface registration algorithm. Merging of CE-MRI meshes with EAM was successful with a registration error of 3.8±0.6mm. After the procedure voltage amplitudes of each mapping point were superimposed on the corresponding CE-MRI location using the reversed registration matrix. Infarcts on CE-MRI were categorized by transmurality and signal intensity. Local bipolar and unipolar voltages decreased with increasing scar transmurality and were influenced by scar heterogeneity. VT reentry circuit isthmus sites were correlated to CE-MRI scar location. In 3 patients VT isthmus sites were located in scar areas not identified by EAM. This study showed the feasibility of integration of MRI derived scar maps with EAM during VT ablation. CE-MRI identifies non-transmural scars and infarct gray zones not detected by EAM according to currently used voltage criteria and may provide important supplementary substrate information.

Epicardial substrate determination and RFCA for VA is limited by the presence of coronary arteries and epicardial fat. In **Chapter 6** we aimed to evaluate epicardial ablation failure using real-time integration and reversed registration of MDCT data and EAM. Twenty-eight patients underwent combined endo-epicardial EAM. Cardiac MDCT was performed to visualize coronary anatomy and epicardial fat distribution. Prior to ablation, MDCT these data were loaded into the 3D EAM system. Irrigated-tip ablation was withheld within 5mm from a coronary artery confirmed by coronary angiography. All EAM data were extracted and superimposed on the MDCT using reversed registration matrix. In all patients image registration was successful and accurate (registration accuracy 2.8±1.3mm). Forty-six VA were induced, 25(54%) were abolished by catheter ablation, and 21(46%) were not. In 10 VA no target site was identified. In 7 VA of ablation was withheld due to proximity of coronary arteries and in 2 to proximity of the His-bundle at the target site. In 4 VA applied RF energy was not effective. At ineffective ablation sites the mean epicardial fat thickness was 16.9±6.8mm (range 7.3– 22.2mm). In contrast, epicardial fat thickness at successful ablation sites was 1.5±2.1mm (range 0–6.1mm, $p<0.001$). In conclusion Real-time image integration of pre-acquired MDCT information is feasible and accurate. Epicardial fat layers of >7mm and the presence of coronary arteries are important reasons for epicardial ablation failure which can be predicted based on MDCT integration.

Part II

Improvement of left ventricular ejectionfraction (EF) after RFCA of frequent premature ventricular contractions (PVCs) has been reported. However, most patients with frequent

PVCs have normal LVEF. In these patients subtle and early forms of PVC induced left and right ventricular (RV) impairment may not be detected by standard echocardiographic techniques. **Chapter 7** aimed to assess the effect of frequent PVCs on ventricular function in patients with preserved LVEF.

Forty-nine patients with recent onset, frequent PVCs (burden 26±13%) and 25 healthy controls were studied. Thirty-four patients with PVCs underwent successful RFCA. Two-dimensional echocardiography was performed at baseline and follow-up. LV volumes and LVEF were calculated by Simpson's rule. Tricuspid annulus plane systolic excursion and fractional area change were calculated to assess RV function. Multidirectional LV strain (radial, circumferential, longitudinal) and RV free wall longitudinal strain were calculated by two-dimensional speckle tracking imaging. At baseline LVEF, volumes and RV dimensions were normal in patients and controls. Speckle tracking imaging demonstrated reduced LV and RV strain in PVC patients as compared to controls. At follow-up there were no changes in LVEF, LV volumes and RV dimensions and function in successfully treated by RFCA and untreated patients. However, radial, circumferential and longitudinal strain improved significantly in patients after RFCA but remained unchanged in untreated patients. Frequent PVCs can induce subtle cardiac dysfunction detected by speckle tracking imaging analysis in patients without apparent cardiomyopathy. RFCA can successfully eliminate PVCs and improve cardiac function.

In **chapter 8** long-term arrhythmia recurrence rate and outcome in patients with scar-related right VT with and without a diagnosis of arrhythmogenic right ventricular cardiomyopathy (ARVC/D) was assessed. Sixty-four patients presenting with non ischemic scar-related VT of RV origin were studied. Scar was identified by electroanatomical mapping, contrast-echocardiography and/or MRI.Twenty-nine (45%) patients were diagnosed with ARVC/D according to TF criteria (TF+) and 35 (55%) with RV scar of undetermined origin (TF-) at the end of follow-up (64±42 months). Patients were treated with anti-arrhythmic drugs, RFCA and/or ICD implantation. VT recurrence-free survival for TF+ and TF- was 76% vs. 74% at 1yr and 45% vs. 50% at 4yr (p=ns). Patients with fast index VT (CL≤250ms, n=31) were more likely to experience a fast VT during follow-up than patients with a slow index VT (CL>250ms, n=33) (61% vs. 3%, $p<0.001$). We concluded that scar-related RV VTs have a high recurrence rate in TF+ and TF- patients. Patients presenting with a fast index VT are at high risk for fast VT recurrence and may benefit most from ICD therapy.

Chapter 9 aimed to to extend the findings demonstrated in chapter 4 in a larger population of post AMI patients who underwent electrophysiological evaluation prior to implantation of an implantable cardioverter defibrillator (ICD). Five-hundred-six patients with prior MI who underwent electrophysiology study before implantation of an ICD for primary or secondary prevention were assessed. Patients were classified according to the reperfusion

strategy (reperfusion (thrombolysis (n=44) or percutaneous coronary intervention (n=65)) vs. no reperfusion (n=397)) during AMI.

Monomorphic sustained VT was inducible in 351 (69%) patients. Inducibility in reperfused and non-reperfused patients was similar in primary prevention patients (56% vs. 58%) but significantly higher for non-reperfused patients in secondary prevention patients (56% vs. 79%, p=0.001). Induced VT cycle length was shorter (247±40 vs.287±63, p<0.001) and very fast VT (cycle length ≤250 ms) was more often induced in reperfused patients (71% vs.47%, p=0.001). In primary prevention patients, non-reperfusion was associated with a doubled risk for first spontaneous VT during follow-up. This study showed that there are important differences in VT inducibility, induced VT cycle length and occurrence of spontaneous VT in the chronic infarct healing phase between patients with and without successful reperfusion during AMI. These findings suggest differences in the chronic arrhythmogenic substrate and extend the findings of chapter 4.

After surgical ventricular restoration (SVR) for heart failure in ischemic cardiomyopathy, ventricular tachycardias are an important reason for postoperative morbidity and mortality.

Chapter 10 aimed to elucidate the VT substrate, VT characteristics and outcome of catheter ablation in patients with VT after SVR. Twelve (3%) of 416 patients referred for RFCA for VT after AMI in three centers had underwent previous SVR. After induction of VT, LV EAM was performed. Ablation target sites were identified by entrainment, substrate and/or pace mapping. Four (33%) patients presented within the perioperative period after surgery with an incessant VT, 8(67%) presented with incessant or recurrent VT late after SVR (VT cycle length 453±102ms). The region of surgical scar was identified by EAM in 11 patients. Twenty-eight VTs (cycle length 384±95ms) were induced. The VT exit was bordering the surgical scar in 20(71%) VTs. All VT were abolished in 5 patients, in 4 only the clinical VTs were abolished, in 1 re-inducibility was not tested. In 2 patients ablation failed after which surgical ablation was performed successfully. During follow-up 3 (25%) patients died (non-arrhythmic deaths) all had presented early after SVR. Two (17%) experienced recurrent VT. VT after LV SVR therefore seems to have a bimodal presentation, one third presented with incessant VT in the acute postoperative phase, having a high mortality. Two thirds presented late after SVR, in these patients RFCA is usually effective. Successful ablation sites are frequently located at the border of surgical scars and patch material.

Conclusions en future perspectives

In patients presenting with clinically apparent VA identification and characterization of the underlying substrate is key to the treatment and prognosis.

Initial discrimination between scar-related and idiopathic (non scar-related) VA is mandatory since patients with scar-related VA may be at risk for sudden cardiac death while the latter are generally considered benign. The VA surface ECG may provide an immediate electrocardiographic criterion to indicate whether ventricular scar is likely to be present, and can inform further evaluation. Since the diagnosis of idiopathic VA is still one of exclusion, this evaluation may require extensive non-invasive and invasive assessment and (CE-)MRI is considered as goldstandard to detect scar. However, electroanatomical catheter mapping is a sensitive tool to identify concealed forms of myocardial scar that are not detected by imaging modalities, and is therefore of incremental value.

In contrast to other treatment modalities like antiarrhytmic drugs or implantable defibrillators RFCA has the ability to abolish the substrate of VA. Over the last decades the role of RFCA has expanded due to development of new techniques and broadening of indications.

Idiopathic VA

Despite a good prognosis idiopathic VA can cause severe symptoms. Furthermore frequent idiopathic PVCs have reversible detrimental effects on ventricular function that may range from subclinical dysfunction detected by echocardiographic strain imaging to overt reduction in LV ejection fraction. Due to the high ablation success for idiopathic VA catheter ablation has become a first line therapy for symptomatic VA or VA presumed to cause ventricular dysfunction. The accuracy of catheter mapping to identify ablation target sites can be further improved using 'reversed polarity' as novel criterion in addition to LAT and the presence of a QS morphology of the unipolar signal. The clinical relevance of frequent PVCs in asymptomatic patients without LV dysfunction in the unselected general population is not fully understood. Identification of more sensitive indicators identifying patients who are at risk for clinically significant LV functional deterioration is needed before "preventive" RFCA in these patients can be recommended.

Scar-related VT

The underlying heart disease affects the substrate that determines VT characteristics. Better understanding of the VT substrate in different diseases and individual patients is important for the improvement of mapping and ablation strategies. The majority of patients with scar-related VT has experienced prior myocardial infarction. Much of our understanding of the VT substrate after MI is based on animal models of a chronically occluded coronary artery typically resulting in dense scar with only a small scar borderzone and on interaoperative mapping studies in patients with a chronically occluded artery. However, currently early reperfusion strategies have become the standard treatment of acute MI. Early reperfusion seems to be associated with less dense and less confluent electroanatomical scars, which was confirmed by histology. Small areas of dense scar and thicker infarct border zones may result in shorter isthmus length and faster conduction. This affects spontaneous VT

occurrence, VT inducibility and VT characteristics like cycle length. Whether a patchy pattern of electroanatomic scar after reperfusion will pose a challenge in substrate-based mapping and ablation needs further evaluation

In patients with VT after SVR for ischemic cardiomyopathy the reentry circuit is commonly related to the surgical scar or patch material identified by catheter mapping and RFCA can be highly effective the treatment of VT and prevention of recurrence.

If scar is identified as the substrate for VT originating from the RV patients are at risk for VT recurrence and sudden death irrespectively of the diagnosis of ARVC/D. Patients who present with fast VT and right ventricular scar are at high risk for fast VT recurrence despite intervention and may benefit most from ICD therapy.

Catheter ablation

In patients with scar-related VT development of substrate based techniques, irrigated tip catheter ablation and the introduction of an percutaneous epicardial approach in selected patients has rendered many VT previously considered 'untreatable' approachable for ablation. Advances in substrate imaging technologies and their integration during ablation procedures may provide more insights into the substrates and may guide VT ablation.

CE-MRI allows for the visualisation of the three-dimensional geometry of myocardial fibrosis and is the gold standard for the detection of subendocardial and non-transmural scar. Real time integration of CE-MRI derived scar information with electroanatomical mapping is feasible and accurate and allows for visualisation of intramural or epicardial scars undetected by voltage mapping and scar characteristics during the procedure. After image integration detailed mapping can be limited to the region of interest and areas incorrectly identified as scar can be easily identified. Furthermore, animal studies have shown that the detailed scar geometry as assessed by in vitro CE-MRI can predict the location of VT reentry circuits. Future evaluation should focus on whether and how in vivo CE-MRI can predict the location of reentry circuits which could be of great value aiding catheter ablation.

The determination of epicardial substrate by electroanatomical mapping and catheter ablation is limited by the presence of epicardial fat and coronary arteries. Integration with pre-acquired MDCT images can facilitate real-time visualization of coronary arteries and the distribution of epicardial fat during epicardial mapping and ablation and thereby aid the interpretation of local electrograms and identify potential sites unsuitable for ablation.

Conclusions

It is the underlying substrate determining VA characteristics. Understanding the substrate in different diseases and individual patients is crucial for the treatment of VA. RFCA is able to abolish the substrate causing arrhythmias. The use of new mapping criteria and integration of imaging techniques during RFCA may facilitate successful ablation.

procedure
reperfusie
PVCs
zeer
risic
vroege
katheterablatie
Kathet
straat
tijde
228
technieken
electroan
spontane
meeste
ventriculaire
CT
int
herhaling
vetweefsel
ventrikel
bestudeerd
leiden
CE-MRI
abla
laat
echter
gerelateerd
electrogrammen
gebied
hadden
gere
dysfunctie
minder
beelden
gereperfundeerde
studie
kamer
induceer
strain
ritmestoornissen

Samenvatting en conclusies

Ventriculaire ritmestoornissen (VR) treden op in patiënten met en zonder structurele hartziekten. In patiënten met onderliggende structurele hartziekten is verlittekening van het myocard doorgaans het substraat voor ventriculaire tachycardiën (VT). Het mechanisme dat ten grondslag ligt aan VT is cirkelgeleiding (reëntry) met een kritische isthmus in het litteken gebied. Patiënten die zich met een dergelijke ritmestoornis presenteren lopen risico op acute hartdood. Door het gebruik van inwendige cardioverter defibrillator (ICD) kan dit risico sterk worden gereduceerd. ICD's kunnen echter optredende VT alleen stoppen, vaak door een electroshock. Aanvulllende behandelingen die VT voorkomen zijn daarom van groot belang. Katheterablatie heeft de potentie, door modificatie van het onderliggend substraat, toekomstige VT in patiënten met structurele hartziekten te voorkomen.

In patiënten zonder structurele hartziekten hebben VR vaak een focale oorsprong. Idiopatische ritmestoornissen worden over het algemeen als benigne beschouwd en hebben een goede prognose. Deze VR kunnen wel tot klachten leiden en in enkele gevallen de hartfunctie negatief beïnvloeden. Daarom heeft katheterablatie ook bij de behandeling van deze ritmestoornissen toenemend een belangrijke plaats.

Het doel van dit proefschrift was enerzijds het bestuderen van de determinanten van het substraat dat VT veroorzaakt, VT eigenschappen en het beloop na invasieve behandeling van VT. Anderzijds werd beoogd technieken te ontwikkelen die katheter ablatie ondersteunen en daarmee mogelijk verbeteren.

In **hoofdstuk 1** wordt een overzicht gegeven van de huidige literatuur betreffende de verschillende typen substraat voor monomorfe VT en de toegepaste ablatie technieken.

In **deel I** worden determinanten van het VR substraat en technieken voor substraat identificatie bestudeerd in patiënten die werden verwezen in verband met katheterablatie van VR. Na identificatie en lokalisatie van het substraat kan dit door katheterablatie gericht worden behandeld waardoor herhaling van de ritmestoornis kan worden voorkomen. Verder worden de voordelen van de integratie van beeldvorming van substraat en omliggende anatomische structuren met electroanatomische mapping bestudeerd.

Deel II behandelt de invloed van verschillen in het substraat tussen individuele patiënten op klinische uitkomstvariabelen.

Deel I

Het onderscheid tussen idiopatische (niet litteken gerelateerde) en litteken gerelateerde linker bundeltak blok type VR heeft belangrijke klinische implicaties. In **hoofdstuk 2** werd geëvalueerd of de QRS morfologie van het VR oppervlakte ECG kan discrimineren tussen litteken en niet litteken gerelateerde VR.

Twaalf-afleidingen ECG's van 297 linker bundel tak blok (LBTB) type monomorfe VR werden vastgelegd tijdens catheter ablatie procedures. QRS morfologische eigenschappen die gerelateerd zijn met litteken gerelateerde VA werden geïdentificeerd in een retrospectieve analyse van 118 LBTB type VR om een algoritme te ontwikkelen dat vervolgens prospectief werd getest in 179 LBTB type VR. De aanwezigheid van myocard litteken werd gediagnostiseerd op basis van het sinusritme ECG, cardiovasculaire beeldvorming en elecroanatomical katheter mapping. Een precordiale transitie verder dan V4, notching van de S-wave downstroke in afleiding V1 of V2 en een duur van het begin van het QRS complex tot de nadir van de S-wave in V1 >90ms waren onafhankelijke voorspellers voor litteken gerelateerde VR. Het voorgestelde algoritme classificeerde een VR als litteken gerelateerd als deze aan een van deze criteria voldeed. Als geen van deze 3 criteria van toepassing waren werd een VR als niet litteken gerelateerd geclassificeerd. Het algoritme bleek zeer sensitief (96%) en specifiek (83%) voor het identificeren van litteken gerelateerde LBTB type VR in de prospectieve evaluatie. De conclusie van deze studie was derhalve dat de QRS morfologie van een VR verschilt tussen litteken gerelateerde en niet litteken gerelateerde VR. Litteken gerelateerde VR kunnen worden geïdentificeerd aan de hand van een eenvoudig ECG algoritme waarop verdere diagnostiek kan worden ingezet.

In **hoofdstuk 3** wordt geëvalueerd of omgekeerde polariteit (reversed polarity) van aangrenzende bipolaire electrogrammen terechte ablatiepunten voor het behandelen van idiopatische rechter ventrikel uitstroombaan (RVOT) VR kunnen identificeren. Vijfentwintig patiënten die katheter ablatie voor RVOT VR ondergingen werden bestudeerd. Electrogrammen van ablatie punten en mapping punten in een 15mm radius werden beoordeeld op locale activatietijd, de morfologie van het unipolaire signaal en het voorkomen van reversed polarity van bipolaire electrogrammen. Electrogram eigenschappen van geslaagde en niet geslaagde ablatiepunten werden vergeleken. Verder werd de partiële distributie van elk electrogram bestudeerd. Electrogrammen met een unipolair QS morfologie werden gevonden in een relatief groot gebied rondom het geslaagde ablatiepunt. Mapping gebaseerd op locale activatie tijd en reversed polarity kon een goed ablatiepunt beter voorspellen dan mapping gebaseerd op unipolaire QS morfologie en locale activatietijd. Reversed polarity heeft daarom een sterke voorspellende waarde voor geslaagde ablatie in focale idiopatische RVOT VR. Het gebruik van reversed polarity kan resulteren in een verminderd aantal katheter ablatie applicaties.

Reperfusie therapie tijdens een acuut myocard infarct (AMI) leidt tot minder schade aan het myocard en een betere cardiale functie. Vroege reperfusie therapie kan echter ook het substraat voor later optredende VT's beïnvloeden. In **hoofdstuk 4** wordt electroanatomische mapping en beoordeling van infarct histologie gebruikt om de invloed van reperfusie behandeling op substraat en VT eigenschappen laat na het myocard infarct te beoordelen.

Veertien patiënten met VT die vroege reperfusie hadden ondergaan tijdens het AMI werden vergeleken met 22 patiënten met VT die geen reperfusietherapie hadden ondergaan tijdens het AMI. Zevenentwintig patiënten werden behandeld met katheterablatie en 10 met chirurgischekamer reconstructie met chirurgische cryoablatie in 9. De cyclus lengte van spontane en geïnduceerde VT was significant korter in patiënten die reperfusie therapie hadden ondergaan. In gereperfundeerde patiënten was het electroanatomische litteken minder homogeen dan in niet gereperfundeerde patiënten. Histologische evaluatie van het litteken in geopereerde patiënten toonde dikke lagen van overlevend myocard in gereperfundeerde maar niet in niet gereperfundeerde patiënten.

Litteken grootte en patroon verschillen tussen vroeg gereperfundeerde en niet gereperfundeerde patiënten. Minder homogeen litteken en vroege reperfusie tijdens AMI zijn geassocieerd met snellere VT.

Katheterablatie gericht op substraat gebruikt electronanatomical voltage mapping om litteken te visualiseren. Contrast enhanced MRI (CE-MRI) is de gouden standaard om de 3-dimensionale structuur van verlittekend myocard te visualiseren. **Hoofdstuk 5** onderzoekt de relatie tussen locale electrogram amplitudes (voltages) en littekengegevens gevisualiseerd door MRI in vijftien patiënten die een ablatie ondergingen voor VT na een myocardinfarct. CE-MRI gegevens konden tijdens de ablatie procedure nauwkeurig worden samengevoegd met de electroanatomische voltage maps. Hierbij kon CE-MRI in een derde van de patiënten littekengebieden identificeren die niet waren gedetecteerd door voltagemapping. Verder werden locale voltages vergeleken met de gegevens van de CE-MRI en bleek er een duidelijke relatie tussen afnemend electrogramvoltage en toenemende litteken transmuraliteit en intensiteit. Deze studie heeft laten zien dat integratie van CE-MRI met kathetermapping tijdens ablatie procedures van aanvullende waarde kan zijn.

Identificatie van epicardiale substraat en ablatie van epicardiale VR wordt bemoeilijkt door de aanwezigheid van coronair arteriën en epicardiaal vetweefsel.

In **hoofdstuk 6** wordt het gebruik van computed tomography (CT) beelden om coronair en vet anatomie tijdens ablatie te visualiseren geëvalueerd. CT scans werden gemaakt in 28 patiënten die een endo- en epicardiale VT ablatie ondergingen. CT beelden werden succesvol geintegreerd met electranatomical mapping tijdens de ablatie procedure. Tijdens en na de prodecure werden CT, coronair angiografie en mapping en ablatie gegevens vergeleken. CT scan bleek een adequate 3-dimensionale anatomie van de coronairen weer te geven. In 7 van de 46 opgewekte VR is afgezien van ablatie omdat de oorsprong te dicht bij een coronair arterie lag. Verder was er bij toenemende dikte van de epicardiale vetlaag een afname van locaal gemeten voltage. De dikte van epicardiaal vet ter plaatse van niet effectieve ablatie applicaties was 16.9±6.8mm (range 7.3– 22.2mm). Op locaties waar ablatie succesvol was 1.5±2.1mm (range 0–6.1mm, $p<0.001$). Concluderend kan integratie van

CT data met electroanatomische mapping worden gebruikt om de anatomie van coronair arteriën en epicardiaal vetweefsel te visualiseren tijdens ablatie procedures. Een epicardiale vetlaag van >7mm en de aanwezigheid van coronair arteriën zijn belangrijke factoren die het falen van ablatie kunnen veroorzaken.

Deel II

Het is beschreven dat de linker kamer ejectiefractie (EF) kan verbeteren na ablatie van frequente premature ventriculaire extrasystolen (PVCs). De meeste patiënten met frequente PVCs hebben echter een normale ejectiefractie. Subtiele en vroege vormen van PVC geïnduceerde verminderde cardiale functie kunnen echter worden gemist door conventionele echocardiografische technieken. In **hoofdstuk 7** wordt het effect van frequente PVCs op de ventriculaire functie in patiënten met een behouden EF bestudeerd.

Met behulp van 2D echocardiografie werd in 49 patiënten met frequente PVC's (waarvan 34 een geslaagde ablatie onderging) en 25 controle patiënten de ventriculaire functie geëvalueerd. Naast LVEF, ventriculaire volumina en tricuspid annulus plane systolic excursion werd ook multidirectionele strain gecalculeerd op basis van speckle tracking imaging.

Bij presentatie waren de LVEF, volumina en RV dimensies normaal in patiënten en controles. Speckle tracking imaging toonde echter verminderde strain in patienten met frequente PVC's in vergelijking met controles. Na verloop van tijd was er geen verandering in LVEF, volumina en RV dimensies in patienten die al dan niet een geslaagde catheter ablatie ondergingen. Strain parameters echter verbeterde significant in patiënten na een geslaagde ablatie. Hieruit volgt dat frequente PVC's subtiele cardiale dysfunctie kunnen veroorzaken die kan worden gedetecteerd met speckle tracking evaluatie in patiënten zonder evidente cardiomyopathie. Catheter ablatie kan resulteren in eliminatie van PVC's en verbetering van subtiele dysfunctie.

In **hoofdstuk 8** wordt het herhaalrisico en uitkomsten in 64 patiënten met litteken gerelateerde VTs uit de rechter ventrikel bestudeerd. Negenentwintig patiënten met en 35 zonder de diagnose van arrhythmogene rechterkamer cardiomyopathie (ARVC) werden vergeleken.

Litteken werd geïdentificeerd door middel van electroanatomische mapping, echocardiografie en/of MRI. De behandeling bestond uit medicamenteuze therapie catheter ablatie en/of ICD implantatie. Het optreden van VTs was vergelijkbaar tussen patiënten met en zonder ARVC. De recidief kans was hoog ondanks behandeling. Patiënten die presenteerden met een snelle VT (CL≤250ms) hadden een hoger risico op een recidief snelle VT en hebben om die reden waarschijnlijk het meeste baat bij een ICD.

Hoofdstuk 9 beoogt de bevindingen gedaan in hoofdstuk 4 te staven in een grotere populatie van 506 patiënten na een myocardinfarct. Deze patiënten ondergingen een electrofysiologisch onderzoek voor implantatie van een ICD voor primaire of secundaire preventie van ventriculaire ritmestoornissen. Zij werden geclassificeerd naar vroege reperfusie behandeling (groep 1: reperfusie (trombolyse & percutane coronaire interventie), groep 2: geen reperfusie).

Tenminste 1 monomorfe VT was induceerbaar in 69% van de patiënten.

In de populatie met een ICD implantatie voor primaire preventie was de induceerbaarheid vergelijkbaar tussen groep 1 en 2. De induceerbaarheid was echter significant hoger in groep 2 in de subpopulatie van patiënten met een ICD voor secundaire preventie. De cycluslengte van de geïnduceerde VTs was korter in groep 1 in vergelijking met groep 2. Verder was non-reperfusie geassocieerd met een verdubbeling van het risico op optreden van VT in de primaire preventie populatie. Deze studie laat zien dat er belangrijke verschillen zijn in VT induceerbaarheid, VT cycluslengte en optreden van spontane VT tussen gereperfundeerde en niet gereperfundeerde patiënten.

Ventriculaire ritmestoornissen zijn een belangrijke oorzaak van postoperatieve mortaliteit en morbiditeit na een chirurgische linker kamer reconstructie (SVR) als behandeling voor ischaemisch hartfalen.

In **hoofdstuk 10** wordt het substraat, VT eigenschappen en uitkomst na katheterablatie in patiënten na SVR belicht. Uit een populatie van 416 patiënten in 3 centra verwezen voor katheterablatie van late VT na AMI hadden 12(3%) een SVR ondergaan.

Vier (33%) presenteerden zich met aanhoudende VT in de perioperatieve periode en 8 (67%) met aanhoudende of herhaalde VT laat na de operatie. In 11 patiënten kon het operatie litteken worden geïdentificeerd met catheter mapping. Eenenzeventig procent van de VT had een reentrycircuit grenzend aan chirurgisch litteken. In 9 patiënten konden alle of alleen de klinische VT succesvol worden geableerd. Presentatie in de vroege postoperatieve fase was geassocieerd met een hoge mortaliteit. Daar tegenover staat dat katheterablatie laat na SVR een hoge slagingskans heeft.

Conclusies en toekomstperspectief

In patiënten die zich met VR presenteren is identificatie en karakterisering van het substraat van centraal belang voor het bepalen van behandeling en prognose.

Initieel heeft het maken van onderscheid tussen litteken gerelateerde en niet litteken gerelateerde VR vergaande consequenties, aangezien litteken gerelateerde VR kunnen leiden tot acute hartdood en niet litteken gerelateerde VR vaak goedaardig zijn.

Het oppervlakte ECG van de VR kan in een vroeg stadium een indicatie geven of er myocardiaal litteken aanwezig is en de aanleiding zijn voor verdere evaluatie. Aangezien 'idiopathische VR' een diagnose is die 'per exclusionem' wordt gesteld kan dit leiden tot uitvoerige non-invasieve en invasieve onderzoeken. Op dit moment wordt CE-MRI beschouwd als de gouden standaard voor de detectie van littekenweefsel. Kathetermapping is echter een zeer gevoelig instrument om verborgen vormen van myocardiaal litteken te identificeren en is daarom van aanvullende waarde naast beeldvorming.

In tegenstelling tot farmacotherapeutische behandeling of behandeling met een ICD heeft katheterablatie het vermogen substraat van VR weg te nemen. De rol van katheterablatie is in de afgelopen jaren aanzienlijk gegroeid door de ontwikkeling van nieuwe technieken en verbreding van indicatiestelling.

Idiopathische VR

Ondanks het feit dat idiopatische VR een goede prognose heeft kunnen deze wel tot ernstige symptomen leiden. Verder kunnen idiopathisch PVC's, een vaak reversibel, negatief effect hebben op de ventriculaire functie. Deze afname van functie varieert van een subklinische dysfunctie alleen detecteerbaar door middel van strain echocardiografie tot duidelijke afname van de linker kamer ejectiefractie. Dankzij de hoge slagingskans is katheterablatie voor idiopathische VR de belangrijkste behandeling geworden voor symptomatische PVC's en voor PVC's waarvan wordt aangenomen dat ze de kamerfunctie beïnvloeden.

De nauwkeurigheid van kathetermapping om ablatie target sites te identificeren kan worden verbeterd door 'reversed polarity' als mapping criterium te gebruiken naast locale activatietijd en morfologie van het unipolaire signaal.

De klinische relevantie van frequente PVC's in asymptomatische patiënten zonder LV dysfunctie in de algemene populatie is niet volledig begrepen. Voordat 'preventieve' PVC ablatie kan worden aanbevolen is het belangrijk gevoeligere indicators te identificeren om patiënten met een risico op achteruitgang van de LV functie te detecteren.

Litteken gerelateerde VT

Het is het onderliggend ziektebeeld dat het substraat voortbrengt. De morfologie van het substraat bepaalt vervolgens de eigenschappen van de VT. Kennis van het VT substraat in verschillende ziektebeelden en individuele patiënten is belangrijk voor het verbeteren van mapping- en ablatie strategieën.

Het grootste deel van de patiënten met litteken gerelateerde VT heeft daarvoor een AMI doorgemaakt. De meeste kennis van het VT substraat na AMI is gebaseerd op diermodellen van een chronisch geoccludeerde coronair arterie en intraoperatieve mapping studies in patiënten met een chronisch geoccludeerde coronair. Dit resulteert gewoonlijk in een dens litteken met daaromheen een beperkt randgebied. Op dit moment is echter vroege reperfusie de standaard behandeling van AMI. Vroege reperfusie is geassocieerd met minder dens

en minder homogeen electroanatomisch litteken, dit werd bevestigd met histologie. Kleine gebieden van dens litteken en meer infarct randgebied kan resulteren in kortere isthmus lengte en snellere geleiding. Dit beinvloed het optreden van spontane VT, VT induceerbaarheid en eigenschappen zoals cyclus lengte. Of substraat gebaseerde ablatie bemoeilijkt wordt door een patchy litteken patroon moet verder worden geëvalueerd.

In patiënten die zich presenteren met VT na SVR voor ischaemische cardiomyopathie is het reëntry circuit vaak gerelateerd aan chirurgisch litteken of patch materiaal. Katheterablatie kan zeer effectief zijn dit type VT te behandelen en herhaling te voorkomen.

Bij litteken gerelateerde VT uit de rechter kamer is er een aanzienlijk risico op herhaling en mogelijk acute hartdood onafhankelijk of de diagnose ARVC al dan niet wordt gesteld. Patiënten die zich met een snelle rechter ventrikel tachycardie presenteren hebben een hoog risico op opnieuw snelle VT in de toekomst en hebben daarom waarschijnlijk het meeste baat bij ICD therapie.

Katheterablatie

De ontwikkeling van substraat gerichte technieken, gekoelde katheterablatie en de introductie van de percutane epicardiale benadering heeft er toe geleid dat veel eerder als 'onbehandelbaar' beschouwde VT nu benaderbaar zijn voor ablatie. Vooruitgang in beeldvorming van het substraat en de integratie hiervan tijdens ablatieprocedures kan het inzicht in het substraat voor VT verbeteren en leidend zijn voor ablatie.

CE-MRI kan de 3-dimensionale geometrie van myocardiale fibrose visualiseren en is de gouden standaard voor het detecteren van subendocardiaal en non-transmuraal litteken. CE-MRI informatie kan worden geïntegreerd met electroanatomische mapping tijdens de ablatie procedure. Hiermee kunnen epicardiaal en intramuraal litteken worden gedetecteerd dat gemist wordt door enkel voltage mapping. Na CE-MRI integratie kan gedetailleerde mapping worden beperkt tot een interessegebied en kunnen gebieden die onterecht als laag voltage zijn aangemerkt worden geïdentificeerd. Hierbij komt dat in diermodellen is aangetoond dat litteken geometrie afgebeeld met hoge resolutie CE-MRI de locatie van reëntrycircuits kan voorspellen. Verder onderzoek naar of en hoe CE-MRI reëntrycircuits kan voorspellen in patiënten is noodzakelijk aangezien dit van aanzienlijke waarde kan zijn bij catheterablatie.

Een belangrijke beperking van epicardiale substraatmapping is de aanwezigheid van epicardiaal vetweefsel en coronairarteriën. De integratie van CT beelden met electroanatomische mapping kan de anatomie van epicaridaal vet en coronairen visualiseren. Deze techniek kan bijdragen aan correcte interpretatie van electrogrammen en plaatsen identificeren waar het epicardiale vet te dik is voor ablatie.

Conclusies

Het onderliggend substraat bepaalt de eigenschappen van een VT. Kennis en begrip van het substraat in verschillende ziektebeelden en in individuele patiënten is cruciaal voor de behandeling van VT. Katheterablatie kan het substraat dat ritmestoornissen veroorzaakt wegnemen. Het gebruik van nieuwe mapping criteria en integratie van beeldvormende technieken tijdens katheterablatie kan het succes van de procedure faciliteren.

gouden
hartdood
populatie
hoofdstu
gegevens
geassocieerd
myocard
arteriën
belangrijke
verbeteren
voorkomen
hoge
vet
MRI
geïdentificeerd
geslaagde
reperfusie
PVCs
zeer
risico
procedure
vroege
katheterablatie
238
Katheter
tijden
technieken
electroana
spontane
meeste
ventriculaire
CT
integ
herhaling
vetweefsel
ventrikel
bestudeerd
CE-MRI
laat
leiden
echter
gerelateerd
electrogrammen
gebied
hadden
dysfunctie
minder
beelden

List of publications

From wastepaper basket; Total AV block?!
Wijnmaalen AP, van den Berg TM, Delemarre BJM.
Neth Heart J 2006; 6, 232 & 238.

Patients with scar-related right ventricular tachycardia: determinants of long-term outcome.
Wijnmaalen AP, Schalij MJ, Bootsma M, Kies P, DE Roos A, Putter H, Bax JJ, Zeppenfeld K.
J Cardiovasc Electrophysiol. 2009 Oct;20(10):1119-27.

Early reperfusion during acute myocardial infarction affects ventricular tachycardia characteristics and the chronic electroanatomic and histological substrate.
Wijnmaalen AP, Schalij MJ, von der Thüsen JH, Klautz RJ, Zeppenfeld K.
Circulation. 2010 May 4;121(17):1887-95.

Beneficial effects of catheter ablation on left ventricular and right ventricular function in patients with frequent premature ventricular contractions and preserved ejection fraction.
Wijnmaalen AP, Delgado V, Schalij MJ, van Huls van Taxis CF, Holman ER, Bax JJ, Zeppenfeld K.
Heart. 2010 Aug;96(16):1275-80.

Head-to-head comparison of contrast-enhanced magnetic resonance imaging and electroanatomical voltage mapping to assess post-infarct scar characteristics in patients with ventricular tachycardias: real-time image integration and reversed registration.
Wijnmaalen AP, van der Geest RJ, van Huls van Taxis CF, Siebelink HM, Kroft LJ, Bax JJ, Reiber JH, Schalij MJ, Zeppenfeld K.
Eur Heart J. 2011 Jan;32(1):104-14.

Ventricular tachycardia ablation: indications and techniques.
Wijnmaalen AP, Zeppenfeld K.
Minerva Cardioangiol. 2011 Apr;59(2):149-69.

ECG Identification of Scar-Related Ventricular Tachycardia with a Left Bundle Branch Block Configuration.
Wijnmaalen AP, Stevenson WG, Schalij MJ, Field ME, Stephenson K, Tedrow UB, Koplan BA, Putter H, Epstein LM, Zeppenfeld K.
Circ Arrhythm Electrophysiol. 2011 Apr 1;4(2):195-201.

Early reperfusion therapy affects inducibility, cycle length, and occurrence of ventricular tachycardia late after myocardial infarction.
Wijnmaalen AP, Piers SR, Borleffs CJ, van Huls van Taxis CF, Thijssen J, van Rees JB, Cannegieter SC, Bax JJ, Schalij MJ, Zeppenfeld K.
Circ Arrhythm Electrophysiol. 2011 Apr 1;4(2):195-201.

Catheter ablation of ventricular tachycardia after left ventricular reconstructive surgery for ischemic cardiomyopathy.
Wijnmaalen AP, Roberts-Thomson KC, Steven D, Klautz RJM, Willems S, Schalij MJ, Stevenson WG, Zeppenfeld K.
Heart Rhythm. 2012 Jan; 9(1):10-7

Longitudinal mechanics of the periinfarct zone and ventricular tachycardia inducibility in patients with chronic ischemic cardiomyopathy.
Bertini M, Ng AC, Borleffs CJ, Delgado V, **Wijnmaalen AP**, Nucifora G, Ewe SH, Shanks M, Thijssen J, Zeppenfeld K, Biffi M, Leung DY, Schalij MJ, Bax JJ.
Am Heart J. 2010 Oct;160(4):729-36.

Epicardial ablation for ventricular tachycardia: a European multicenter study.
Della Bella P, Brugada J, Zeppenfeld K, Merino J, Neuzil P, Maury P, Maccabelli G, Vergara P, Baratto F, Berruezo A, **Wijnmaalen AP**.
Circ Arrhythm Electrophysiol. 2011 Oct;4(5):653-9.

Reversed polarity of bipolar electrograms for predicting a successful ablation site in focal idiopathic right ventricular outflow tract arrhythmias.
van Huls van Taxis CF, **Wijnmaalen AP**, den Uijl DW, Gawrysiak M, Putter H, Schalij MJ, Zeppenfeld K.
Heart Rhythm. 2011 May;8(5):665-71.

Real-time integration of MDCT derived coronary anatomy and epicardial fat: Impact on electroanatomical mapping and ablation for ventricular arrhythmias.
van Huls van Taxis CF, **Wijnmaalen AP**, Piers SR, van der Geest RJ, Schalij MJ, Zeppenfeld K.
Submittted

Real-time integration of intracardiac echocardiography to facilitate atrial tachycardia ablation in a patient with a Senning baffle.
den Uijl DW, Blom NA, **Wijnmaalen AP**, Bax JJ, Schalij MJ, Zeppenfeld K.
Circ Arrhythm Electrophysiol. 2009 Oct;2(5):e28-30

PVC's
eigensch
voorspellen
behandelin
morfologie
gouden
hartdood
populatie
hoof
gegevens
geassocieerd
belan
verbeteren
voorkomen
MRI
geïdentificeerd
gesla
reperfusie
PVCs
zeer
procedure
vroege
katheterablat
ubstraat
tij
technieken
electro
litteke
spontane
meeste
ventriculaire
CT
abl
herhaling
vetweefsel
bestudeerd
CE-
leiden
laat
echter
gerelateerd
electrogramm
hadden

Dankwoord

Dit boek was er niet geweest zonder de hulp en steun van velen. Ik heb met veel plezier aan dit proefschrift gewerkt. Mijn dank gaat uit naar al diegenen die de afgelopen jaren hierbij betrokken waren. Zonder anderen tekort te doen wil ik graag een aantal mensen persoonlijk noemen.

De onderzoeken beschreven in dit proefschrift werden gedaan op de afdeling hartziekten van het Leids Universitair Medisch Centrum. Dank aan iedereen met wie ik de afgelopen jaren heb samengewerkt. Dank in het bijzonder aan de dames en heer van het cathlab voor de gezelligheid, effectieve samenwerking en koffie in de vele uren achter 'Prucka' en 'CARTO'.

Alle collega's uit 'de Tuin': Dennis, Maaike, Ellen, Roxana, Jaël, Jan, Jan Willem, Jaap, Rutger, Roderick, Mark, Leontine, Louisa, Joanne, Claudia, Laurens, Sjoerd, Yvo, Daniël, Robert, Hans, Sum-Che, Stijntje, Fleur, Joëlla, Joep, Mihály en Cees, we hebben een geweldige tijd gehad! Dank voor alle lol, creativiteit en adviezen op de werkvloer en tijdens borrels, etentjes en congressen.

Carine en Sebastiaan dank dat jullie het stokje hebben overgenomen, jullie doen het geweldig.

Verder wil ik mijn collega's uit het Sint Franciscus Gasthuis in Rotterdam en mijn huidige collega's in het LUMC danken voor hun ondersteuning en flexibiliteit.

Veel dank ben ik verschuldigd aan vrienden die een belangrijke bijdrage hebben geleverd aan het hooghouden van de moraal. Pieter, Marcel, Tim, Timon, Arian, Leon, Corné, Ruben, Hans, Cornelis en Ab, bedankt voor alle mooie en uitdagende momenten op de fiets en ernaast.

Martijn dank voor alle morele support en de vele verhelderende avonden de afgelopen jaren. Pim, jouw verfrissende blik op de zaken blijft een bron van inspiratie. Ik ben blij dat jullie mijn paranimfen willen zijn.

Ben en Marjan, jullie staan altijd voor ons klaar, dank dat jullie de ´ideale´ schoonouders zijn. Becky, as a mother at distance you have managed to support me nevertheless. Lennard, Thomas en Benno, als broers hoor je een gezond kritische blik te hebben, bedankt voor de goede tijd de afgelopen jaren.

Pap en mam mijn dank voor de basis die jullie hebben gelegd en jullie blijvende steun is niet in een paar woorden uit te drukken, ik ben blij met en trots op jullie.

Anna en Ard, met jullie is het leven iedere dag opnieuw een feestje! Jullie maken me tot een ongekend trotse vader, binnenkort met z´n drieën!

Lieve Menke, leven zonder jou is niet voor te stellen. Dank voor wie je bent. Dank voor je onvoorwaardelijke liefde. Ik bewonder je. Ik heb je lief.

PVC's
eigenschap
voorspellen
behandeling
morfologie
gouden
hartdood
populatie
myocard
gegevens
geassocieerd
verbeteren
voorkomen
MRI
geïdentificeerd
geslaagd
reperfusie
PVCs
zeer
risic
procedure
vroege
katheterablatie
littekens
tijde
technieken
electroan
spontane
meeste
ventriculaire
CT
int
herhaling
vetweefsel
ventrikel
bestudeerd
leiden
laat
echter
gerelateerd
electrogrammen
hadden
gebied

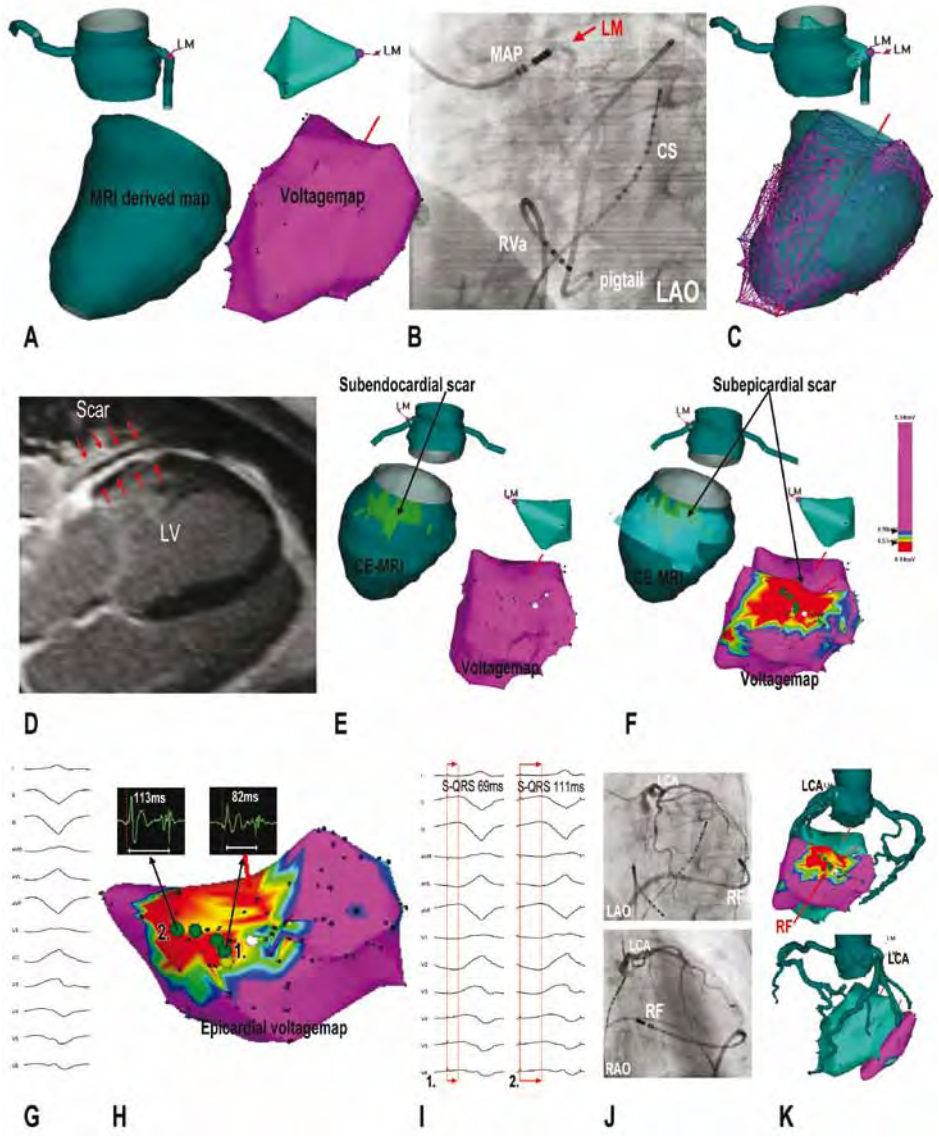
Curriculum Vitae

De auteur van dit proefschrift werd geboren op 2 juli 1980 te Rotterdam. In 1997 en 1999 behaalde hij achtereenvolgens het HAVO diploma aan scholengemeenschap Willem van Oranje te Oud-Beijerland en het VWO diploma aan het Albeda college te Rotterdam. Hierna startte hij met de opleiding Geneeskunde aan de Universiteit Leiden. Na het behalen van het artsexamen in november 2005 heeft hij 10 maanden gewerkt als arts-assistent op de afdeling cardiologie van het HAGA ziekenhuis (opleider Dr. B.J.M. Delemarre).

Van 2006 tot 2009 deed hij klinisch promotieonderzoek aan de afdeling cardiolgie van het Leids Universitair Medisch Centrum onder leiding van Prof. Dr. M.J. Schalij en Dr. K. Zeppenfeld naar het substraat van ventriculaire tachycardiën. De resultaten hiervan zijn beschreven in dit proefschrift.

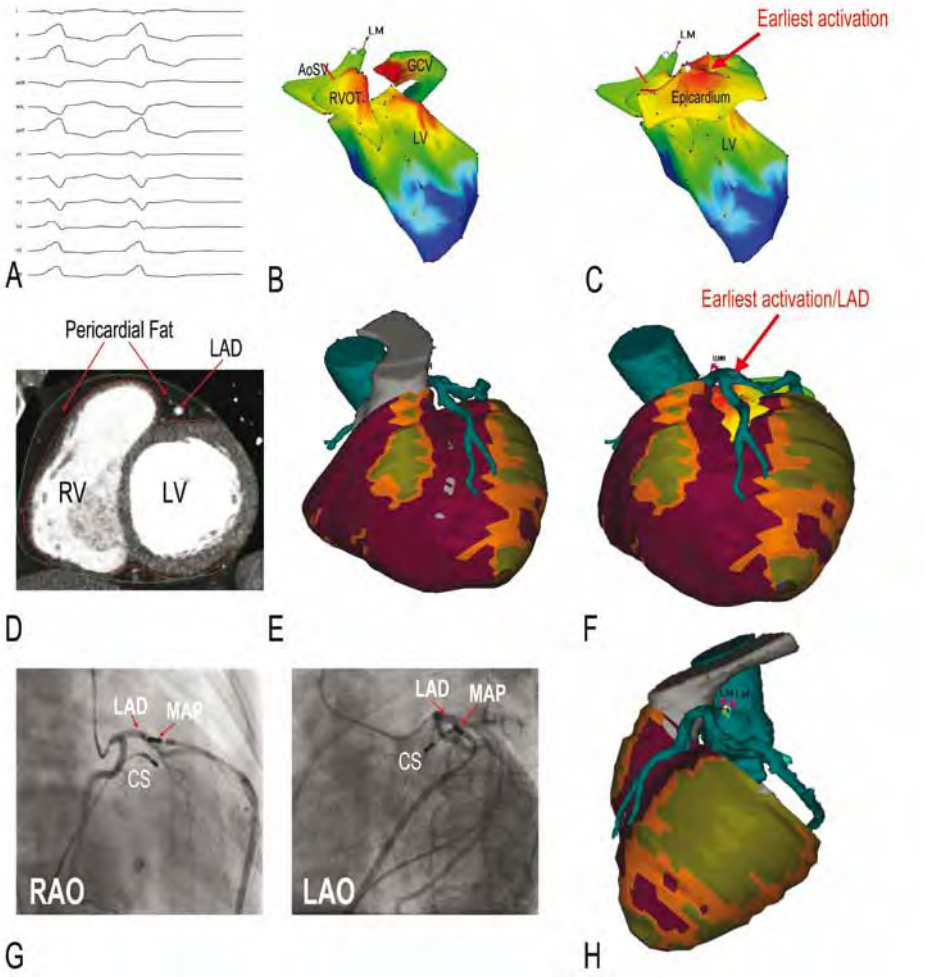
Per 1 november 2009 startte hij met de opleiding cardiologie. Deze werd aangevangen met de vooropleiding Interne Geneeskunde in het Sint Franciscus Gasthuis te Rotterdam (opleider A.P. Rietveld). November 2011 is hij teruggekeerd naar het LUMC voor het vervolg van de opleiding cardiologie (opleider Prof. Dr. M.J. Schalij).

Color section figures



Page 17 Figure 2. Image integration of electroanatomical voltage mapping and CE-MRI derived data on anatomy and scar characteristics

Example of a patient presenting with VT due to non-ischemic cardiomyopathy in whom combined endocardial and epicardial catheter ablation was performed using image integration of CE-MRI derived data sets and electroanatomical substrate mapping techniques during sinus rhythm.
A and C. Successful integration of the CE-MRI derived LV and aortic cusp anatomy with the LV endocardial electroanatomical voltage map (EAVM) (voltages>1.5mV defined as normal and color coded in purple) using the left main coronary artery (LM) as a single landmark for registration.
B. The fluoroscopy image shows contrast injection through the ablation catheter (MAP) to confirm its position in the LM. Other catheters shown are located at the right ventricular apex (RVa), coronary sinus (CS) and a pigtail catheter in the pericardial space.



Page 19 Figure 3. Integration of electroanatomical activation mapping and MSCT derived anatomy during epicardial ablation

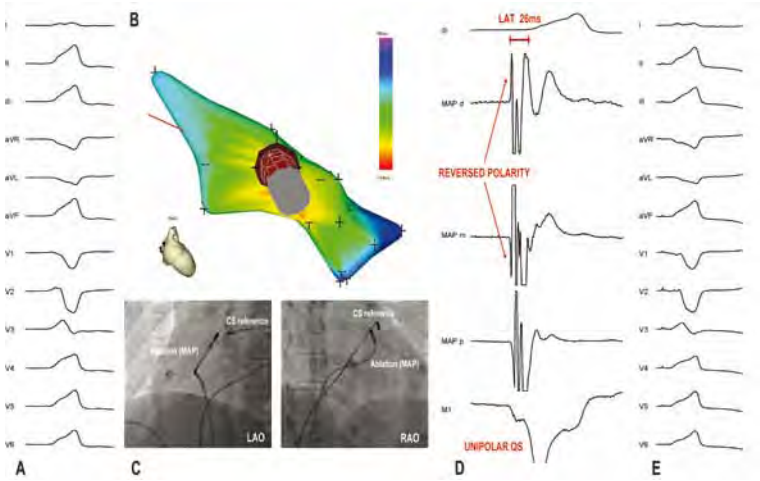
Example of a patient presenting with frequent highly symptomatic non-sustained idiopathic VT in whom combined endo- and epicardial electroanatomical mapping and ablation was performed facilitated by integration of CT derived anatomy.

A. 12-lead QRS of the non-sustained VT.

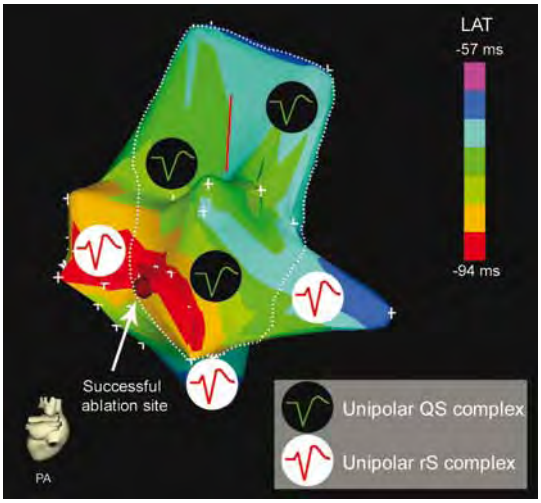
B. Endocardial activation mapping showing limited maps of the aortic cusps (AoSV), great cardiac vein (GCV), right ventricular outflowtract (RVOT) and left ventricle (LV). Earliest local activation time (LAT) was recorded in the GCV but ablation at this site was not successful. C. A limited epicardial activation map overlaying the endocardial maps; epicardial LAT during VT is earlier than the earliest LAT in the GCV.

D. Short axis slice of contrast enhanced multislice computed tomography scan (CT) showing the left and right ventricles (LV and RV) and pericardial fat in the interventricular groove and RV lateral wall.

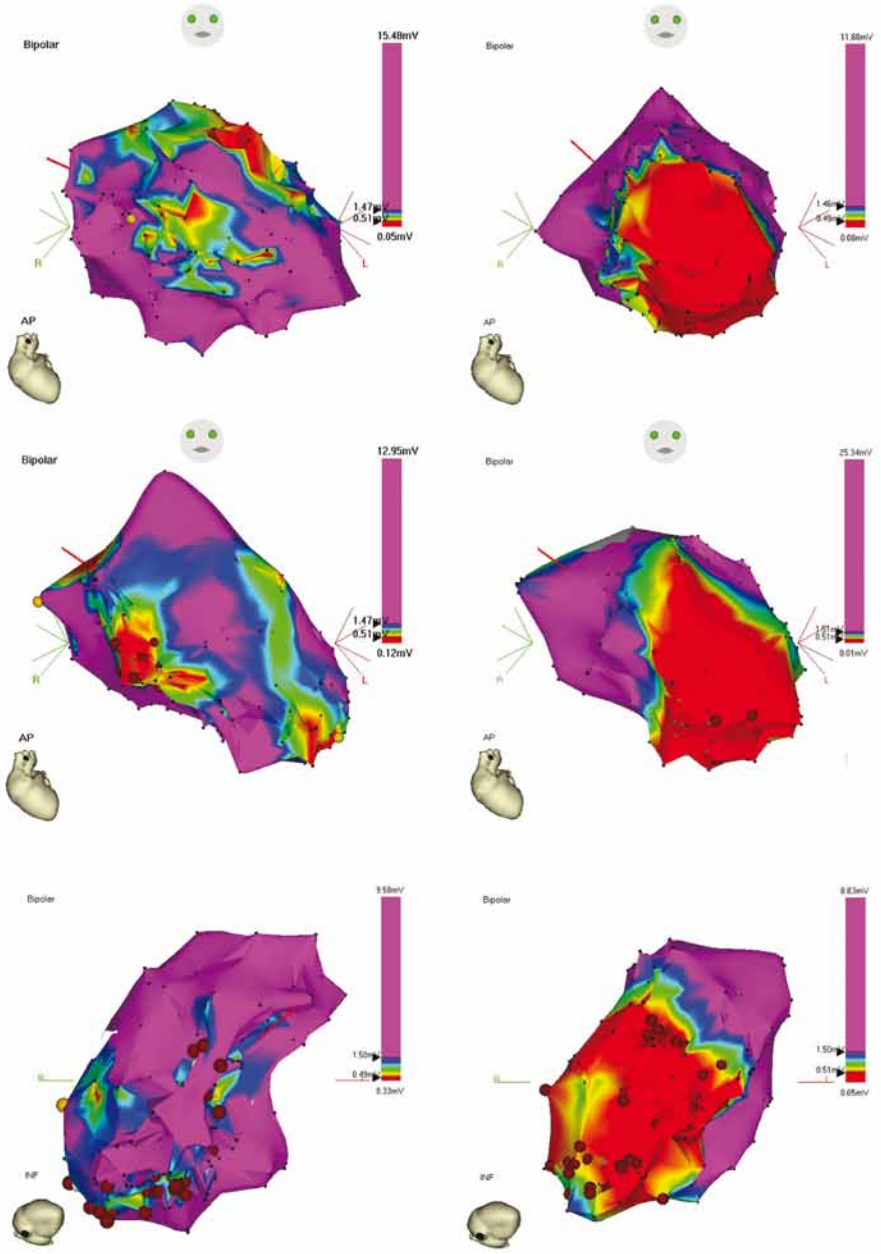
E and H. Different views of CT derived anatomy showing the proximal aorta, left main coronary artery and pulmonary artery with overlaying CT derived mesh of the epicardial surface. Color



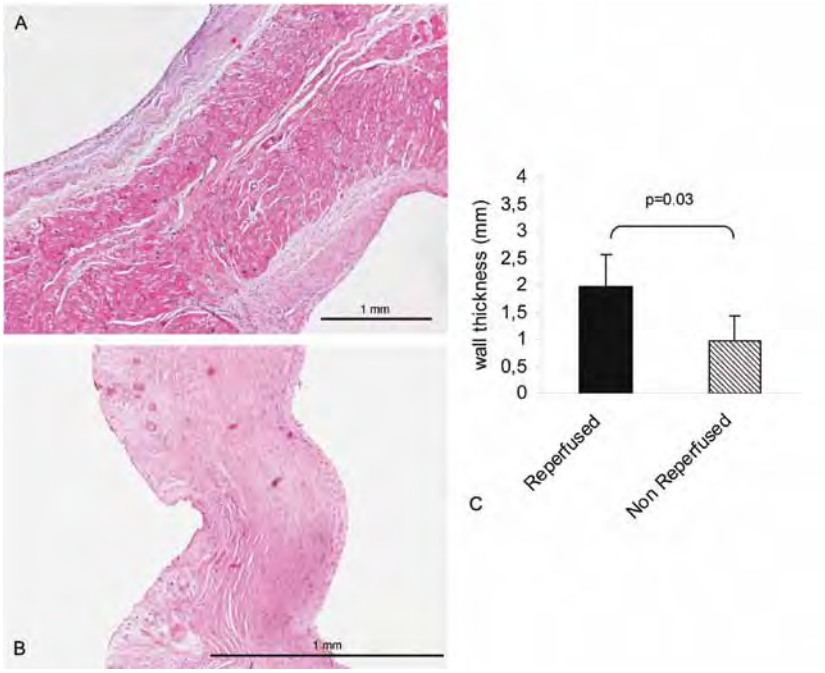
Page 23 Figure 4. Mapping criteria for focal idiopathic ventricular arrhythmias
Example of a patient presenting with frequent symptomatic premature ventricular contractions (PVCs) successfully ablated from the right ventricular outflow tract (RVOT).
A. 12-lead ECG of the PVC QRS. B. Limited activation map or the RVOT (local activation time (LAT) color coded according to the colorbar, reference R-peak of surface ECG lead II)
C. Fluoroscopy images showing the left anterior oblique (LAO) and right anterior oblique (RAO) views. The ablation catheter is located at the successful ablation site (MAP) and the reference catheter in the CS/GCV.
D. Intracardiac signals at the successful site show (1) LAT of 26ms prior to the PVC QRS onset, (2) the presence of reversed polarity of bipolar adjacent electrograms recorded from the distal and mid electrode pair of the mapping catheter and (3) an unipolar QS configuration.
E. Good pace-match of the PVC QRS with the paced QRS at this site.



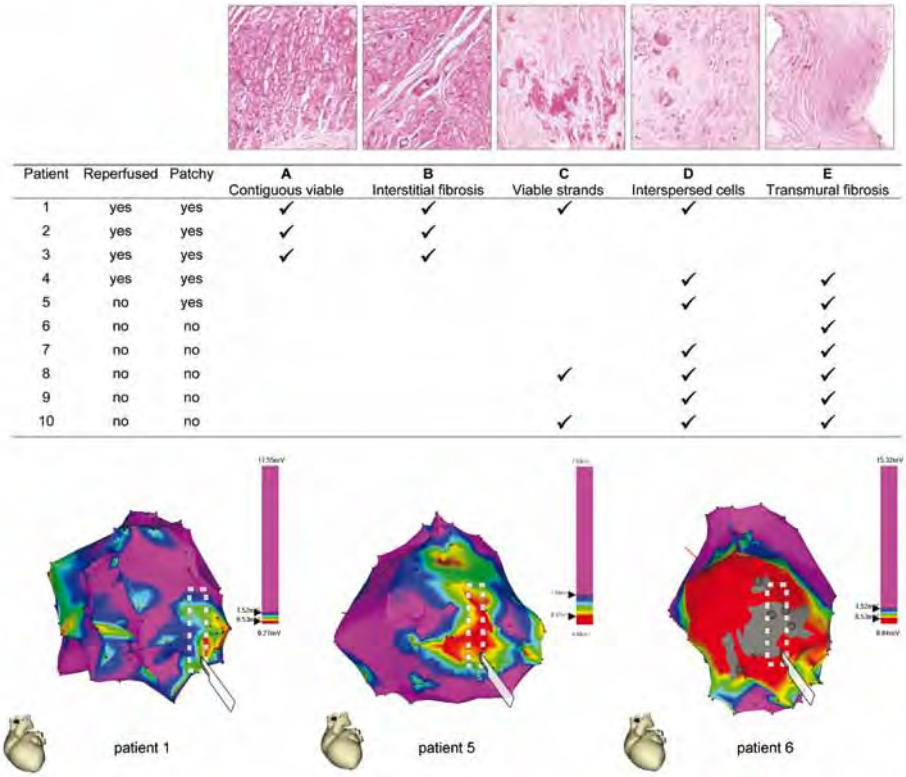
Page 72 Figure 3. Electroanatomical activation map of a right ventricular outflow tract arrhythmia (posterior view). Local activation time (LAT) is color coded with isochronal steps of 5 ms according to the color bar. The white dotted line delineates the area around the successful ablation site (red tag) that demonstrated a unipolar QS-configuration. Black-with-green icons indicate areas demonstrating unipolar QS-configuration and white-with-red icons correspond to the area demonstrating a unipolar rS configuration.



Page 90 Figure 2. Left ventricular electroanatomical voltagemaps of six patients. Bipolar voltages are color coded according to the colorbar. Voltages <1.5mV were considered abnormal. The 3 maps on the left hand side are obtained in reperfused patients and the 3 on the right in non-reperfused patients. The scar pattern is patchy in reperfused and homogeneous in non-reperfused patients.

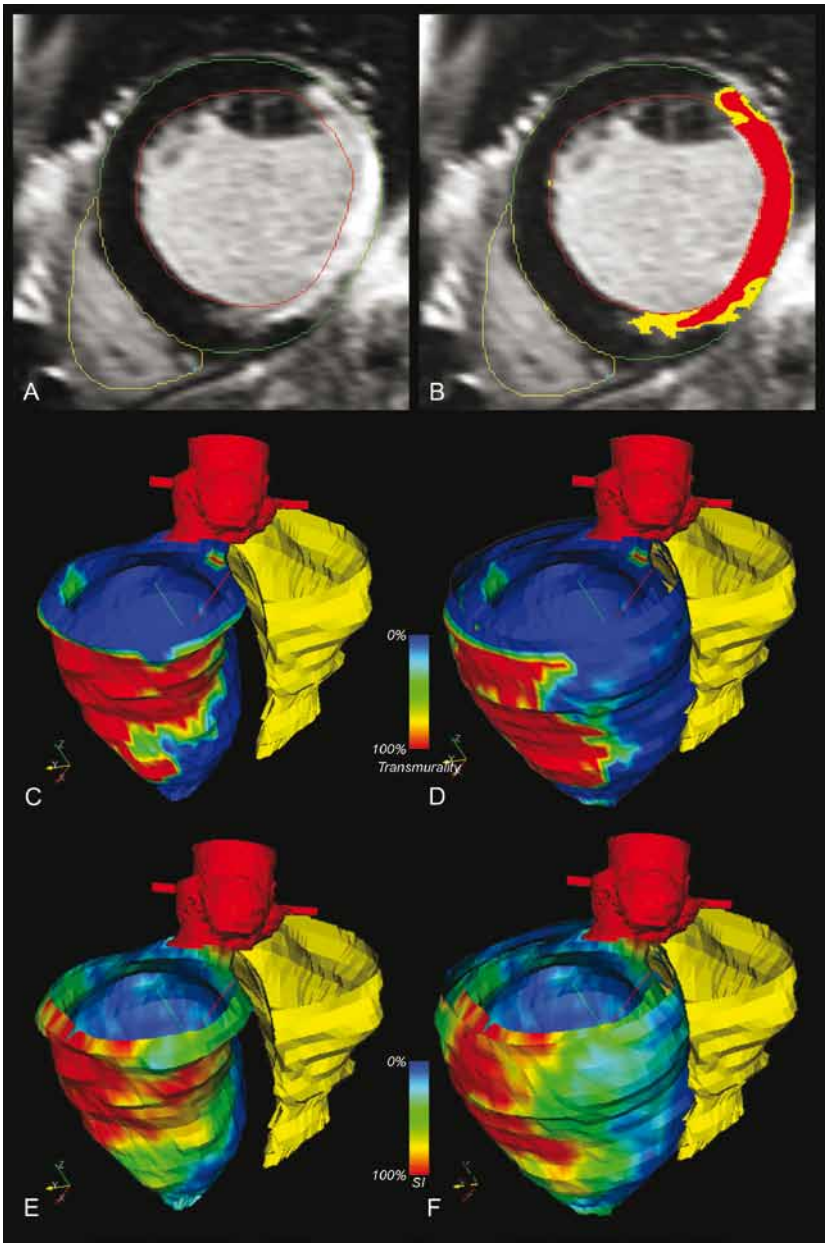


Page 93 Figure 3. Representative slides of transmural biopsies from the core infarct zone in 2 patients (H&E stain). Panel A: small mid wall fibrosis surrounded by thick viable myocytes bundles in a patient after early reperfusion and with a patchy pattern of EA scar. Panel B: mural thinning with dense transmural fibrosis in a non-reperfused patient with a homogeneous pattern of EA scar with only interspersed cardiomyocytes. Panel C: average wall thickness of the area of most extensive fibrosis in myocardial biopsies of reperfused (n=4; 2.0±0.6 mm) and non-reperfused (n=6; 1.0±0.5 mm) patients.

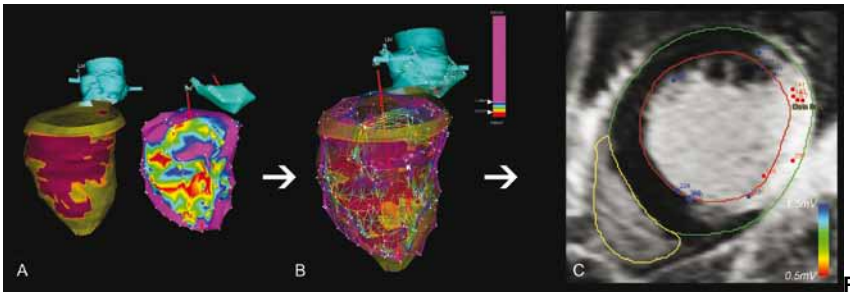


Patient	Reperfused	Patchy	A Contiguous viable	B Interstitial fibrosis	C Viable strands	D Interspersed cells	E Transmural fibrosis
1	yes	yes	✓	✓	✓	✓	
2	yes	yes	✓	✓			
3	yes	yes	✓	✓			
4	yes	yes				✓	✓
5	no	yes				✓	✓
6	no	no					✓
7	no	no				✓	✓
8	no	no			✓	✓	✓
9	no	no				✓	✓
10	no	no			✓	✓	✓

Page 94 Figure 4 The relation between viable myocytes and fibrosis was characterized. Five patterns of local histological scar were identified (A-E). The presence of any of these types in the assessed core infarct region was scored and compared to the presence of reperfusion and the pattern of electroanatomical scar in the 10 patients in whom histological assessment was performed. Three representative examples of EA maps (patient 1, 5 and 6) are shown, the assumed area that was resected by the surgeon is indicated.



Page 105 Figure 1. Preprocedural processing consisted of drawing endo- and epicardial ventricular contours using the short axis CE-MRI slices (panel A), defining intensity and transmurality of scar (yellow= gray-zone, red= core infarction, panel B) and creating color coded endocardial (panel C&E) and epicardial (panel D&F) surface meshes. Panels C&D show coding for percentage of transmurality and panels E&F show the same meshes coded for signal intensity according to the colorbar.



Page
106 **Figure 2.** During the procedure 3-D CE-MRI derived meshes (purple represents scar, green represents normal myocardium) were integrated with the electroanatomical voltage maps (color-coding as in the colorbar). After the procedure color-coded mapping points were superimposed on the CE-MRI slice at the corresponding location (color-coding as in the colorbar).

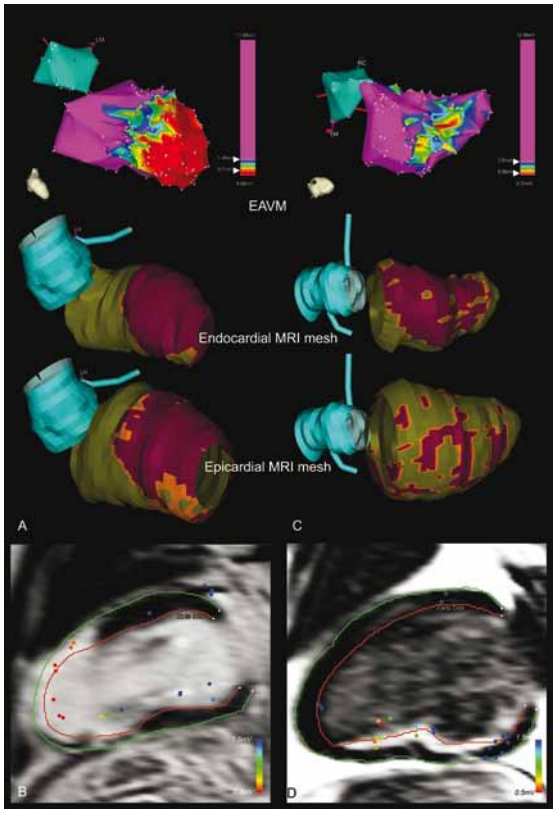
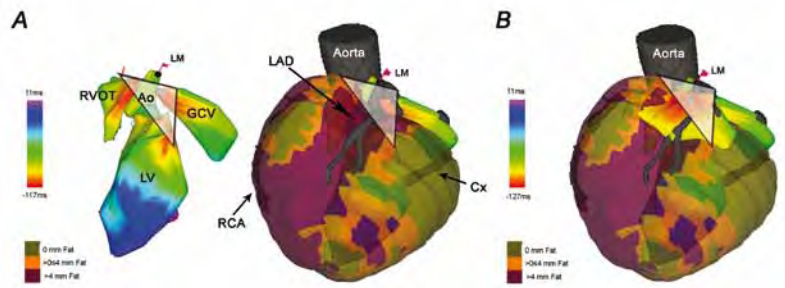
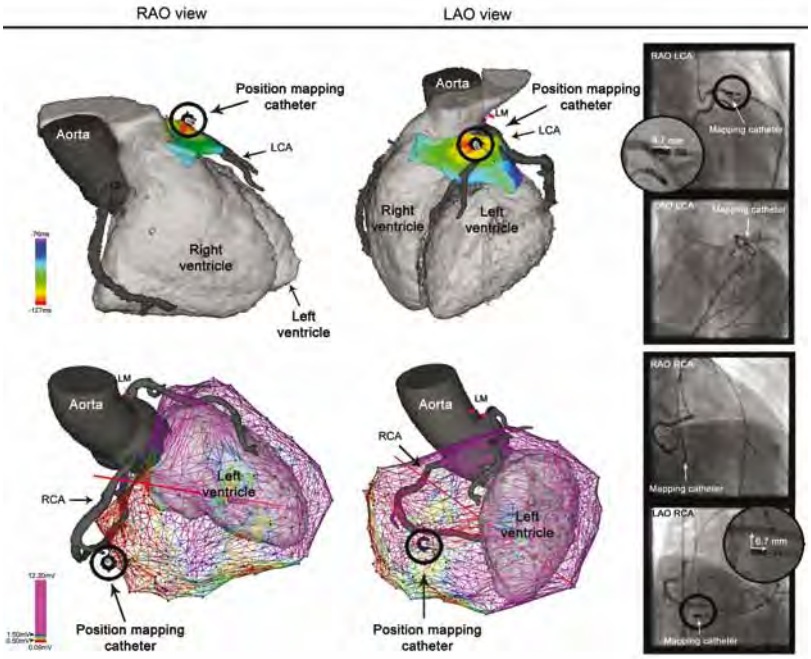


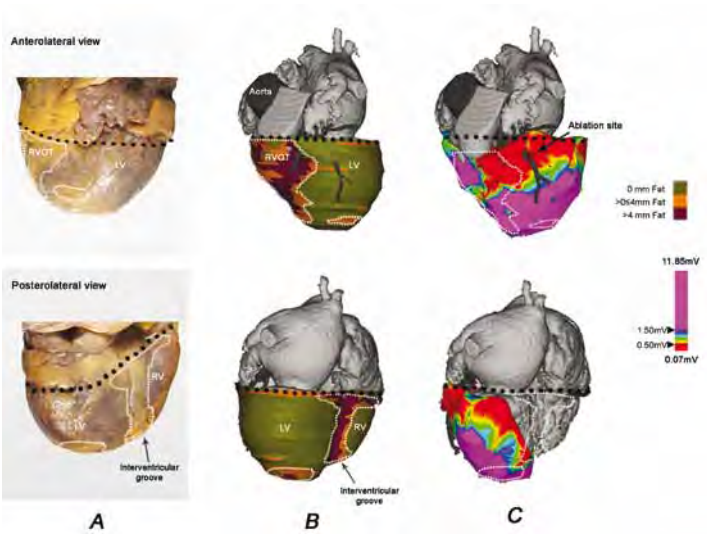
Figure 4. Representative examples of a patient in whom CE-MRI derived mesh matched the EAVM (panel A, B) and of a patient with additional scar-areas identified by CE-MRI not detected by EAVM (panel C, D). Panels A and C show the bipolar voltage maps (color-coding as in the colorbar) and corresponding endo- and epicardial MRI derived surface meshes coded for transmurality (purple represents scar, green represents normal myocardium). Panels B and D show a representative long axis CE-MRI slice with superimposed mapping point locations (mapping point bipolar amplitudes are color coded as in voltage maps).



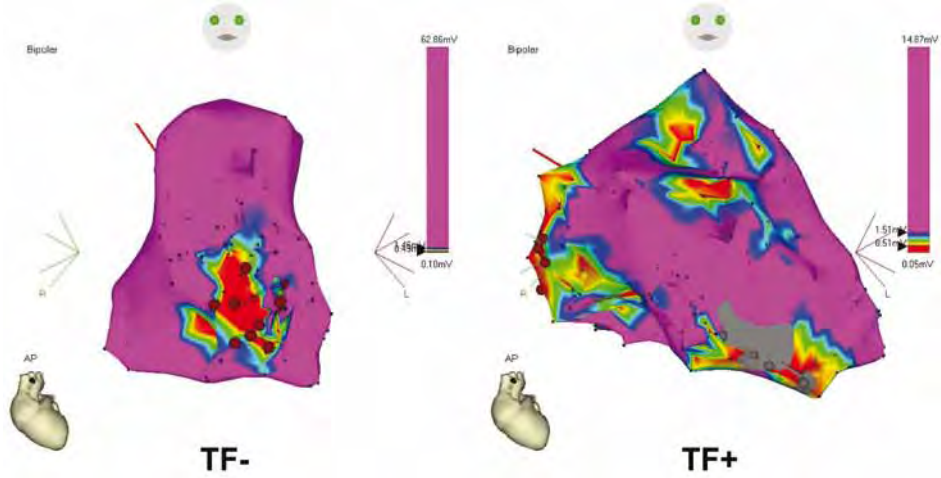
Page 126 Figure 2. Electroanatomical activation map (EAAM) of an idiopathic ventricular arrhythmia and image integration. Panel A: Endocardial EAAM of the left ventricle (LV), right ventricle outflow tract (RVOT), aorta (Ao) and great cardiac vein (GCV). Similar activation time of the LV, RVOT and GCV was observed. The final fusion image (FFI) was registered with the endocardial EAAM, using the left main artery (LM) (right). The white triangle demonstrates the predicted epicardial target site in the vicinity of the left anterior descending artery (LAD), covered by >4mm fat. Panel B: Limited epicardial EAAM confirmed the earliest activation within the predicted site not suitable for ablation. Cx=Circumflex coronary artery; RCA=right coronary artery.



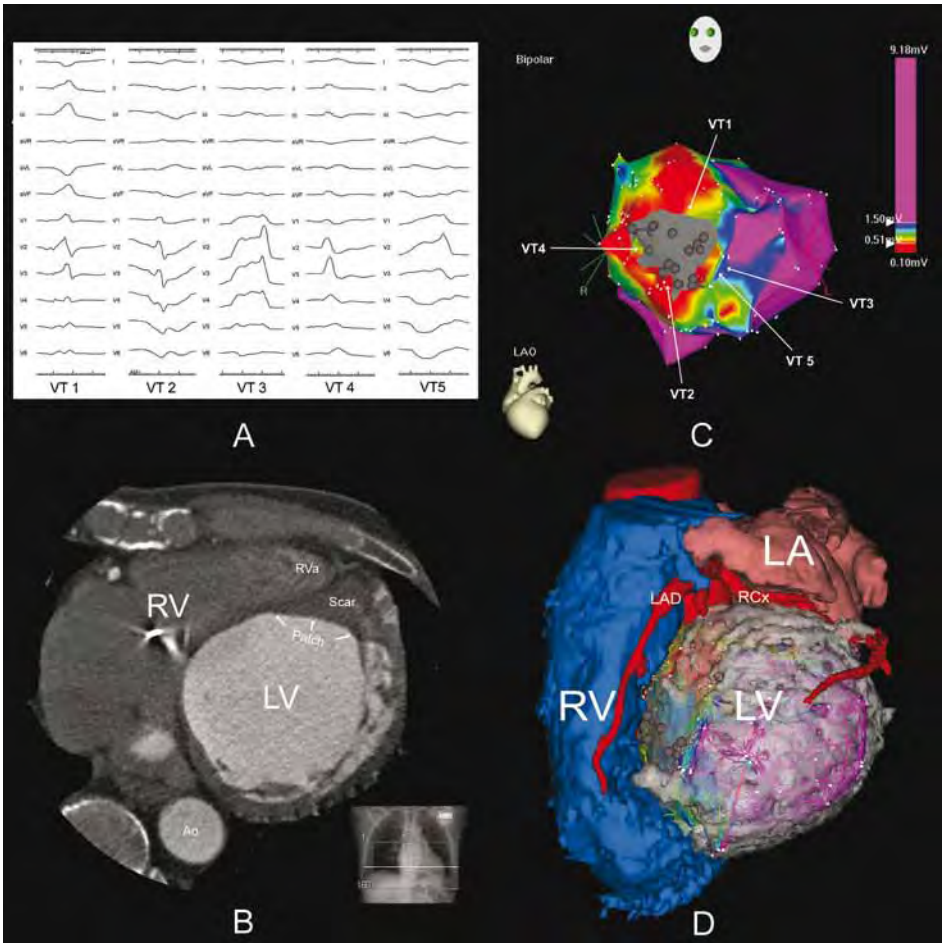
Page 127 Figure 3. Registration accuracy in 2 patients comparing the distance between the catheter tip and coronary arteries on integrated multi-detector computed tomography (MDCT) images and coronary angiography in a right (RAO) and left (LAO) anterior oblique view. Upper panel: limited activation mapping identified a target site located on the left anterior descending artery (LAD) on both MDCT and angiography. Lower panel: the target site (based on pace-mapping) was located <7mm from the right coronary artery (RCA) confirmed by angiography.



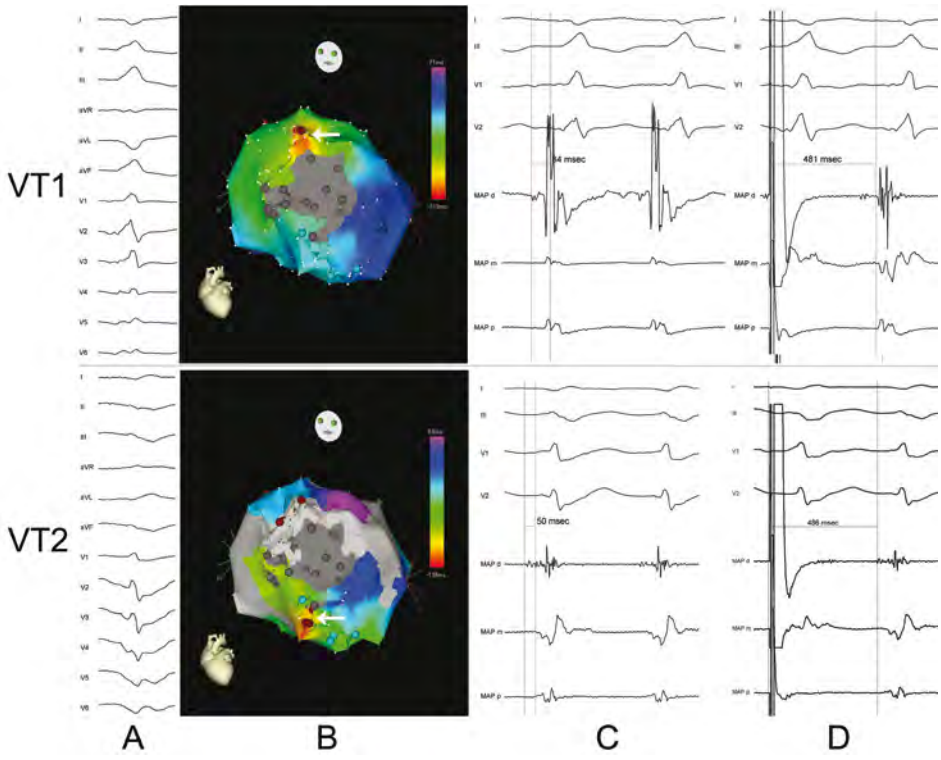
Page 136 Figure 6. Panel A: Gross pathology of the heart of the patient who died 4 weeks after ablation. Panel B: Final fusion image. Panel C: Fusion of the multi-detector computed tomography (MDCT) anatomy with the epicardial electroanatomical voltage map in a modified anterolateral (top) and posterolateral (bottom) view. The ablation site in the vicinity of the circumflex coronary artery is indicated. Comparison of panel A and B shows a good correlation between epicardial fat distribution by pathology and the MDCT derived epicardial fat mesh (white dotted lines). The black line indicates the atrioventricular groove; the anterolateral low voltage area (color coded as indicated) is compatible with subepicardial scar in the absence of epicardial fat.
LV=left ventricle, RV=right ventricle, RVOT=right ventricle outflow tract.



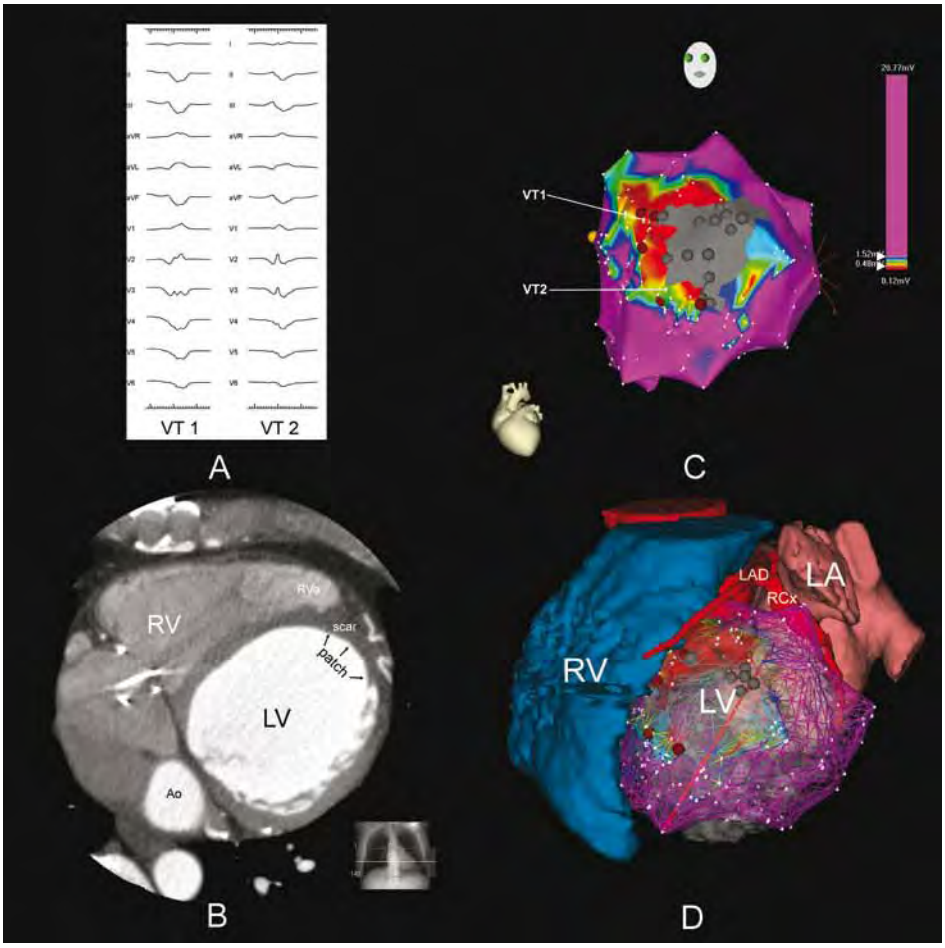
Page 176 Figure 5. Right ventricular 3-D electroanatomical bipolar voltage maps of a TF- (left) and a TF+ (right) patient. Voltages are color-coded according to the corresponding color bar. Normal voltage is defined as electrogram amplitude >1.5mV displayed in purple. The TF- patient had recurrent VT's with different morphologies originating from a single small RV free wall scar area. Scar was only identified by voltage mapping. The TF+ patient had multiple low voltage areas. VT was successfully terminated at the lateral tricuspid annulus.



Page 210 Figure 1. Patient 5, in whom RFCA failed to abolish any of the 5 VTs that appeared to originate from behind the endoventricular patch. Panel A shows the morphologies of VT 1-5 (sweep-speed 100mm/s). Panel B shows the sagittal plane of a multislice CT scan after intravenous contrast demonstrating a space occupied with scar tissue (indicated by the word 'scar') that is excluded from the left ventricular cavity by the endoventricular patch. Panel C shows the endocardial bipolar voltage map with the locations of the exit sites of VT 1-5 bordering the endoventricular patch and indicated by arrows. (colorcoding as in the colorbar, gray is electrically unexcitable scar representing the patch), voltage >1.5 mV is purple. Panel C shows the 3-dimensional reconstruction of the CT images merged with the endocardial voltage map.



Page 211 Figure 2. Example showing the activation and entrainment mapping of VT1 and VT2 in patient 5 (figure 1). The exits of VT3 – VT5 were identified using only activation or pacemapping. Panel A: 12 lead QRS morphology of VT1 and VT2. Panel B: Electroanatomical activation maps of the LV during VT1 (top) and VT2 (bottom). The endoventricular patch was identified as an area of unexcitable scar and tagged in gray. Activation time is according to the colorbar with the earliest activation displayed in red. The white arrows indicate the site of earliest endocardial activation, entrainment mapping and RF application (red tags). Panel C: Intracardiac bipolar electrograms recorded from the distal, mid and proximal electrode pairs of the ablation catheter at the border of the endoventricular patch for VT1 and VT2. Panel D: Entrainment mapping of VT1 shows concealed entrainment while capturing the second electrogram component with an S-QRS interval of 25ms identical with the E-QRS, which is consistent with a VT exit site. Pacing at this site entrained the VT with concealed fusion with a post pacing interval (PPI) of 481ms, which equaled VTCL. VT2 could be entrained with concealed fusion with a PPI of 486ms (VTCL = 504ms) and a S-QRS interval of 50ms.



Page 215 Figure 3. Patient 7, in whom RFCA was successful, abolishing 2 VTs by applying RF energy at the septal side of the endoventricular patch. Panel A shows the morphologies of VT 1-2 (sweep-speed 100mm/s). Panel B shows the sagittal plane of a multislice CT scan after intravenous contrast showing a small apical scar behind the endoventricular patch if compared to patient 5 (figure1). Panel C shows the endocardial bipolar voltage map with the locations of the exit sites of VT 1-2 bordering the endoventricular patch and indicated by arrows (color coding as in the color bar, gray is electrically unexcitable scar representing the patch). Panel C shows the 3-dimensional reconstruction of the CT images merged with the endocardial voltage map.